DIGITALCOMMONS
@WAYNESTATE

Wayne State University

Wayne State University Theses

1-1-2013

Lithogeochemical And Stable Isotope Characteristics Of Bristol And Northern Thorneloe Townships And Its Correlation With Gold Mineralization

Zachary Grant Stevison
Wayne State University,

Follow this and additional works at: http://digitalcommons.wayne.edu/oa_theses

 Part of the Geochemistry Commons, and the Geology Commons

Recommended Citation
Stevison, Zachary Grant, "Lithogeochemical And Stable Isotope Characteristics Of Bristol And Northern Thorneloe Townships And Its Correlation With Gold Mineralization" (2013). *Wayne State University Theses.* Paper 246.

This Open Access Thesis is brought to you for free and open access by DigitalCommons@WayneState. It has been accepted for inclusion in Wayne State University Theses by an authorized administrator of DigitalCommons@WayneState.

Lithogeochemical and Stable Isotope Characteristics of Bristol and Northern Thorneloe Townships and its Correlation with Gold Mineralization

by

Zachary G. Stevison

THESIS

Submitted to the Graduate School

of Wayne State University,

Detroit, Michigan

in partial fulfillment of the requirements

for the degree of

MASTER OF SCIENCE

2013

MAJOR: GEOLOGY

Approved by:

5/3/2013

Advisor Date

DEDICATION

I would like to dedicate this personal and academic accomplishment to my most devoted supporters, Barbara M. Stevison, Brent M. Stevison, and Randy A. Stevison. Each of these individuals supplied necessary personal, spiritual, and financial assistance that made completion of this endeavor possible, aptly expressed in the quote, “The only rock I know that stays steady, the only institution I know that works is the family.” -Lee Iacocca. This project not only furthered my academic understanding of the dynamic and beautiful geological world, but also supplied important lessons of dedication and motivation that can be applied in all aspects of life.

ACKNOWLEDGMENTS

My appreciation and thanks to my graduate advisor Dr. Edmond H.P. van Hees for his support and guidance through the course of this project. His geological knowledge of gold deposition and his intimate experience with the Porcupine Mining Camp made the research project successful. I would also like to acknowledge the field work opportunities organized for me by Dr. van Hees that provided invaluable experience in "real life" geological applications.

West Timmins Mining (now Lake Shore Gold Corporation) provided financial support for the research project and provided access to drill core. Xstrata Copper – Kidd Creek Exploration Division made available historic geochemical data for six townships, including Bristol and Thorneloe Townships, that was incorporated into the research project.

I would like to thank my thesis committee members, Dr. Mark Baskaran and Dr. Jeffrey Howard, for their encouragement and contributions to the completion of this thesis. Their availability and expedient response on critical issues made completion of my graduate studies possible.

Several individuals have assisted in my geological knowledge used during my research project. Each individual provided necessary data, interpretation and/or useful insight related to gold deposition. I want to thank Ann Wilson of the Ontario's Ministry of Northern Development and Mines, Jacques Samson of Lake Shore Gold Corporation, Corey Lambert and Carl Freeman of Wayne State University for generating geochemical data and helping interpret the results as they pertain to this study. Thanks are also due to Wayne Corstorphine and Patrick Hourican, former West Timmins Mining

Corporation consultants, for providing important geological knowledge pertaining to gold deposition in the Porcupine Mining Camp.

Lastly, I would like to acknowledge a close network of friends who provided much appreciated support during my graduate school tenure. Craig Champagne, David Elliott, Joseph Letourneau, William Rose Jr., Jasper Sciuto, and Jason Thomas offered motivation, personal support and at a times a gratuitous roof over my head.

TABLE OF CONTENTS

APPENDICES

LIST OF TABLES

LIST OF FIGURES

Chapter I – Introduction

Geochemical tools have been utilized extensively by the gold mining and exploration industry to identify exploration targets. Major, minor and trace element abundances of country rocks provide information about rock mineralogy and mineral alteration patterns throughout the study area. Quartz vein samples were also analyzed to determine their carbon ($\delta^{13}C$) and oxygen ($\delta^{18}O$) isotopic ratios that are characteristic of the hydrothermal fluids that formed the quartz-carbonate veins.

The area of interest is the Bristol-Thorneloe area located in the Abitibi Greenstone Belt, a prolific base and precious metallogenic province of Canada. The study area is located in the Porcupine Gold Camp fifteen kilometers southwest of the center of the City of Timmins, Ontario. The Porcupine Mining Camp has produced over 75 million ounces of gold since 1909 and is only second in gold production to that of the Kalgoorlie Golden Mile in Western Australia. The Porcupine gold deposits are characterized by mesothermal quartz vein that are enveloped by strong hydrothermal alteration haloes. Most auriferous vein systems in the region occur in close proximity to the Porcupine-Destor Fault Zone, which extends from west of Timmins to the eastern edge of the Abitibi greenstone belt in Quebec, at a distance of approximately 450 km (Fig. 1).

The western extension of the Timmins Mining Camp, including the Bristol-Thorneloe Study Area, has seen extensive exploration for its economic mineral potential during the past decade. In 2008, Lake Shore Gold Corporation began development of their Timmins West Mine that is reported to have an estimated gold reserve of 905,000 ounce (25,637 kg) (Cavey 2006). This new mine represents an opportunity to discover

geochemical indicators that can be used to explore for new gold mineralization on the Lake Shore Gold properties as well as throughout the Porcupine Mining Camp.

The objective of this study is to analyze the lithogeochemical characteristics of the Bristol-Thorneloe Township Study Area rocks and establish their relation to gold mineralization. Determining the nature of country rock alteration and isotopic signature of quartz-carbonate veins that were formed by auriferous hydrothermal fluids, might result in the identification of exploration vectors to gold mineralization. Unique geochemical characteristics of auriferous zones might help to identify new exploration targets or extend known mineralized zones in the Timmins West mine.

1.1 Geologic Setting

The study area (Fig. 1) is located in Bristol and Thorneloe townships in the southwestern end of the Archean age Abitibi Greenstone belt in the Superior Province of the Canadian Shield. These townships are located approximately fifteen kilometers southwest of the center of the Porcupine Gold Camp / City of Timmins, Ontario, around the junction of highways 144 and 101.

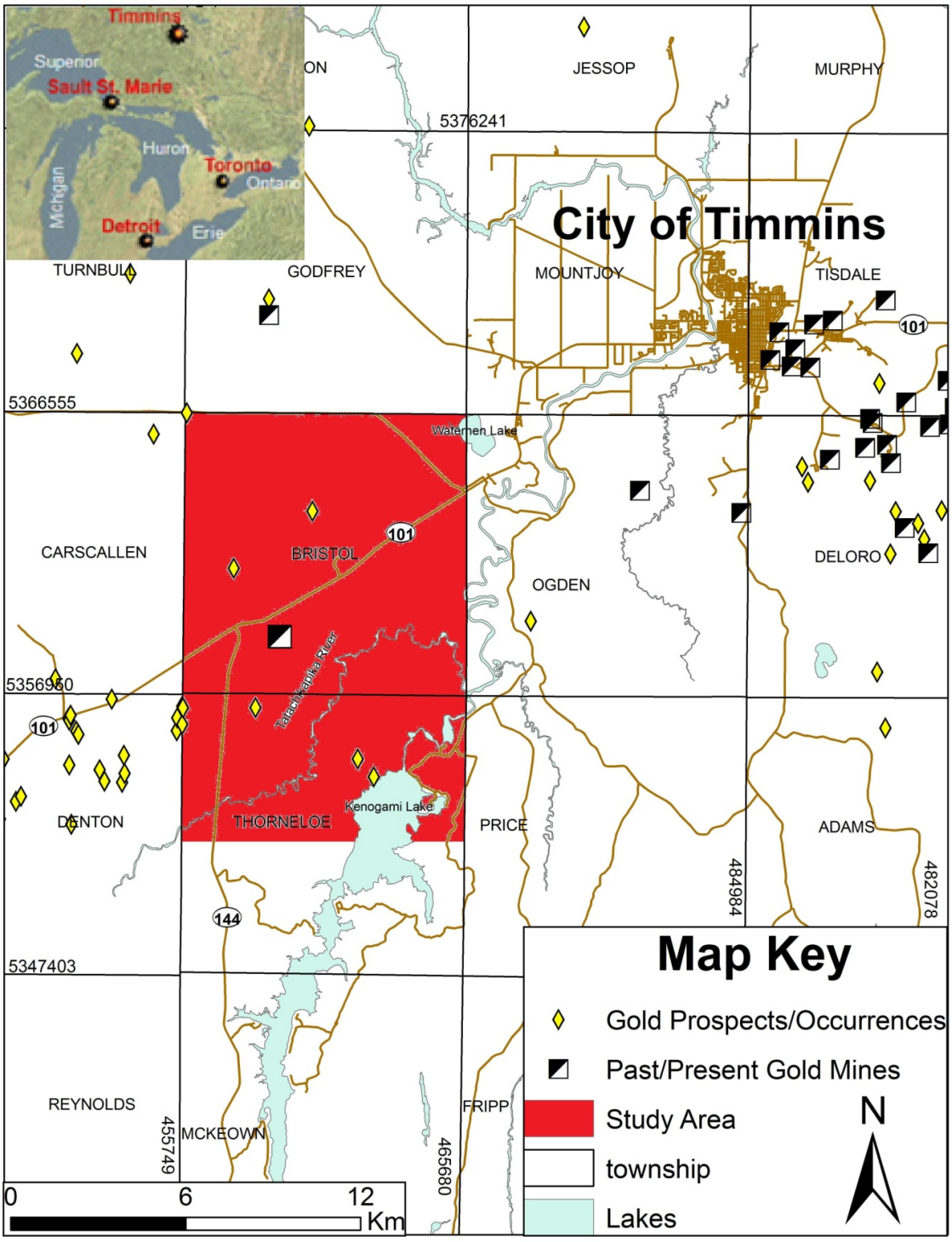

Figure 1 Location of the Bristol-Thorneloe Study Area. Map modified from Ayer et al. 2005

Previous geological mapping in the area was done by Hawley (1926), Ferguson (1957), Pyke (1975, 1980, and 1982), Choudry (1989), Barrie (2000), Vaillancourt (2000), Cavey (2006), and Thurston et al. (2008). Geological units in the study area strike 60° to 70° and dip steeply to near vertical to the southeast. Bristol and northern Thorneloe Township are underlain by the same lithological units (Deloro, Kidd-Munro, Tisdale, Porcupine, and Timiskaming units) that host gold mineralization elsewhere in the Porcupine Camp (Fig. 2). The Destor-Porcupine Fault Zone, an important geologic structure associated with gold mineralization in the Porcupine Camp, also cuts through the study area.

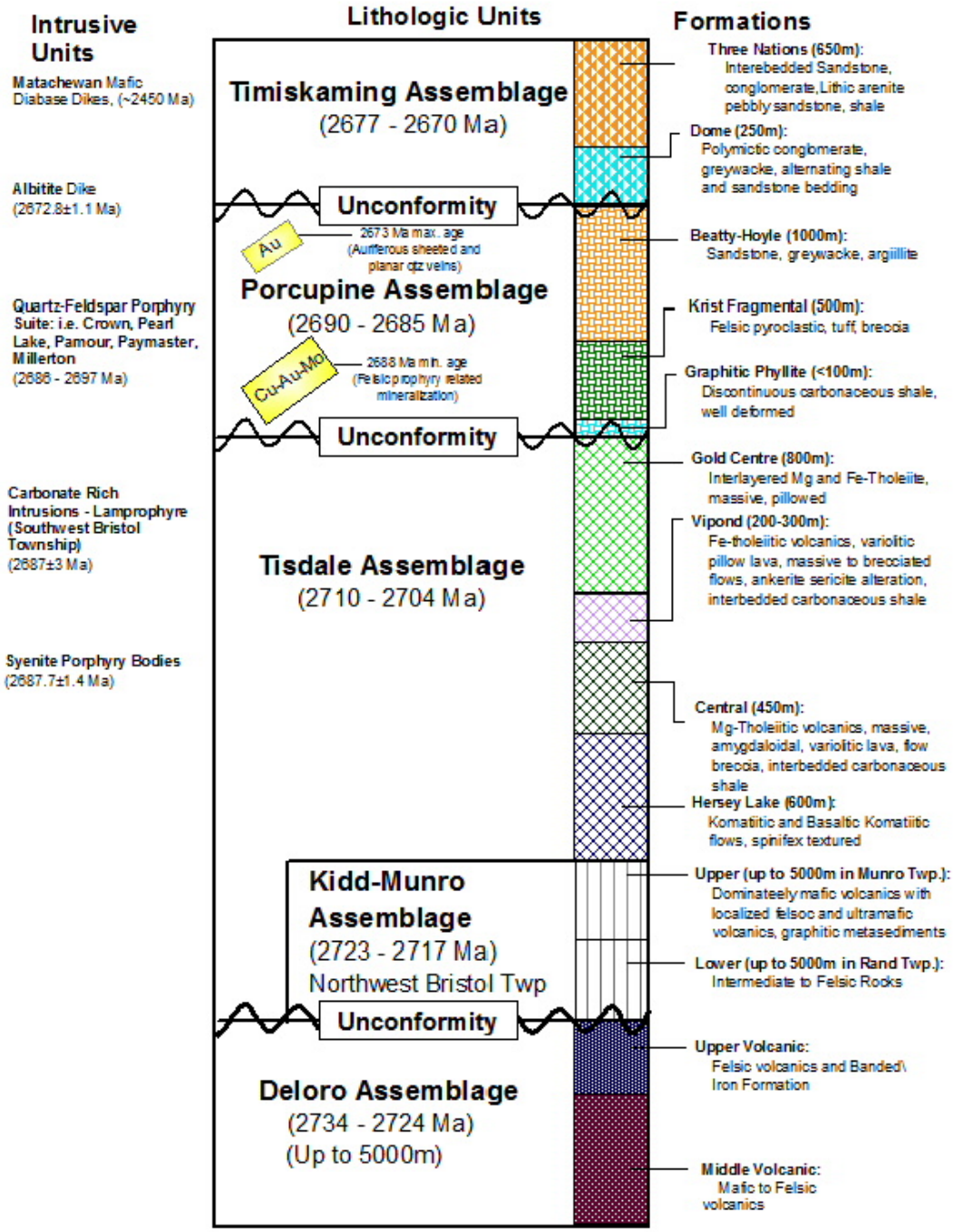

Figure 2 Simplified Stratigraphic section of the Porcupine Mining Camp. Modified from Bateman et al. 2008 and Thurston et al. 2008. Dates were obtained from Corfu et al. 1989, Barrie 2000, Ayer et al. 2005, and MacDonald et al. 2005.

The northwest corner of Bristol Township is underlain by the Kamiskotia Volcanic Complex (KVC), a 2.714 Ga felsic metavolcanic unit of tholeiitic origin (Barrie 2000). The rocks that underlie one third of the study area were mapped by Ferguson (1957) as quartz rhyolite and massive rhyolite. He described the massive rhyolitic bodies as having a cherty texture and being a southward extension of the rock units found to the north and northwest in Godfrey and Turnbull Townships, respectively. These felsic metavolcanic rocks are overlain locally by thin lenses of primitive mafic metavolcanic rocks (Bajc et al. 2001; Barrie, 2000).

Vaillancourt (2000) interpreted the rock units that were mapped in the southwestern third of Bristol Township as belonging to the Upper Kidd-Munro Assemblage and those in the northeast two thirds of the township as belonging to the Upper Blake River Assemblage. Recent geological and geochronology studies in northwestern Bristol Township by Ayer et al (2002, 2005) have subdivided the KVC rocks into the Upper Kidd-Munro and the Upper Blake River assemblages. There are varying opinions on whether the Blake-River Assemblage is part of the rock sequence in Bristol Township. Given the uncertainty of the distribution of rock units, the felsic volcanic rocks in Bristol Township will be treated in this study as a single unit.

A wide band (2 to 3.5 km) of mafic volcanic rocks belonging to the Tisdale Assemblage strikes 60° to 70° across the center of the study area (from southwest to northeast corner Bristol Township). The unit consists predominantly of pillow and amygdaloidal-textured volcanic rocks as well as minor coarse-grained subvolcanic-sills (Ferguson, 1957). Ultramafic komatiite flows, like those found in the Tisdale

Assemblage in the Porcupine Camp, occur interbedded within the mafic unit. The center of Bristol Township is underlain by an agglomerate that contains rhyolitic fragments embedded in a mafic matrix containing dark-green chlorite (Hawley, 1927). Subsequent geological analysis of the area determined them to be mafic-intermediate tholeiitic rocks of the Lower Tisdale Assemblage. The Lower Tisdale group rocks are predominantly of Mg-tholeiitic composition and occur interbedded with carbonaceous shale and ultramafic rocks (Thurston et al. 2008; Bateman et al. 2008).

The southeast corner of the study area is underlain by metasedimentary rocks of the Porcupine Group with polymictic metasedimentary rocks of the Timiskaming Group interbedded locally in the south. The Porcupine rocks include turbiditic argillite, medium- to coarse-grained greywacke, and small amounts of polymictic conglomerates that unconformably overly the Tisdale Assemblage to the north (Cavey, 2006). Pyke (1982) recognized the northwesterly striking contact between the mafic metavolcanic rocks of the Tisdale Assemblage and the Whitney Formation of the Porcupine Group. The Porcupine metasedimentary rocks increase in thickness southeast from the contact and are unconformably overlain by Timiskaming sedimentary rocks at the southern edge of the study area.

The Bristol-Thorneloe study area, like other auriferous areas in the Porcupine Camp, has younger intrusive rocks that crosscut the dominant lithologies. The history of Porcupine Camp intrusive rocks is complex and has been described in detail by Ferguson (1968), Mason and Melnik (1986), Barrie (2000), Bateman et al., (2005), MacDonald et al. (2005), and Finnamore (2008). Their work identified a uniform fine-

grained dark-grey diorite that intrudes the rhyolite exposed in the northwest corner of Bristol Township. Throughout the study area small diorite and gabbro intrusions and dikes, composed primarily of plagioclase and pyroxene, cut the volcanic units (Vaillancourt 2000). Central-eastern Bristol and north-central Thorneloe Townships have large porphyritic felsic intrusions into the sedimentary and mafic tholeiitic band of rocks. These large bodies are characterized by <1-4 mm quartz and feldspar phenocrysts hosted in a matrix that contains biotite (Vaillancourt 2000). There is a 600 meter diameter syenite pluton in southwest Bristol Township that ranges from aphanitic to porphyritic in texture (Vaillancourt, 2000). A suite of lamprophyre dikes unique to the southwestern Superior Province was also identified in western Bristol Township, on the Croxall and Holmer properties (Barrie, 2000). The lamprophyre dikes have three dominant lithologies that grade into each other including: (1) Biotite lamprophyre on the margin; (2) Diopside-rich material, and (3) Garnetite and Garnet-rich feldspathic dikes. Ultramafic peridotite intrusive bodies are found in the southwest corner of the study area, near the contact of the metasedimentary rocks and the base of the Tisdale Assemblage. Some of the peridotite intrusions are located proximal to the Lake Shore Gold Timmins Mine and are associated mineralization elsewhere. The last intrusive event in Bristol and Thorneloe Townships is the emplacement of three different generations of Proterozoic diabase dikes that crosscut all other lithologies. Vaillancourt (2000) grouped these dikes into the northwest trending Paleoproterozoic age Matachewan swarm, east-northeast trending Mesoproterozoic age Abitibi swarm, and west-northwest trending Mesoproterozoic age Sudbury swarm.

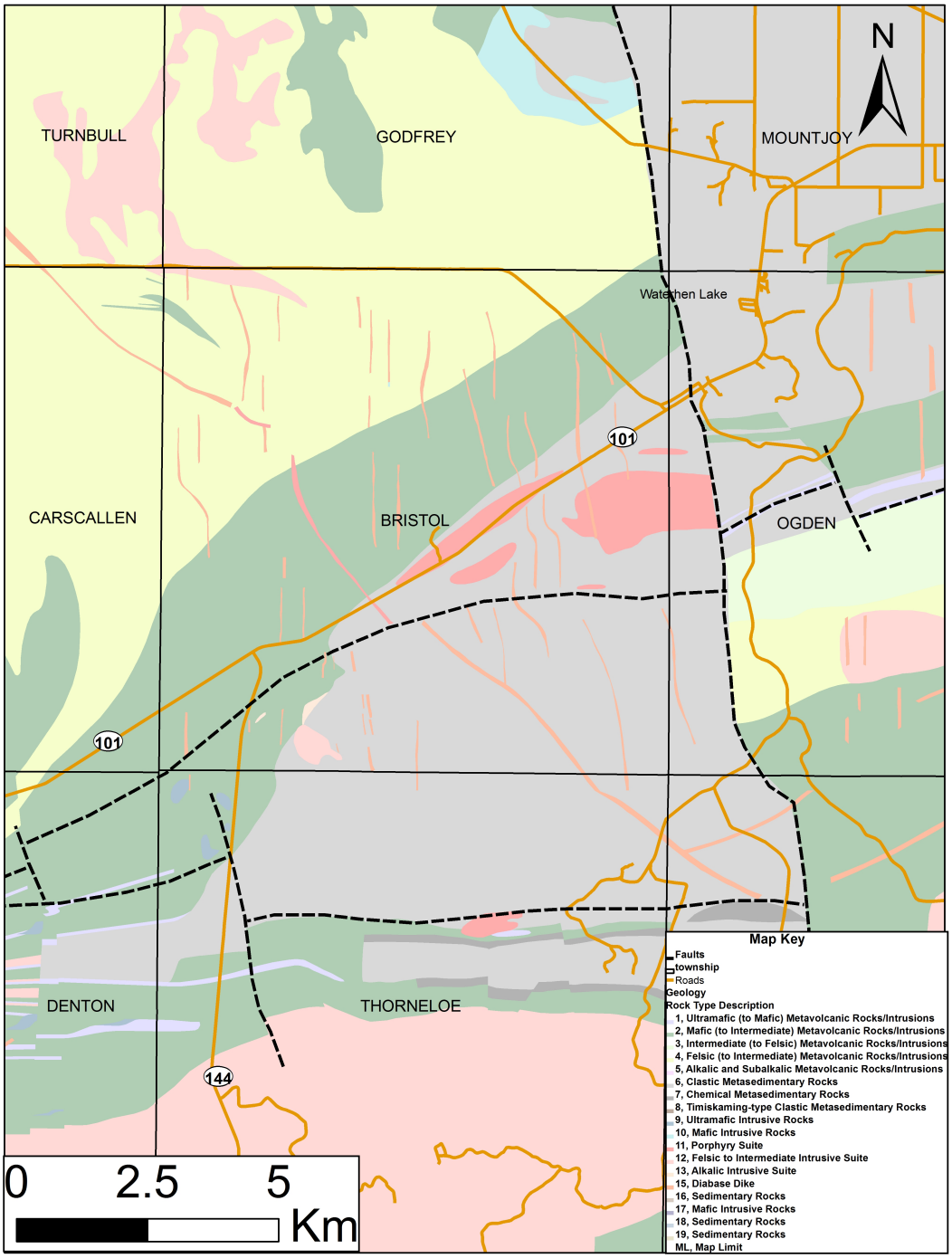

Figure 3 Regional Geological map of the Bristol-Thorneloe Study Area. Modified from Ayer et al. 2005.

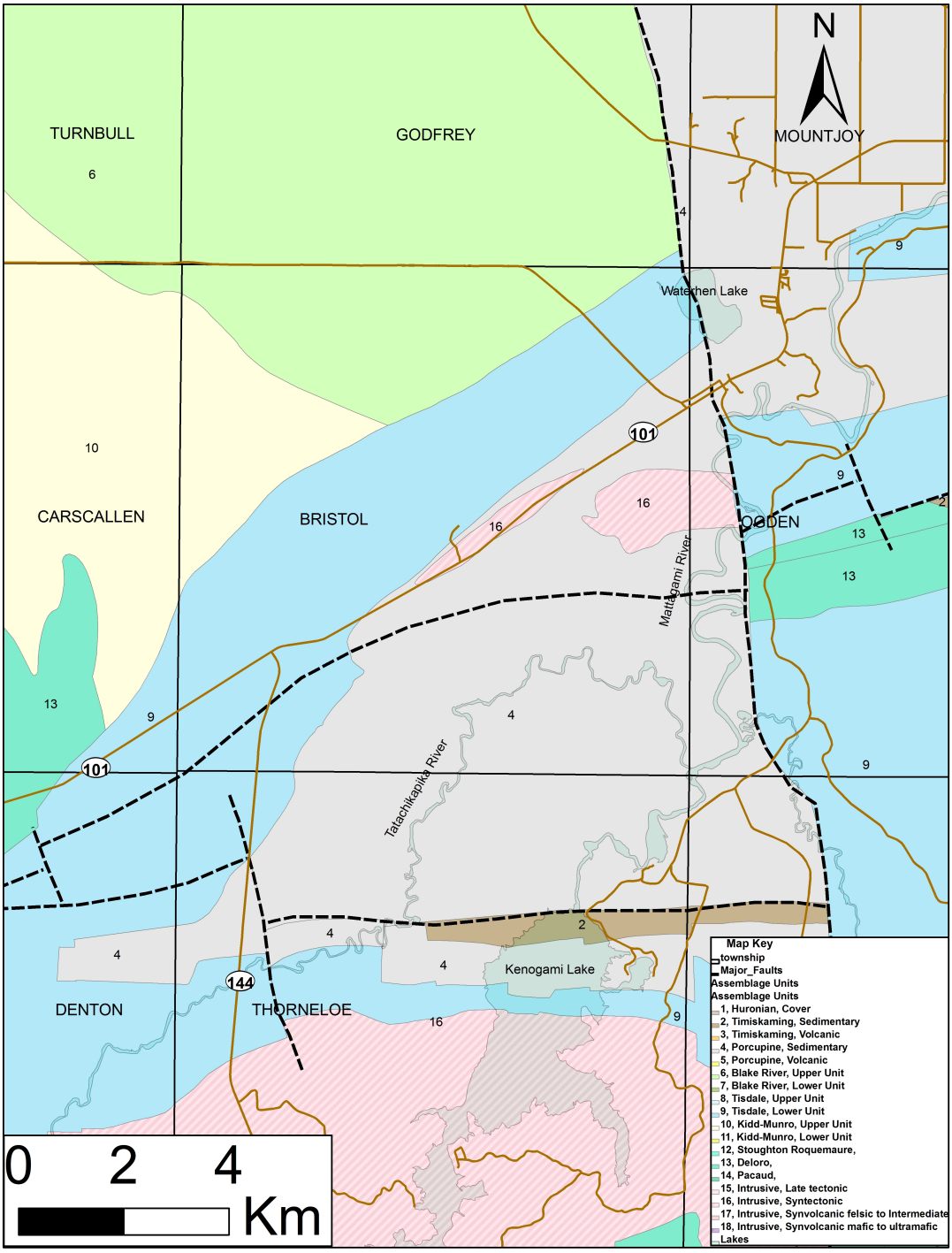

Figure 4 Geological Assemblage map of the Bristol-Thorneloe Study Area. Modified from Ayer et al. 2005.

1.2 Previous Studies

1.2.1 Lithogeochemical Study

The rocks of the Porcupine Mining Camp and surrounding areas have been extensively analyzed using mobile and immobile geochemical constituents and their association with gold mineralization in the camp. The important lithogeochemical studies that can be used to evaluate the Bristol-Thorneloe study area were conducted by Gorman et al. (1981), Davies et al. (1978, 1979, 1982), Kerrich and Hodder (1982), Smith and Kesler (1985), Wood et al. (1986), Barrett and MacLean (1993, 1994, 1995), Melnik-Proud (1997), MacDonald (2005), Dinel et al. (2006, 2008), and Washington et al. (2009). Their results can be used understand the composition and alteration of parent lithologies, as well as extent of various alteration halos.

Preliminary studies by Smith and Kesler (1985) chemically analyzed a suite of mineralized and unmineralized samples in and around the Hollinger-McIntyre Mine, located in the heart of the Porcupine Camp. Their “mineralized” samples were collected within 150 meters of gold-bearing zones. They concluded that alteration zonation around auriferous zones is an important exploration tool, and identified five major assemblages using the dominant minerals. They describe a pervasive regional greenschist alteration (Assemblage I), that was interpreted to be the background alteration throughout the Porcupine Camp, and increases in intensity to quartz-albite-ankerite-sericite alteration (Assemblage IV) directly related to “ore grade mineralization.” Along with these mineral alteration zones they found enrichment of Barium (Ba) that increased from a background on ~200 ppm to over 400 ppm near auriferous zones.

These mineral alteration and Ba enrichment zones exist both vertically and laterally around the gold mineralization.

A study by Davies et al. (1982) explored the chemical / mineralogical variations in carbonate alteration halos in known auriferous zones. They employed a CO_2/CaO molar ratio that distinguished the dominant carbonate mineral in a given area. This ratio is a normative calculation that identifies the dominant carbonate mineral species. Molar ratio values of <1 indicate the presence of Ca-silicate minerals, values of 1 indicate the presence of calcite, values of 2 correspond with dolomite/ankerite, values between 2 and 3 indicates a mixture dolomite-ankerite-siderite-magnesite (Davies et al. 1982). Davies et al. (1982) proposed that CO_2/CaO values greater or equal to 1.5 are associated with gold mineralization and can be used as a geochemical vector for gold exploration.

Understanding the host rock and how alteration affects the composition from its original composition is essential during a lithogeochemical study. Barrett and MacLean (1993) used immobile elements in the volcanic rocks to discern the character of the original host rock. They employed the immobile constituents aluminum (Al), titanium (Ti), yttrium (Y), zirconium (Zr), and niobium (Nb) to characterize the chemical composition of the igneous suite. MacLean and Barrett (1993) used Zr/Y ratios to distinguish tholeiitic from calc-alkaline suites. They use ratios that range from ~3 to 5 for tholeiites, and those ranging from ~7 to 30 to recognize calc-alkaline units (Barrett and MacLean 1993). Identifying alteration zones and their extent around mineral deposits is an important exploration tool and can be achieved by using ratios of mobile and

immobile elements. Barrett and MacLean (1993) used the intersection of alteration and fractionation lines of immobile compatible –incompatible element pairs. Knowing the original (unaltered) concentration of elements in individual magmatic rock units, the type and relative strength of metasomatic alteration can be characterized by the depletion or enrichment of these elements. When the concentration increases along the alteration line toward the origin, it is attributed to depletion of the elements associated with mass gain and away from the origin is attributed to the concentration of elements caused by mass loss (Barrett and Maclean 1993).

The Hollinger-McIntyre-Coniaurum (HMC) mine complex is located northeast and along strike of the Bristol-Thorneloe study area. The HMC has been subjected to lithogeochemical studies by Davies and Luhta (1978), Melnik-Proud (1997), and Washington et al. (2009). The preliminary work by Luhta and Davies (1978) identified alteration elemental zonation. They discovered high Na_2O, MgO, and Fe_2O_3, in the peripheral albite zone and an abrupt increase in the K_2O and CaO content associated with the sericite-rich core of the McIntyre porphyry copper deposit (Davies and Luhta 1978). The addition of K_2O and removal of Na_2O were assumed to be caused by movement of fluid from high to low pressure, where changes in acidity and varying stabilization of oxides in solution would result in mineralogic/chemical alteration halo. The localized low pressure dilation zones appeared to be controlled by structural components associated with movement along the Hollinger fault (Davies and Luhta 1978). Melnik-Proud (1997) expanded on previous alteration studies and argued that the albitite dikes and related mineralizing fluids generated the albite alteration halos found around auriferous veining

at the HMC deposit. She also found that the HMC deposit relies on a brecciated porphyry as a porous medium for the movement of hydrothermal fluids (Melnik-Proud 1997). Washington (2009) continued the research at the HMC deposit by employing lithogeochemical contouring along a cross section in the mine and that allowed for interpretation of changes across lithological and structural formations. Washington was able to argue that the HMC deposit is a product of two separate mineralizing fluids that traveled through different structures before deposition (Washington 2008; Washington et al. 2009). Evidence to support the conclusions involved two distinct lithogeochemical alteration patterns and corresponding oxygen isotope and fluid inclusion differences (Washington 2008; Washington et al. 2009).

Analysis of the Hoyle Pond Mine by Dinel et al (2008) identified elemental anomalies associated with gold-bearing veins and the lithological host units. His discoveries at the Hoyle Pond Mine might be relevant to the Bristol-Thorneloe study area because it has similar geological setting and location relative to DPFZ. The immobile elements were diluted because of massive influx of hydrothermal elements Na_2O, K_2O, Cr_2O_3, Rb, CaO, Eu, FeO, and MgO. Magnesium tholeiites have the greatest enrichment in mobile elements adjacent hydrothermal veining (Dinel et al. 2008b). Magnesium tholeiites typically have chromium contents of 150 to 250 ppm that are characteristic of oceanic crust, and can reach concentrations of up to 1200 ppm in close proximity to auriferous quartz-carbonate veining. These localized enrichments were interpreted not to be related to their igneous origin because nickel and magnesium values did not follow the same trend (Dinel et al. 2008b). Dinel et al. (2008) argued that

the immobile Cr^{3+} was oxidized to mobile Cr^{6+} by higher pressure fluids of approximately 350°C (Dinel et al. 2008b). The mobile Cr was deposited by decreasing fluid temperatures and reaction with reducing agents such as Fe (II), Fe-sulfides, thiols, hydrogen sulfides, and organic matter available in the wall rock (Dinel et al. 2008b).

1.2.2 Stable Isotopes

Stable isotope analysis of carbonate, quartz and tourmaline samples collected from the Bristol-Thorneloe Study area can be interpreted using results obtained from other locations in the Porcupine Camp and other mining districts. Stable isotope studies were done in the Porcupine camp by Woods (1986), Fyon (1986), Kerrich and Hodder (1982), Gorman et al. (1981), van Hees (1993), and Washington (2008). These researchers obtained and analyzed $\delta^{18}O$ and $\delta^{13}C$ data and were able to establish the temperatures and origin of paleo-fluids, and the characteristic range of oxygen isotope values for barren and mineralized vein systems in the area.

Kerrich and Hodder (1982) established the range of $\delta^{18}O$ values in auriferous veins and estimated hydrothermal fluid temperatures in and around the Porcupine Mining Camp using $\delta^{18}O$ values obtained from vein quartz and carbonate. Their study estimated fluid temperatures for gold-bearing systems to be 320-480°C with $\delta^{18}O$ values in the 11 to 15‰ range. At the Dome Mine, quartz has a $\delta^{18}O$ range of 14-15.2‰ (Kerrich and Hodder 1982). They concluded that auriferous hydrothermal fluids in the Porcupine Camp were produced by prograde metamorphism related to increased temperatures caused by the progressive accumulation of volcanic sequences rather than magmatic fluids. The temperature buildup caused both the dehydration and

released CO_2 from the rocks generating auriferous metamorphic hydrothermal fluid that form the gold-rich veins (Kerrich and Hodder 1982).

Isotopic studies by Woods et al., (1986) of the HMC concluded that the mineralizing fluids in this deposit had a lower temperature and different fluid source. Their study determined the $\delta^{18}O$ and $\delta^{13}C$ values of the mineralizing fluid that formed the HMC deposit were derived from a magmatic source with temperatures that range between 270 to 300°C. Some $\delta^{18}O$ values overlapped with the lower limit of the metamorphic field that they concluded was caused by wall rock interaction. The $\delta^{13}C$ values obtained are inconclusive and can be attributed to both a metamorphic and magmatic source.

Further work done at the HMC deposit by Washington (2008), Washington et al., (2009) determined that multiple fluids were involved in its formation. The $\delta^{18}O$ isotopic values are different in the Au-Cu and Au mineralized sections of the mine, where calculate fluid values are ~12‰ and ~4‰, respectively (Washington et al. 2008). The different episodes of gold mineralization were assumed to have been emplaced at different stages of regional rock deformation. The authors were also able to relate the mineralizing fluids to episodes of regional deformation and thereby assign relative times of gold deposition. The Au-Cu fluid predates the Au fluid and assumed to have been deposited during regional D2 deformation to early regional D3 tectonic events. This event was followed by the Au mineralizing fluid migration along the Hollinger Shear Zone (HSZ) during the D3 structural deformation episode in the Porcupine Camp. The deformation episodes are described in detail in Ayer et al. (2005).

1.2.3 Stratigraphy

The preliminary stratigraphic lithologies of the Bristol-Thorneloe study within the Porcupine Mining Camp were largely based on the work performed by Burrows (1915, 1924), Hawley (1926), Harding and Berry (1939), Ferguson (1957 and 1959), Pyke (1972, 1973, 1975,1978a, 1980, and 1982), and Choudhry (1982 and 1989). Initial fieldwork completed in the study area by Hawley (1926) and Ferguson (1957 and 1959) provides detailed descriptions of the rock units but does not link them to the stratigraphic assemblages of the Porcupine Mining Camp. Pyke's work (1982), in and around the Porcupine Camp, identified two Supergroups that he named the Lower Deloro Supergroup and Upper Tisdale Supergroup. With increased exploration and mining activity in the camp, further studies by Barrie (1992), Vaillancourt (2000), Barrie (2000), Hall (2001, 2002), Bateman et al. (2005), MacDonald et al. (2005), Thurston et al. (2005), and Barr et al. (2007) provided more accurate geological information for the Bristol-Thorneloe study area at the western end of the Porcupine Mining Camp.

The stratigraphic column in Bristol-Thorneloe Township study area is presented in Figure 2. Deloro Assemblage rocks occur at the base of the stratigraphic sequence and have U/Pb zircon ages of 2734 to 2724 Ma. The Deloro Assemblage is overlain by felsic metavolcanic rocks of the Kidd-Munro Assemblage and have ages of 2717 to 2712 Ma (Ayer et al. 2005b; Thurston et al. 2008). This assemblage was superseded by tholeiitic basalts of the Lower Tisdale assemblage that has U/Pb zircon ages of 2710-2706 Ma (Thurston et al. 2008). These volcanic units are dominantly overlain by turbiditic metasedimentary units of the Porcupine Assemblage and minor overlying polymicitic

conglomerates of the Timiskaming Assemblage at southeastern end of the study area (Vaillancourt, 2000). The sedimentary rock units have U/Pb minimum ages of 2690 to 2685 Ma and 2677 to 2670 Ma, respectively (Ayer et al. 2005b).

Multiple generations of intrusions crosscut the metavolcanic rock units of Bristol and northern Thorneloe Townships. A number of different quartz-feldspar porphyry bodies occur in the Porcupine Camp that have ages ranging from 2687 to 2691 Ma and indicate that they are a genetically equivalent to the metavolcanic units found in the study area (Corfu et al. 1989; Dinel et al. 2008b; Vaillancourt, 2000). The felsic intrusive rock units were subdivided into five separate trends allowing for classification of each using their genetic, geochemical, and geochronology signature (MacDonald et al. 2005). West trending ellipse-shaped syenite bodies, that have a U/Pb age of 2687.7 ± 1.4 Ma, occur around Bristol Lake, Thunder Creek and the southwest corner of Bristol Township. Vaillancourt (2000) also recognized a carbonate-rich ultramafic intrusive body, but it requires additional work to fully characterize the rock type and its affiliation (Vaillancourt, 2000). This intrusive body has been assigned a tentative age of 2687±3 Ma (Barrie 2000). Lastly, three swarms of diabase dikes that crosscut all lithologies in the study area belong to the Matachewan (Paleoproterozoic age), Abitibi (Mesoproterozoic), and Sudbury (Mesoproterozoic) dike swarms. The oldest Matachewan dikes have age U/Pb ages of ~2641±2 Ma (Heaman 1988).

Mineralization in the Porcupine camp was described by Gray and Hutchinson (2001). They suggest that gold deposition in the area consists of broad episodes that they described as: 1) An early period of gold deposition that occurred prior to the

development of the Timiskaming unconformity surface, 2) An epigenetic Cu-Au-Mo event that was contemporaneous with felsic magmatic activity, and 3) An economically important gold-vein forming event that postdates felsic magmatic activity, porphyry emplacement, and Timiskaming sedimentation (Gray and Hutchinson 2001). The authors also correlated petrological, geochemical, and field observations from around the Porcupine camp with U/Pb isotopic dating in order to establish an approximate age for these three gold depositing episodes. The pre-Timiskaming mineralization in the Pamour conglomerate is assumed to have a minimum U/Pb age of 2679 ± 4 Ma. The epigenetic Cu-Au-Mo event was inferred to have taken place after 2688 ± 2 Ma and before albitite dike emplacement at 2673 $\pm^{6}_{2}$ Ma, because of its close association with quartz-feldspar porphyry magmatic activity. The economically most important gold veining episode was assigned a maximum age of 2673 $\pm^{6}_{2}$ Ma, because it crosscuts the albitite dikes in the McIntyre deposit (Gray and Hutchinson 2001)

1.2.4 Structural Formation

The complex structural formations of the Porcupine Camp are spatially related to economic mineralization in the area. The earliest structural geology interpretation of the Bristol-Thorneloe study area were performed by Hawley (1926), Ferguson (1957), and Choudry (1989), and those of the Porcupine camp were done by Dunbar (1948), Hogg (1950), Ferguson (1968), and Pyke (1982). The Porcupine camp is associated with the Destor-Porcupine Fault Zone (DPFZ), a major east-west shear zone that has a minimum width of 150 meters and extends approximately 440 kilometers (Pyke, 1982) and passes to the south of the mineralized portion of the camp. Ferguson (1968) was

the first to analyze this structure and associate it with the vein structures of the Porcupine Camp. The DPFZ is described as a normal fault with the south side moving up and north side down (Pyke 1982). This structure also has a sinistral strike-slip movement determined by the position and symmetry of the Porcupine Syncline and Whitney Anticline (Pyke 1982). Pyke also found a close association between ultramafic volcanism, sedimentation and the DPFZ, in the southwest portion of the Bristol-Thorneloe study area. Benn et al. (2001) and Bateman (2008) also discuss multiple episodes of deformation associated with the PDFZ. They describe the rocks in the area as having been deformed by four possible episodes but that they are not found uniformly throughout the camp (Benn et al. 2001; Bateman et al. 2008).These recent structural studies are important because they permit individual gold deposits in the Porcupine region to be assigned to specific deformation events.

1.2.5 Metamorphic Studies

The metamorphic and alteration characteristics of the Western Abitibi Greeenstone Belt, Porcupine Camp and Bristol-Thorneloe study area, were originally described by Jolly (1978). He described regional-scale metamorphic facies found in the metavolcanic rocks and labeled them as metamorphic zones 1 through 5 that have increasing metamorphic grade and a characteristic mineral assemblage (Jolly 1978).

Jolly's work provided valuable regional information but is not useful on a township or mineral deposit scale. Thompson (2002 and 2005) studied the metamorphic variation using minimally altered samples collected throughout the Timmins-Kirkland Lake area. Using characteristic mineral assemblages and index minerals for each lithological unit,

he identified five zones of metamorphism in the Timmins Mining Camp and labeled them the Amphibolite, Transition, Upper Greenschist, Lower Greenschist, and Sub-Greenschist Isograd Zones (Thompson 2005). Locations with higher grade metamorphic isograds were frequently found to be spatially associated with known past and current gold producers. The zones are thought to have been caused by igneous bodies intruding relatively close to the surface into rocks with temperatures of 100°C or lower (Thompson, 2005). Steep temperature gradients caused the small localized amphibolite and transition isograds (Thompson 2005). He proposed that areas containing higher grade metamorphic zones and structurally complex zones, would make ideal exploration targets.

Thompson's study mapped zones of higher metamorphic grade in the Bristol-Thorneloe study area. These zones are located in close proximity with known gold mineralized prospects along DPFZ and north-south fault structures. Northwest Thorneloe and southwest Bristol Townships have a transition isograd that envelops current gold exploration targets, and occurs less than 1.5 km from the Lake Shore Gold Timmins Mine (Fig. 5).

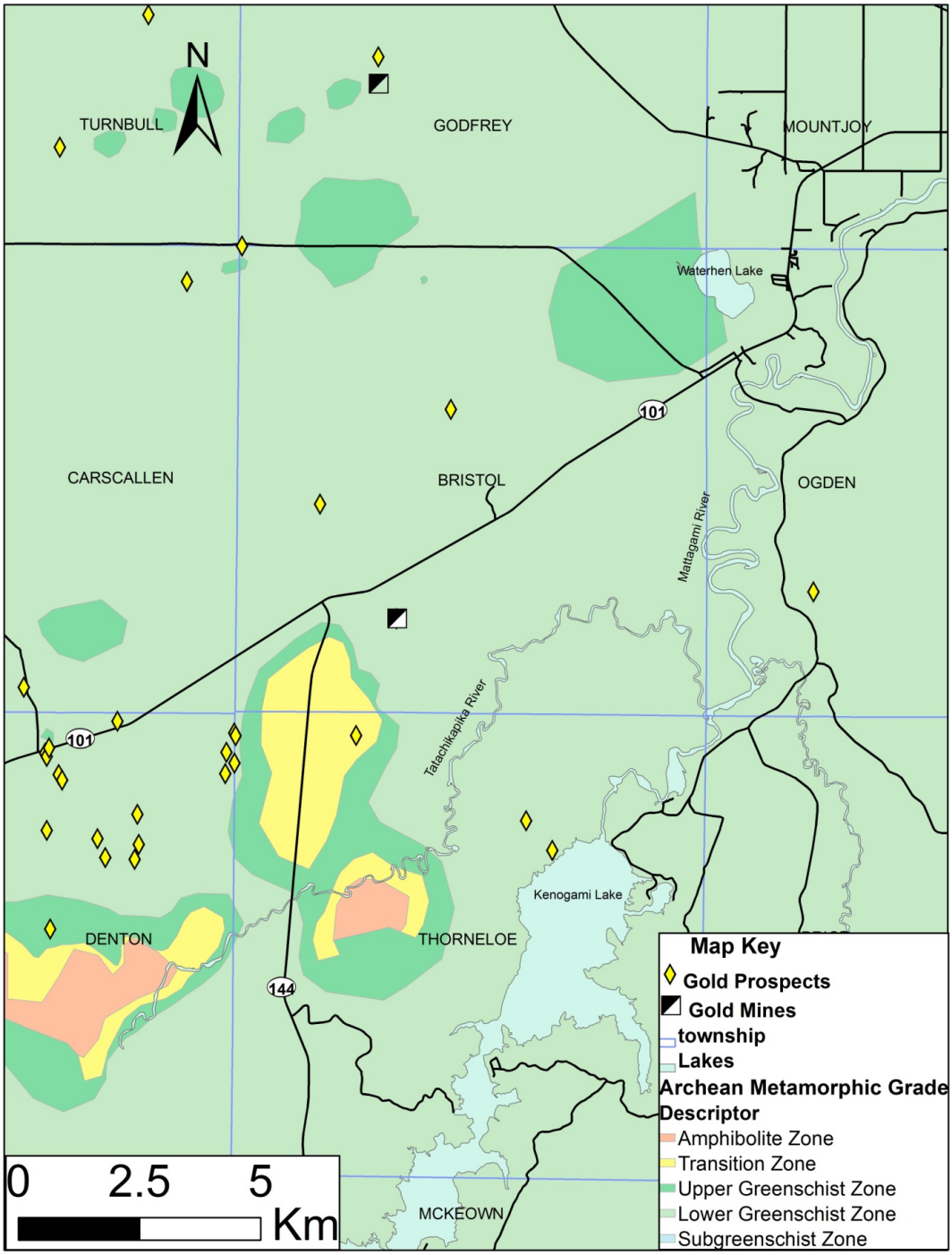

Figure 5 Regional metamorphic grade map of Bristol-Thorneloe Township. Modified from Thompson 2005 and Ayer et al. 2005.

The goal of this study is to gain understanding of the fluid history by identifying alteration zones, relative intensity and specific geochemical characteristics associated with the local gold deposition. By analyzing the $\delta^{18}O$ and $\delta^{13}C$ of quartz-carbonate vein and whole rock geochemical (major, minor, and trace elements) data of host/country rocks a geochemical signature might be determined to assist in local exploration and mining efforts. Finding zones of strong hydrothermal alteration that are accompanied by geochemical characteristics similar to gold mineralized prospects and deposits might extend the deposit at Lake Shore Gold Timmins West Mine or find new exploration target(s) in the study area. Lastly, the multiple elements analyzed of the country rocks might uncover a new hydrothermally mobile element or an anomaly that might be useful to identify potential exploration targets. Towards this goal, 178 wall rock samples were collected and Al_2O_3, CaO, K_2O, MgO, MnO, Na_2O, P_2O5, TiO_2, Y, CO_2, and LOI (Loss on Ignition), and a suite of elemental concentrations that include Sc, Sr, Zr, Ag, Au, Ba, Cu, Ni, Pb, Zn, and Cr data were obtained. Combining the data obtained in this study with that of other studies (e.g. Xstrata Copper - Kidd Creek Exploration data), the variations of these elements have been evaluated. Sixty four (64) quartz-carbonate vein samples have been analyzed for their carbon ($\delta^{13}C$) and oxygen ($\delta^{18}O$) isotopic composition. Five tourmaline samples were also collected from veining in the West Timmins mine and Allerston property for potential use as a hydrothermal fluid thermometer. The outcome of this study might generate results that are relevant to identification of gold exploration targets.

Chapter 2 Analytical Methodology

This study of Bristol and Thorneloe townships was conducted to determine the lithogeochemical characteristics associated with gold deposition in the area using stable isotope and whole rock lithogeochemical data obtained by analyzing rock and veins collected from archived drill core in the MDNM core library in Timmins and surface samples collected in areas where there was inadequate drill core coverage. . Analytical results obtained, along with data acquired from published sources and Xstrata Copper – Kidd Creek Exploration were plotted and contoured using ArcGIS©. Information obtained from drill holes was projected to surface throughout the study area before interpretation of the data. ArcGIS© contoured data plots were superimposed on geological base maps obtained from the Ontario Geological Survey and a geological map created by Lake Shore Gold for their property.

2.1 Whole Rock Lithogeochemical Analysis

The chemical composition of the major, minor and trace elements contained in rock samples collected in the Bristol-Thorneloe study area were determined at Wayne State University, obtained from data published by the Ontario Geological Survey and Xstrata Copper - Kidd Creek Exploration Division. The carbonate analysis was completed at Oakland University. Each analysis was performed on a representative sample obtained by pulverizing the rock to a fine-grained homogenous pulp. Methods used to determine the composition of rock samples collected from the study area are described below.

The major, minor and trace elements were determined at Wayne State University using an ICP-OES (Inductively Couple Plasma Optical Emission Spectrometer). The

samples were prepared by measuring out exactly 200 mg of the homogenized sample pulp and combining it with 600mg $LiBO_2$ (Lithium Metaborate) and small amount of LiBr (Lithium Bromide) in a platinum crucible. The crucible is then placed in oven heated to approximately 1100°C to produce a molten homogenous bead. The bead is dissolved in a Teflon beaker containing trace metal grade 10% Nitric acid (HNO_3) at approximately 70°C, then diluted to 100mL with distilled de-ionized water. The solution produced is used to measure the minor and trace element concentrations using the ICP-OES. The major element analysis is measured using a 20% diluted solution. The sample solutions are aspirated into the ICP-OES where the plasma ionizes the solution producing photons. The presence and concentration of an element is determined using the strength of a characteristic light wavelength emitted by the plasma compared to that of a series of standards with different concentrations for each element. Quality control during analysis was done using known standard solutions developed from high purity elemental concentrates. Standard samples were placed in the sample series after every 10 test samples. The results were also compared against BIR-1 (U.S. Geological Survey's Icelandic Basalt) that underwent identical sample preparation as test samples. Lastly, "blank" DDI (distilled de-ionized) water samples were used after 5 consecutive test samples.

2.2 Carbonate Analysis

The carbonate content of the rock samples was measured at Oakland University using Tekmar Dohrmann solids analyzer connected to Tekmar Dohrmann Pheonix with infrared detection. Each of the 178 rock samples were analyzed using 5-10 mg of

homogenous rock pulp. The sample is placed in a furnace heated to 1,000°C and the carbonate driven off and recorded as Total Carbon (in ppm). The organic carbon content of the samples was not measured because it is unlikely to occur in the Archean Age igneous and highly altered rocks of the study. The Total Carbon recorded is related directly to carbonate mineralization that occurs in the altered country rocks found in the study area. Davies et al. (1982) CO_2/CaO calculation was used to establish the type of carbonate alteration present in the Porcupine Mining Camp. Accuracy of results was based on calibration with known standards to develop a calibration curve. During analysis of the samples duplicates were run every five samples, and a standard run every ten samples to verify the accuracy of the calibration curve. This method identified any deviation in the instrument output and quantified the extent to which results needed to be corrected.

2.3 Gold Analysis

Actlabs located in Ancaster, Ontario performed the gold analyses of 164 samples using the Fire Assay Method with an Atomic Absorption finish (Hoffman et al. 1998). The 1A2--50 method provides a 5 ppb detection limit. A 30 g sample of the rock was crushed and pulverized to a homogenous pulp before submitting them to Actlabs for assaying. The pulp is mixed with various fire assay fluxes (borax, soda ash, silica, and litharge) and a silver (Ag) collecting agent in a clay crucible. The crucible is placed in a furnace and subjected to 60-minute incremental increase in temperature to fuse the mixture. The temperature of the furnace is first brought up to 850°C followed by an intermediate 950°C, and then finished at 1,060°C. The crucible is then removed from

the furnace the molten mixture poured into a mold to cool. The lighter slag is removed leaving a lead button. The lead button is placed on a bone-ash cupel and heated to 950°C in a furnace. The cupel absorbs the lead leaving behind an Ag doré bead that contains any Au present. The doré bead is then dissolved with Agua Regia (1:3 ratio nitric and hydrochloric acid) and the gold content analyzed using AA (Atomic Absorption). This method determines the elemental concentration of gold by ionizing the sample in solution and each element absorbs light at a characteristic wavelength. The absorption is recorded by the reduction of light intensity at each characteristic wavelength and correlates directly with elemental concentration (Hoffman et al. Hoffman 1998).

2.4 Stable Isotope Analysis

The $\delta^{13}C$ and $\delta^{18}O$ isotope values for the stable isotope study were determined on quartz-carbonate vein samples collected from drill core and outcrop in the study area. The samples were prepared by separating pure carbonate from the quartz vein and then manually pulverized it using a dedicated mortar and pestle. The samples were sent to Isotope Tracer Technologies Inc., in Waterloo, Ontario for analysis. They placed a 4 mg sample in a vial from which air is purged using helium and then it is quickly capped with a silicon/Teflon cap. The sample vials and the 103% phosphoric acid (H_3PO_4) that was used to liberate the CO_2 from the carbonate are heated in an oven to 50°C. A 1 mL aliquot of the phosphoric acid is injected into each sample vial through the septum cap using a small syringe. Following injection of the acid, the vials were put back in the oven

for 24 hours. This heating time is required to ensure that all carbonates types (calcite, dolomite, ankerite, and siderite) are fully digested and CO_2 is completely liberated.

The final stage of analysis involves the liberated CO_2 being measured using a mass spectrometer. Each sample was quickly removed from the oven and injected into the mass spectrometer to ensure that the CO_2 did not cool before analysis and cause a shift in the isotopic value.

2.5 Quartz-Tourmaline Thermometry

The temperature of the hydrothermal fluids in the study area was determined using five quartz-tourmaline sample pairs. This method utilizes the $\delta^{18}O/^{16}O$ values measured on quartz and tourmaline mineral pairs found in each vein sample.

The thermometry analysis was done using four available tourmaline- quartz drill core samples and one rock sample collected in the study area. Pure tourmaline and quartz samples are necessary to produce accurate oxygen isotope results. Tourmaline grains were first manually extracted and pulverized from the drill core samples. The remaining massive quartz was removed and pulverized. Both quartz and tourmaline pulps were placed in a magnetic separator to separate the minerals. Following mechanical separation the tourmaline samples were placed in a Teflon beaker and treated with 50% hydrofluoric acid (HF) and heated to 40-60°C. They were allowed to rest in the HF acid for 4 hours to dissolve any remaining quartz as well as carbonate and sulfide mineralization. The HF acid solution was decanted from the beakers and the tourmaline was rinsed using methanol to remove any remaining HF from the beaker. The quartz samples were treated with Aqua Regia (50:50, nitric and hydrochloric acid) to dissolve

any carbonate and sulfide minerals in the quartz matrix. All samples were dried and placed in vials. They were sent to Queens University in Kingston, Ontario for oxygen isotope analysis. Oxygen was liberated from the minerals using a silicate line in which they were combined with BrF_5 and reacted at 500°C. The oxygen was converted to CO_2 using a carbon rod heated to 1,000°C and then transferred to a mass spectrometer to measure its $\delta^{18}O/^{16}O$ values.

The $\delta^{18}O/^{16}O$ values for the five samples were interpreted using the research results of Blamart (1991). His work established that quartz-tourmaline oxygen fractionation varies with temperature and can therefore be used as a thermometer. This method was determined empirically by establishing isotopic fractionation signatures verified using microthermometric quartz fluid inclusion and quartz-biotite vs. quartz-muscovite thermometric methods (Blamart, 1991). Using his results, Blamart developed the formula $\sqrt{\frac{2.23*10^6}{\Delta\delta_{qtz-tour}^{18}O+1.07}}$ - 273.15 to predict the temperatures of fluids that co-precipitated the quartz and tourmaline. His method has an error of ± 50°C when compared to other thermometry methods (Blamart, 1991).

2.6 GIS Geostatistical Map Analysis

2.6.1 Establishing Sample Locations

The quartz and rock samples used in the study were collected from the Ontario Ministry of Northern Development and Mines drill core library in Timmins, Ontario, drill core belonging to West Timmins Mining, Lake Shore Gold, several other junior mining companies, and samples collected by the author from outcrop in Bristol and Northern

Thorneloe Townships. The samples were collected during the summer of 2008 through to the fall of 2010 because new exploration core became available during that time. The location of each sample was recorded in Universal Transverse Mercator (UTM) coordinates to simplify plotting of the data. The elevations (depth), bearing and dip of the holes were taken into account so that the lithogeochemical data projected properly to surface. Locations of the archived drill core were all converted to the North American Datum 83 (NAD83 – Zone 17N) format and accuracy of the information verified using assessment files for each hole. The geochemical data provided by the exploration / mining companies was accompanied by the collar co-ordinates for each diamond drill hole. The location of rock samples collected from outcrops and some drill holes lacking collar information were obtained using a handheld Global Positioning Satellite (GPS) unit. These systems provided easting and northing UTM coordinates with a ±3m error in accuracy. The rock and quartz vein sample co-ordinates were recorded in separate spreadsheets and plotted using ArcMap© Geographic Information System (GIS).

All samples were plotted with map layers obtained from the 2005 Digital Compilation that accompanies the Discover Abitibi Initiative study, a collaborative multifaceted geologic effort (MRD 186). The digital information is available in map layers that are formatted for ArcGIS© applications. The geological layers of the rock units and assemblages in the study area were generated using mapping efforts conducted by Ferguson (1957), Pyke (1982) and later updated by Vaillancourt (2000).

2.6.2 Surface Geology Map Preparation

The geological base map for the study was obtained from the Ontario Geological Survey (OGS) 2005 Discover Abitibi Initiative. Miscellaneous Release - Data 186 contains digital data for the entire Abitibi Greenstone Belt and subfile, Miscellaneous Release – Data 155, that focuses on the Timmins-Kirkland Lake region. This file supplied the geological interpretation of the study area, various map overlays of gold-bearing zones, road, infrastructure, surface water features, township boundaries, and assemblage maps (Ayer 2005a). The map covers the entire Bristol-Thorneloe Township study area. The rock unit code used is that of the Ontario Geological Survey and is used throughout the Abitibi Greenstone Belt.

A smaller scale geological map of the Timmins Mine Property was supplied by Lake Shore Gold Corporation and provided their interpretation of the geology of the gold mineralized zone. The map has differences in the Porcupine-Tisdale Assemblage contact, extensions of existing intrusions, and the addition of an ultramafic intrusion unit, ultramafic volcanic unit and diabase dikes. This map was directly imported into ArcMap© with its accompanying co-ordinate system. The description of each rock unit is that used by Lake Shore Gold Corporation and differs from the OGS scheme.

All samples were plotted on the geological maps using the NAD83 Northing and Easting UTM coordinate system. Individual rock unit geochemical characteristics were defined by the samples that lie within each unit. It is important to note that subsurface bedrock mapping is not available on a regional scale, so surface projections of drill core samples was the only possible option to define lithological units.

2.6.3 Kriging Contour Methods

All Kriged contoured maps were made using ArcMap© 9.3 Geostatisical Analyst extension. The contours were overlaid on the geological base map obtained from MRD 186 by Ontario Geological Survey. The scale used is 1:67,500 which covers the study area and has minor extensions into neighboring townships to show regional geological trends.

The contour plots used the ordinary Kriging method producing prediction maps of the distribution of each element/oxide and alteration index. All contour intervals were adjusted individually to allow for best interpretation of the data. This approach was used so that each element or alteration index either followed individual rock units or crossed lithological boundaries. Each individual anomaly was then analyzed for its potential of being a hydrothermally mobile component transported by the mineralizing fluids.

The parameters set under the ordinary Kriging method were consistent for all maps. Each contour used a Gaussian model and an anisotropy setting because of directional variance caused by the orientation of the geologic units. The ellipse size and sample set used the default five neighboring samples considered with a minimum of 2. Lastly, the ellipse was oriented at azimuth of 70°, consistent with overall trend of the geology in the study area.

Chapter 3 - Results

3.1 Aluminum (Al_2O_3)

The aluminum oxide (Al_2O_3) content of the rocks in the Bristol-Thorneloe Study Area and the neighboring townships range 0.12 to 28.59 wt% Al_2O_3 (Fig. 6). Typical

values for aluminum in the study area are ≤13 wt% Al_2O_3. The Al_2O_3 contours cross lithological boundaries to form a consistent band through the study area. The overall trend of Al_2O_3 is similar to many other elements because it has a northeast orientation.

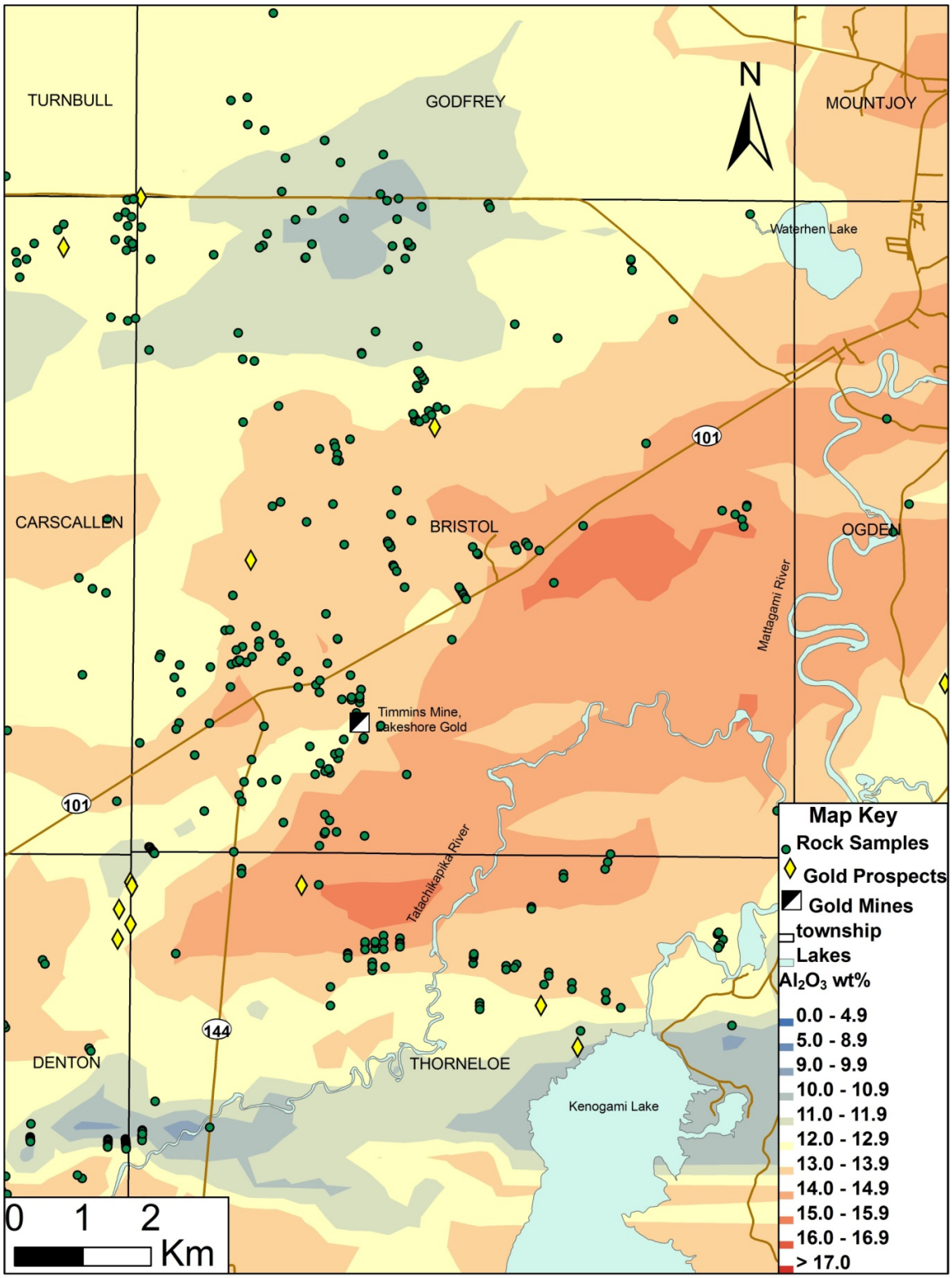

Figure 6 Kriged map of weight percent Al_2O_3 projected to surface

In east central Bristol Township a zone of higher Al_2O_3 values can be found approximately 500 m east of Highway 101, and 3.5 km north of the Thorneloe Township border (Fig. 6). The anomaly has a ”convex lens-shape" with the nose of the lens oriented north-northwest. It is approximately 3.5 km long and 1.25 km wide with a tail structure extending northeast to a cluster of samples. The zone of higher values has Al_2O_3 concentrations ≥15 wt% with the highest sample containing 18.21 wt%. The higher values appear to be associated a felsic porphyry body that intrudes the metasedimentary rocks of the Porcupine Assemblage.

A second "trapezoidal-shaped" anomaly with Al_2O_3 values ≥15 wt%, occurs in north-central Thorneloe Township and is hosted by metasedimentary rocks of the Porcupine Assemblage (Fig. 6). It is located approximately 400 m south of Bristol Township border and 400 m west of the Tatachikapika River. The dimension of the anomaly is 750 m wide and 1.9 km long with trapezoid peak pointing south. This anomaly encompasses or is in close proximity to the Golden River West, Sand Porphyry, Red Porphyry, and No. 14 gold zones.

There is a zone of lower Al_2O_3 values in the northwest corner of Bristol Township that extends from eastern Carscallen to southwest Godfrey Township (Fig. 6). This anomaly is defined by more than 60 data points with Al_2O_3 values <12 wt% and some below 6 wt%. The anomaly is a discontinous band of pod-shaped structures. Overall, it extends for approximately 14.5 km in a southwest direction and has a maximum width of 4.5 km. The host is a felsic metavolcanic rock belonging to the Upper Kidd-Munro and Upper Blake River Assembalges, as well as a felsic instrusive unit that extends into the

anomaly. The zones that have anomalously low Al_2O_3 concentrations do not envelop any gold prospects, however, the Larchmont and KennCo gold showings do occur along strike (Fig. 35 and Table 6).

3.2 Calcium (CaO)

The calcium oxide (CaO) in the study area ranges from 0.03 to 29.55 wt% (Fig. 7). The country rocks in Bristol-Thorneloe Townships have background values of <1 wt% to ≤4 wt%. Higher CaO values form a major “S-shape" anomaly extending from southwest corner of Mountjoy to the northeast corner of Denton Townships.

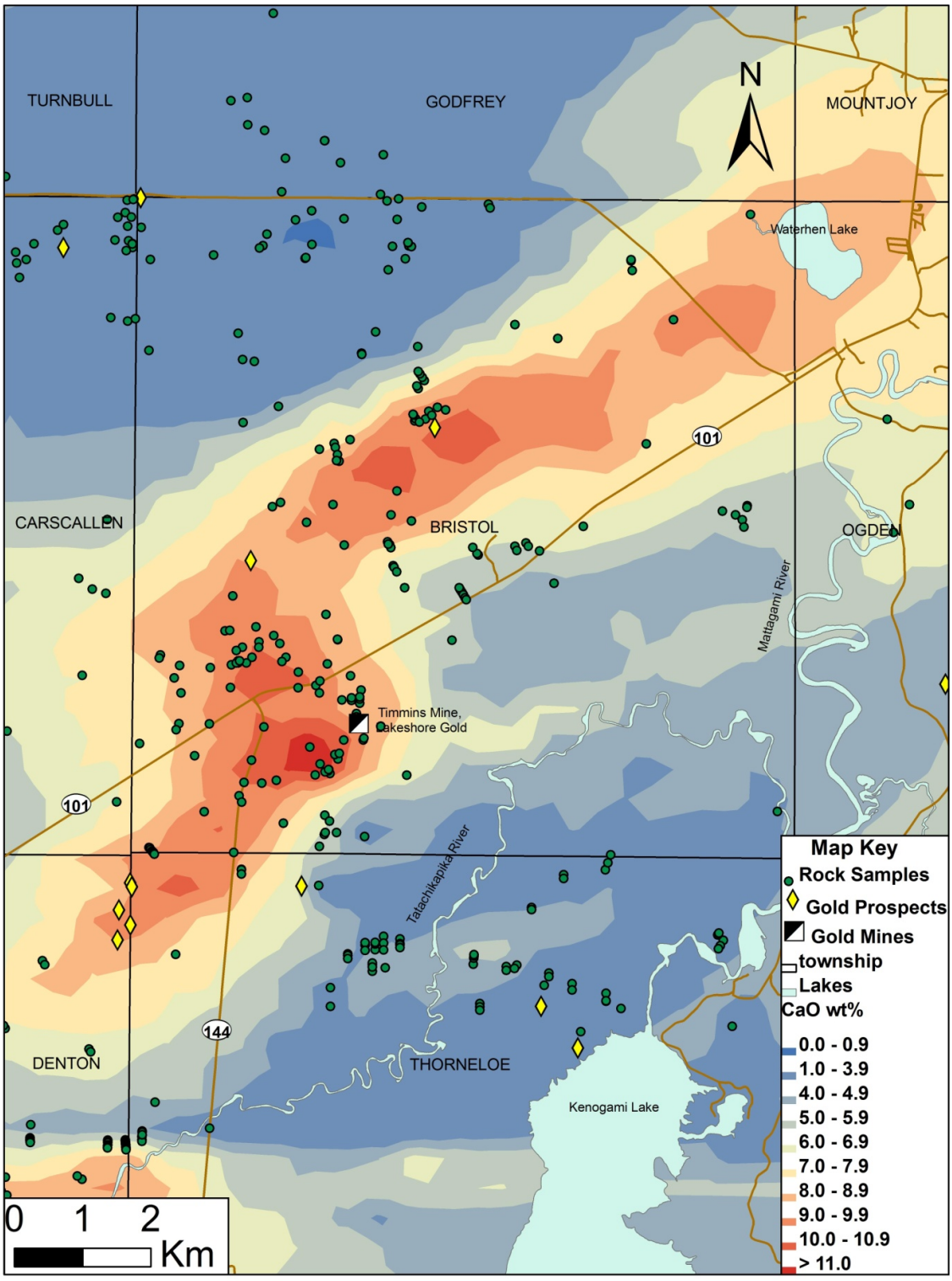

Figure 7 Kriged map of weight percent CaO projected to surface

The band is approximately 2 km wide and 20 km long, and the bend in the “S” is located in the southwest corner of Bristol Township at the junction of Highway 101 and 144. The anomaly contains elevated CaO values of >7 wt% and is conformable with the mafic metavolcanic rocks of the Lower Tisdale Assemblage that extends diagonally across Bristol Township. The highest values in this anomaly are located in a structural deformation zone associated with the contact between altered metasedimentary and ultramafic intrusive rocks of the area. The “S-shaped” anomaly encompasses the Timmins Gold deposit, as well as the Rusk and Highway 144 gold zones.

A second, weak CaO anomaly occurs in the north-central part of Thorneloe Township where typical values are 5 to 6 wt% and the maximum value is 10.6 wt% (Fig. 7). It has a flatten “pancake-shape" with a east-northeast to west-southwest trend. The anomaly is approximately 1 km wide and 4 km long. This anomaly could be a continuation of the “S-shaped" anomaly to the north, but that possibility is uncertain because of the limited amount of data in northern Thorneloe Township. The anomaly extends over the Kapika, No.14, and the western extent of the Golden River East gold zones, all of which are located approximately 3.5 km south-southwest of the Timmins Gold Deposit (Fig. 35 and Table 7).

3.3 Iron (Fe_2O_3)

The iron oxide content of the rocks in the Bristol-Thorneloe Township study area range from 0.0 to 52.56 wt% with background values <4 wt% (Fig. 8). Higher Fe_2O_3 values mimic the “S-shaped" anomaly seen in the CaO results where the higher values appear to be associated with the mafic metavolcanic band of rocks that stretch

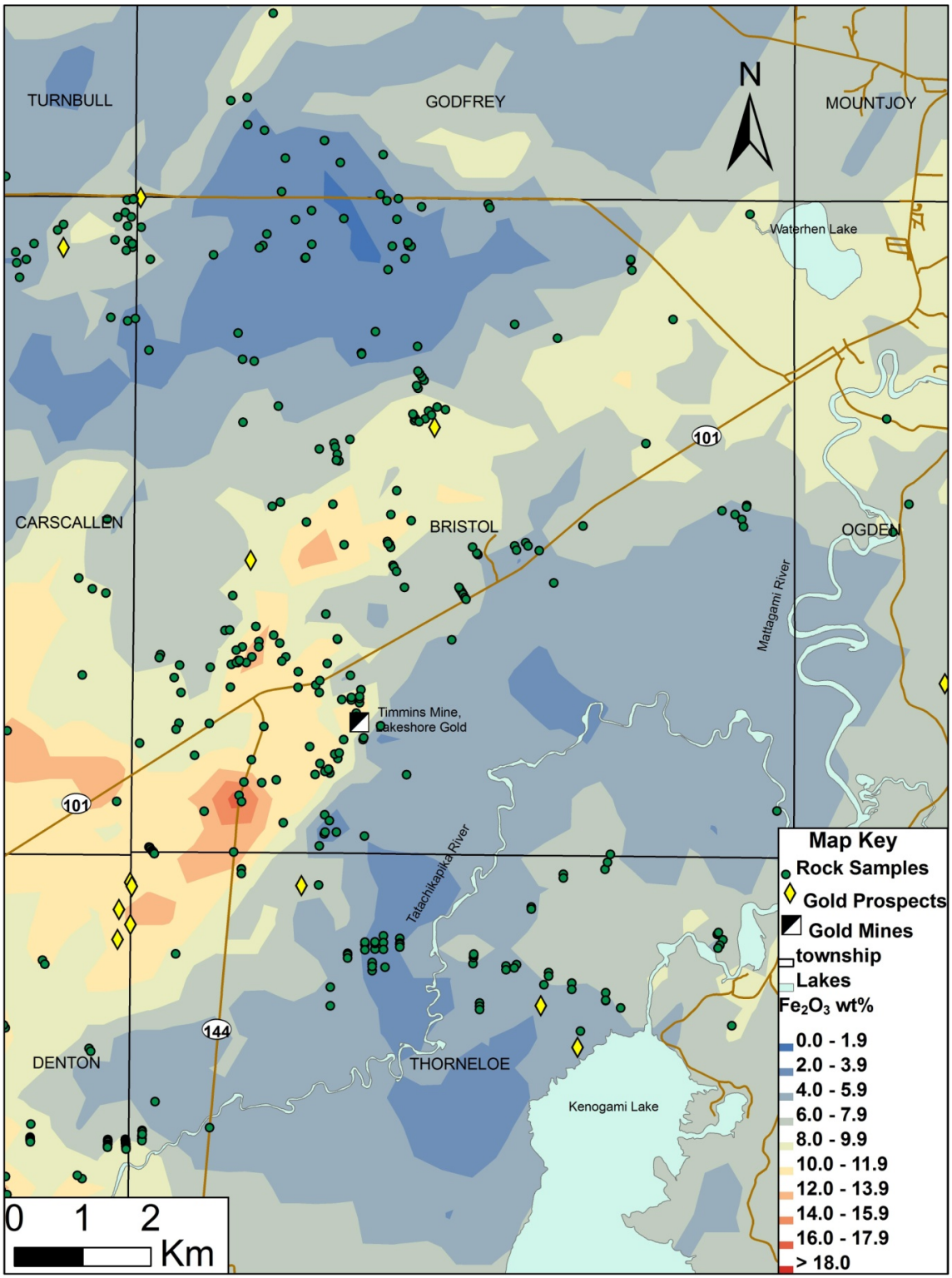

Figure 8 Kriged map of weight percent Fe_2O_3 projected to surface

diagonally across the study area. The anomaly is defined by Fe_2O_3 values >8 wt% with areas locally having values >14 wt%. It is not as well-defined as the CaO anomaly, however, they appear to be related to one another. The Fe_2O_3 anomaly differs from CaO because it follows the Lower Tisdale assemblage rocks northeast from the junction of Highway 101 & 144 into Carscallen Township. The Fe_2O_3 anomaly is not closely association with any known structural elements thereby indicating that it is probably independent of alteration.

A second, smaller anomaly is located in the northwest corner of Carscallen Township that has higher Fe_2O_3 values that range from ≥6 to ≤10 wt% (Fig. 8). It is approximately 1 km wide (east-west) and 2 km long (north-south). The highest value contour is not supported by sample data and is an artifact generated by the ArcGIS© program. However, the higher Fe_2O_3 values coincide with a small mafic metavolcanic / intrusive rock unit located within the felsic metavolcanic rocks in the northern section of the study area. The two anomalies with higher Fe_2O_3 values are similar in that both occur where there are altered mafic metavolcanic rocks.

3.4 Magnesium (MgO)

The MgO content of the country rocks in the Bristol-Thorneloe study area range ≥0.03 to 39.75 wt% (Fig. 9). Typical MgO values for rocks in the study area and neighboring townships is ≤3.5 wt%. Higher concentrations of MgO in the study area and neighboring townships appear to follow the mafic metavolcanic lithological units.

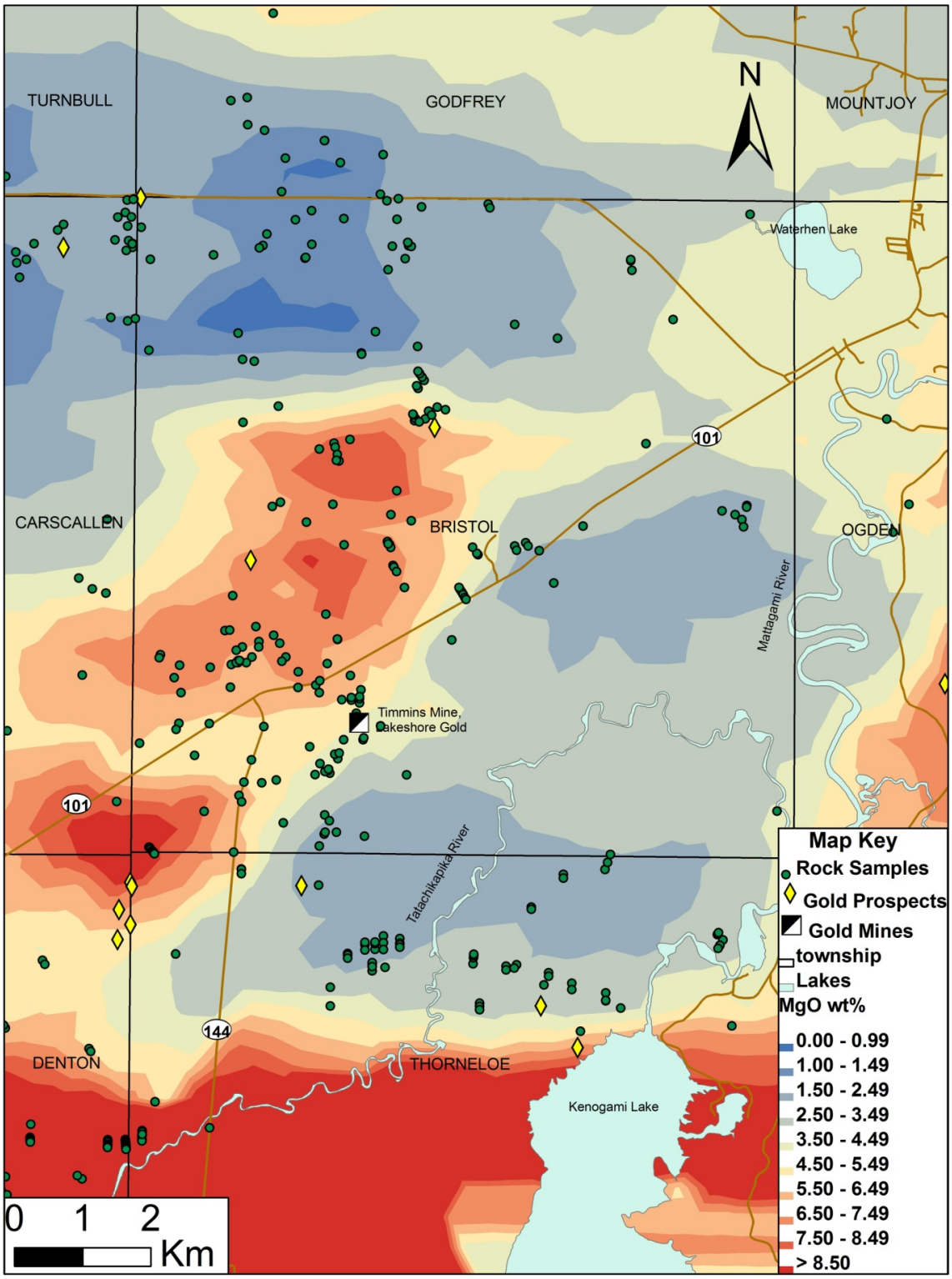

Figure 9 Kriged map of weight percent MgO projected to surface

MgO forms an anomaly similar to but less well-defined that the “S-shaped" CaO structure that extends from northeast Bristol to northeast Denton Township (Fig. 9). Typical values in the anomaly are 5.5 to 8.5 wt% with some ≥26.0 wt%. The anomaly appears to continue from the northeast corner of Bristol Township southeast into Ogden and Price Townships. Unlike CaO, the MgO anomaly has a clearly defined fold-nose structure and eastward trending limb. This geochemical feature closely follows the mafic metavolcanic rocks of the Lower Tisdale Assemblage and the fold structure outlined by geological maps of the area (Ferguson, 1957; Pyke, 1982).

The anomaly continues eastward from northeastern Denton Township to northeast Thorneloe Township. This trend follows the southern limb of the fold that host Tisdale mafic metavolcanic, ultramafic, and metasedimentary rocks. The samples along this limb are primarily found in the interbedded ultramafic and mafic metavolcanic rock units. Samples in the metasedimentary rocks form the periphery of the anomaly of lower MgO concentrations, interpretted by ArcGIS©. The anomaly envelops the R.E. Halpenny, Cripple Creek Zone 16, Karvinen and Darry gold occurences (Fig. 35 and Table 1).

3.5 Manganese (MnO)

The MnO content of the country rocks in the study area range from 0.00 to 2.35 wt% MnO (Fig. 10). Typical MnO background concentrations in the rocks are ≤0.10 wt% with lower zones containing <0.05 wt% MnO. The MnO values appear to follow lithological boundaries where higher concentrations are associated with the mafic metavolcanic rock units of the Lower Tisdale Assemblage.

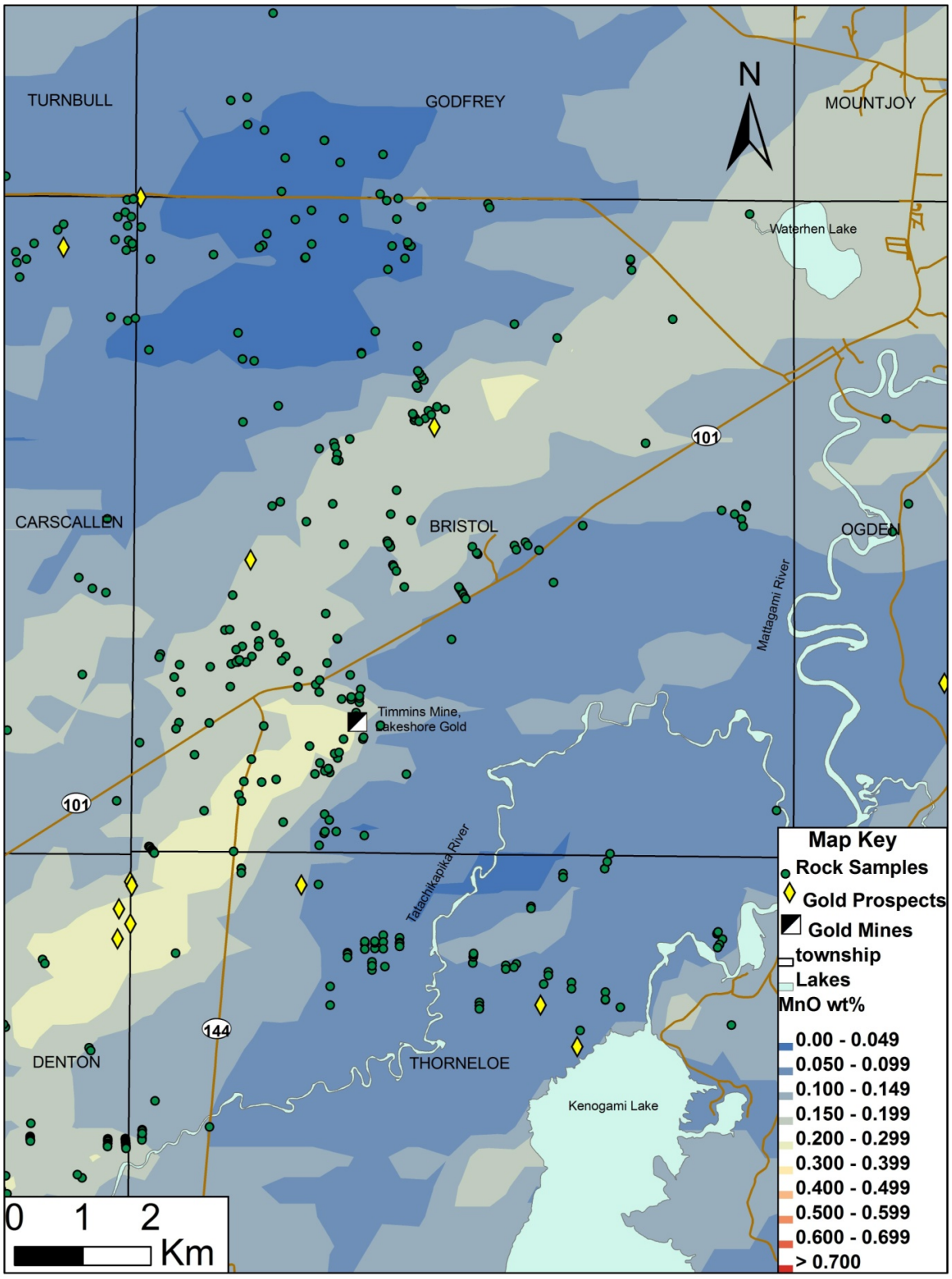

Figure 10 Kriged map of weight percent MnO projected to surface

MnO forms an “S-shaped" anomaly that spans from northeast Bristol to the west-central part of Denton Township and has typical values between ≥0.15 wt% to >0.40 wt%. The location and shape of the MnO anomaly closely mimics the MgO and CaO anomalies (Fig. 10).

3.6 Sodium (Na_2O)

The Na_2O content of the country rocks in the study area range from 0.00 to 8.97 wt% (Fig. 11). Typical background Na_2O values are ≤2.49 wt% with low values being <1.00 wt%. Concentrations cross lithological boundaries as well as vary within mapped lithological units. Higher values (>2.50 wt%) are typically found in the metasedimentary rocks as well as felsic rock units.

A circular Na_2O anomaly occurs in the northwest corner of Bristol Township and the neighboring townships (Turnbull, Carscallen, and Godfrey). This anomaly is approximately 2.7 km in diameter and has typical Na_2O values >3.00 wt%. This anomaly is hosted by felsic metavolcanic, mafic metavolcanic, and felsic to intermediate intrusive rocks. It is centered on the contact between the Upper Blake River and Upper Kidd-Munro Assemblages. The Larchmont 65-5 and KennCo gold prospects lie within the anomaly.

A larger oval-shaped anomaly occurs in the southeast corner of Bristol Township. It is approximately 9 km by 3 km in area and extends from west-central Ogden to south-central Bristol Township. Typical Na_2O values in this anomaly are ≥3.00 wt% and <4.00 wt%. The anomaly is hosted by metasedimentary rocks of the Porcupine Assemblage, felsic to intermediate intrusive and “porphyry suite” rocks. The Rusk mineralized corridor

and Mahoney Creek Occurrence #1 lie within the anomaly and the Lake Shore Timmins West Gold Mine is found approximately 100 m northwest of the Na_2O anomaly.

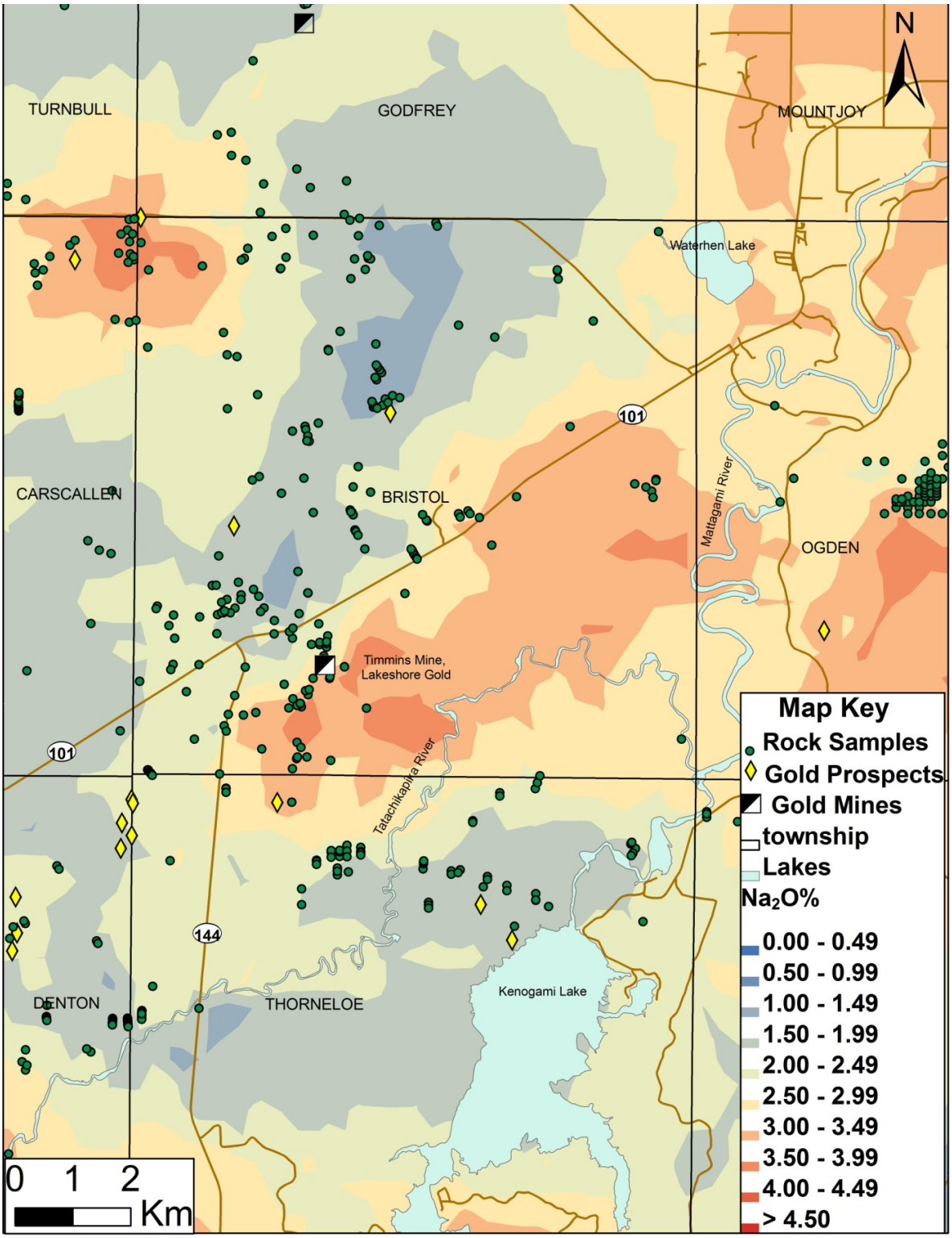

Figure 11 Kriged map of weight percent Na_2O projected to surface

3.7 Potassium (K_2O)

The K_2O content of the wallrocks in the Bristol-Thorneloe study area ranges from 0.0 to 39.60 wt% (Fig. 12). The typical background K_2O values throughout the study area are 0.50 to 1.25 wt%, with some zones containing <0.25 wt%. Higher K_2O values occur predominately in the felsic metavolcanic rocks at the north and northeast edge of the study area, as well as felsic-intermediate intrusive rocks.

The K_2O anomalies in the study area are spatially associated with felsic intrusive and metavolcanic rock units. Approximately 1.5 km southeast of the junction of Highway 101 & 144, higher K_2O values form an “v-shaped" anomaly that trends from north-northwest to south-southeast and crosses several lithological boundaries (Fig. 12). It is defined by the 2 wt% K_2O contour and contains a maximum value of 8.73 wt%. The highest K_2O concentrations in this anomaly coincide directly with a suite of alkalic and felsic intrusive rocks bodies at the Lower Tisdale-Porcupine assemblage contact. The “arrow-shaped" anomaly does not coincide with any known mineralized gold zones or prospects in the Bristol-Thorneloe study area, but does lie just south of the West Timmins Gold Mine.

A second, larger anomaly passes through the northwest corner of the study area at the Bristol-Godfrey Township boundary (Fig. 12). It is defined by >50 data points and forms a “wedge-shaped" structure that extends from north-central Carscallen to north-central Godfrey Township. The northeast to southwest trending anomaly is approximate 6.5 km wide and 17.5 km long. The rocks that underlie this anomaly have K_2O concentrations of 2 to >5 wt% with local values of up to >9 wt%. The K_2O anomaly is largely interpreted by ArcGIS© because of the increase in distance from the immediate

study area and the limited number of data points. The highest K_2O concentrations are found in felsic metavolcanic country rocks and occur in close proximity to felsic-intermediate intrusive bodies. There do not appear to be any gold-bearing zones in the study area that have a clear association with higher K_2O values.

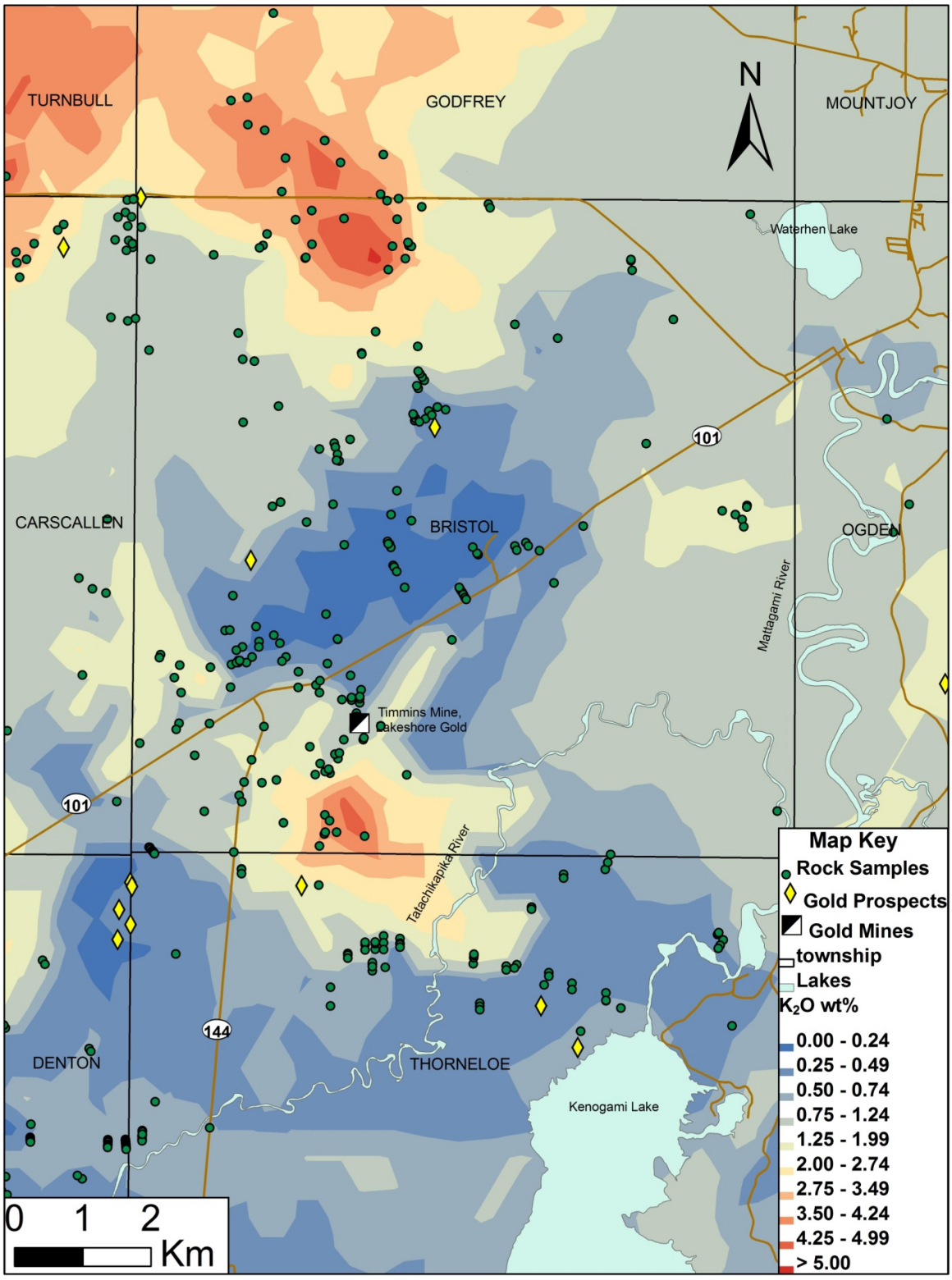

Figure 12 Kriged map of weight percent K_2O projected to surface

3.8 Phosphorus (P_2O_5)

The P_2O_5 content of the country rocks in the Bristol-Thorneloe Township study area and seven immediately adjacent townships ranges from 0.00 to 6.53 wt% (Fig. 13) and is typically $\leq$0.2 wt%. These low concentrations extend across lithological boundaries and occur in close proximity to north–northwest trending diabase dikes. Rock samples collected <1 km from the Timmins mine have higher P_2O_5 contents than the surrounding townships and define a 3 by 4 km anomaly with a maximum value of 4.3 wt%. This anomaly appears to consist of two closely spaced, parallel anomalies the western half of which is defined by >25 data points and the eastern half is largely interpreted from nearby results. The P_2O_5 anomaly envelops the Timmins mine and nearby Thunder Creek gold zones, as well as the Rusk and Highway 144 gold zones, located just south of the junction of Highway 101 & 144 (Fig. 35 and Table 1). Rocks located in the center of the Bristol-Godfrey Townships boundary have P_2O_5 concentrations that range up to 0.5 wt%. This smaller anomaly is defined by fewer samples and was interpreted by the ArcGIS© software and extends out of the study area (Fig. 13).

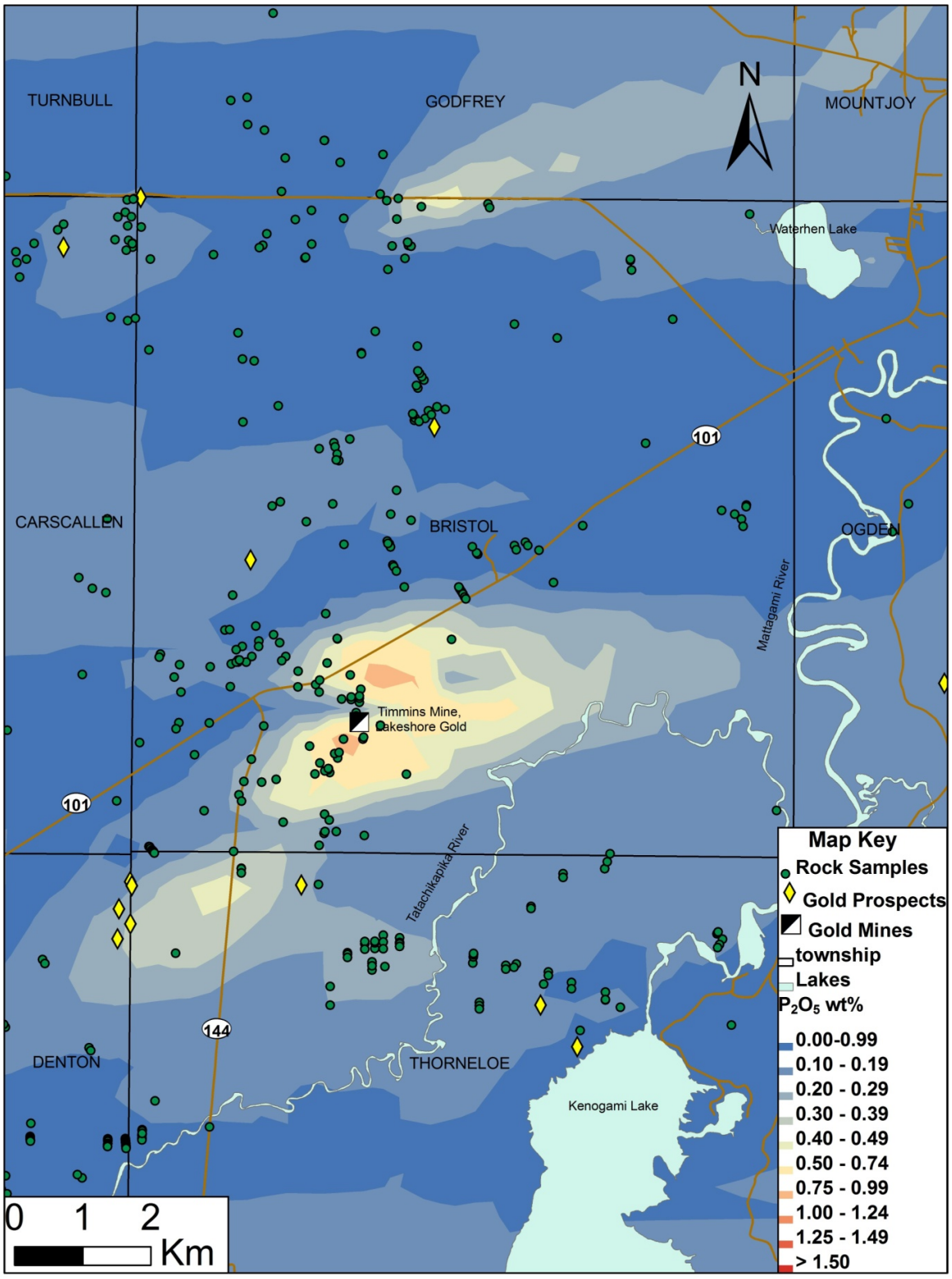

Figure 13 Kriged map of weight percent P_2O_5 projected to surface

3.9 Titanium (TiO_2)

The TiO_2 content of the country rocks in the Bristol-Thorneloe study area and surrounding townships ranges from 0.00 to 3.16 wt% (Fig. 14). Typical TiO_2 background values in the area are ≤0.60 wt%. Higher TiO_2 concentrations have a weak association with the mafic metavolcanic rocks of the Lower Tisdale Assemblage.

An "S-shaped" anomaly with higher TiO_2 concentrations appears similar to those identified for CaO, MgO and Fe_2O_3, and is centered in the southwest corner of Bristol Township (Fig. 14). The 21 km long and 5 km wide anomaly extends from central Bristol to the southwest corner of Denton Township and has TiO_2 values that range from ≥0.60 to ≥1.50 wt%. The anomaly might have a fork that extends into northern Ogden and central Godfrey Townships. These discontinuous limbs coincide with mafic metavolcanic rocks that would account for the higher TiO_2 concentrations. The Rusk occurrence and Timmins Mine are the only gold-bearing zones that coincide with the northeast periphery of this anomaly.

An "hourglass-shaped" TiO_2 anomaly with values ≤0.30 wt% occurs in the northwest corner of Bristol Township (Fig. 14). The approximate dimensions of this northerly orientated anomaly is 4 km long and 3.5 km wide. The low concentration anomaly is defined by >40 data points and coincides with the felsic metavolcanic rocks of the Upper Blake River and Upper Kidd-Munro Assemblages.

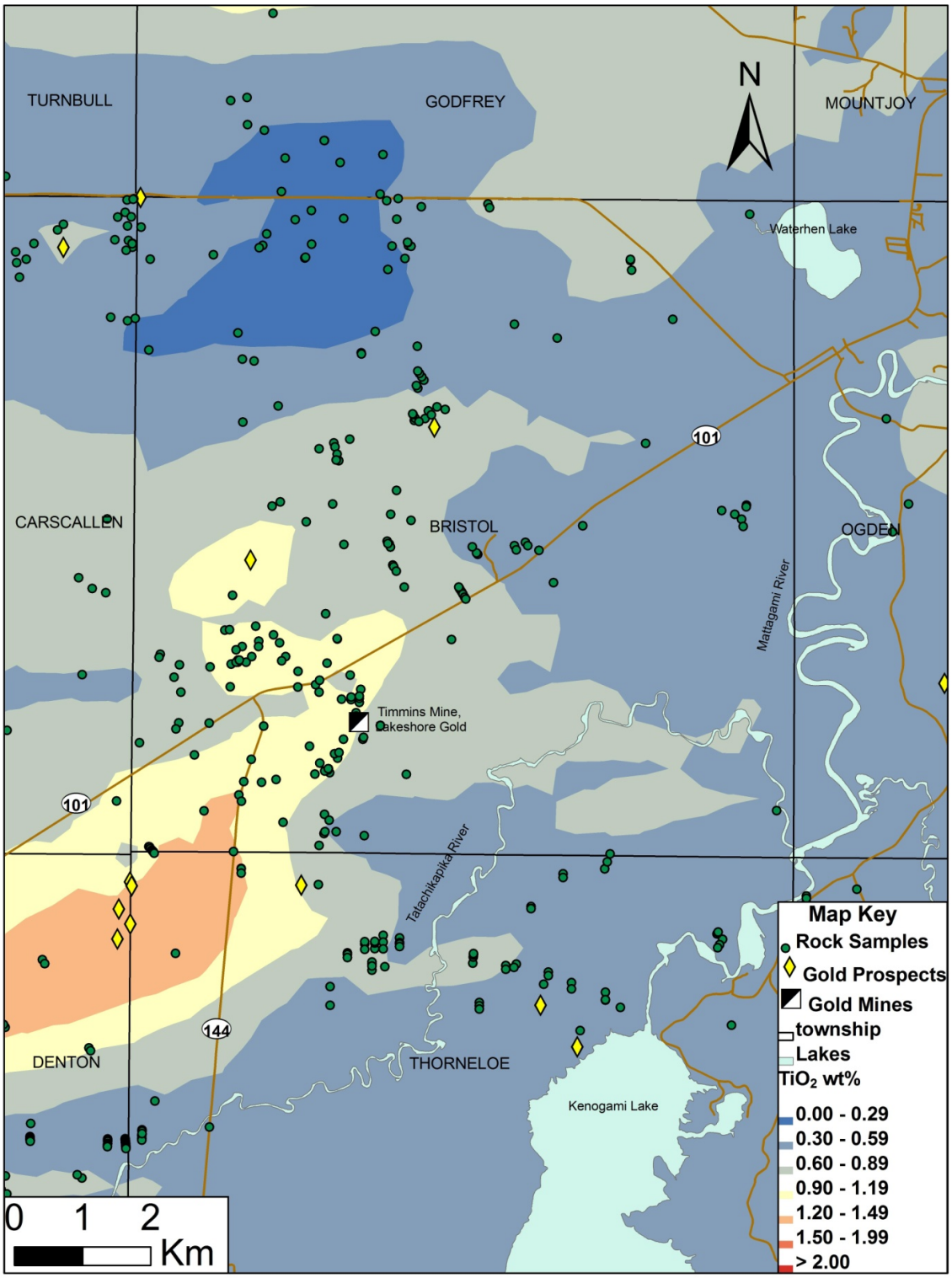

Figure 14 Kriged map of weight percent TiO_2 projected to surface

3.10 Gold (Au)

The gold (Au) content of the country rocks in the Bristol-Thorneloe Study Area and neighboring townships range from 0 to 10,674 ppm and have typical background values of <25 ppb (Fig. 15).

Gold values in bedrock form a somewhat dumbbell-shaped anomaly. This north-south oriented anomaly measures 4.2 km by 2.0 km and straddles the boundary between southwest corner of Bristol Township and the northwest corner of Thorneloe Township (Fig. 15). The gold values that define the anomaly are typically >150 ppb and are hosted in the complex Porcupine metasediment – Lower Tisdale mafic metavolcanic contact zone that includes metasedimentary, ultramafic intrusive, Tisdale mafic metavolcanic, and felsic to intermediate intrusive rocks. The rocks that host the gold anomaly are located between the Bristol and Destor-Porcupine faults, two major breaks in the study area. The Lake Shore Timmins West Gold Mine and Rusk Mineralized Corridor occur within this anomaly.

A second and smaller “bulls-eye–shaped” anomaly is located in north-central Thorneloe Township, approximately 1.3 km northwest of Kenogami Lake (Fig. 15). This smalleranomaly has a diameter of 750 m and is defined by three gold values that range from 100 to 150 ppb. The gold anomaly is hosted by the Porcupine clastic metasedimentary rocks and envelops the Kapika and Golden River East Mineralized Zones located ~650 m west of the Tatachikapika River (Fig. 35 and Table 1).

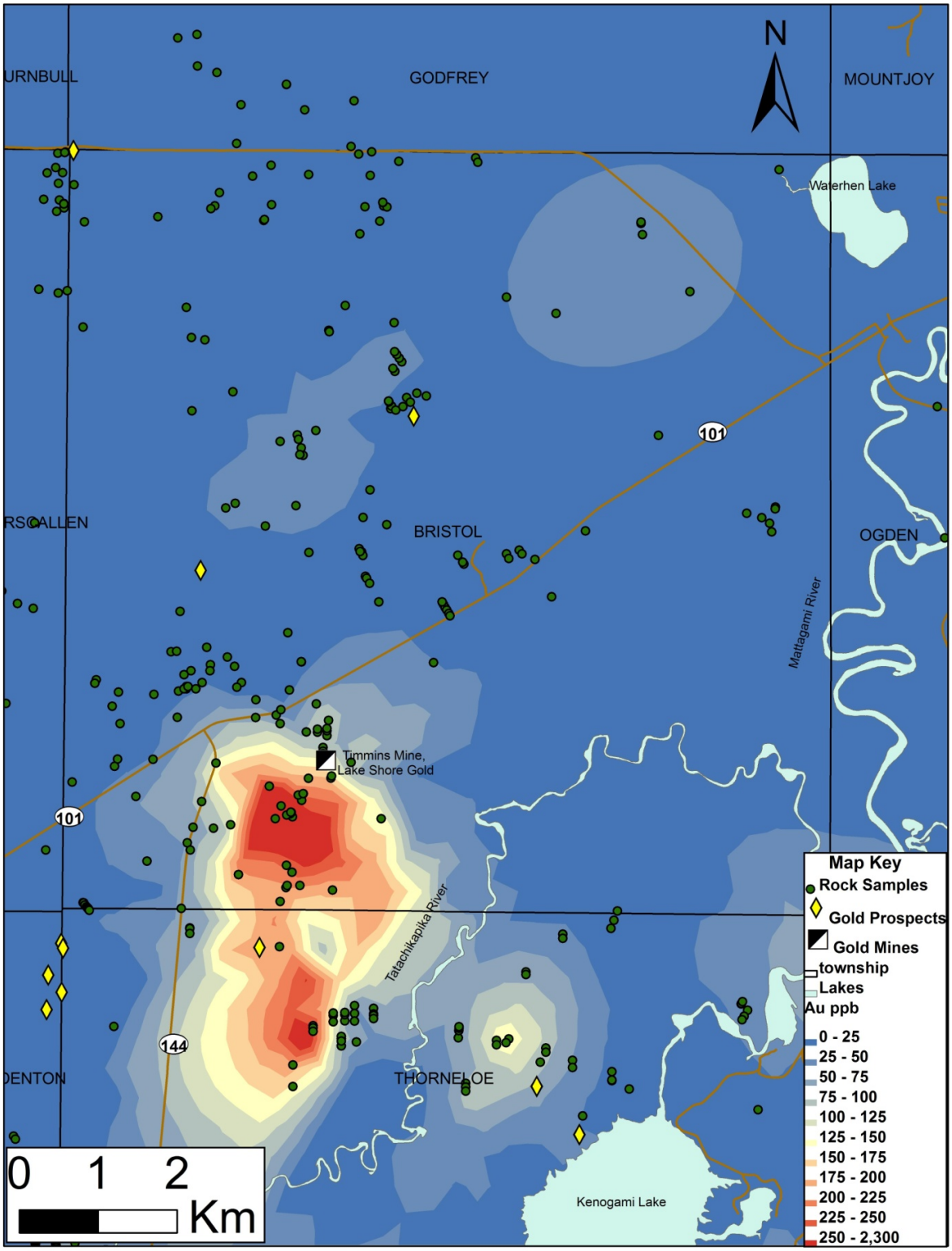

Figure 15 Kriged map of Gold in ppb projected to surface

3.11 Zirconium (Zr)

The Zirconium (Zr) content of the country rocks in Bristol-Thorneloe study area and neighboring townships ranges from 0 to 2,488 ppm and has typical background values of ≤125 ppm (Fig. 16). Similar zirconium values cross lithological boundaries.

A 3.5 by 1.25 km “pancake-shaped" anomaly located in southwest corner of Bristol Township has Zr concentrations that typically range between 175 and 325 ppm (Fig. 16). This anomaly has a southwest-northeast orientation and is located approximately 750 meters from the junction of Highway 101 & 144. The anomaly is centered on the Rusk gold occurrence and also envelops the Timmins gold mine. A branch of the anomaly that has Zr values between 175 and 225 ppm, extends south and intersects the Golden River West gold zone.

A second, elliptical anomaly (13 by 4.5 km) extends from southwest Godfrey to northeast Carscallen Township (Fig. 16). Typical Zr values found in the zone range from 225 to 375 ppm. Much of the anomaly, found in southeast and south-central Godfrey Township, is an artifact of the ArcGIS© interpretation because it is not supported by any data points. This zone appears to be related to the small lens of mafic metavolcanic rocks found in northwestern Bristol Township. The Zr anomaly encompasses the KennCo and Larchmont 65-5 gold prospects located in the northwest corner of Carscallen Township (Fig. 35 and Table 1).

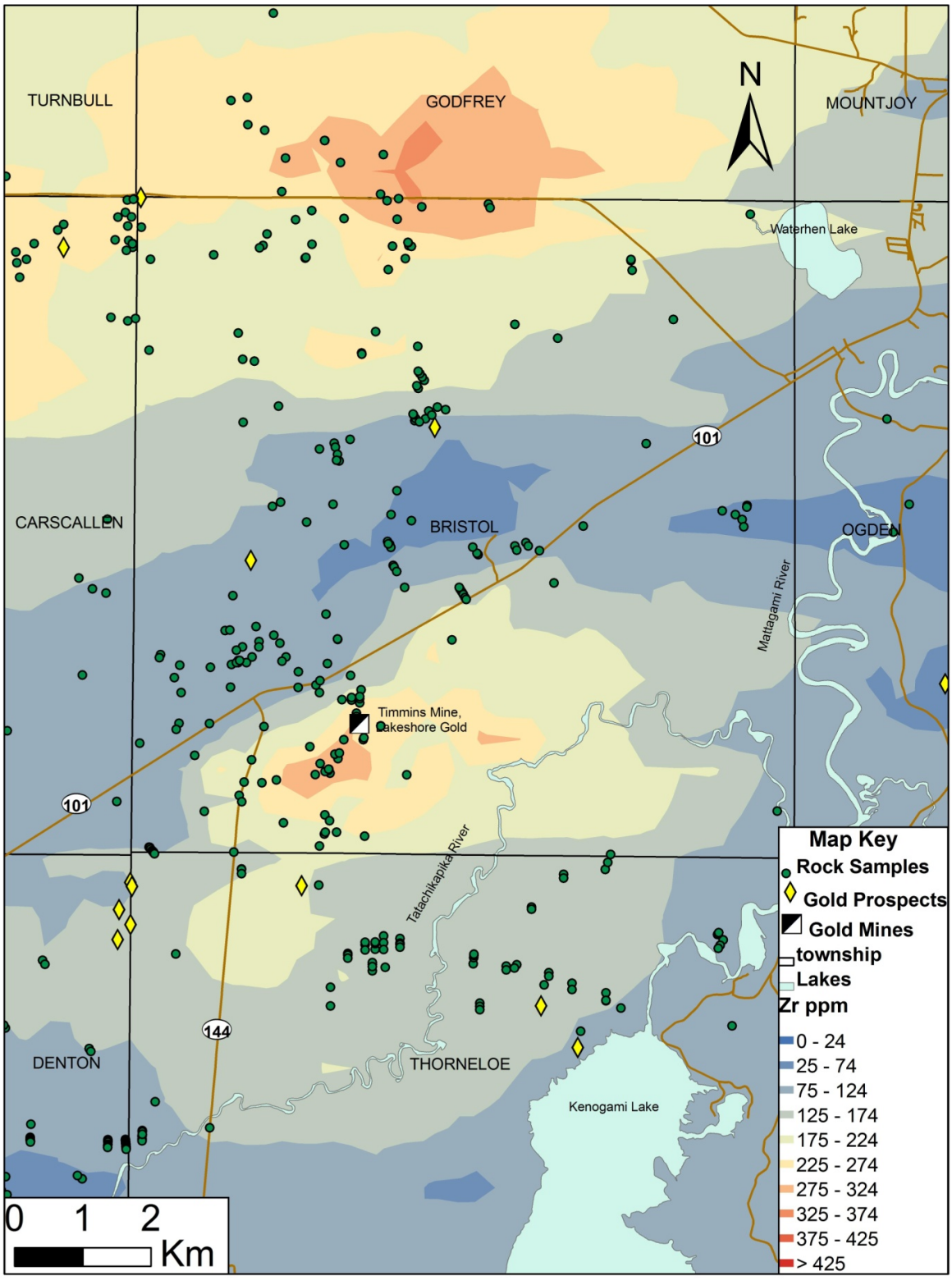

Figure 16 Kriged map of Zirconium in ppm projected to surface

3.12 Strontium (Sr)

The Sr content of the country rocks in the Study Area and surrounding townships range from 1 to 7,301 ppm (Fig. 17) and have typical background values of <180 ppm. Zones with similar concentrations extend across lithological boundaries with the highest values found at or near the metasediment (Porcupine) – mafic metavolcanic (Lower Tisdale) rock contact with associated ultramafic and felsic intrusive bodies.

Located in southwestern Bristol Township, 750 meters southeast of the junction of Highway 101 & 144, is a flattened “bullseye-shaped" anomaly (Fig. 17). The structure is approximately 3.5 km long and 1.5 km wide and trends parallel to Highway 101. The Sr values found in this area typically range from 750 to 1,500 ppm with concentrations >1,500 ppm found locally. The center of the Sr anomaly and highest values are centered directly on top of the Rusk gold occurrence and the outer boundary envelops the Timmins West Gold Mine (Fig. 35 and Table 1). This Sr anomaly is found within a much broader anomaly that has values between 250 and 749 ppm and covers the south and southeastern part of Bristol Township below Highway 101 (Fig. 17). This anomaly is defined largely by samples collected from around its boundary.

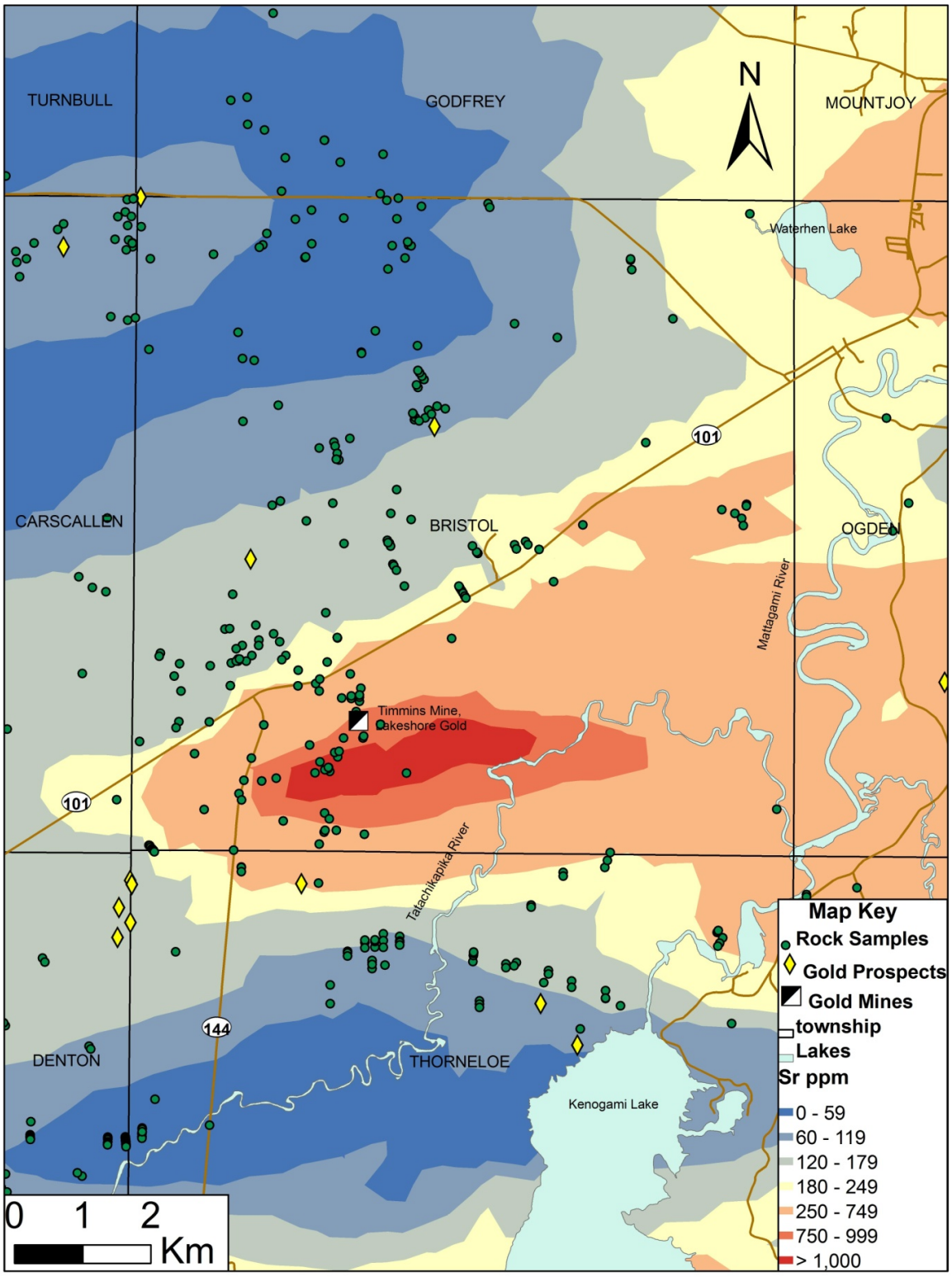

Figure 17 Kriged map of Strontium in ppm projected to surface

3.13 Barium (Ba)

The Ba content of the country rocks in the Bristol-Thorneloe Study Area and the neighboring townships range from 3 to 8,168 ppm and have typical background concentrations of <400 ppm (Fig. 18). Zones with similar Ba content extend across lithological boundaries indicating that there is no direct association with rock type.

There is a trianglular anomaly with approximate dimensions of 2.5 by 2.25 km located in the southwest Bristol Township 800 meters southeast of the junction of Highway 101 & 144, that has typical Ba concentrations >600 ppm (Fig. 18). The highest values occur near the center of the anomaly and are associated with a complex contact between the mafic metavolcanic (Lower Tisdale Assemblage) and clastic metasedimentary rocks (Porcupine Assemblage), as well as with the associated felsic and ultramafic intrusive bodies. The highest values are centered on the Rusk gold occurrence and the northeast edge of the anomaly envelops the Timmins West Gold Mine (Fig. 35 and Table 1).

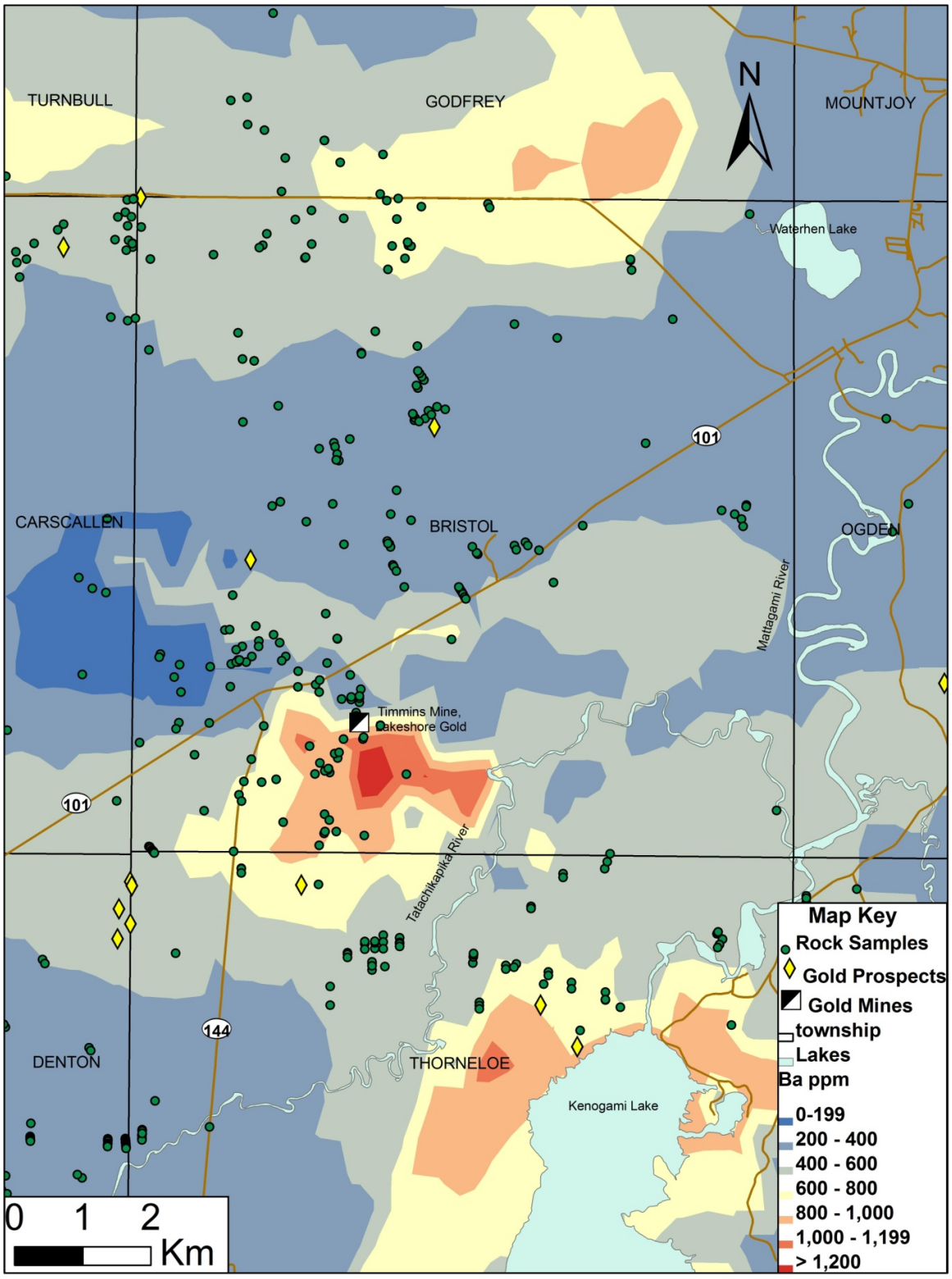

Figure 18 Kriged map of Barium in ppm projected to surface

The south-southwest limb of the anomaly lies approximately 300 m north of the Mahoney Creek gold occurrence and 200 m east of a cluster of samples with high gold values near Highway 144.

A second “wedge-shaped anomaly" is located midway along the Bristol - Godfrey Township border. It is approximately 3 km long and has values of up to 800 ppm. The zone is hosted by felsic metavolcanic rocks of the Upper Blake River Assemblage. No known gold prospects are located in or close to the anomaly.

A "lens-shaped" anomaly that extends approximately 6 km east-west and 2.5 km north-south envelops the north end of Kenogami Lake, located in the northeast corner of Thorneloe Township. Typical Ba concentrations in this area range from 600 to 1200 ppm. This anomaly coincides with the thinly laminated contact zone between the clastic metasedimentary rocks and mafic metavolcanic rocks (Porcupine Assemblage, Lower Tisdale Assemblage, and Timiskaming Assemblage). A porphyry intrusion is found at the center of the anomaly. Structurally, the Ba anomaly coincides with the south limb of a regional fold in the Destor-Porcupine Fault Zone. The highest Ba concentrations envelops known gold occurences icluding the Kapika Zone, Golden River East Zone, and Darry Prospects.

3.14 Yttrium (Y)

The Y content of the country rocks in the study area and neighboring townships range from 0 to 238 ppm. Typical Y background values in the region are >30 ppm and extend across lithological boundaries.

Anomalously high Y concentrations underlie northern Bristol, northeast Carscallen, southeast Turnbull, and Godfrey Townships (Fig. 19). These values appear to be associated with the felsic metavolcanic rocks of the Upper Blake River and Upper Kidd-Munro Assemblages and have ArcGIS© interpreted contours that extend across lithological boundaries. Typical Y concentrations found in the anomalous zone are >50 ppm. The KennCo and Larchmont 65-5 gold prospects, located in the northeast corner of Carscallen Township, and the Genex Mine of southwest Bristol Township are enveloped by this anomaly.

A second "arrow head-shaped" Y anomaly is located 700 meters southeast of the junction of Highway 101 & 144 in southwest Bristol Township (Fig. 19). This northeast oriented anomaly is approximately 1.2 km by 1.6 km and has Y concentrations between 40 and 50 ppm. It coincides with the rocks near the Lower Tisdale and Porcupine Assemblage contact and extends into a ultramafic intrusive between them. This anomaly envelops Lake Shore Timmins Mine and the Rusk mineralized occurrence.

A third Y anomaly is located in northeast Thorneloe Township enveloping the north end of Kenogami Lake (Fig. 19). The anomaly has a northeast trend and Y values that increase from 40 ppm at the northeast end to 59 ppm at the south end in southern Thorneloe and Price Townships. The highest Y concentration is located 700 meters northeast of Kenogami Lake. The ArcGIS© interpretation of the data suggests that the anomaly continues southeast into south-central Price Township, however, that extension is unsupported by data points. The area underlying the anomaly is the

characterized by the clastic metasedimentary rocks of the Porcupine Assemblage. The Darry gold prospect lies within this Y anomaly.

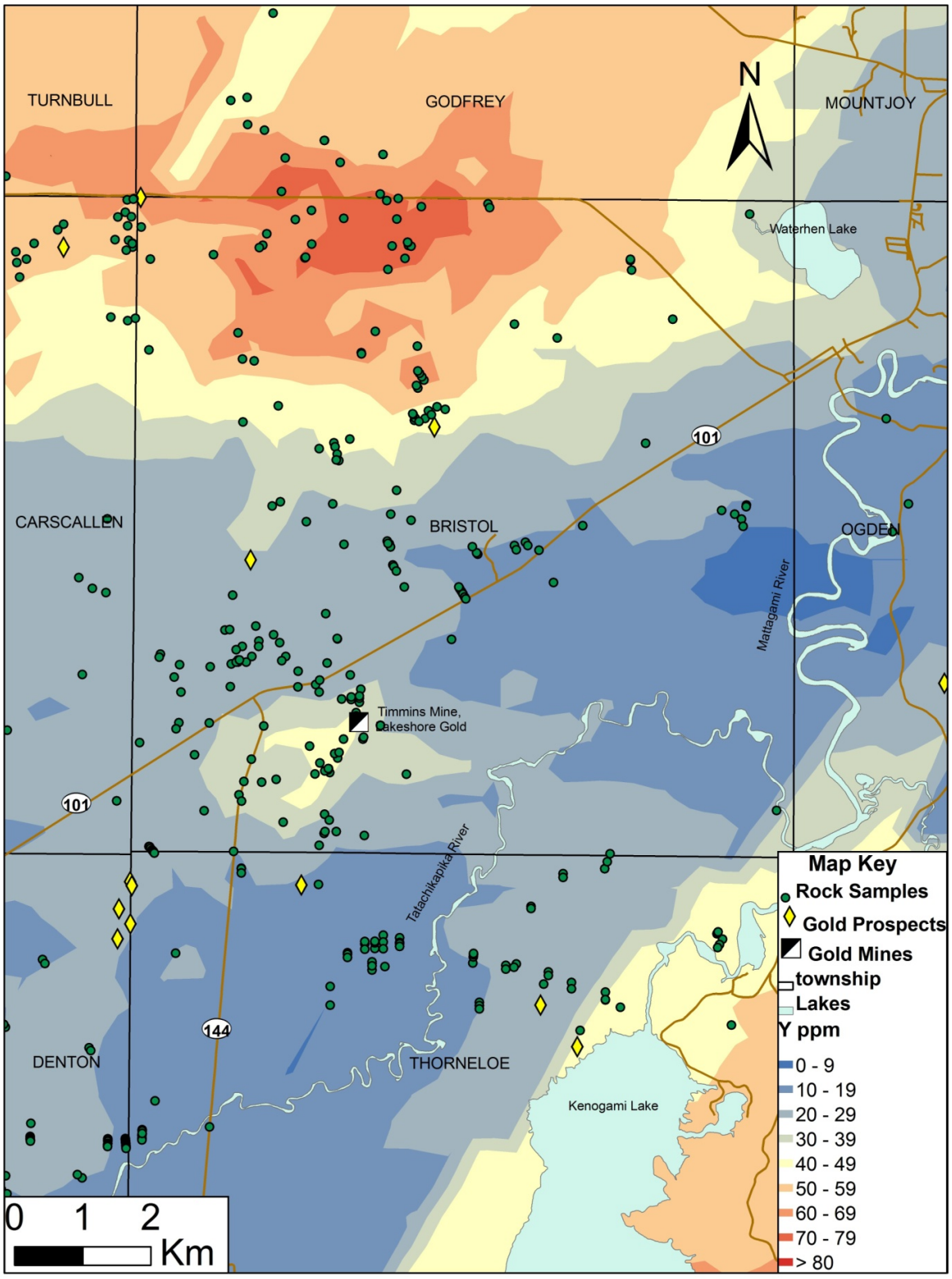

Figure 19 Kriged map of Yttrium in ppm projected to surface

3.15 Scandium (Sc)

The Sc content of the country rocks in the study area and neighboring townships ranges from 0 to 67 ppm. Typical background Sc values in the area are <20 ppm and similar concentrations extend across lithological boundaries.

There is a discontinuous band of higher Sc values between 20 and 39 ppm that are located in northeast corner of Bristol Township and extend into northwestern Thornloe Township (Fig. 20). The band has an average width of 2.6 km that decreases to the southwest. The high Sc concentration of the anomaly in the northeast corner of Bristol Township is supported by only one sample and the rest is interpreted by ArcGIS©. The anomaly conforms relatively well with the location of the mafic metavolcanic rocks of the Lower Tisdale Assemblage, but extends across into the felsic metavolcanic rocks of Upper Blake River Assemblage, and clastic metasedimentary rocks of the Porcupine Assemblage. The band has higher Sc values at the southwest end and teminates at the nose of isoclinal fold in north central Denton Township. The band envelops known gold mineralized zones where the northeastern extension coincides with the Rusk Mineralized Corridor, the Lake Shore Timmins West Gold Mine, and McKinely & Molesky gold showing on claim 8405. The southwestern extension envelops multiple gold showings and zones including: Shankman Zones, various Hemlo Gold Reources Prospectors Alliance DDHs (PA97-2, PA97-4, PA97-5), and Battle Mountain DDHs (MC97-9, MC97-18, MC97-20, MC97-21, MC97-22, MC97-26), as well as Cripple Creek Zone 17, AUMO, and AUMO No.3 Vein (Fig. 35 and Table 1).

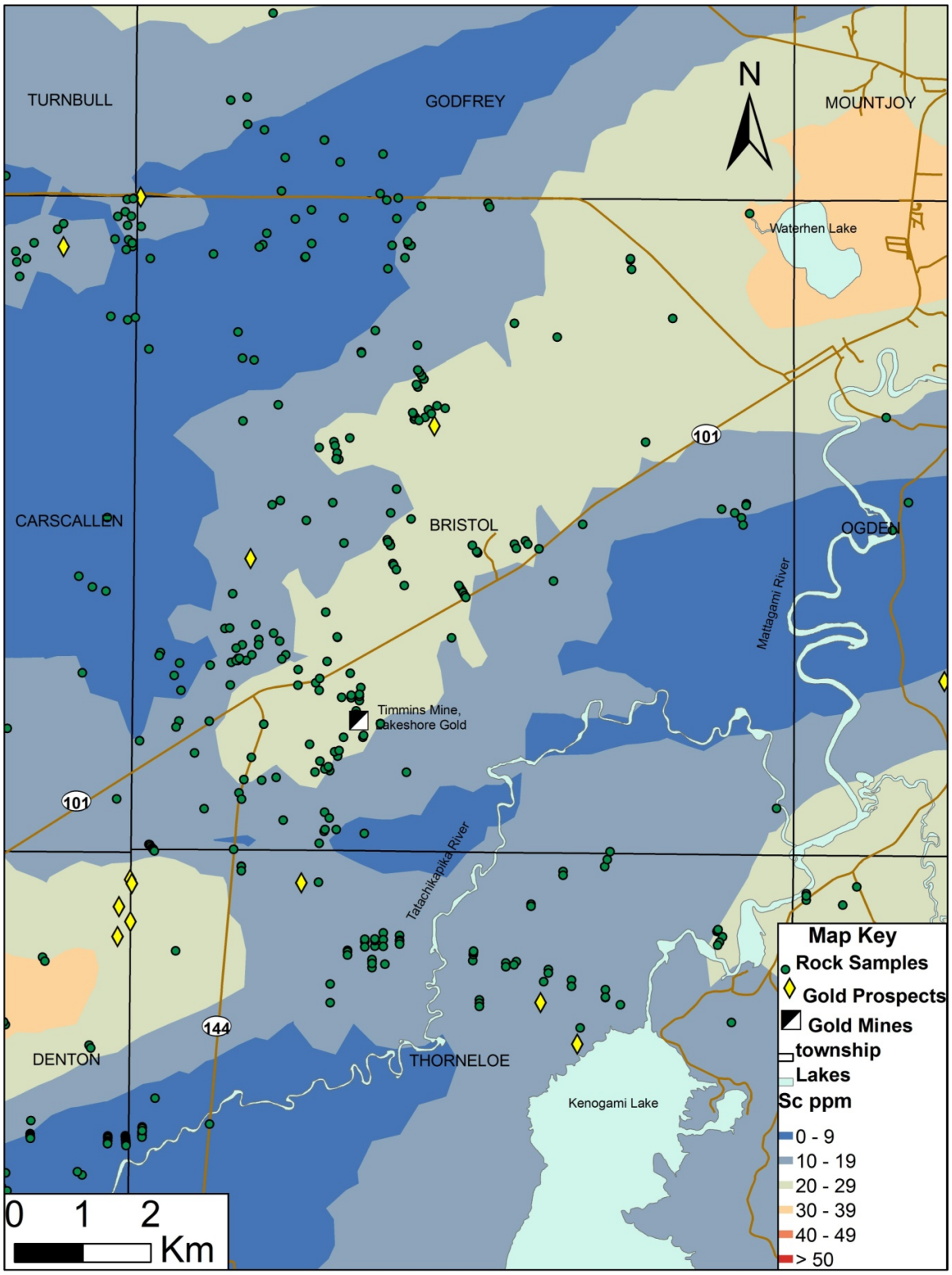

Figure 20 Kriged map of Scandium in ppm projected to surface

3.16 Nickel (Ni)

Nickel content of the country rocks in the study area range from 0 to 4,000 ppm. Typical background values in the study area and surrounding townships is ≤50 ppm. The higher values appear to coincide primarily with the mafic metavolcanic rocks of the Lower Tisdale Assemblage where the highest values occur <500 meters from ultramafic intrusive and metavolcanic rock units (Fig. 21).

In the southwest corner of Bristol Township an “L-shaped"-anomaly extends from southwest Bristol into northeast Denton Township, as well as along the southern border of the study area (Fig. 21). The anomaly is defined by Ni values ≥125 ppm that stretch for ~25 km and has an average width of ~3.5 km. The ArcGIS© interpreted anomaly is largely defined by high Ni values located on the Bristol-Thorneloe Township boundary approximately 1.25 km west of highway 144. This anomaly is in close proximity (<750m) to the Golden River East, Sand Porphyry, No.14, Kapika, and Golden River West gold zones (Fig. 35 and Table 1).

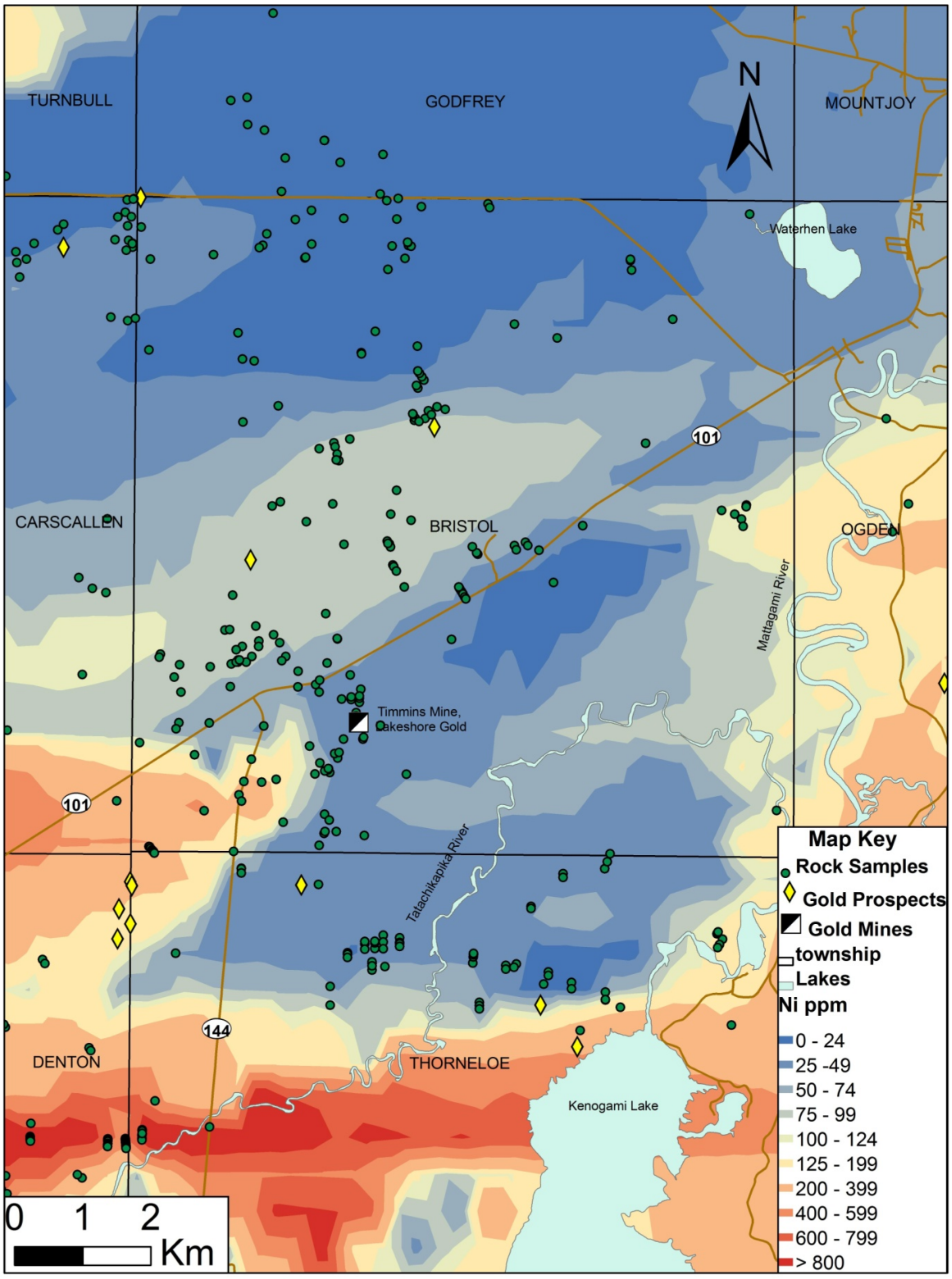

Figure 21 Kriged map of Nickel in ppm projected to surface

3.17 Chromium (Cr)

The Cr content of the country rocks in the Bristol-Thorneloe Township study area and neighboring townships range from 0 to 21,620 ppm and are typically ≤100 ppm. Similar values cross lithological boundaries but are not related to intrusive rock bodies in the area. Contouring of Cr values in the study area was performed by limiting the upper value of Cr to 500 ppm in order to reduce the influence of a highly anomalous value that obscured lower contour values (Fig. 22).

The biggest Cr anomaly is “U-shape", measures 5 by 3.5 km, has the opening oriented north-northwest, and is located in west-central Bristol Township and northwestern Carscallen Township. It is defined by Cr values that range from 200 to 299 ppm. The contours extend across lithological boundaries of the Upper Kidd-Munro and Lower Tisdale Assemblage rocks. The highest Cr concentrations are located 1.5 km northwest of the junction of Highway 101 and 144.

A second Cr anomaly begins in central Denton Township and extends into west-central Thorneloe Township. This anomaly is an oblong lens that is approximately 8.5 km by 3.5 km, orientation east-west, and has Cr values that range from 125 to 599 ppm. The ArcGIS© interpretation has the anomaly extending east and northeast into Price and Ogden Townships, respectively, however these extensions are not supported by any data. The highest Cr values are located on the nose and east striking limb of the regional fold defined by intercalated ultramafic metavolcanic, mafic metavolcanic, felsic and ultramafic intusive rocks. Although it is difficult to assign samples with the highest concentration to a specific lithology, they appear to coincide with or occur in close

proximity to the ultramafic rocks. This Cr anomaly envelops the Karvinen and Halpenny gold ccurences, and gold values encountered in a DDH by Hemlo Gold (Fig. 35 and Table 1).

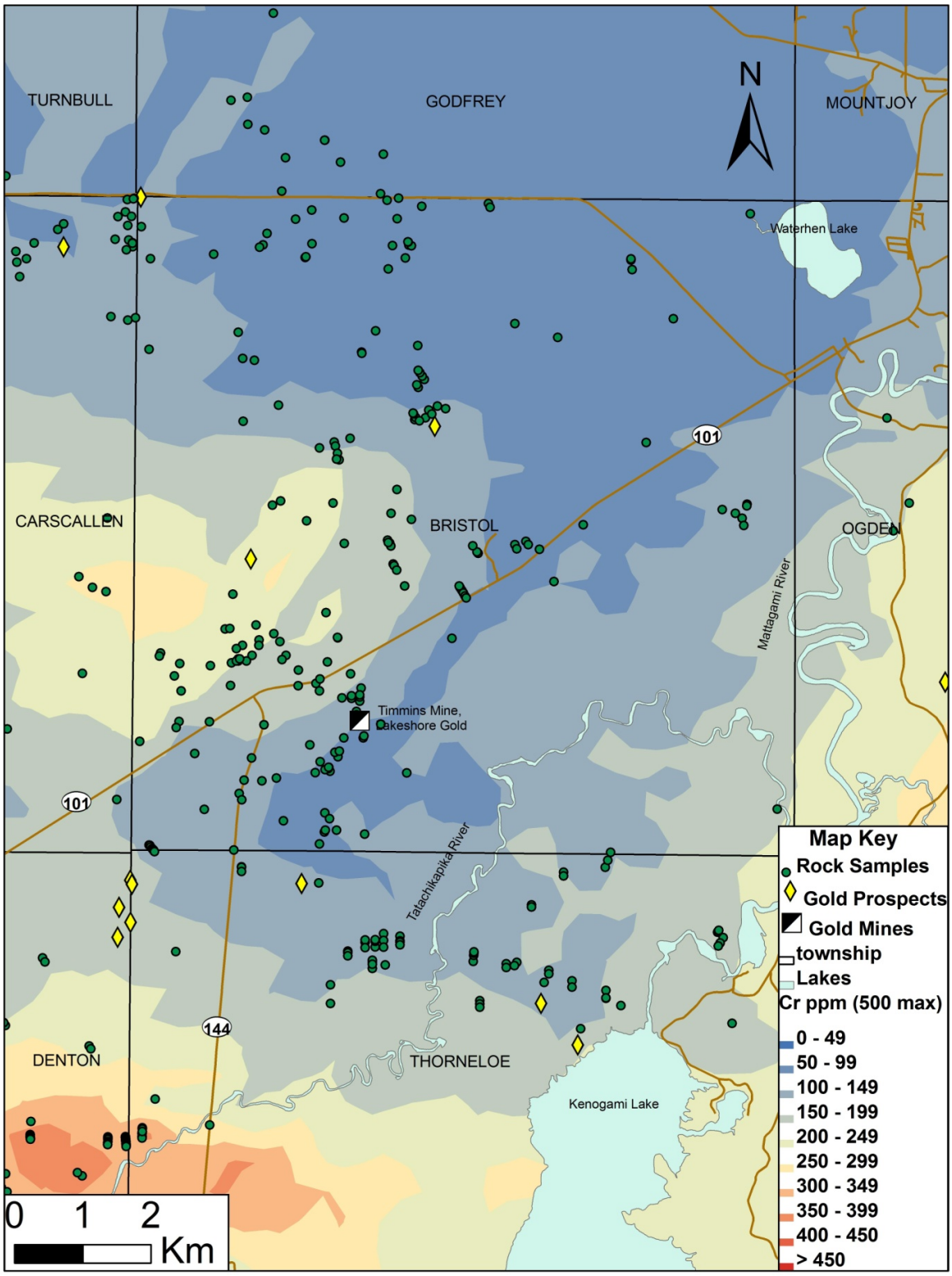

Figure 22 Kriged map of Chromium in ppm projected to surface

3.18 Lead (Pb)

The lead content of the country rocks in the study area and neighboring townships ranges from 0 to 47 ppm Pb. Typical Pb background concentrations are <6 ppm and more commonly <4 ppm. Contours of similar Pb values cross lithological boundaries and do not appear to be related to a specific rock unit (Fig. 23).

There is an oval-shaped Pb anomaly ~6 km by 2.5 km in area, with a “boot-shaped" limb extending 2 km to the north, located in southwestern Bristol and northwest Thorneloe Townships. This anomaly has values that range from 6 ppm to 12 ppm and is centered on a felsic intrusion 1 km south of the Lake Shore Timmins West Gold Mine. The anomaly extends to within <200 meters of the Timmins Mine, envelops the Rusk Mineralized Corridor, as well as the Red Porphyry gold zone in north-central Thorneloe Township (Fig. 35 and Table 1). The northwest limb of the anomaly has lower Pb values of between 6 ppm to 8 ppm, extends northwest across Highway 101 and 144. This limb lies north of the 144 Property.

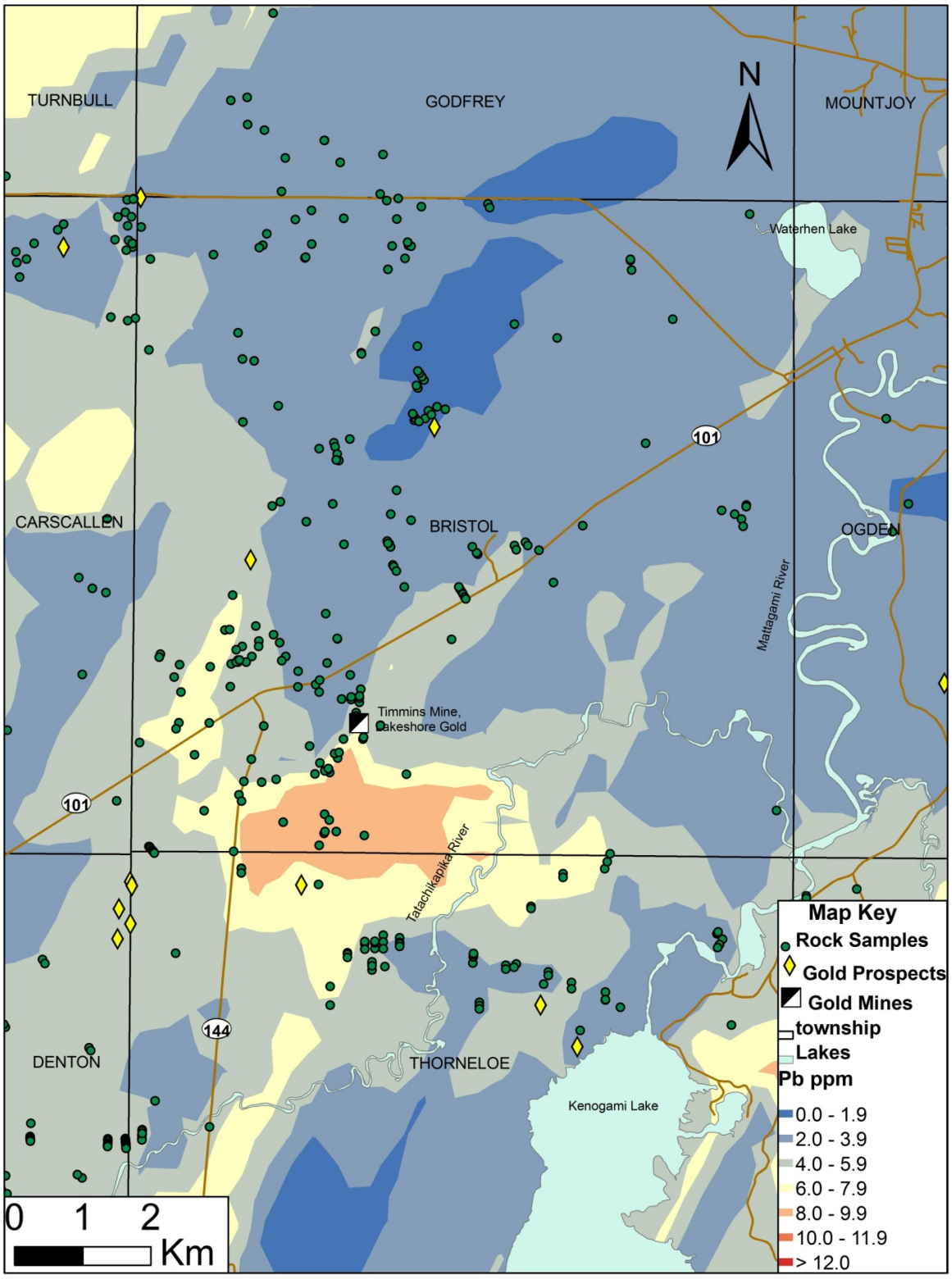

Figure 23 Kriged map of Lead in ppm projected to surface

3.19 Copper (Cu)

The Cu content of the country rocks in the Bristol-Thorneloe Study Area and neighboring townships range from 0 to 2000 ppm but are all >100 ppm and in such a limited range that in the study area there are no anomalous Cu values. The closest anomaly with high Cu values is located in central Godfrey Township >3.5 km from Bristol Township border. The low Cu values extend across lithological boundaries (Fig. 24).

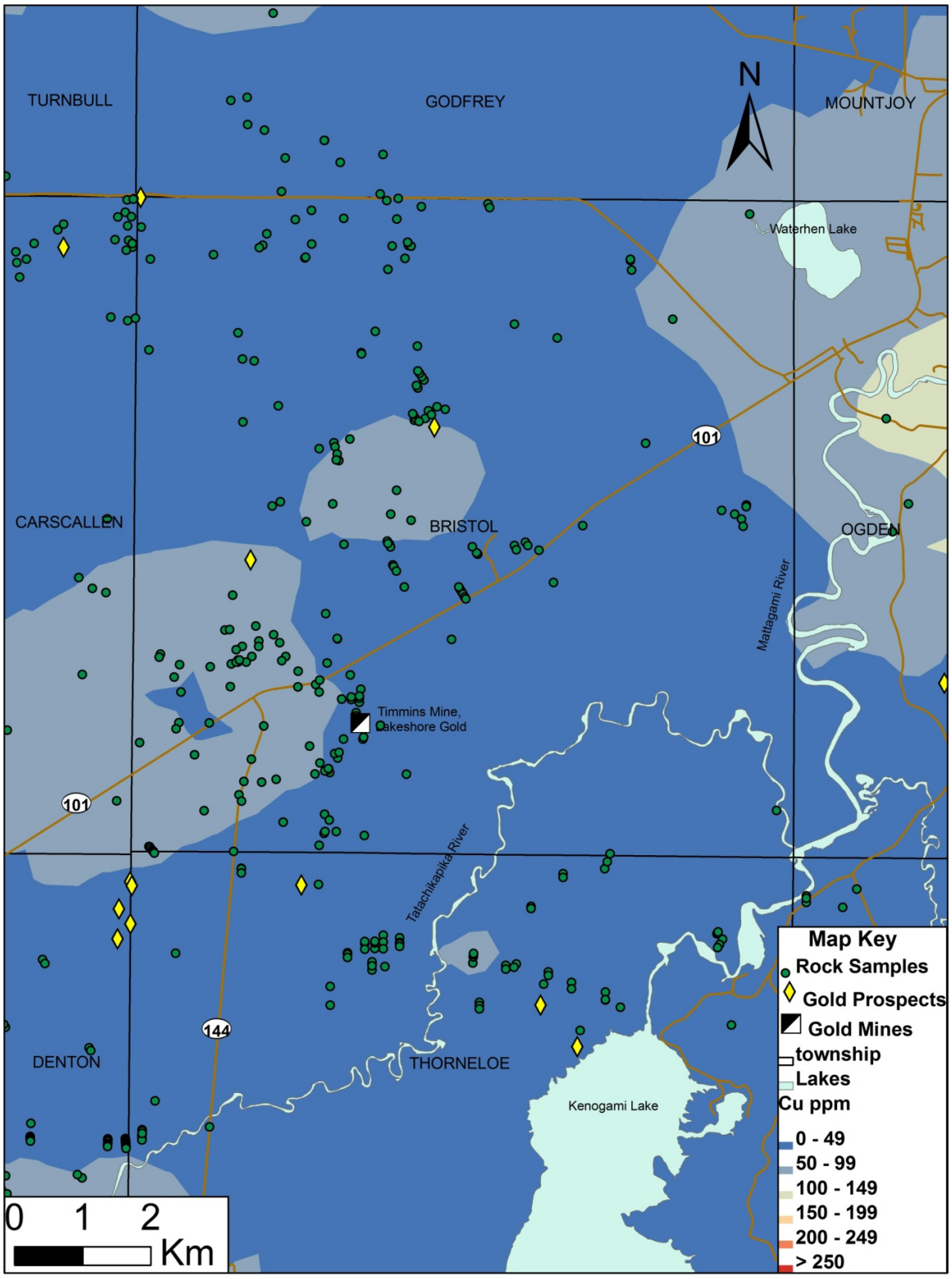

Figure 24 Kriged map of Copper in ppm projected to surface

3.20 Ishikawa Alteration Index

The Ishikawa Alteration (IA) Index (100*(MgO+K_2O)/(MgO+Na2O+CaO+K2O)) values measures the sericite alteration intensity of the country rocks in the study area and surrounding townships. IA index values range from 3.65 to 99.95% and has typical background values of 20 to 40% (Fig. 25). Sericite alteration varies throughout the region and crosses lithologic boundaries.

There is a 3 by 4 km northeast trending "oval-shaped" IA anomaly located along the center of the Bristol-Godfrey Township border that has IA values that range from 50 to 70% sericite. The northeast end of the anomaly has been interpreted by ArcGIS© to have a 1.75 km long northwest extension toward the Genex Mine but there are no data points to support this interpretation (Fig. 35 and Table 1). The "oval-shaped" anomaly is not directly associated with any known gold mineralization but the interpreted northwestern extension envelops both the Genex base metal mine and the Aconda gold deposit.

A second, "cone-shaped" IA anomaly is located in central Bristol Township 3.8 km north-northeast of the junction of Highway 101 & 144. The anomaly has an east-west orientation, measures approximately 575 by 240 m, and has typical IA values between 50 and 60%. The anomally is located on the contact between the mafic metavolcanic rocks of the Lower Tisdale and the felsic metavolcanic rocks of the Upper Kidd-Munro Formations. The anomaly is not associated with any known gold zones or prospects.

A third "fork-shaped" IA anomaly extends from east-central Denton to central Thorneloe Township. The anomaly is approximately 7.5 by 3 km with the highest values

lying beneath the southern end of Highway 144 in the study area. Sericitic alteration values in the area range from 50 to 70%. The IA anomaly is oriented east-west with the extension northeast and southeast, respectively. The anomaly is located in the center of Denton Township and coincides with the nose of the fold defined by thin intercalated ultramafic metavolcanic (Lower Tisdale Assemblage), mafic metavolcanic (Lower Tisdale Assemblage), clastic metasedimentary (Porcupine Assemblage), and the felsic intrusive rock units. The anomaly envelops the Keno gold zone and western end of the Thibault gold horizon.

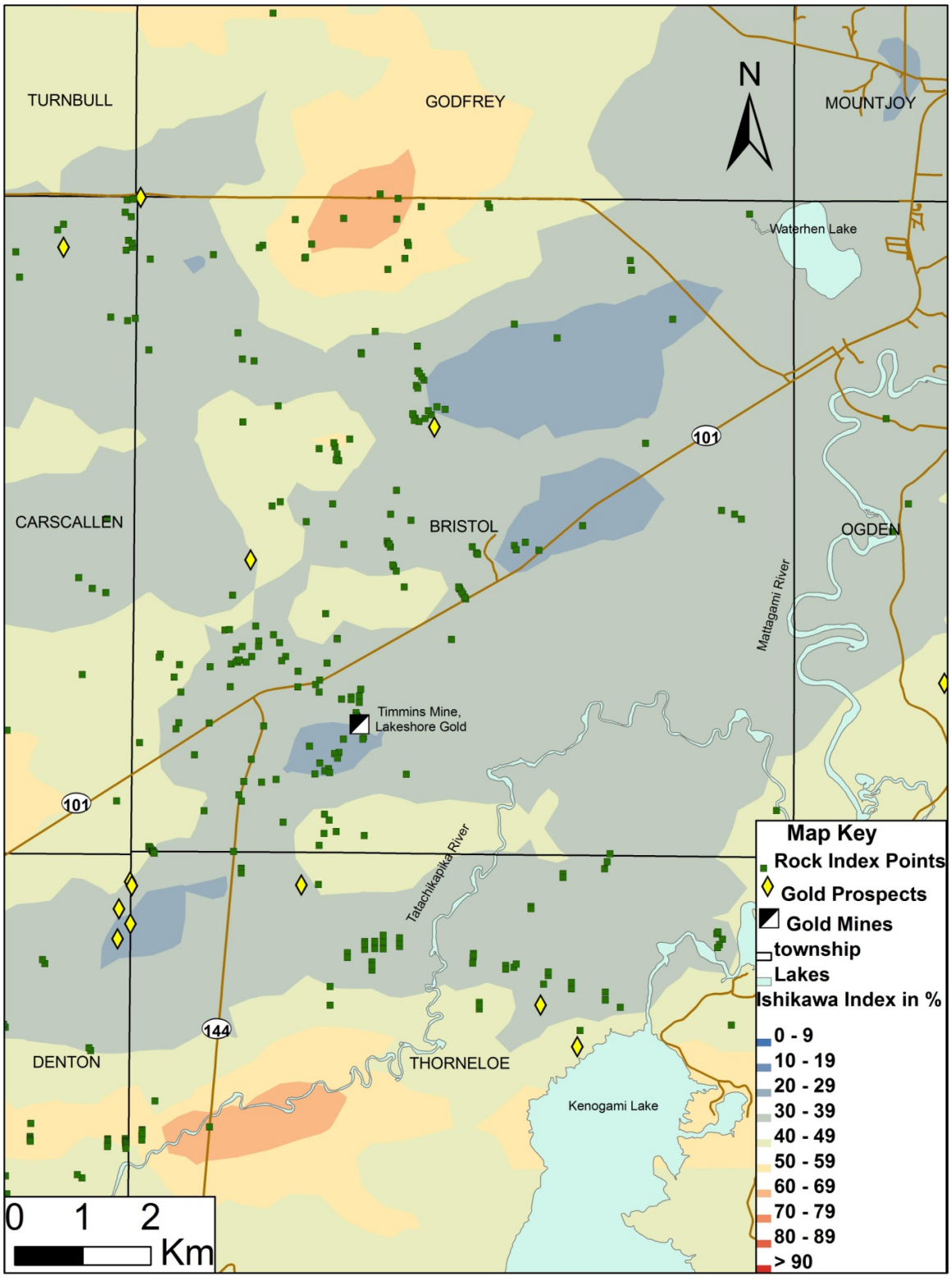

Figure 25 Kriged map of Ishikawa Index projected to surface

3.21 Chlorite Alteration Index

Chlorite Alteration Index ($(Mg,Fe)_3(Si,Al)_4O_{10}(OH)_2 \cdot (Mg,Fe)_3(OH)_6$) values of the country rocks in the study area and neighboring townships range from 0.62 to 99.96% (Fig. 26). Typical background chlorite alteration values in the area are 50 to 70%. Similar values extend across lithological boundaries and regional chlorite alteration appears to be pervasive throughout the Porcupine Mining Camp.

There is a 1.5 by 2.25 km, trapezoid-shaped anomaly with low chlorite alteration values, located in the northwest corner of Bristol Township. The chlorite alteration values in this southeast-oriented area are typically 30 to 40% and coincide with the felsic metavolcanic rocks of the Upper Blake River Assemblage. Also underlying the northwest extension of the anomaly are felsic intrusive and mafic metavolcanic rocks. There are no known gold-bearing zones or prospects that coincide with the low chlorite altered rocks.

There is a second, low chlorite alteration index anomaly located in the south-central Bristol and north-central Thorneloe Townships. The low chlorite alteration anomaly is approximately 2.5 by 1.5 km and has values that range from 30 to 40%. The anomaly coincides with the location of clastic metasedimentary rocks (Porcupine Assemblage) and the felsic intrusive rocks, near the contact between the Lower Tisdale and Porcupine Assemblages. The anomaly envelops the Rusk gold occurrence, ~700 m south of the Lake Shore Gold Timmins Mine, and <500 m from the Mahoney Creek gold occurrence #1 (Fig. 35 and Table 1).

High chlorite alteration extends east to west across Thorneloe Township and passes through the northern end of Kenogami Lake. The band has an average width of 1.5 km and typical chlorite index values between 60 to 69%. The higher chlorite values are hosted by the Timiskaming and Porcupine metasedimemtary, and mafic metavolcanic rocks of the Tisdale Assemblages. No known gold prospects or mines lie within the band.

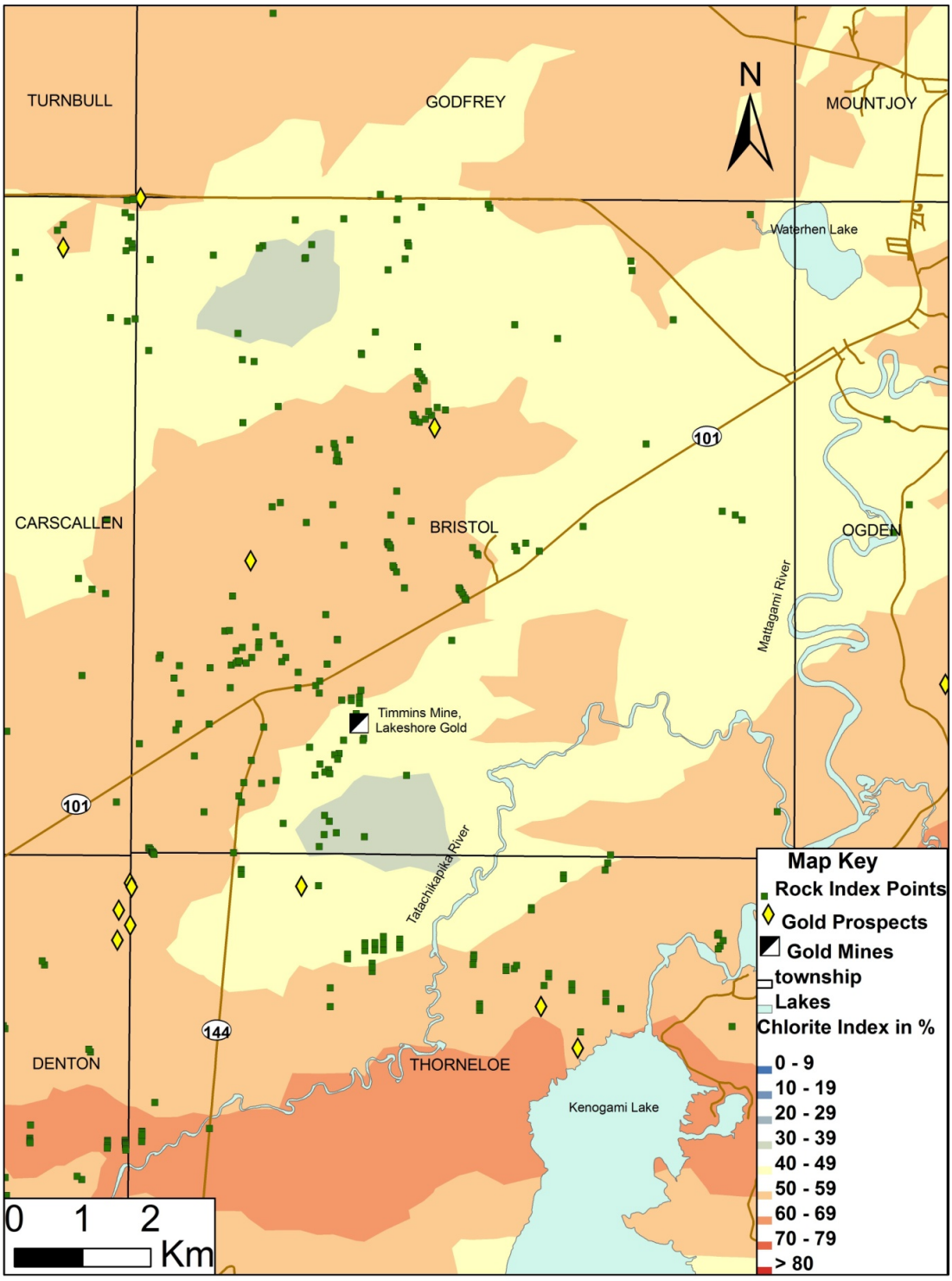

Figure 26 Kriged map of Chlorite Index projected to surface

3.22 Sericite/Chlorite Index (SCI)

The SCI alteration values are calculated using the formula (Sericite Index / (Sericite Index + Chlorite Index))*100 (Washington et al. 2009). This index measures the amount of sericite and chlorite alteration found in the Porcupine Mining Camp. The SCI values for the country rock in the study area (Fig. 27) range from 4.79% to 99.30% (Chlorite dominated and Sericite dominated, respectively). The SCI anomalies with high sericite alteration extend across lithological boundaries.

There is a 3 km diameter "bullseye-shaped" SCI anomaly in northern Bristol Township that coincides with the felsic metavolcanic rocks of the Upper Blake River Assemblage and a southeastern “finger” of a felsic instrusive unit in Bristol, Turnbull and Godfrey Townships (Fig. 27). The SCI values found in this anomaly range from 50 to 79% and are not associated with known gold mineralization in the area.

The second, dome-shaped anomaly measures 2 by 1.5 km and is located in southern Bristol Township and extends into Northern Thorneloe Township (Fig. 27). The anomaly is associated primarily with felsic intrusive rocks at the metasediment-mafic metavolcanic rock contact. The ArcGIS© interpretation that extends the anomaly into the clastic metasedimentary rocks of the Porcupine Assemblage is not supported by any sample data. The SCI values in the anomaly range from 50 to 79% with all samples located close to known gold mineralization and prospects in the study area. The higher SCI values occur within 50 m of the Rusk gold mineralized corridor, 50 m of the Mahoney Creek gold occurrence, and approximately 1 km south of the Lake Shore Timmins West Gold Mine (Fig. 35 and Table 1).

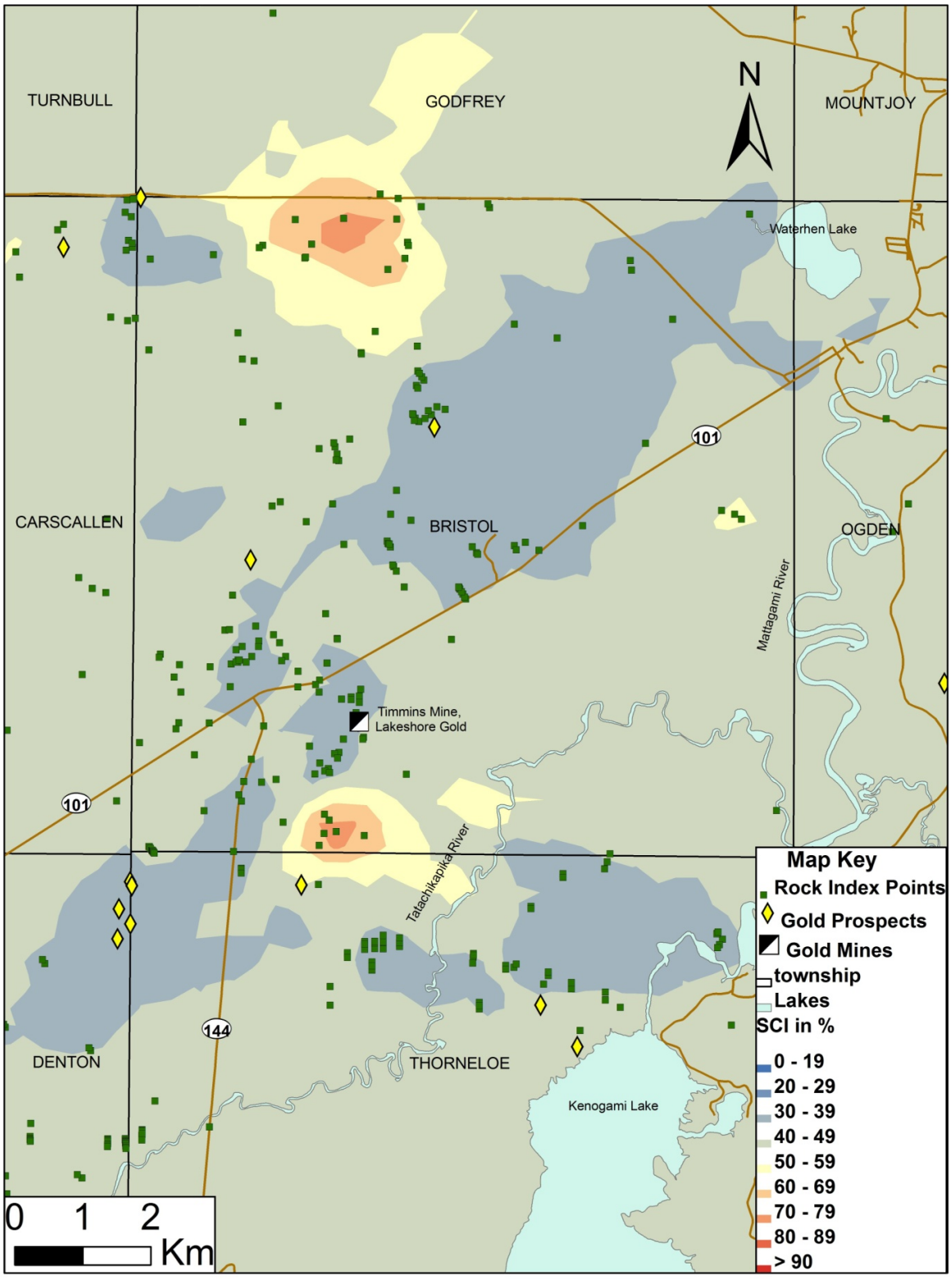

Figure 27 Kriged map of Sericite Chlorite Index projected to surface

3.23 K/Al

The K/Al molar ratio (K(molar)/Al(molar)) of the country rocks in the study area range from 0.00 to 8.05 (Fig. 28). Ratios were capped at a maximum value of 0.75 in order permit proper contouring of anomalies that contained very high value(s). This ratio is used to identify alteration by comparing the concentration of mobile potassium with immobile aluminum in the rocks. There are two anomalies with high values that are associated with the felsic metavolcanic rocks of northern Bristol Township and the felsic intrusive rocks in southern Bristol and northern Thorneloe Townships. The K/Al anomalies with values that range from 0.18 to 0.75, occur in the same locations as the SCI anomalies but are generally larger in area than the SCI anomalies (e,g, K/Al anomalies can be 3 to 4 times larger than its SCI counterpart). The southern anomaly is approximately 4 km long and 2 km wide and extends west to Highway 144 and into the Lower Tisdale mafic metavolcanic rocks. The association of the K/Al anomalies with known gold mineralization and prospects is similar to that of the SCI anomalies. However, the southern K/Al anomaly has a limb that is broader than the SCI anomaly and envelops the Golden River West, No. 14, and Red Porphyry gold zones.

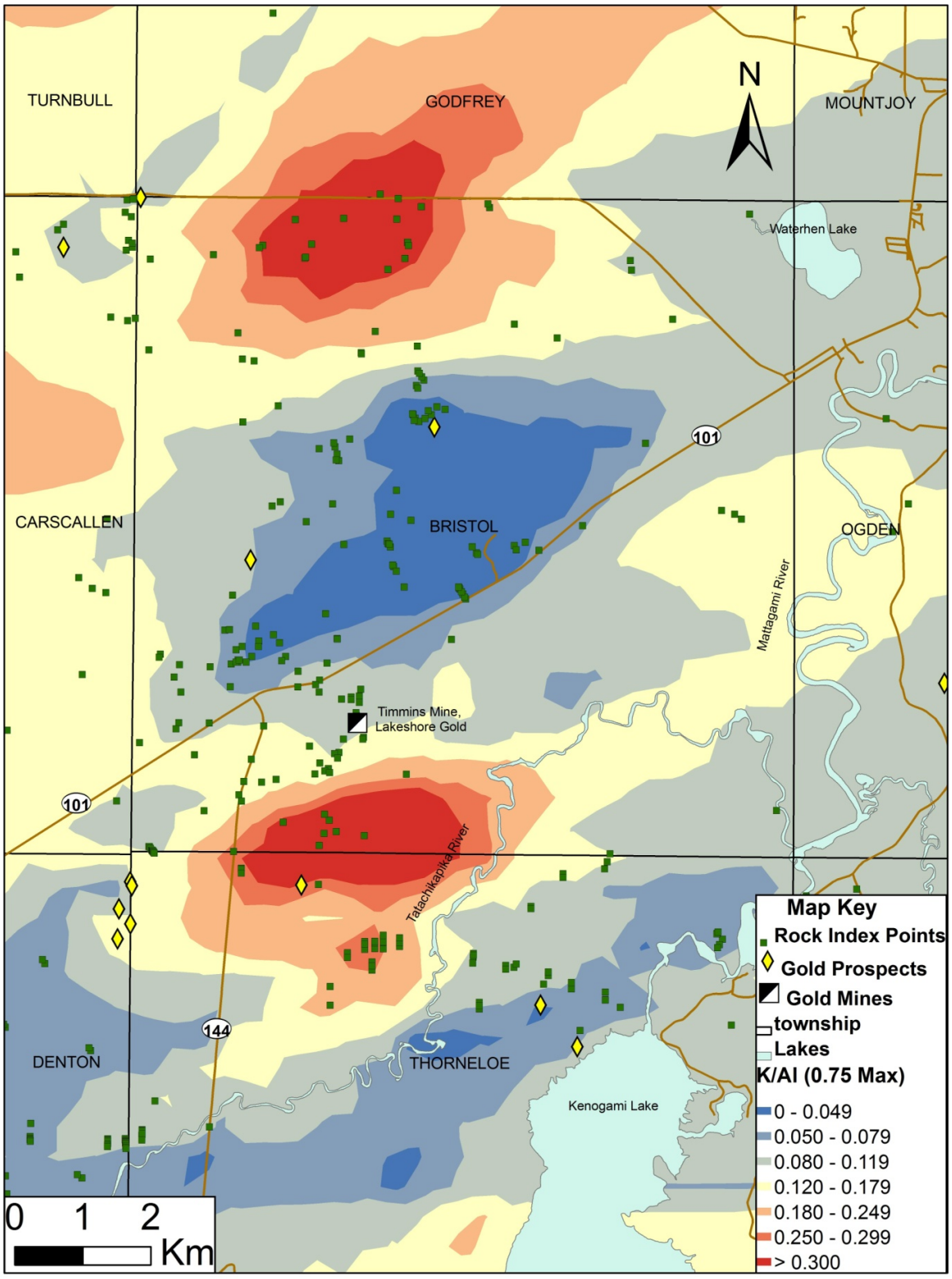

Figure 28 Kriged map of K/Al Index projected to surface

3.24 Fe/Fe+Mg (Fe#)

The Fe# (Fe/Fe+Mg) values of the country rocks in the study area and surrounding townships ranges from 0.14 to 0.99 (Fig. 29). This number enables the identification of iron and magnesium concentrations in the country rocks. Similar values extend across lithological boundaries with low zones (magnesium-rich).

A discontinuous “S-shaped" low Fe# anomaly (high Mg#) occurs in central Bristol Township and extends into southeastern Carscallen Township. The anomaly is approximately 9.5 by 3.5 km in area and trends from northeast to southwest. Values found in this anomaly range from 0.0 to 0.64 and coincide with the mafic metavolcanic rocks of the Lower Tisdale, and the felsic metavolcanic rocks of Upper Kidd-Munro and Deloro Assemblages. This anomaly lies ~2.5 km northwest of the Lake Shore Timmins West Gold Mine. The southern extension of this Fe# anomaly envelops the North Rankin nickel occurrence (contains Ni, Au, Cu) and lies <1 km north of the 144 Property gold prospect in northeast Denton Township (Fig. 35 and Table 1).

Along the southern edge of the study area a second band with low values extends from central Denton to Price Township. This low value band is oriented east to west and is approximately 15 km by 2 km in area. Average values range from 0.0 to 0.59. It appears to be hosted by the southern limb of the fold with low Fe/Fe+Mg values being associated with the interbedded ultramafic volcanic and intrusive units of the Lower Tisdale Assemblage. It is important to note that east of Highway 144, the band of low values is largely interpretted by ArcGIS©, with no sample data supporting the extension

of the anomlay into Price Township. This band of low values is not associated spatially with areas that contain known gold mineralization.

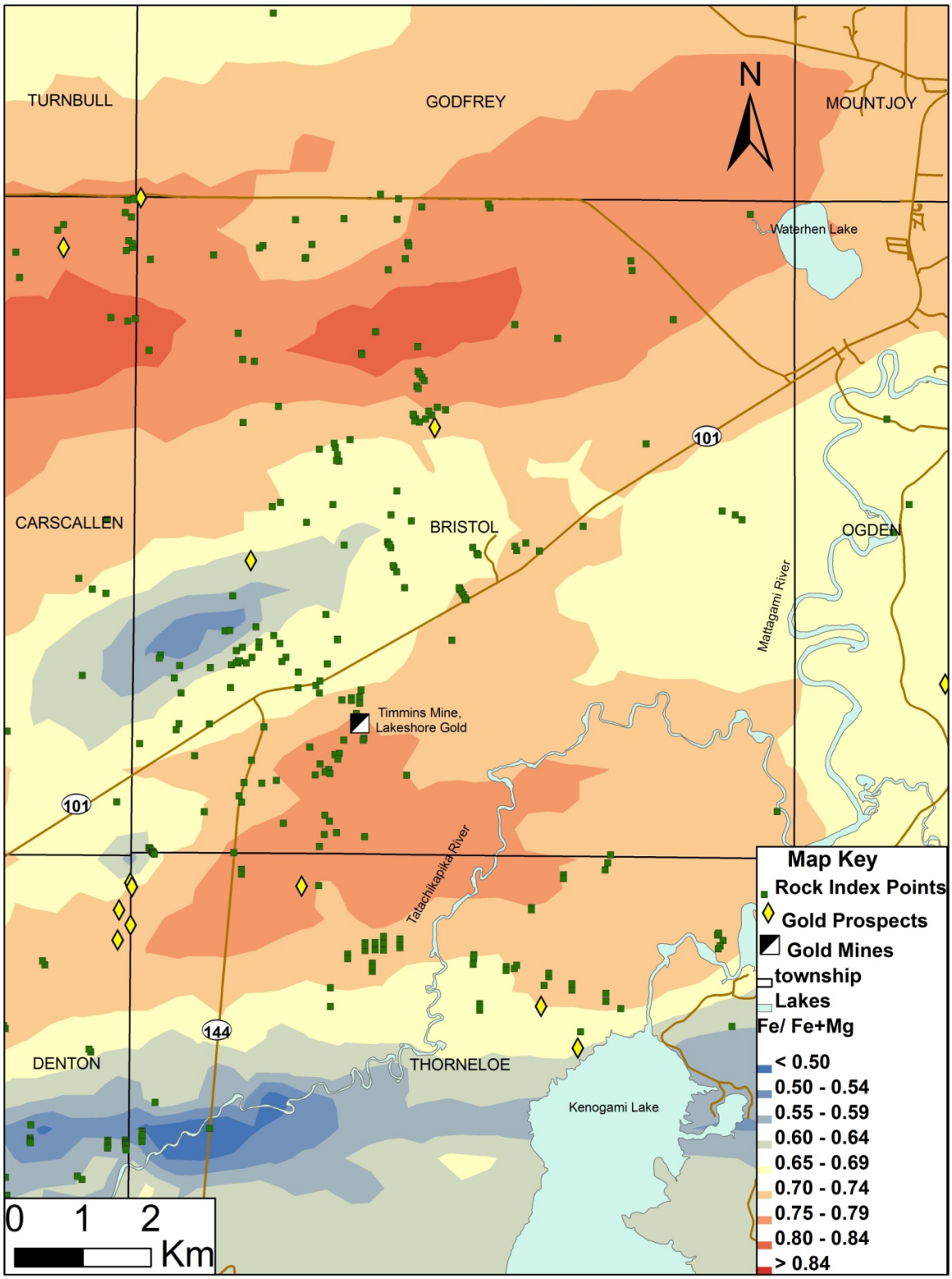

Figure 29 Kriged map of Fe / Fe+Mg Index projected to surface

3.25 Chlorite-Carbonate-Pyrite Index (CCPI)

The CCPI values for the country rocks in the study area and the surrounding townships range from 0.6 to 100. The typical background values are >60, however it varies throughout the study region. Similar values cross lithological boundaries (Fig. 30).

A large “C-shaped" anomaly is located in the center of the study area, stretching from northeast Bristol to central Denton then bending to east-central Thorneloe Townships. The anomaly is conformable to the local geology and roughly follows the mafic metavolcanic rocks of the Lower Tisdale Assemblage that extends across Bristol Township. In Thorneloe Township, the higher CCPI values are hosted primarily by metasedimentary rocks of the Porcupine and Timiskaming Assemblages found in the southern end of the study area. Typical values found here range from 70 to 85. The anomaly envelops nearly all known gold mineralized zones and prospects in the study area. It is important to note that many of the active and current prospects are located in the enclosure of the “C” structure that has similar CCPI values. The Timmins Mine, Rusk Occurrence, Golden River West, Sandhill Porphyry, No.14, Kapika, and Golden River East Zones all associated with CCPI values of 70 to 80 (Fig. 35 and Table 1).

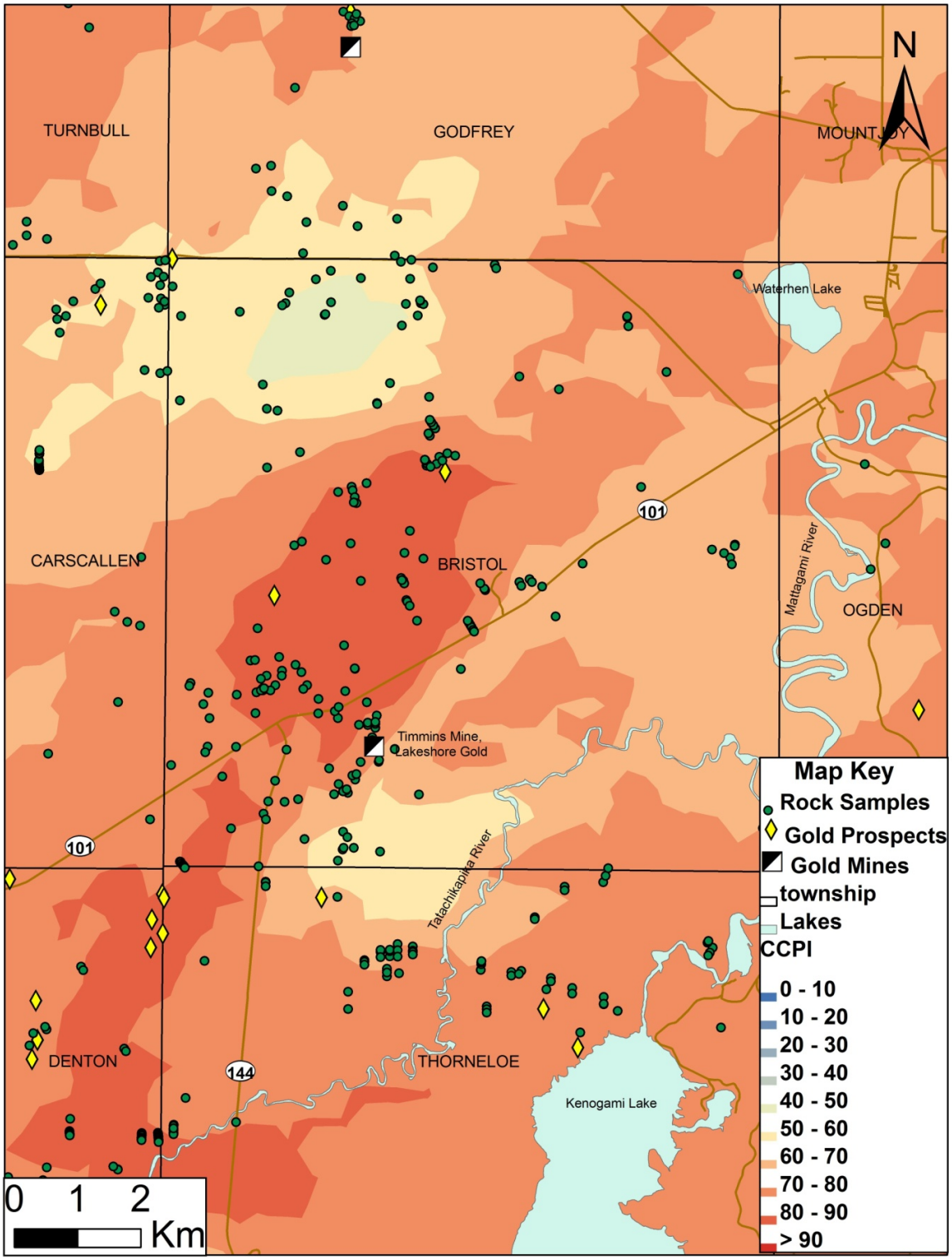

Figure 30 Kriged map of Carbonate Chlorite Pyrite Index projected to surface

3.26 Carbon Dioxide (CO_2)

Carbon dioxide (CO_2) values in the Bristol-Thorneloe Study Area and neighboring townships range from 0.05 wt% to 32.06 wt%. CO_2 content of the rocks is commonly used as an alteration indicator and can be used in conjunction with other constituents to determine the type and intensity of carbonate alteration. Typical background values in the study area are ≤4.0% with similar values crossing lithological boundaries.

A 7.5 km by 1.7 km oval-shaped anomaly extends from central Bristol to east-central Carscallen Township (Fig. 31). The anomaly has a strike of ~70° and CO_2 concentration of >8.0 wt%. The anomaly location coincides with the lithologic contact of the Tisdale mafic metavolcanic, and Kidd-Munro and Blake River felsic metavolcanic rocks. The anomaly envelops the McKinley & Molesky Claim 8405, and is located ~260 m north of the North Rankin Nickel 65-7 (Ni, Au, Cu) occurrence.

A 2.0 km by 0.9 km “oval-shaped” anomaly in southern Bristol Township is centered on the Lake Shore Timmins West Gold Mine and the northern tip of the Rusk Mineralized Corridor. The anomaly has a strike of ~85° and crosses lithological boundaries. Typical values found in the anomaly are 4.0 to 8.0 wt%. The CO_2 anomaly is hosted by the same complex geology setting as the gold values and lies on the Tisdale mafic metavolcanic – Porcupine metasediment rock contact. A 2.2 km by 1.1 km oval-shaped CO_2 anomaly is located in the north-central part of Thorneloe Township. This east-west oriented anomaly contains four values with an average CO_2 value of 12.76 wt% and is hosted by the Porcupine metasedimentary rocks. This alteration anomaly coincides with the gold zone located in north-central Thorneloe

Township. The anomaly also envelops the Golden River East, Golden River West, Kapika, No. 14, and Sand Hill Porphyry mineralized zones (Fig. 35 and Table 1).

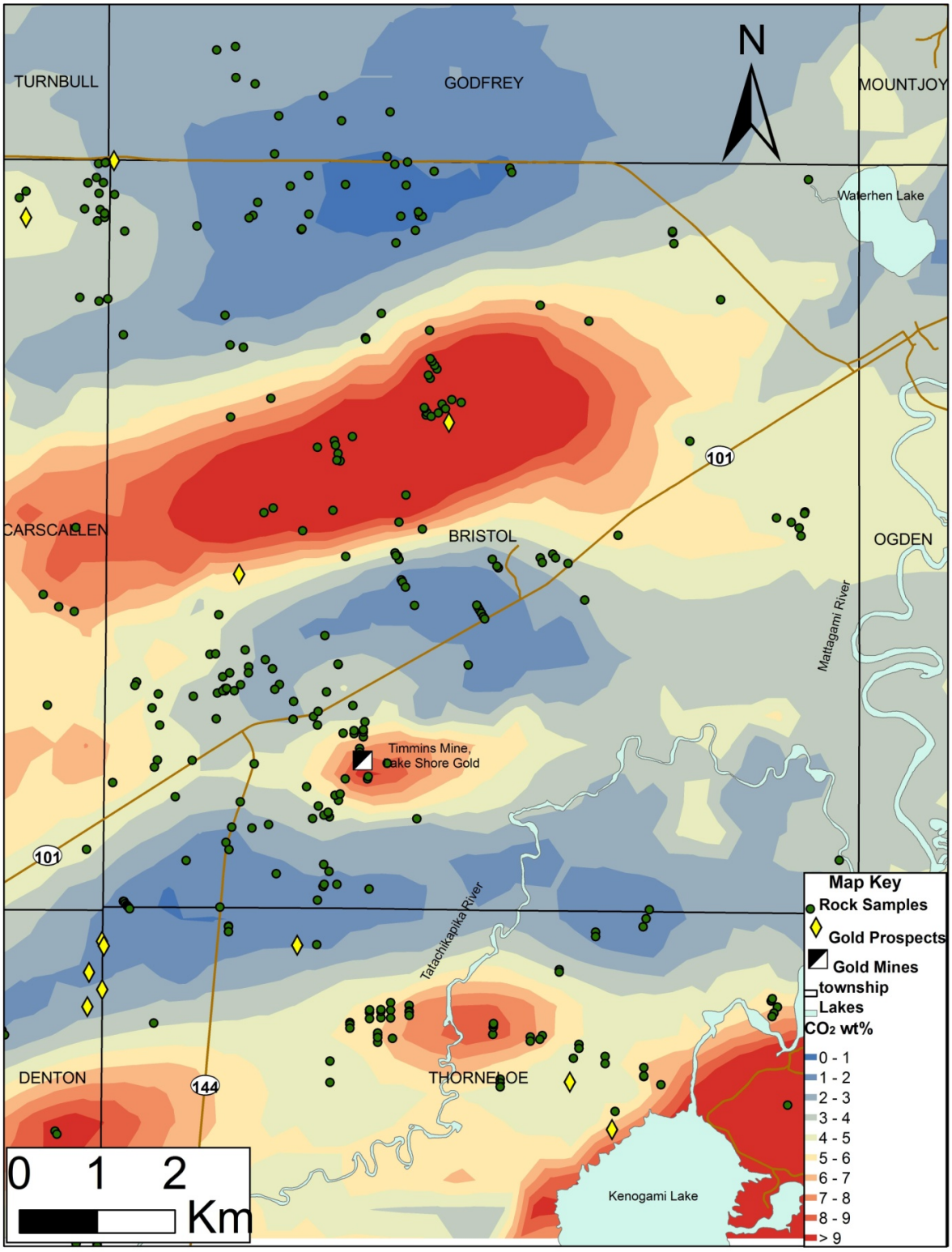

Figure 31 Kriged map of weight percent CO_2 projected to surface

3.27 CO_2/CaO

The CO_2/CaO molar ratio values is a useful method to determine type and intensity of alteration in wallrock in and around hydrothermally altered gold deposits. This method is implemented by taking atomic abundance of carbon dioxide (CO_2) over the atomic abundance of calcium oxide (CaO), that is used to determine the alteration type (Davies et al. 1982). In the Porcupine Mining Camp the carbonate alteration is an important indicator for mineralized systems, where values >1.5 occur proximal to gold-bearing veins where there is a transition from calcitic to dolomitic alteration (Davies et al. 1982). CO_2/CaO values in excess of 2.0 indicate the presence of ferroan dolomite, and 3.0 is ankerite to siderite altered (Davies et al. 1982).

The CO_2/CaO values of the country rocks in and around the study area ranges from 0.0 to 46.9(Fig. 32). The highest values were cut to 3.0 in order to enable accurate contouring of the data. There is a ~4 km wide band of values <1.00 that stretches from northeastern Denton to east central Bristol Township and is thought to coincide with the location of unaltered country rocks (≤0.5) to calcite altered (~1.0)(Davies et al. 1982). This zone crosses lithological boundaries where it is hosted by the mafic volcanics of the Lower Tisdale Assemblage, clastic metasedimentary rocks of the Porcupine Assemblage, and felsic to intermediate intrusive bodies. The low CO_2/CaO band envelop the Lake Shore Timmins West Gold Mine and the Rusk Mineralized Corridor.

A 10 km by 7 km “arrow head-shaped" anomaly with CO_2/CaO values >1.5 is found in the northwest section of the study area. The anomaly has a southwest orientation that is conformable with the local geology. It crosses lithological boundaries and is hosted by

felsic metavolcanic rocks of the Upper Kidd-Munro, Upper Blake River, mafic metavolcanic rocks of Lower Tisdale Assemblages, and felsic to intermediate intrusive suite. The average values indicate carbonate alteration that transitions from calcite to dolomite on the periphery, and consists of a mix of dolomite and ankerite in the center. The anomaly envelops the Kennco and McKinley & Molesky Claim 8405 gold occurences, and lies within 400 m of Larchmont 65-5, and North Rankin Nickel (Ni, Au, Cu) occurences (Fig. 35 and Table 1).

A band of carbonate alteration occurs at the southern end of the study area and extends east-west across Thorneloe Township. Values range from transitional calcite to dolomite at the periphery (~1.5) to ones that are consistent with the presence of iron carbonate (>2.25) (Davies et al. 1982). The band is hosted by Porcupine clastic metasedimentary, Timiskaming chemical sedimentary, and Lower Tisdale mafic metavolcanic rocks. The Destor-Porcupine Fault Zone passes through the center of a carbonate alteration zone that has the strongest carbonate alteration north of the fault. This dolomite/ankerite alteration type coincides with auriferous zones in the Porcupine Camp. The alteration is similar to that found at other gold deposits in that all samples were collected from the Porcupine Assemblage.

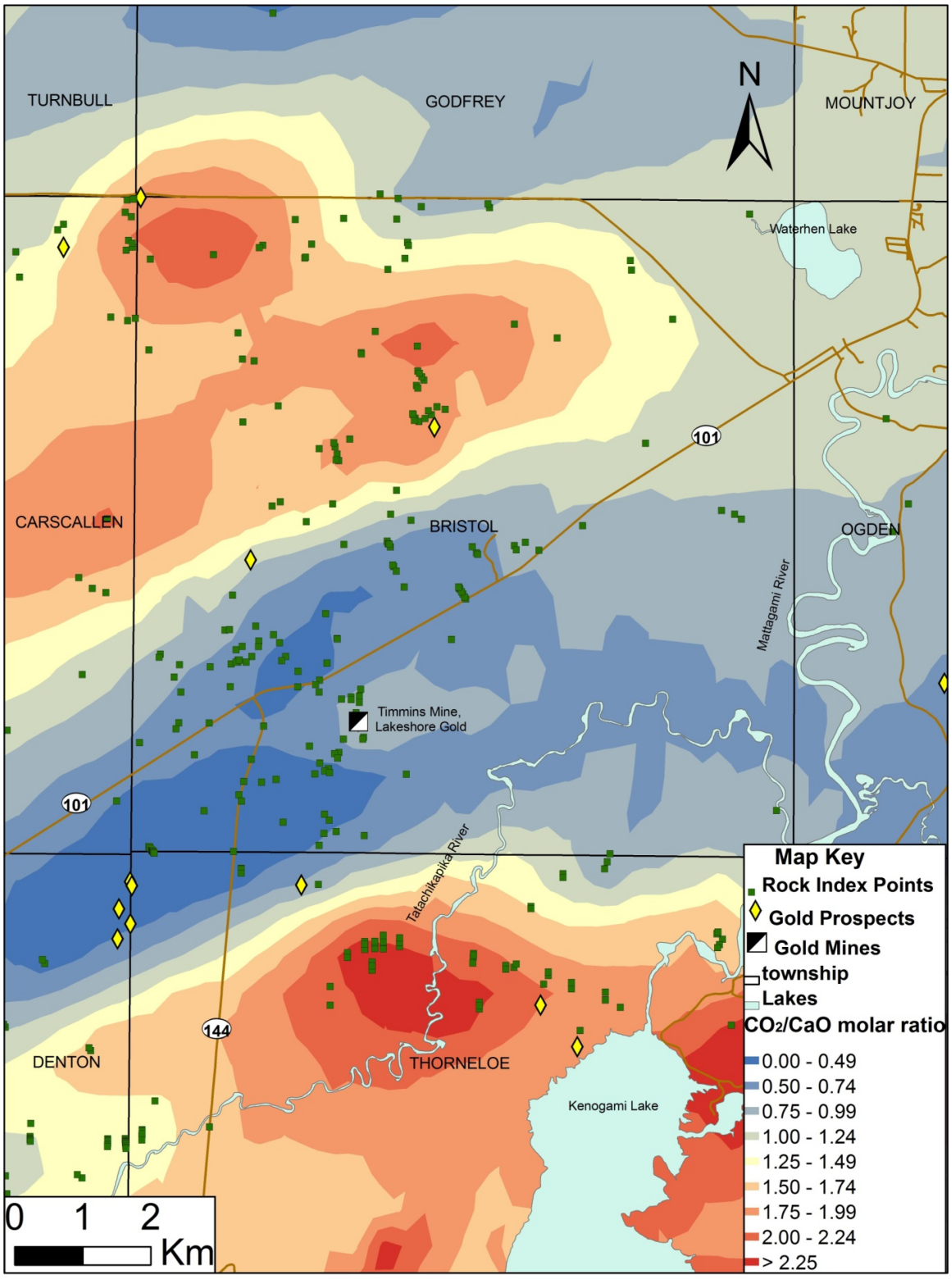

Figure 32 Kriged map of CO_2/CaO molar ratio values projected to surface

3.28 $\delta^{18}O$ Oxygen Isotope

The $\delta^{18}O$ isotope values of the veins in the study area range from 9.87‰ to 18.28‰ (Fig. 33). The overall trend of the $\delta^{18}O$ values is a "V" shape that stretches from northern Bristol to eastern Thorneloe Township, with a southwest-northeast orientation. Similar values cross lithologic boundaries and the highest values occur in the metasedimentary rocks of northern Thorneloe and southern Bristol, and the felsic metavolcanic rocks in northern Bristol Townships.

Higher $\delta^{18}O$ values that range from 14.0‰ to >15.0‰ are located in southwestern Bristol and northern Thorneloe Townships. The "wedge–shaped" anomaly has a northwest-southeast orientation that is approximately 5 km by 4.5 km. The anomaly is predominantly hosted by metasedimentary rocks of the Porcupine and Timiskaming Assemblages, and felsic to intermediate intrusive rocks. Contours that extend into volcanic rock units are artifacts generated by ArcGIS© and are not supported by sample data from the veins. The higher $\delta^{18}O$ values (>13.5‰) are comparable to those measured in gold-bearing quartz veins elsewhere in the Porcupine Mining Camp (van Hees et al., 1998). Similar $\delta^{18}O$ values were found in gold-bearing quartz veins at the Dome Mine on the east end of the Porcupine Camp (Kerrich and Hodder 1982). The higher $\delta^{18}O$ anomaly envelops the Golden River East, Golden River West, No.14, Kapika, Red Porphyry gold mineralized prospects, the Lake Shore Timmins West Gold Mine and the Rusk Mineralized Corridor (Fig. 35 and Table 1). The higher $\delta^{18}O$ values here are associated with past and present gold exploration prospects.

A second north-south orientated "hour-glass" shaped anomaly is located in north-central Bristol Township. The anomaly is approximately 3.2 km by 2.7 km and has $\delta^{18}O$ values that range between 13.5‰ and 14.5‰. The anomaly is hosted primarily by the felsic metavolcanic rocks of the Upper Blake River assemblage. The southeastern edge of the anomaly extends into the mafic metavolcanic rocks of the Lower Tisdale Assemblage, however it is not supported by sample data. The $\delta^{18}O$ anomaly is located approximately 330 m north of the McKinley-Molesky Claim 8405.

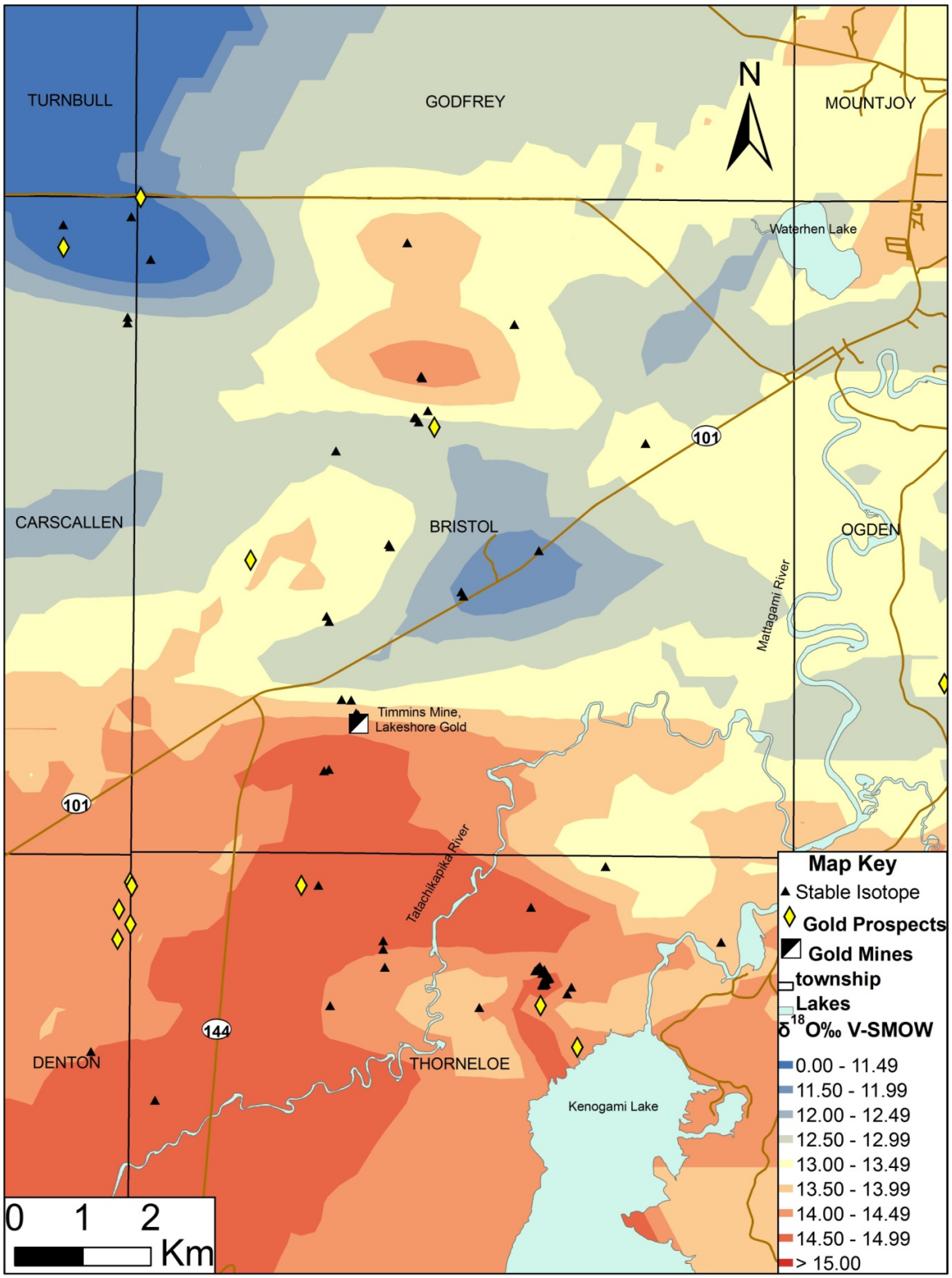

Figure 33 Kriged map of $\delta^{18}O$ ‰ projected to surface

3.29 δ^{13} Carbon Isotope

Along with the $\delta^{18}O$, the $\delta^{13}C$ values were obtained by analyzing carbonate separated from quartz veins collected throughout the study area from drill core and outcrop samples. These values can be used to characterize the local fluids and find $\delta^{13}C$ values associated with gold mineralization (Fig. 34).

The $\delta^{13}C$ values of vein carbonates ranges from -25.63‰ to -1.76‰ in the study area and neighboring townships. Typical background values are >-7.5‰ where similar values cross lithologic boundaries of the quartz veining wallrock (Fig.35).

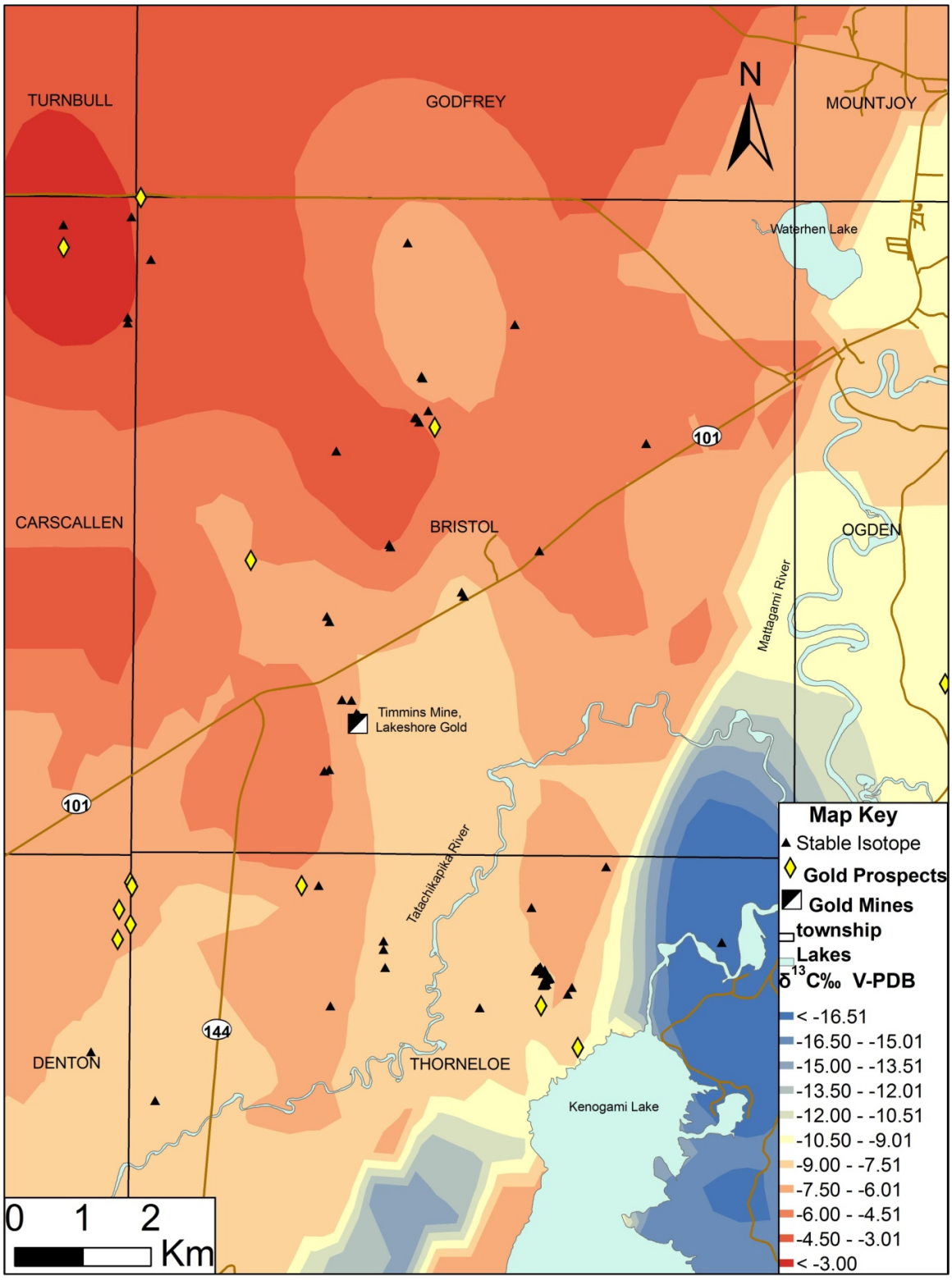

Figure 34 Kriged map of $\delta^{13}C$ ‰ projected to surface

3.29 δ^{13} Carbon Isotope - Cont'd

There is an anomaly defined by a very low $\delta^{13}C$ value that occurs in the southeast corner of the study area. The anomaly is a large concentric oval that has $\delta^{13}C$ values <-12.1‰ and is generated by a single sample point with a $\delta^{13}C$ value of -25.63‰. The north-south oriented anomaly is 3.8 km by 7 km in area. The anomaly coincides with the clastic metasedimentary rocks of the Porcupine Assemblage and is interpretted to extend into the chemical sedimentary rocks of the Timiskaming and mafic metavolcanic rocks of the Tisdale Assemblages. The zone does not have an association with any known gold prospects or deposits.

There is an oval-shaped northwest – southeast oriented anomaly located near the north-central border of Bristol Township that has $\delta^{13}C$ values between -10.5‰ to -9.1‰. This anomaly is an artifact of the ArcGIS© program because it is not supported by any sample data. Given that the anomaly is not supported by any analytical data, the fact that this anomaly coincides with felsic metavolcanic rocks of the Upper Blake River Assemblage but does not coincide with any gold mineralized prospects or mining activity, probably has no significance.

A second, 3.3 km by 2.1 km north-south oriented anomaly with low $\delta^{13}C$ values (-12.5‰ to -9.1‰) occurs approximately 1.8 km east of the junction of Highway 101 & 144 and is also an artifact of the ArcGIS© program because it is not based on any analytical data. The anomaly coincides with the clastic metasedimentary rocks of the Porcupine Assemblage. The surrounding samples that are considered for the anomaly lie within neighboring lithologies. It is within 330 m and 550 m of the Lake Shore

Timmins West Gold Mine and Rusk Mineralized Corridor, respectively (Fig. 35 and Table 1).

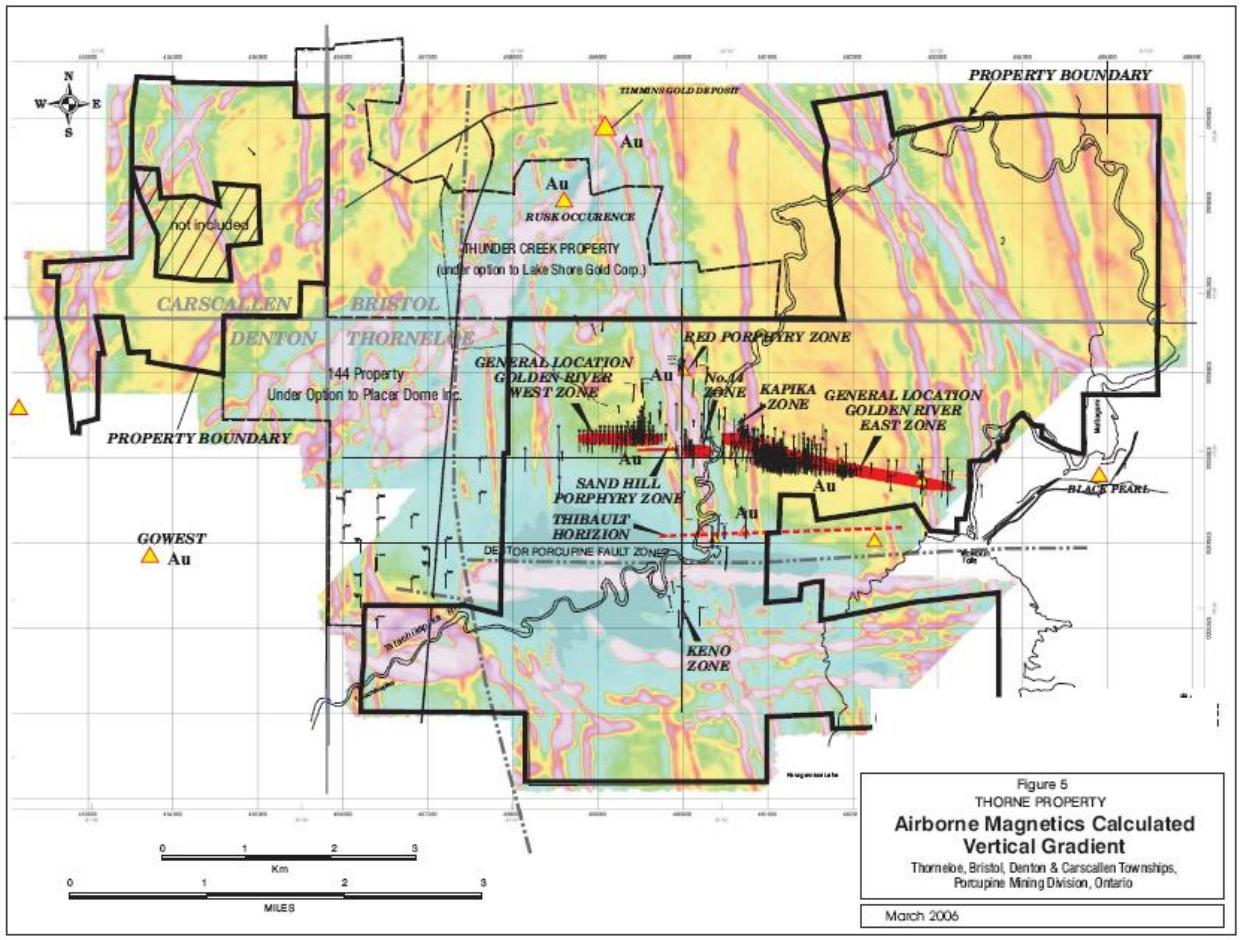

Figure 35 Bristol-Thorneloe Study Area gold occurrence location map. From Cavey 2006.

Gold Occurrence	UTM-Easting	UTM-Northing
Battle Mountain DDH MC97-26	455640	5355670
Battle Mountain DDH MC97-9	453410	5356750
Battle Mountain DDH MC97-21	455660	5356110
Battle Mountain DDH MC97-22	455825	5356510
Battle Mountain DDH MC97-18	455830	5355890
Battle Mountain DDH MC97-20	455850	5356450
Halpenny R.E.	453765	5353903
Hemlo Gold DDH CC95-13	453825	5354830
Hemlo Gold DDH CC93-1	453850	5354210
Pyrotex C-24	454050	5371318
Larchmont 65-5	454848	5365816
KennCo	455982	5366547
North Rankin 65-7	457593	5361230
Manhoney Creek Occurrence #1	458339	5356459
Aconda 75-A	458800	5370450
Genex Mine	458802	5369893
McAuley-Brydge	459173	5358866
McKinley & Molesky Claim 8405	460294	5363181
Esso Kapika T-36	461850	5354700
Darry	462392	5354089
Prospectors Alliance PA97-2	452270	5355540
Prospectors Alliance PA97-4	451950	5356025
Prospectors Alliance PA97-5	451920	5356090
AUMO	452000	5356200
AUMO no.3	452200	5355650
Cripple Creek Zone 17	452999	5354330
Shankman	451480	5357450

Table 1 UTM Coordinates for all other gold occurrences covered that are not included in Fig. 35. Locations form Ayer et al. 2005.

Chapter 4 – Discussion

4.0 Overview

This study of Bristol and northern Thorneloe Townships, west of the historic Porcupine Mining Camp, was conducted to gain an understanding about the lithogeochemical alteration associated with gold mineralization as well as the fluid history of the area. The study set out to determine the nature and size of alteration zones, their relative intensity and determine if the wallrocks near gold mineralization have the same type of alteration as occurs in mesothermal deposits found elsewhere in the Porcupine Mining Camp. While conducting this study, geochemical anomalies associated with gold mineralization were evaluated to determine if they could be used as a vector to aid in the exploration for an extension of the Lake Shore Gold Deposit or help find gold deposits elsewhere in the Porcupine Mining Camp.

Determining the nature of the parent material that makes up the six major rock units that have been mapped in the study area, as well as their alteration, was accomplished by employing the major, minor and trace element analyses and calculations that measured various indexes to establish the type and extent of alteration. The geochemical composition of each unit can be affected differently by hydrothermal fluids and might create localized anomalies that can be overlooked when comparing one lithological unit with another. It is also important to be able to recognize lithologically similar rock units present in the study area because depletion or enrichment of mobile and immobile elements can obscure the real nature of the lithologic unit.

In addition to recognizing individual rock units and their alteration characteristics, the whole rock geochemical data set was used to find alteration halos, some of which, cross lithological boundaries in the study area. These anomalous might identify new exploration targets, or extensions of known gold deposits and prospects in the Porcupine Camp.

Using $\delta^{13}C$ and $\delta^{18}O$ stable isotopic ratios obtained from quartz, carbonate and tourmaline provided information about the fluid history of the study area. These values provided a temperature range for the formation of quartz-carbonate veining calculated using an empirical method developed Blamart (1991). This properly classified the hydrothermal fluid in the study area. The oxygen isotope values were also employed to identify gold-bearing quartz carbonate veining. This was done by comparing the $\delta^{18}O$ distribution with those in gold-enriched zones in Bristol-Thorneloe Townships, as well as using similar $\delta^{18}O$ indicator values at other mesothermal gold deposits. Coupling the isotope values with major and trace element alteration halos of the country rocks might also permit the identification of new exploration targets

4.1 Rock Unit Dependent Elements

Elements that are characteristic of individual rock units in the study area include iron, titanium, chromium, magnesium, aluminum, nickel, scandium, copper, yttrium, and zirconium. The abundance of these elements compares well with published data obtained from unaltered rock units found in the Porcupine Mining Camp and elsewhere in the Canadian Shield (Pyke, 1982)

The metavolcanic rocks and related intrusive equivalents in the Bristol-Thorneloe study area consist of both calc-alkaline and tholeiitic suites that have compositions that range from rhyolitic to ultramafic in composition (Fig. 36). The composition of these rocks correspond closely with published geochemical data for comparable rocks found elsewhere in the Porcupine Mining Camp (Pyke, 1982). The close correlation between the composition of the study area rocks and those analyzed by Pyke (1982) indicates that Fe, Ti, Mg, and Al are primarily associated with the parent material, and not hydrothermally transported. The existence of both calc-alkaline and tholeiitic rock suites in the study area is evident in the Blake River Assemblage at the Genex Mine, located 3 km north of Bristol Township (Hocker, 2005), and is consistent with bimodal volcanism typical of marine rift – and subduction-style tectonic environments like that found in the Porcupine Mining Camp (Ferguson 1957; Thurston et al. 2008).

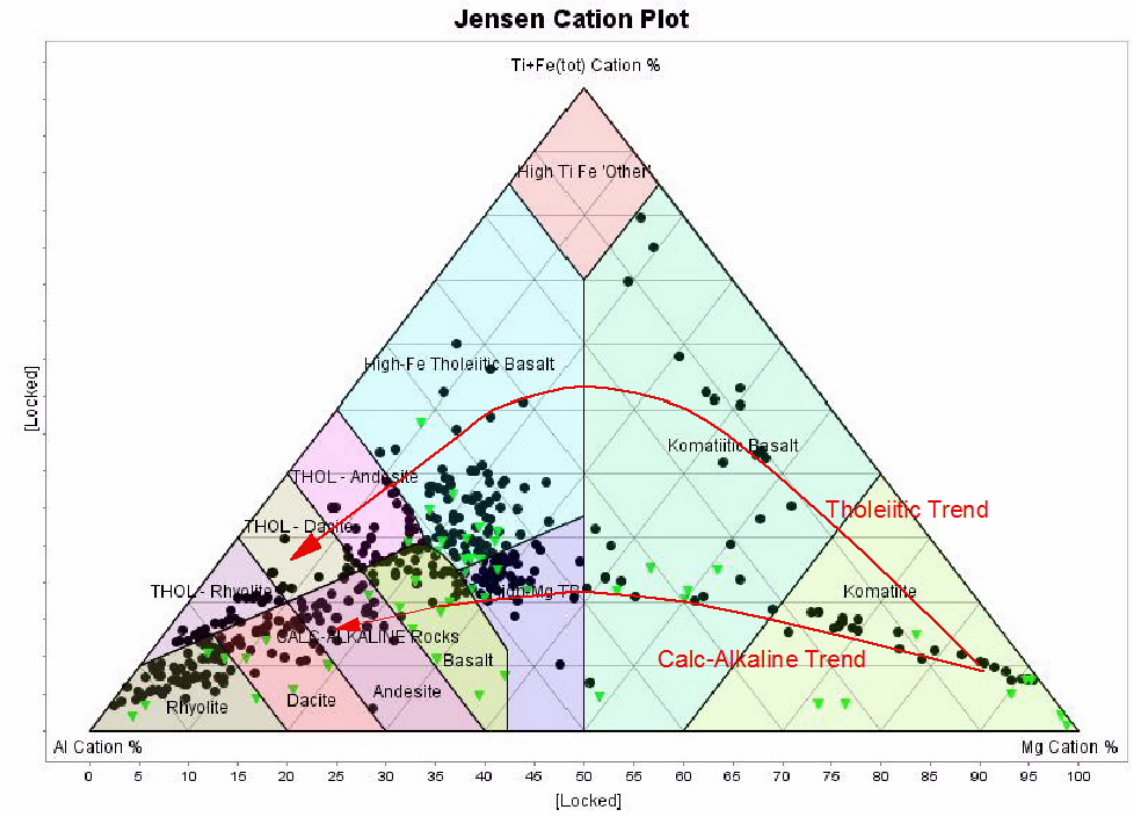

Figure 36 Jensen Cation Plot of published data for unaltered rock units in the Porcupine Mining Camp (Pyke 1982- green triangles) and sample data from this study (black dots). Modified from Jensen, 1976.

The iron, magnesium, and titanium content of rocks in the study area are not noticeably mobilized during alteration (Fig. 36). The study area plots of iron, magnesium manganese and titanium follow lithological unit boundaries with higher values of each found in the Tisdale mafic metavolcanic Assemblage (Figs. 8, 9, 10, and 14). Fe- and Mg-tholeiites in the Porcupine Mining Camp and the Bristol-Thorneloe Study area have comparable average Fe_2O_3 contents of 11.10 wt% and 10.26 wt%, respectively, or only a 0.84 wt% absolute difference (Pyke 1982). The same comparison for the average

MgO, MnO, and TiO_2 contents of the tholeiites results in absolute differences of only 1.22 wt%, 0.04 wt%, and 0.07 wt%, respectively. These differences are similar to the Fe_2O_3 wt% variation observed and supports the interpretation that the Fe- and Mg-tholeiitic rock units in the Bristol-Thorneloe study area are comparable to those found elsewhere in the Porcupine Mining Camp.

Chromium and nickel content of the rocks can be used to discriminate between various mafic to ultramafic rock units because chromium is only mobile under a limited number of conditions (Kerrich and Hodder 1982). Using Cr in this manner is supported by Porcupine Mining Camp data that has a mutual increase in chromium and nickel content from the rhyolite through ultramafic rock units (Pyke 1982). Calc-alkaline rhyolite-dacite have Cr contents that average ~30ppm that range up to ~2350 ppm in peridotitic komatiites (Pyke 1982). The variation of chromium content is essentially independent of alteration because it undergoes minimal hydrothermal transport (Dinel et al., 2008a). Nickel has a similar trend as chromium with Ni contents increasing from felsic to ultramafic rocks and is supported by the immobility of Ni (ppm) and MgO (wt%) in the Porcupine Camp rocks (Fig. 4.1.2, (Brand 2004)). Unaltered (Pyke, 1982) and the study area samples were plotted together and have a linear increase in both MgO wt% and Ni ppm from basalts through peridotite (Fig. 37).

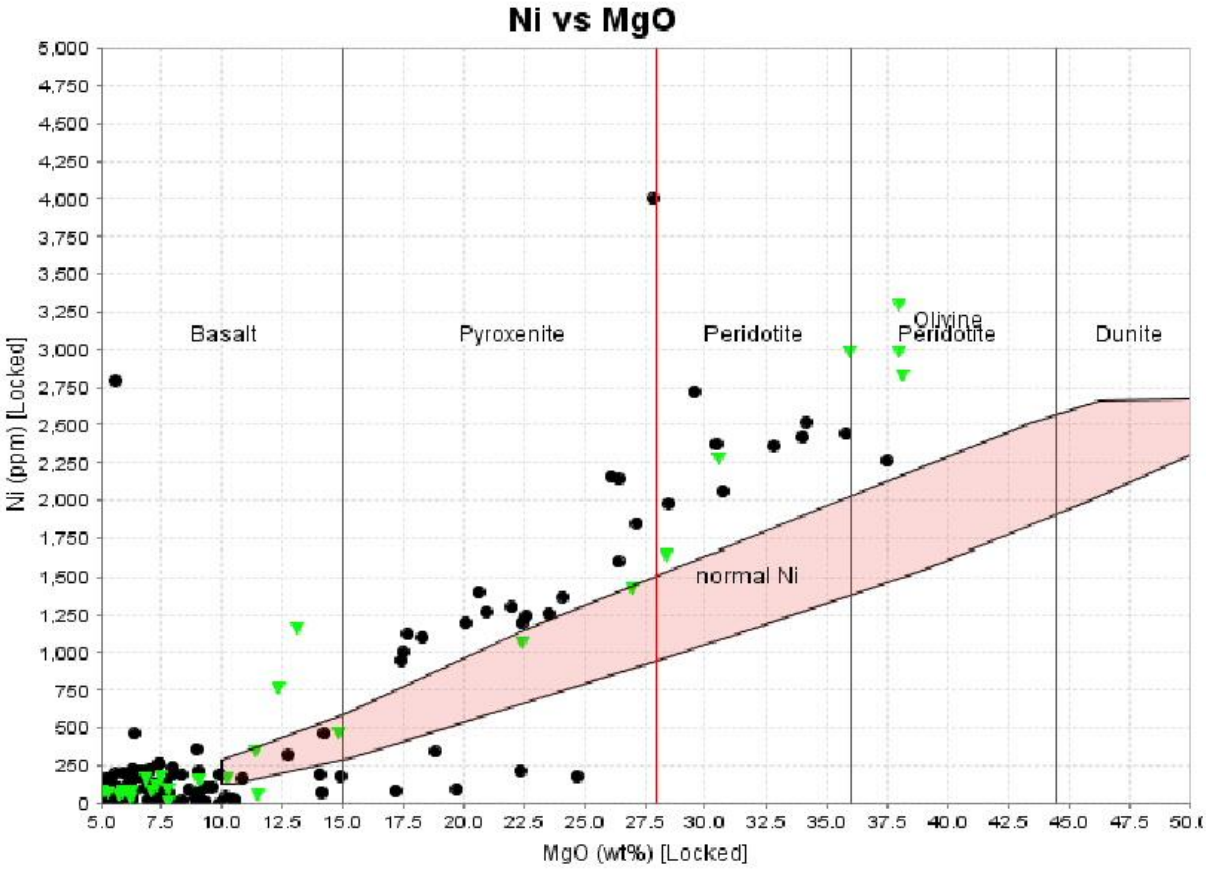

Figure 37 Nickel versus MgO of all Bristol-Thorneloe Study Area samples and selected unaltered rock data from the Porcupine Camp. Black dots indicate study area samples and green triangles are unaltered samples collected by Pyke (1982) from each mafic to ultramafic rock unit. Modified from Pyke, 1982 and Brand, 2004.

Higher scandium contents (>20 ppm) are associated with the Tisdale mafic metavolcanic rock band that extends through the center of Bristol Township and around the nose of the fold into central Denton Township (Fig. 20). Sc behaves similar to Cr and Ni with higher concentrations following the mafic rock units. Similar patterns occur in the Hollinger-McIntyre Mine where Sc concentrations of <30 ppm are associated with felsic rocks and vein systems (Washington 2008) and Sc concentrations >40 ppm are found in mafic country rocks (Washington et al. 2009). This close association between

Sc content and mafic rocks supports that Sc concentration in the Bristol-Thorneloe Study Area are dependent on the rock units.

Calcium (CaO) contents >7.0 wt% closely follows the Tisdale mafic metavolcanic rocks in Bristol Township and isoclinal fold into Denton Township. Calcium is a mobile constituent of hydrothermal systems but in the Bristol-Thorneloe study area the highest CaO values closely follow the mafic metavolcanic rock band (Fig. 7). This close association of CaO and mafic rocks is probably attributable to the abundance of Ca-plagioclase (Anorthite) commonly found in mafic rock units. The size of the study area, wide spacing of the samples and high relative concentration of CaO in mafic rocks obscures small, localized areas of CaO enrichment associated with hydrothermal related wall rock alteration. Given the close association of CaO with the wall rocks, it is treated as a rock dependent in this study. This interpretation is supported by Fe and Mg tholeiites that have average CaO contents of ~9.9 wt% that gradually decreases to average of ~2.3 wt% in rhyolite and dacite in the Porcupine Mining Camp (Pyke 1982). A similar difference in CaO content was observed between the mafic and felsic metavolcanic rocks, with average values being ~10.0 wt% and ~4.1 wt%, respectively.

Copper concentration is low throughout most the study area and only has a modest increase to 50 to 100 ppm in the band of Tisdale mafic metavolcanic rocks that pass through the center of Bristol Township (Fig. 24). Samples collected around the Lake Shore Timmins West Gold Mine have Cu concentrations that can be >100 ppm but these tend to be variable and do not have a clear association gold mineralization. Cu contents of rocks in the Hollinger-McIntyre Mine do not have a clear relation with

hydrothermal alteration because Cu concentrations are similar both proximal and distal to quartz veining (Washington 2008). Mafic rocks that are closely related to porphyry intrusions in the Hollinger-McIntyre Mine were also found to contain higher copper concentrations (Washington 2008). This association of Cu with mafic rocks near the porphyry intrusions can likely be explained by the introduction of Cu-Au-Mo mineralization in the intrusive rocks (Washington, 2008).

Yttrium and zirconium concentrations in the felsic rock units of the Bristol-Thorneloe study area are higher than those measured in mafic rock units (Figs. 16 and 19). The highest Y and Zr concentrations of >50 ppm and >175 ppm, respectively, occur in the felsic metavolcanic rocks of northwestern Bristol Township. These results are comparable to the Y and Zr concentrations of 215 to 410 ppm, respectively, measured in the same rhyolitic rocks (Barrie, 2000). High zirconium concentrations (>225 ppm) also occur around the Timmins Mine where they are associated with felsic-intermediate intrusive bodies at the mafic metavolcanic – metasedimentary rock contact (Fig. 3). Zr and Y are both considered to be immobile and incompatible elements and that helps to explain their relatively uniform and higher concentrations in felsic rock units (Davies et al. 1978).

4.2 Mobile Elements

The movement of certain chemical constituents by hydrothermal fluids affecting whole rocks has been documented by a number of workers e.g. (Davies et al. 1982; Melnik-Proud 1997; Kerrich and Hodder 1982; Washington 2008). The mobile elements

in the study area were identified primarily by similar values of an element extending across lithological boundaries and therefore appearing to be independent of initial composition of the rocks. All mobile elements/alteration types will be addressed further for each individual rock unit. The whole rock constituents that appear to have been mobilized during alteration are Na_2O, K_2O, P_2O_5, Ba, CO_2, Sr, Au, Pb and locally Cr. Although these elements and oxides can be used to define parent lithologies, interpretation of data obtained from the study area supports they have been mobilized by hydrothermal fluids.

Carbon, phosphorus, strontium, and barium (CO_2, P_2O_5, Sr and Ba) concentration in the rocks were compared against their gold (Au) content using Spearman's Rank Correlation Coefficient, a measurement of the relation between two variables. Higher concentrations of each element were found to have a statistical relation with gold in all rock units in the study area, independent of their primary rock composition. Na_2O and K_2O are commonly mobilized during hydrothermal alteration, and primary components assessing alteration types to locate gold-bearing zones. These two major whole rock elements are used to calculate CCPI, Chlorite, Sericite, and Ishikawa Alteration Indices.

Geochemical alteration of rocks in the Porcupine Mining Camp has been recognized previously including enrichment of: phosphorus (P_2O_5) and potassium (K_2O) with Volcanogenic Massive Sulphide (VMS) deposits in the Kamiskotia Area (Hart 1984) and (Barrie, 2000); barium (Ba) and carbon dioxide (CO_2) associated with gold mineralization in the Hollinger-McIntyre mine (Smith and Kesler, 1985); and Sr, K_2O andNa_2O in porphyritic intrusions of the study area (MacDonald, 2005).

Chromium (Cr) concentrations in the study area rocks cross lithological boundaries and appear to have been mobilized slightly. Cr concentrations are commonly used to recognize lithologic types with the highest concentrations typically found in ultramafic rocks decreasing to the lowest contents in felsic rock units. Dinel et al., (2008) documented enrichment of Cr in altered wall rock at the Hoyle Pond Mine and attributed it to the mobility of Cr in oxidizing fluids (uncommon in gold mobility). Similar Cr enrichment was not observed around gold mineralized zones in the Bristol-Thorneloe Study Area. Chrome (Cr) is not considered to be an indicator of alteration in this study because of the rare conditions needed to mobilize Cr and the lack of Cr enrichment around the Lake Shore Timmins West Gold Mine.

4.3 Porcupine Metasedimentary Rocks

Clastic metasedimentary rocks that occur in the southeastern part of the study area consist primarily of turbidites that were deposited in a marine environment (Cavey 2006). The strata in these rocks commonly have thinly laminated “slump” features characteristic of soft-sediment deformation. These rocks are classified predominantly as iron shales and shales that contain minor amounts of iron sandstone and greywacke. The rock types were determined using a $\log(\frac{Fe_2O_3}{K_2O})$ versus $\log\left(\frac{SiO_2}{Al_2O_3}\right)$ plot developed Herron (1988) (Fig. 38).

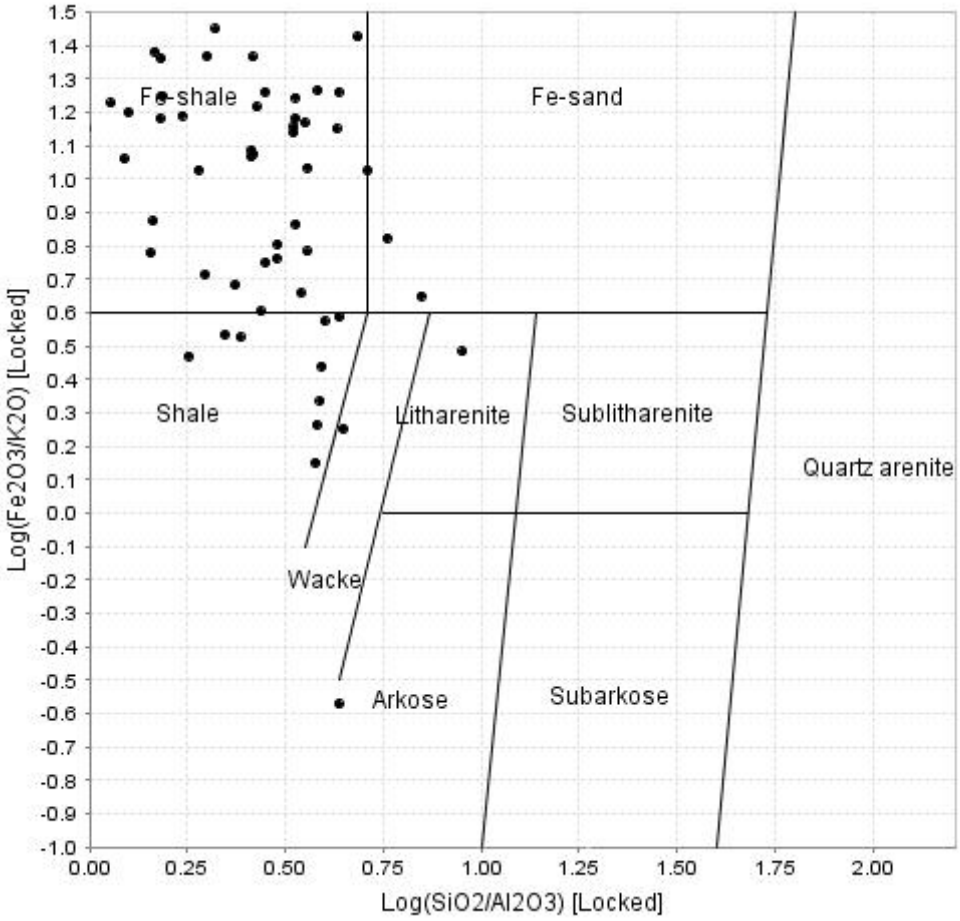

Figure 38 Porcupine metasedimentary rock classification diagram in Bristol-Thorneloe Township. Modified from Herron, 1988.

Metasedimentary rocks found in northern Thorneloe Township have varying types and intensities of hydrothermal or regional metamorphic alteration. The rocks underwent Na-depletion and carbonatization, as well as potassium metasomatism. Na_2O has been removed from approximately half of the samples collected in Northern Thorneloe (Fig. 39). The lower Na_2O concentrations can be explained byeither Na_2O being leached from the rocks during hydrothermal alteration or weathering of the source rock to form potassium-rich clays. Weathering of feldspars in the source rock is the most likely

explanation for the lower Na_2O and higher K_2O values, as well as the high concentation of clay minerals characteristic of the Fe-shale and shale lithologies.

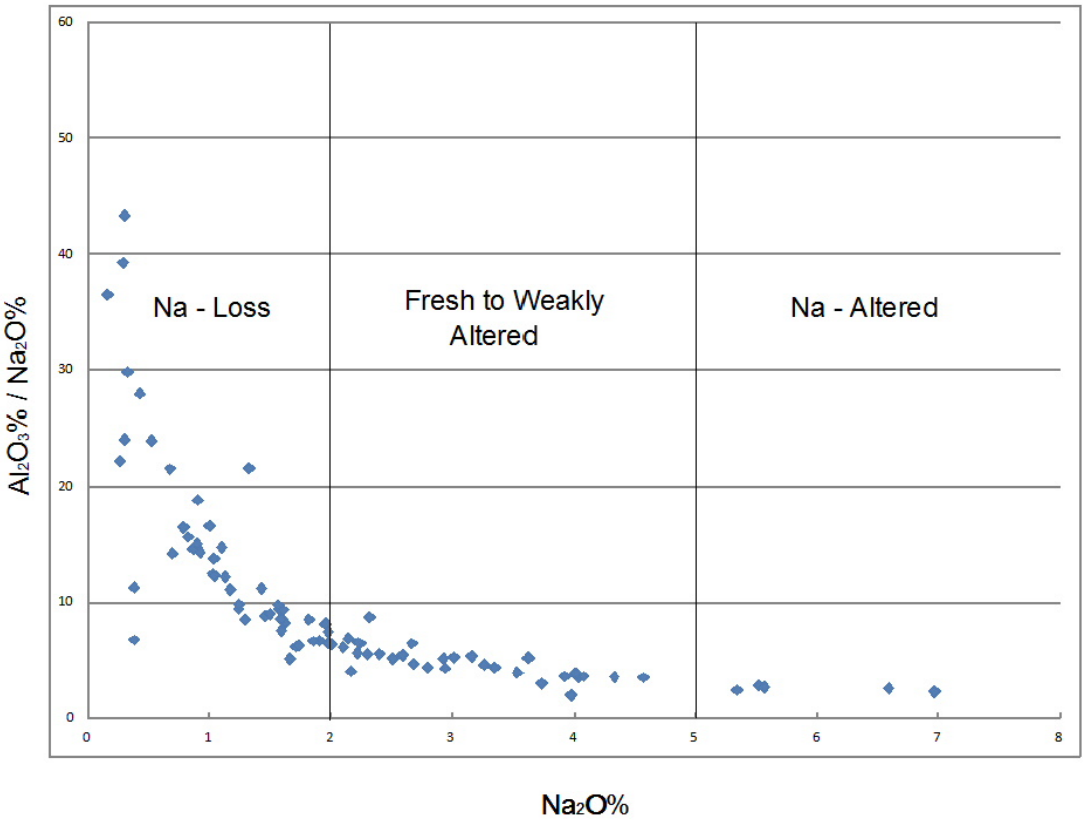

Figure 39 Sodium alteration diagram of the Porcupine metasedimentary rocks in Bristol-Thorneloe Townships Modified from MacDonald, 2005.

Na-depletion also appears to be related to K-enrichment (Fig. 40), with approximately half of the metasedimentary rocks demonstrating K-metasomatization (MacDonald 2005). It is unclear if the altered rocks were affected pre- or post- sedimentation.

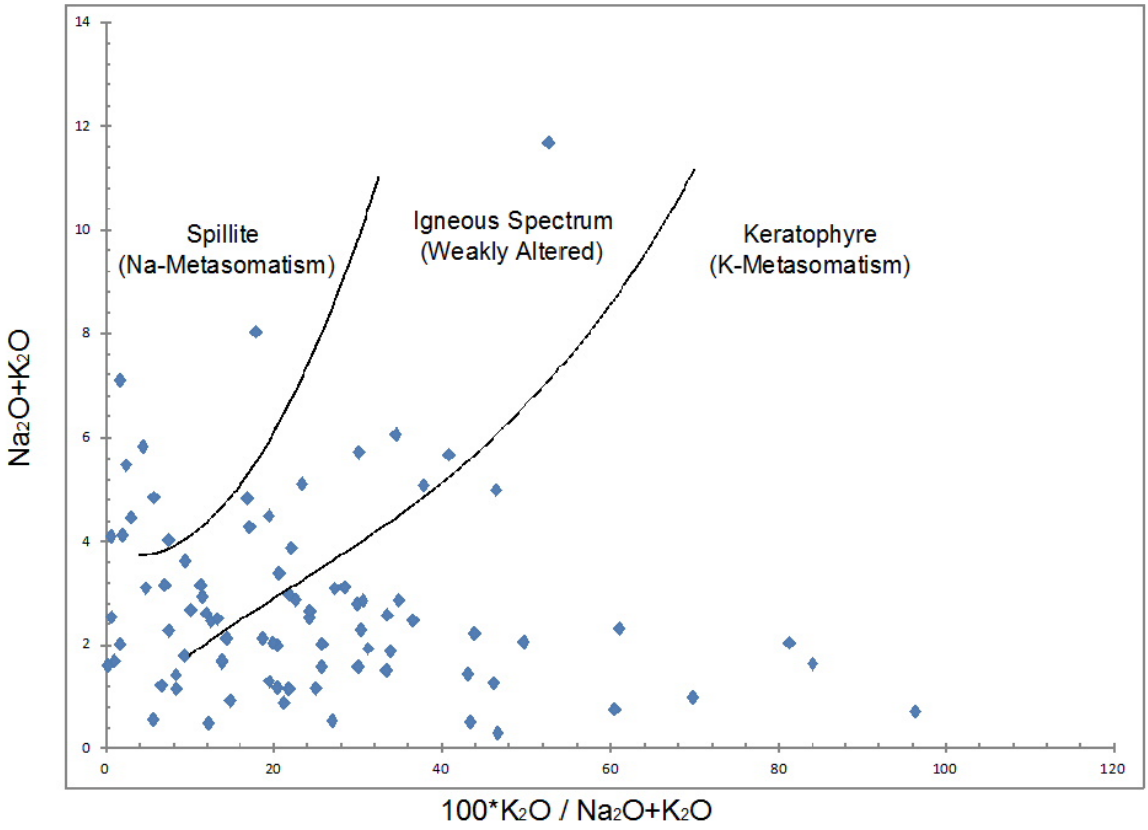

Figure 40 Plot of Na_2O+K_2O vs. $100*K_2O / Na_2O+K_2O$ of metasedimentary rocks in Bristol-Thorneloe Township to evaluate the type of metasomatic alteration present. Modified from MacDonald, 2005.

Approximately one third of the clastic metasedimentary rock samples have been carbonate altered (dolomite-ankerite) as indicated by the plot of the Chlorite Carbonate Pyrite Index (CCPI) versus Alteration Index (Ishikawa Index) (Fig. 41) (Large et al. 2001). This plot was originally designed to characterize the alteration of volcanic rocks, the presumed source of the sediments that formed the shales. Using this diagram to characterize alteration in the metasedimentary rocks appears to be valid because most

of the samples plot in the basalt field and that appears to support that the mafic rocks of the Tisdale Assemblage are the source material.

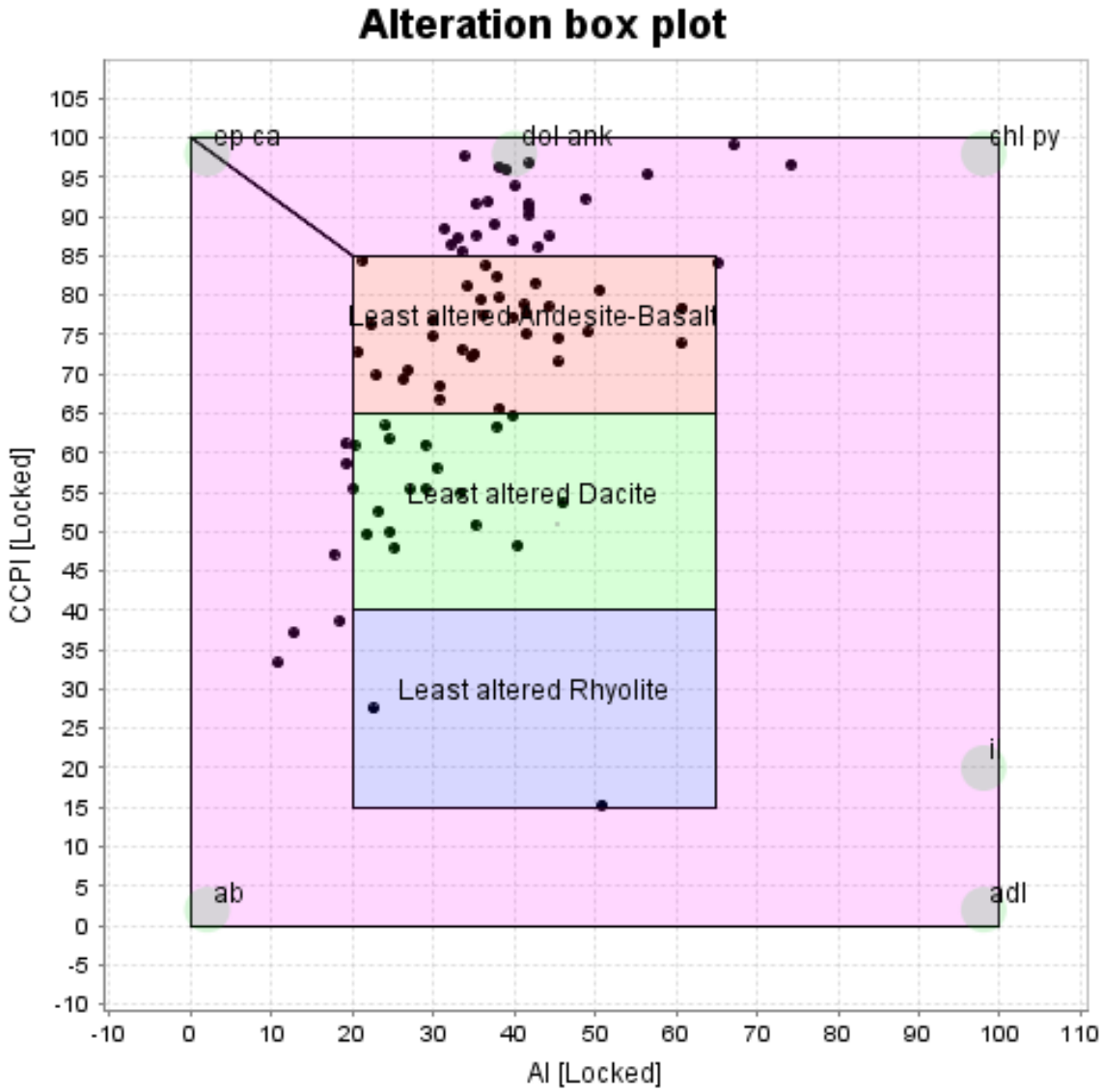

Figure 41 Alteration Box Plot of the metasedimentary rocks in Bristol-Thorneloe Township. Modified from Large et al., 2001.

Throughout the Porcupine Mining Camp, carbonate alteration halos occur around the gold deposits, with calcite and dolomite/ankerite deposited distal and proximal, respectively, to gold-bearing quartz veins (Davies 1982). Metasedimentary rocks in the

study area appear to have a similar relation with high gold concentrations being associated with ankerite/dolomite alteration. This close association is evident when the highest gold values are plotted on a carbonate discriminant plot (Stanley and Madeisky 1996). The plot indicates that the highest gold values are closely associated with dolomite/ankerite mineralization but calcite alteration is not (Fig. 42).

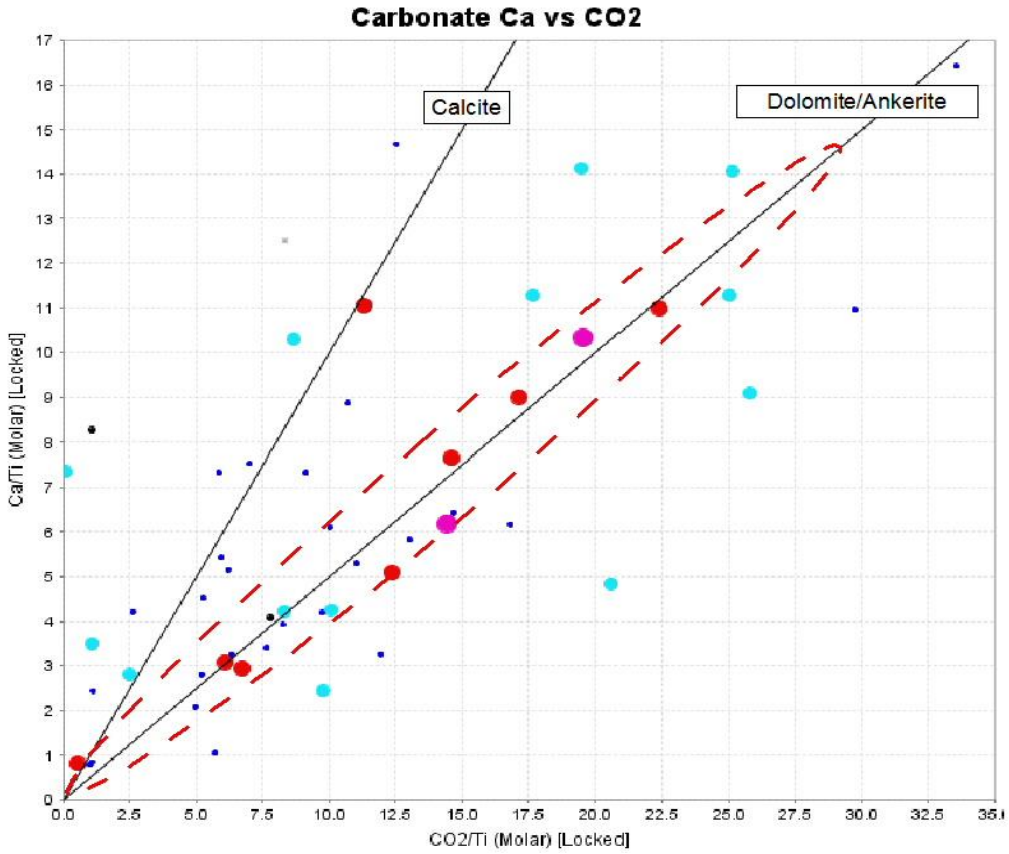

Figure 42 Plot of gold association with carbonate type of the metasedimentary rocks in Bristol-Thorneloe Township. Au abundance corresponds to dot size and color, Dark Blue <5 ppb, Light Blue – 5 to 30 ppb, Red – 100 to 500 ppb, Purple >500 ppb. Modified from Stanley and Madeisky, 1996.

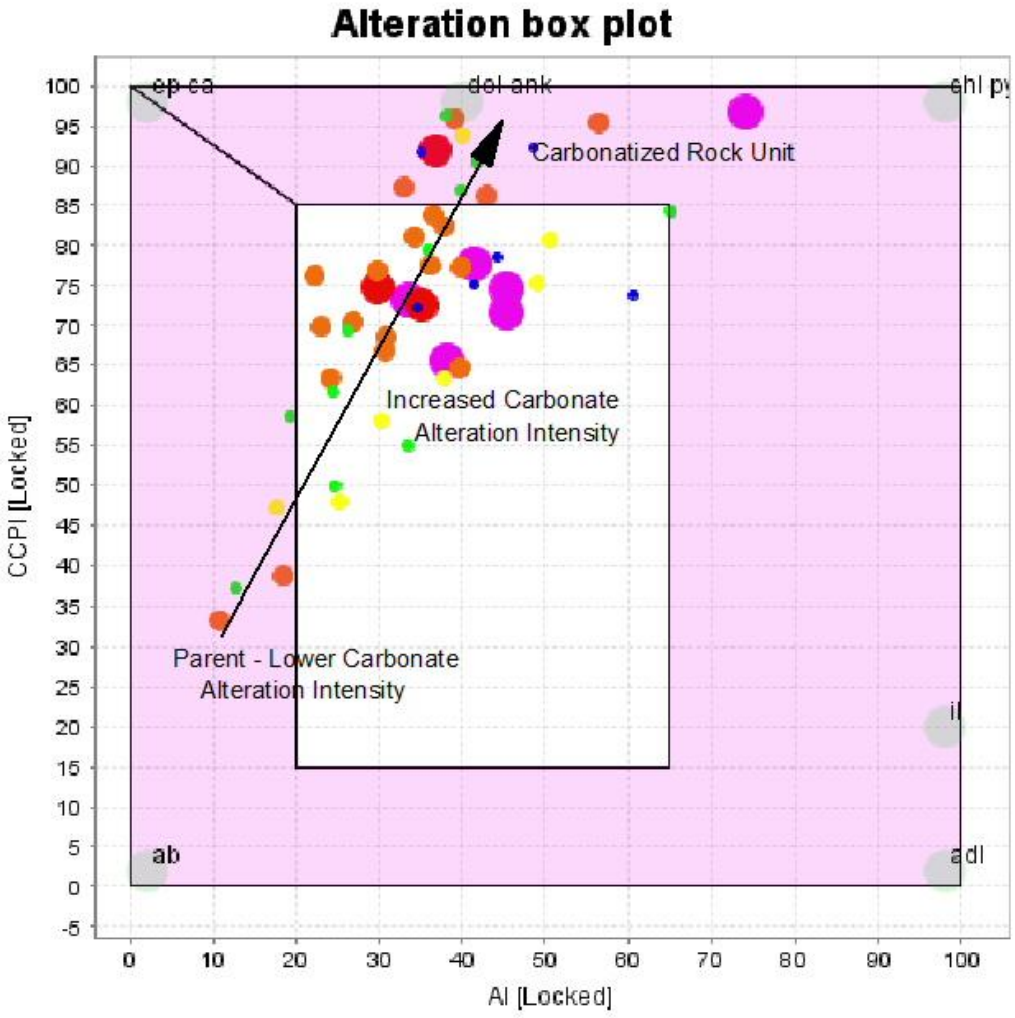

Figure 43 Alteration Box Plot diagram of the Bristol-Thorneloe Township metasedimentary rocks with CO_2/CaO values. CO_2/CaO values correspond to dot size and color Dark Blue – < 0.5, Green – 0.5 to 1.0, Yellow – 1.0 to 1.5, Orange 1.5 – 2.0, Red – 2.0 to 2.5 Purple - > 2.5,. Modified from Large et al. 2001.

The majority of higher gold values are associated with CO_2/CaO values between 1.5 and 2.0 and only two samples with geochemically anomalous gold values are associated with CO_2/CaO values less than 1.0 (Fig. 44). The CO_2/CaO values between 1.5 to 2.0 indicate a zone where carbonate compositions are transitioning from a calcite-

dolomite mixture to pure dolomite/ankerite. The close association between higher gold values and dolomite/ankerite is comparable to the results obtained by Davies et al., (1982) and exceed the CO_2/CaO values of 1.5 that they suggested is the threshold that should be used for gold exploration. When CO_2/CaO values exceed 2.0, gold concentrations are much lower but still exceed background values of 5 ppb, so it is likely that gold depositing conditions are not as favorable when the hydrothermal system is depositing siderite-magnesite dominant mineralization.

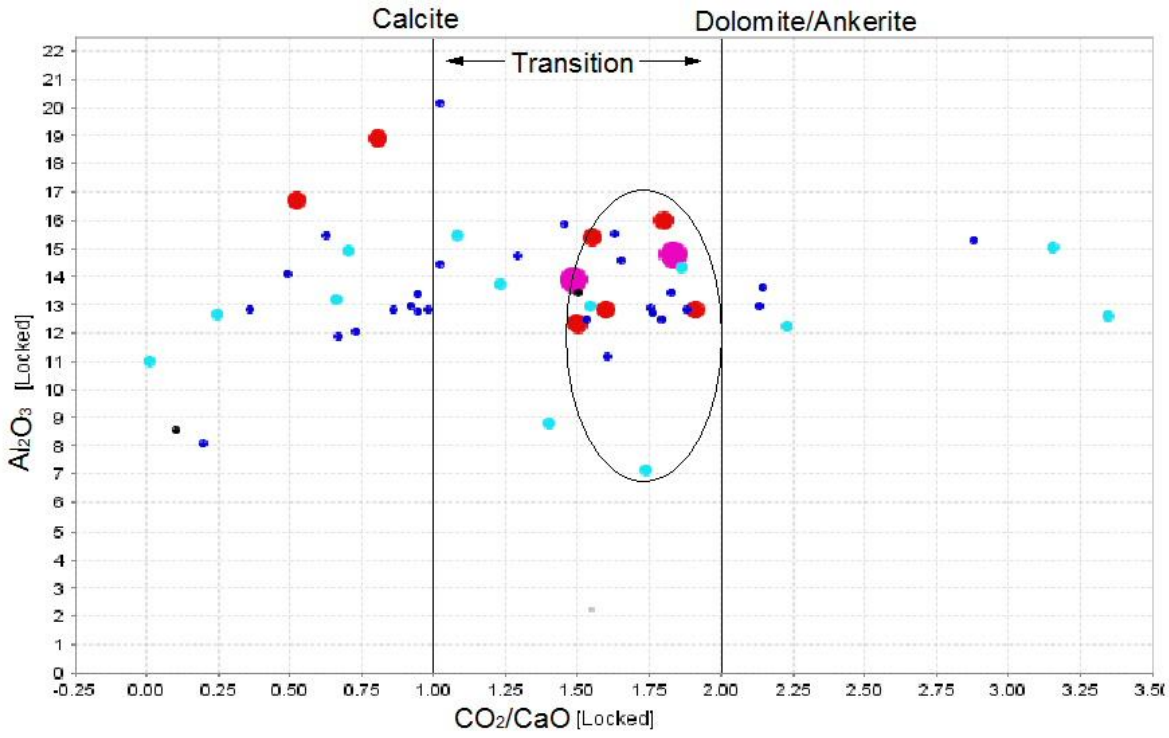

Figure 44 Wall rock gold concentration plotted on a Al_2O_3 wt% versus CO_2/CaO diagram of the Porcupine Metasedimentary rocks in Bristol-Thorneloe. Dot size and color correspond to gold concentration, Small Dark Blue <5 ppb, Light Blue – 5 to 30 ppb, Green 30 to 45 ppb, Yellow – 45 to 60 ppb, Orange - 60 to 100 ppb, Red – 100 to 500 ppb, Large Purple >500 ppb. Modified from Davies et al., 1982.

In addition to CO_2/CaO values that indicate the deposition of dolomite/ankerite, higher barium (Ba) concentrations (>280 ppm) are also found associated with gold in alteration zones associated with metasedimentary rocks in the study area(Fig. 45). This association is comparable to that found in the Hollinger-McIntyrre mine where Ba concentrations >200 ppm and up to more than >400 ppm occurred in close proximity to mineralized veins (Smith and Kesler, 1985). Barium (Ba), gold (Au) and carbonate (CO_2) deposition appear to be related because 7 of 9 samples in the study area that have higher Au values are associated with Ba values >280 ppm and CO_2/CaO molar ratios 1.5 and 2.0 that indicate the rocks underwent dolomite-ankerite carbonate alteration (Fig. 45).

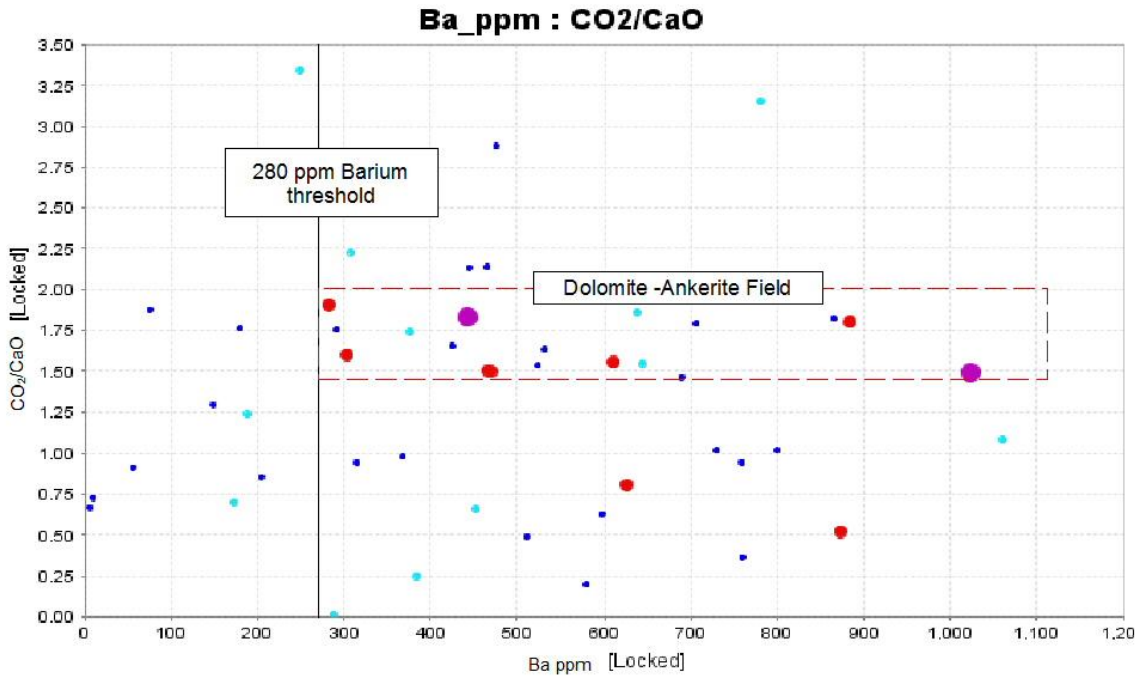

Figure 45 Gold concentrations plotted on a CO_2/CaO versus Ba ppm diagram of the Porcupine metasedimentary rocks in Bristol-ThorneloeTownship. Dot size and color correspond to gold concentration, Small Dark Blue <5 ppb, Light Blue – 5 to 30 ppb, Green 30 to 45 ppb, Yellow – 45 to 60 ppb, Orange - 60 to 100 ppb, Red – 100 to 500 ppb, Large Purple >500 ppb.

Strontium (Sr) and Phosphorus P_2O_5 wt% both increase with barium (Ba) in the altered metasedimentary rocks (Fig. 46) There is a linear relation between Ba and Sr. The P_2O_5 values are highest when Ba values exceed 260 ppm. These three elements also coincide with anomalous gold concentrations (> 25 ppb) and CO_2/CaO molar ratios >1.5 in alteration zones and interpreted to be transported in auriferous hydrothermal fluids. Barium and strontium both form halos around gold deposits and prospects in the study area (Figs. 17 and 18), and have been observed in other Archean greenstone gold deposits, and are therefore considered useful gold exploration indicators (Manikyamba et al. 2003). Sr exists with calcium in calcite/dolomite mineralization, and

Sr and Ba concentrations are increased during potassium metasomatism, which has been documented in the Porcupine metasedimentary rocks (Manikyamba et al. 2003).

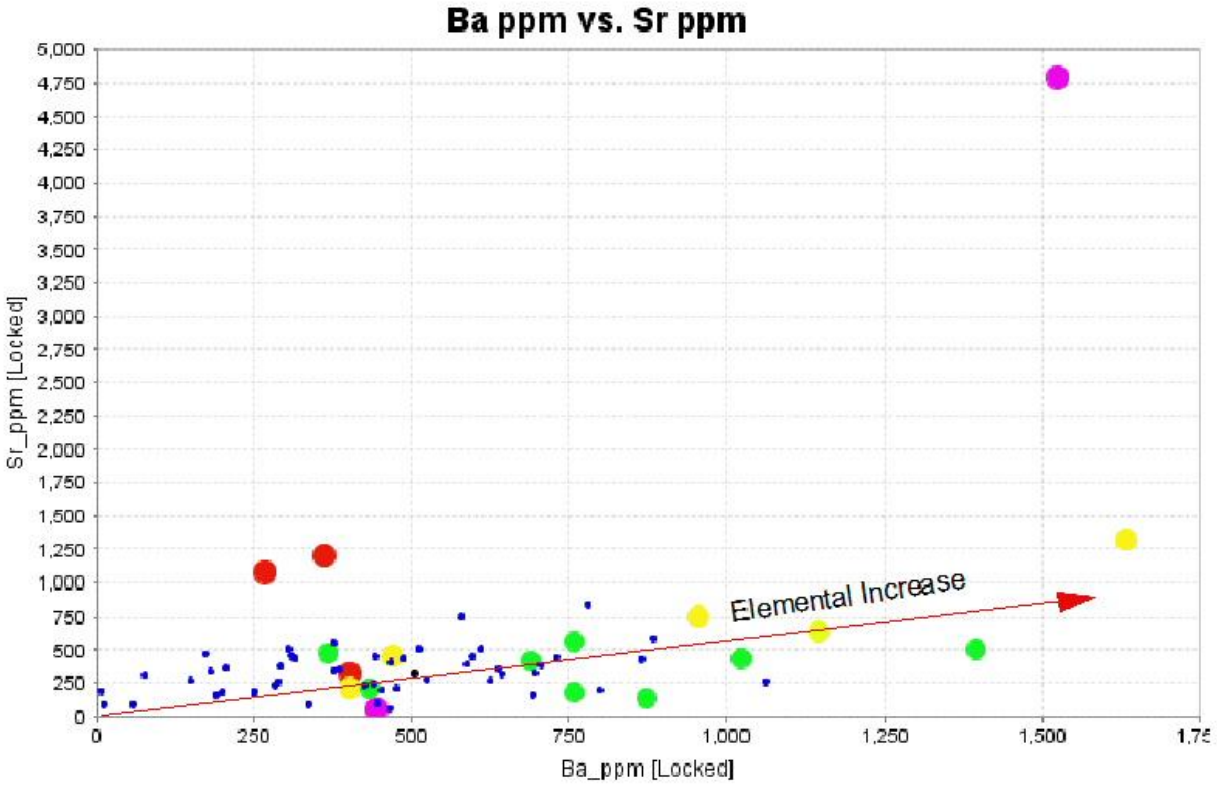

Figure 46 P_2O_5 (wt%) values on a Strontium versus Barium plot of the Porcupine metasedimentary rocks in Bristol-Thorneloe Township. Bigger dot size and color intensity correspond with higher wt% P_2O_5 values, Small Blue - < 0.15,Green 0.15 to 0.20, Yellow - 0.20 to 0.25, Orange - 0.25 to 0.30, Red – 0.30 to 0.35, Large Purple >0.35.

4.4 Tisdale Mafic Metavolcanic Rocks

The Tisdale assemblage mafic metavolcanic rocks that form the band that stretches from northeast to southwest across the study area, plots predominantly as Mg- and Fe-tholeiites on the Jensen Cation Plot as is typical of the Upper Tisdale Assemblage (Rollinson 1993). The rocks have bimodal compositions with the tholeiitic rhyolites to

komatiites extending into the calc-akaline volcanic field (Jensen 1976). Volcanic rocks with bimodal compositions are common in the Porcupine Camp and occur in areas that have both rift and subduction related tectonic regimes (Corfu et al. 1989; Thurston et al. 2008). The mafic metavolcanic unit has a tholeiitic and calc-alkaline compositions on the AFM diagram, which has been previously interpreted in the Tisdale Assemblage.

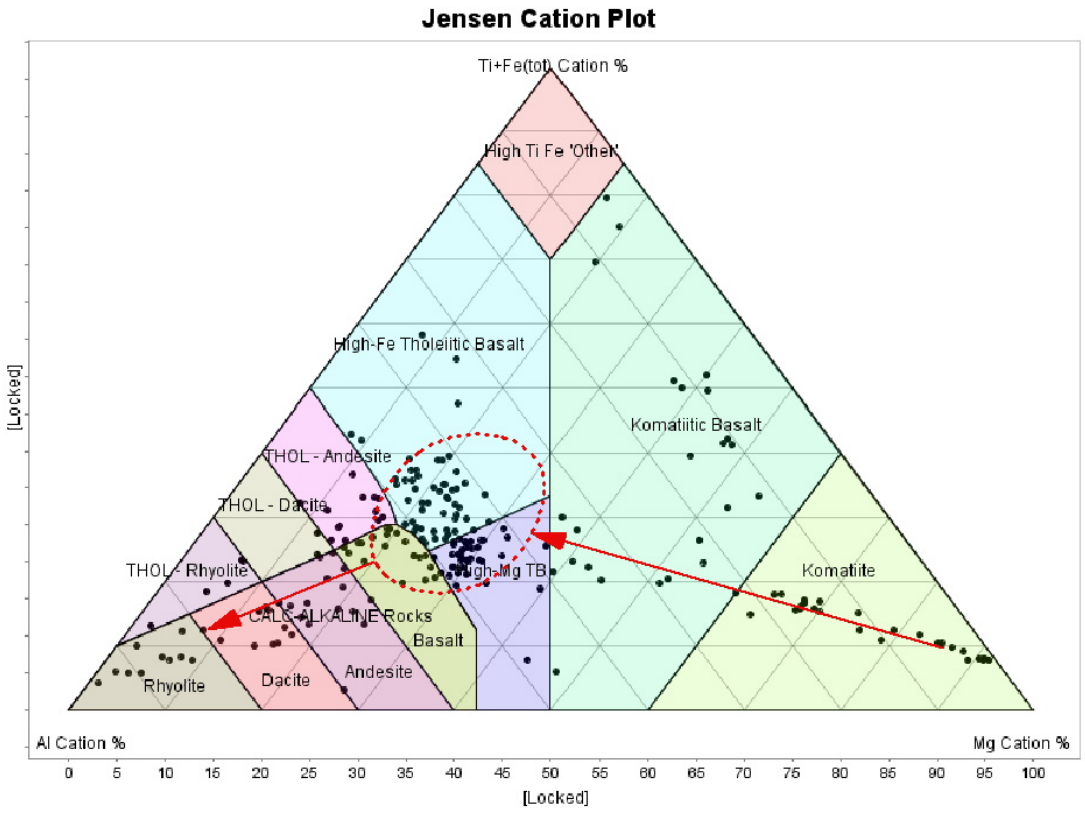

Figure 47 Jensen Cation Plot of the Tisdale Assemblage mafic metavolcanic rocks in Bristol-Thorneloe Township. Data points plot in both tholeiitic and calc-alkaline fields indicating that the area experienced bimodal volcanism. Modified from Jensen, 1976.

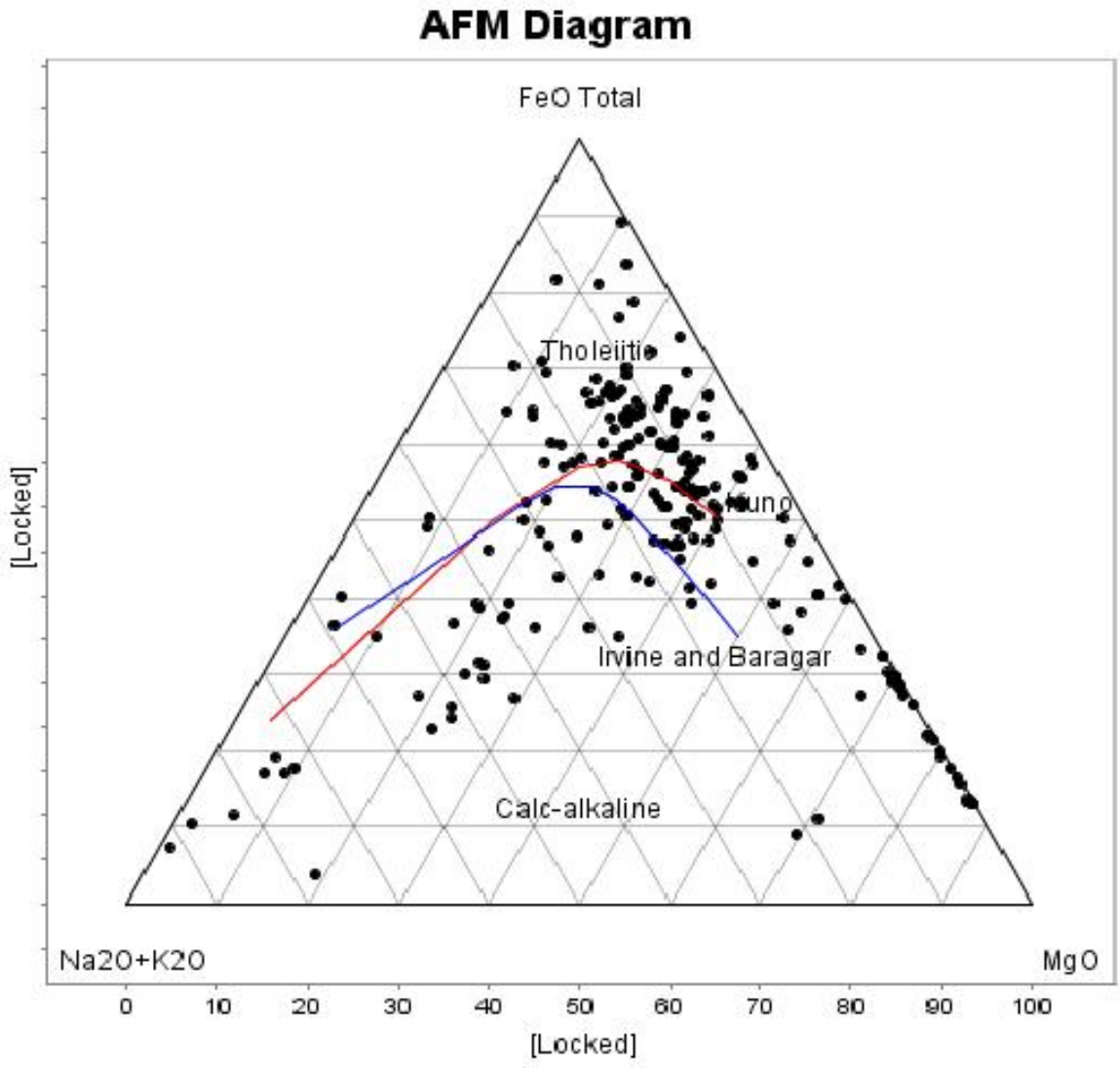

Figure 48 AFM plot of a tholeiitic trend in the Tisdale mafic metavolcanic rocks in Bristol-Thorneloe Township. Data points follow the Irvine and Baranger (1971) (blue line), and Kuno (1968) (red line) tholeiitic fractionation trend line toward the Fe-rich corner and then to the Na_2O+K_2O corner. Modified from Rollinson, 1993.

The alteration and related gold deposition of the mafic metavolcanic rocks in the study area differs from that found in the clastic metasedimentary rocks outcropping to the immediate southeast. Tisdale Assemblage rocks in the study area have an overall "weaker" intensity of alteration (Fig. 49). The figure has a large number of samples that

plot between calcite-epidote and dolomite-ankerite alteration points, and a few samples that plot as pure dolomite-ankerite alteration (Large et al. 2001). This alteration type most likely indicates that there is zonation with these rocks because they are distal from the auriferous fluid source. A second alteration trend extends from the least altered basalts to chlorite-pyrite alteration corner (Fig. 49). This trend was probably formed by regional greenschist metamorphism found throughout the study area. With lower grade hydrothermal alteration like that found in the metavolcanic rocks, gold values becomes less frequent and highly variable in the country rocks compared with its abundance in metasedimentary rocks. Similar results were found in the Hollinger-McIntyre Mine (Smith and Kesler, 1985), where evidence was found that supported carbonate zonation around auriferous zones. The calcite and transition into dolomite-ankerite altered rocks found in the study area are similar to assemblage II and III identified by Smith and Kesler (1985).

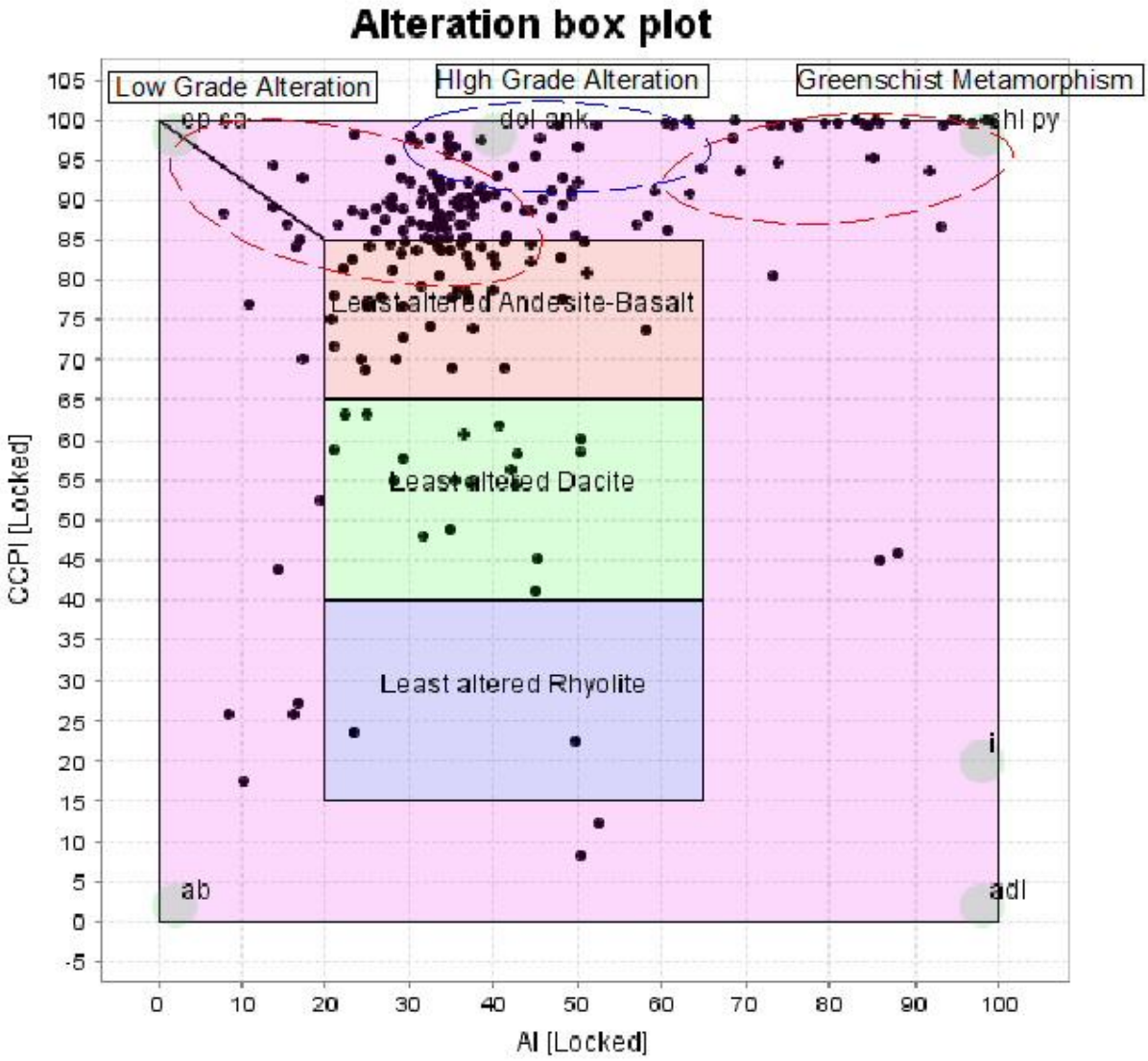

Figure 49 Alteration Box Plot of the Tisdale mafic metavolcanic rocks in Bristol-Thorneloe Township. Red circles envelop low-grade hydrothermal alteration and regional metamorphism. Blue circle envelops high-grade carbonate alteration. Modified from Large et al., 2001.

Carbonate alteration in the study area is dominated by calcite and calcite-ankerite mix that is transitional to dolomite-ankerite formation. Where carbonate alteration is characterized by dolomite-ankerite it is usually associated with geochemically anomalous gold values (Fig. 50). This carbonate alteration is similar to that seen in the

metasedimentary rocks. Rocks with little or no alteration have primary Ca-silicate dominated compositions that plot parallel and close to the Y axis (Ca/Ti molar values) between CO_2/Ti molar values of 0 to 5.

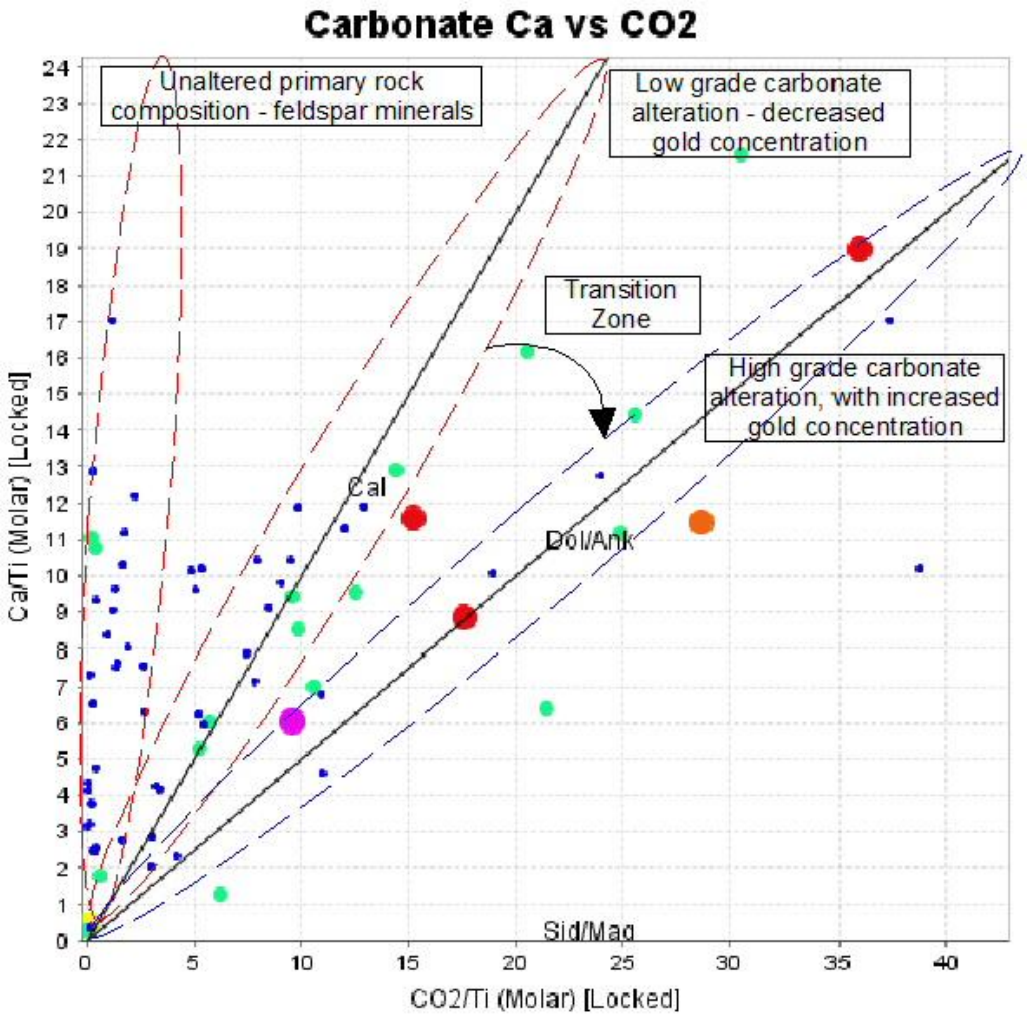

Figure 50 Gold concentration plotted on a Ca/Ti vs. CO_2/Ti Carbonate Discriminant Figure of the Tisdale mafic metavolcanic rocks of Bristol-Thorneloe Township. Dot size and color correspond to gold concentration, Small Dark Blue <5 ppb, Light Blue – 5 to 30 ppb, Green 30 to 45 ppb, Yellow – 45 to 60 ppb, Orange 60 to 100 ppb, Red – 100 to 500 ppb, Large Purple >500 ppb. Modified from Stanley and Madiesky, 1996.

Barium (Ba), strontium (Sr) and phosphorous (P_2O_5 wt%) concentrations increase in altered Tisdale mafic metavolcanic rock but without the close association with dolomite-

ankerite found in altered metasedimentary rocks. High concentrations of Ba, Sr and P_2O_5 occur in close proximity to one another suggesting that they were subjected to similar alteration conditions. The mutually enriched metavolcanic rock samples are located at or near the contact of mafic metavolcanic with ultramafic instrusive or metasedimentary rocks and have Sr, Ba, and P_2O_5 values in excess of 1,000ppm, 750 ppm, and 0.75 wt%, respectively (Fig. 51). This nonconformity could represent a structural weakness or zone allowing hydtrothermal fluid to effectively travel.

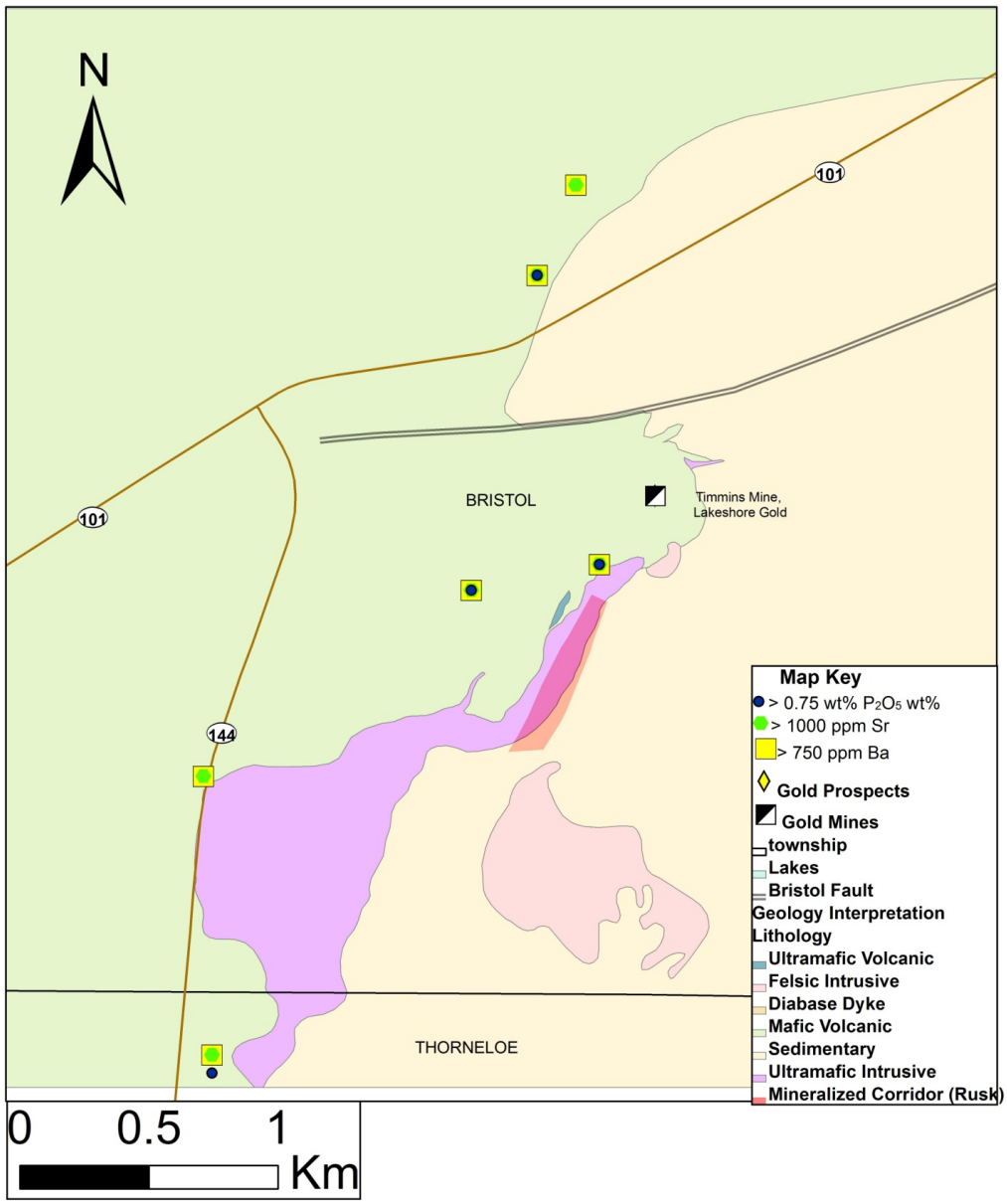

Figure 51 Location of Tisdale mafic metavolcanic samples containing high concentrations of P_2O_5, Sr and Ba. Blue dots indicate samples with >0.75 wt% P_2O_5, green dots indicate samples with >1000ppm Sr, and yellow squares indicate samples with >750ppm Ba.

Sr, P_2O_5 and to lesser extent Ba in the Tisdale mafic rocks have concentrations that are close to that of typical fractionation trends in mafic rocks (Figs. 52 A through C) (Stanley and Madeisky 1996). Plotting the Sr and P_2O_5 contents of mafic rocks on Pearce Element Ratio diagrams that use zirconium as the conserved element and have a basalt control line with a slope of 1, results in these being concentrated close to the end of basaltic fractionation plot that has little to no hydrothermal mobility (Fig. 52 A&B). Barium has samples with high concentrations that cluster near the presumed primary fractional crystallization line, however, mobilization of Ba can be seen in the trendline that diverges from the fractionation line. High silicon and barium concentrations occur together and that supports both being mobilized during hydrothermal alteration. The conditions experienced by the Tisdale mafic metavolcanic rocks appear to have weakly mobilized barium, but strontium and phosphorus remain immobile.

A.)

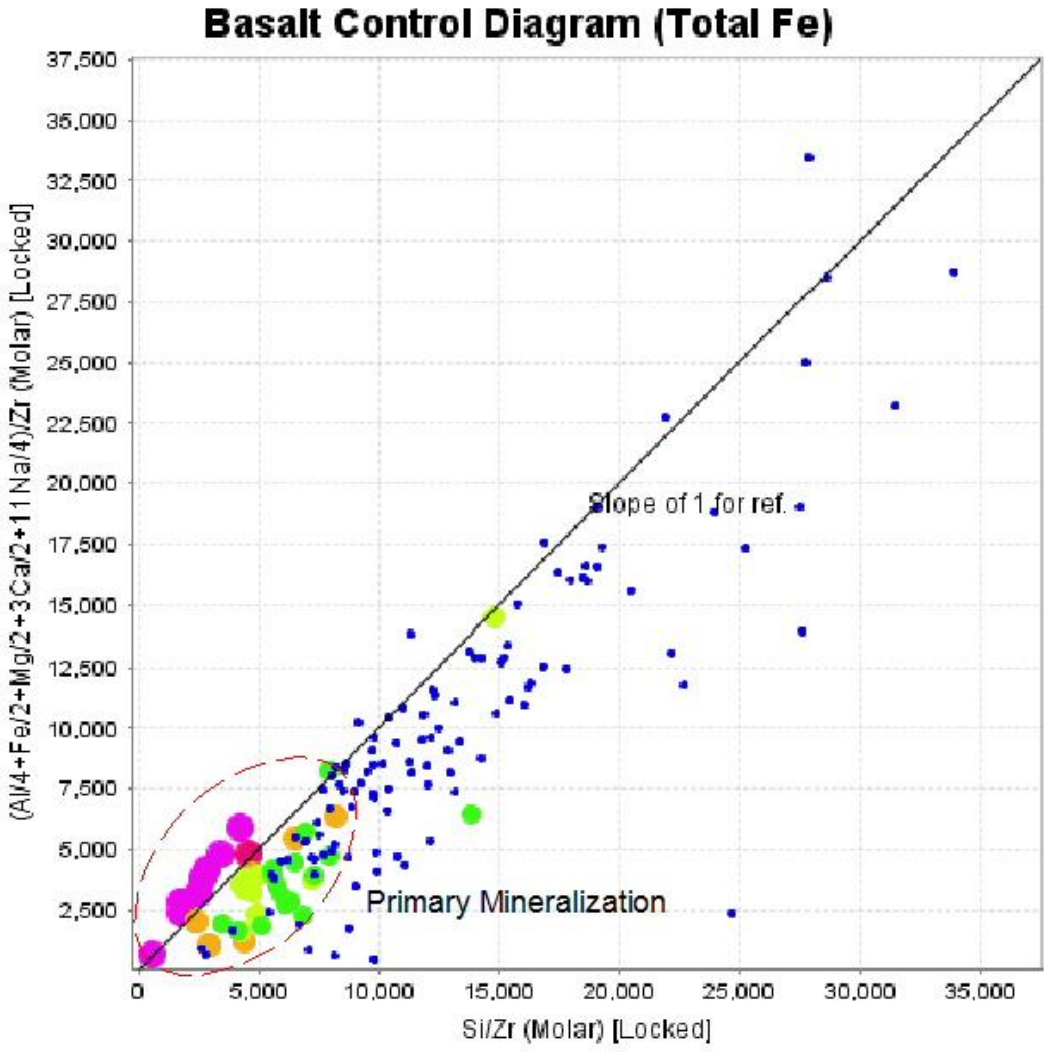
Basalt Control Diagram (Total Fe)
(Al/4+Fe/2+Mg/2+3Ca/2+11Na/4)/Zr (Molar) [Locked]
Si/Zr (Molar) [Locked]
Slope of 1 for ref.
Primary Mineralization
37,500
35,000
32,500
30,000
27,500
25,000
22,500
20,000
17,500
15,000
12,500
10,000
7,500
5,000
2,500
0
5,000
10,000
15,000
20,000
25,000
30,000
35,000

B.)

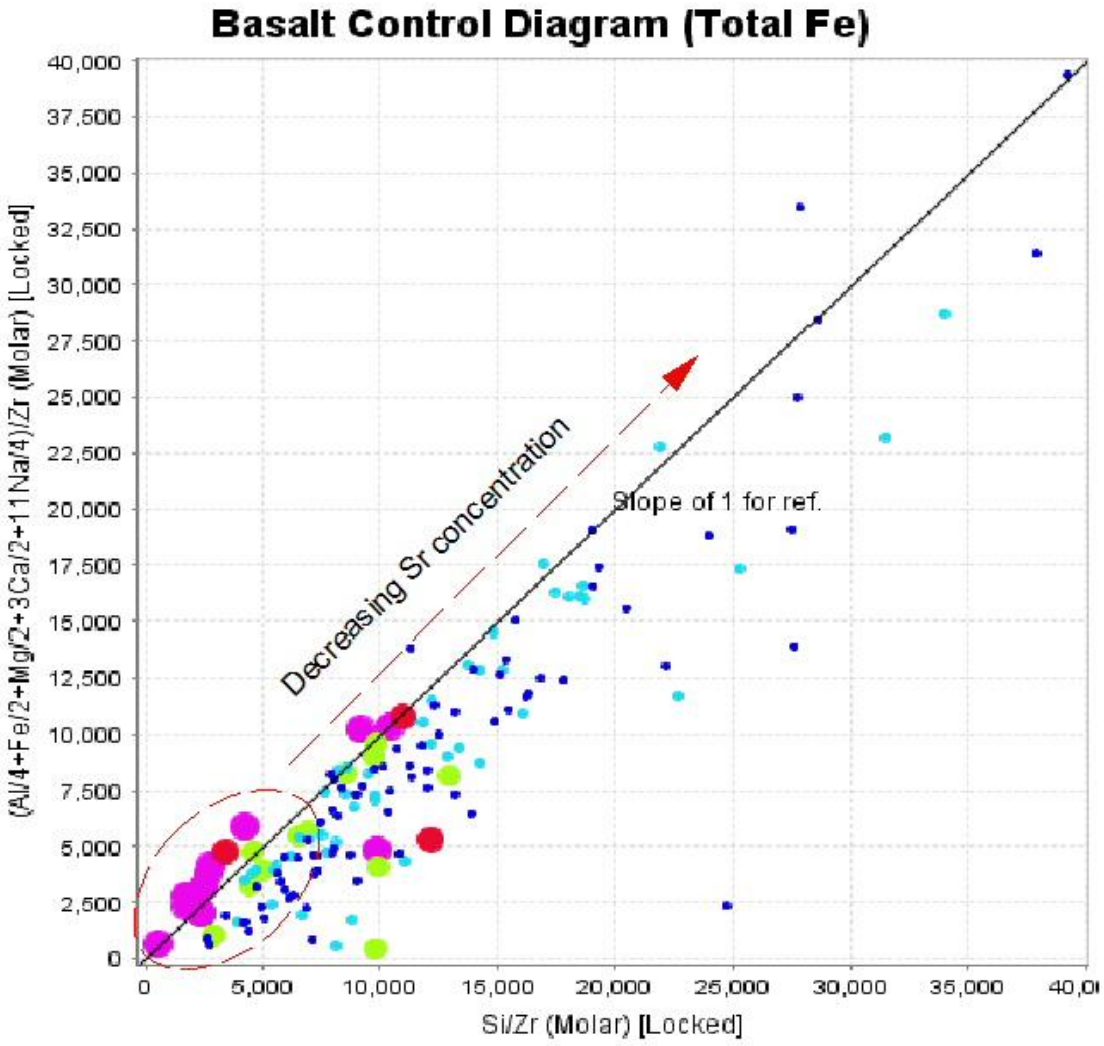
Basalt Control Diagram (Total Fe)
(Al/4+Fe/2+Mg/2+3Ca/2+11Na/4)/Zr (Molar) [Locked]
Si/Zr (Molar) [Locked]
Decreasing Sr concentration
Slope of 1 for ref.
40,000
37,500
35,000
32,500
30,000
27,500
25,000
22,500
20,000
17,500
15,000
12,500
10,000
7,500
5,000
2,500
0
0
5,000
10,000
15,000
20,000
25,000
30,000
35,000

C.)

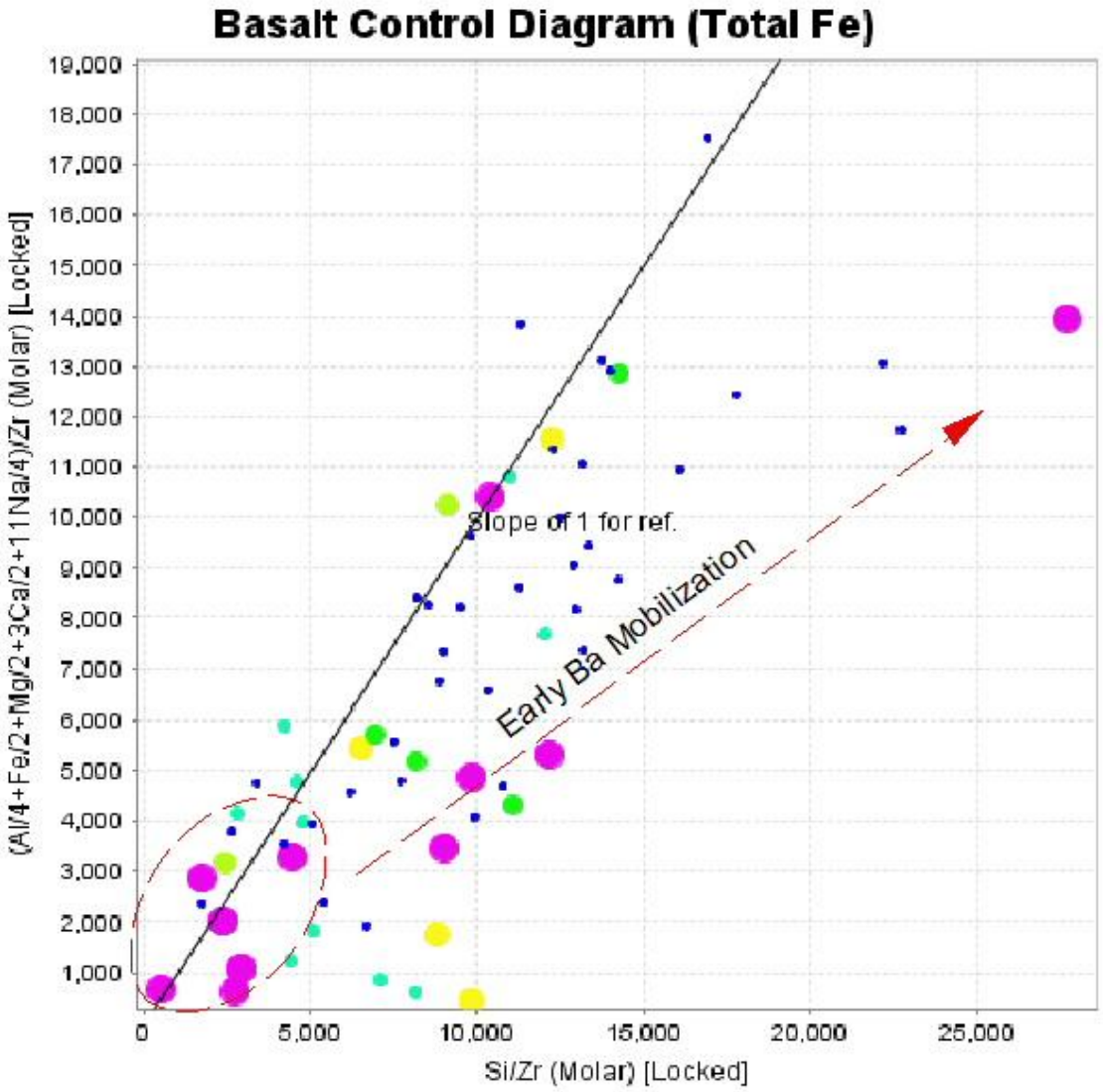

Figure 52 A through C, Basalt fractionation trend lines plotted using Si/Zr versus (Al/4+Fe/2+Mg/2+3Ca/2+11Na/4)/Zr (Molar) of the Tisdale mafic metavolcanic rocks in Bristol-Thorneloe Township **A.)** Phosphorus concentration is proportional to dot size, larger dots correpond to higher P_2O_5 wt%. **B.)** Strontium concentration is proportional to dot size, larger dots correspond to higher Sr ppm. **C.)** Barium concentration is proportional to dot size, larger dots correspond to higher Ba ppm. Modified from Stanley and Madeisky, 1996.

Figures 53 A though D are plots of immobile aluminum, chromium, magnesium, and yttrium. Each of these elements are considered because they are relatively immobile

and important in rock identification. Figure 53A depicts aluminum fractionation that has no variation throughout mineral formation. This plot provides evidence of feldspar formation that remains constant during crystallization and is common during transitional basaltic rock fractionation. The lack of variation also indicates that aluminum concentration has not undergone dilution or enrichment that can occur during hydrothermal alteration. Figure 53B plots higher magnesium concentrations away from the origin where the fractionation line begins. Figure 53C plots chromium in approximately the same location as magnesium. Both Cr and MgO are expected to occur together during crystallization and are commonly found in higher concentrations in mafic-ultramafic rock units. Figure 53 D plots yttrium, an immobile-incompatible element, opposite of magnesium and chromium. The highest Y concentrations plot at the end of fractionation line nearest the origin along with the incompatible elements strontium and barium.

A.)

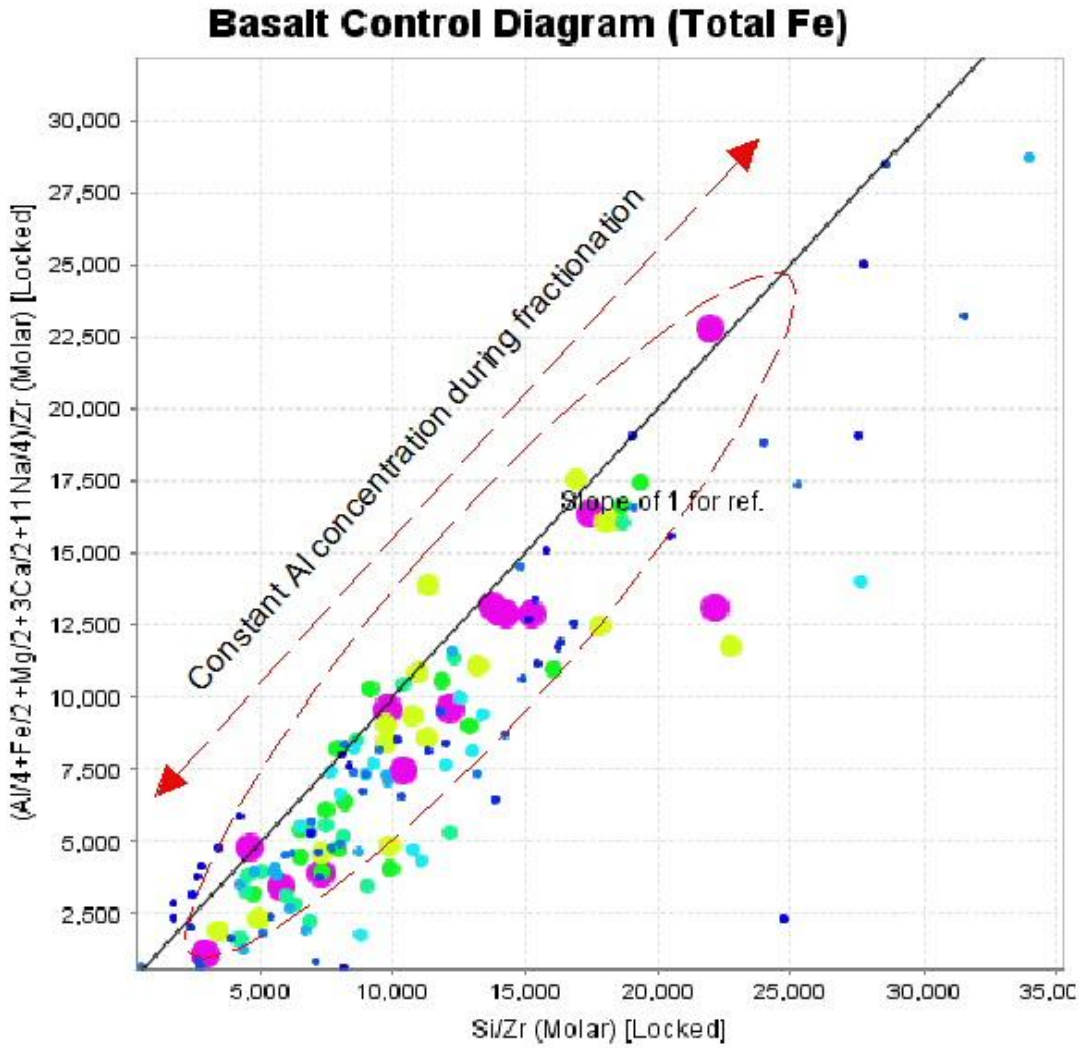
Basalt Control Diagram (Total Fe)
(Al/4+Fe/2+Mg/2+3Ca/2+11Na/4)/Zr (Molar) [Locked]
Si/Zr (Molar) [Locked]
Constant Al concentration during fractionation
Slope of 1 for ref.
30,000
27,500
25,000
22,500
20,000
17,500
15,000
12,500
10,000
7,500
5,000
2,500
5,000
10,000
15,000
20,000
25,000
30,000
35,00

B.)

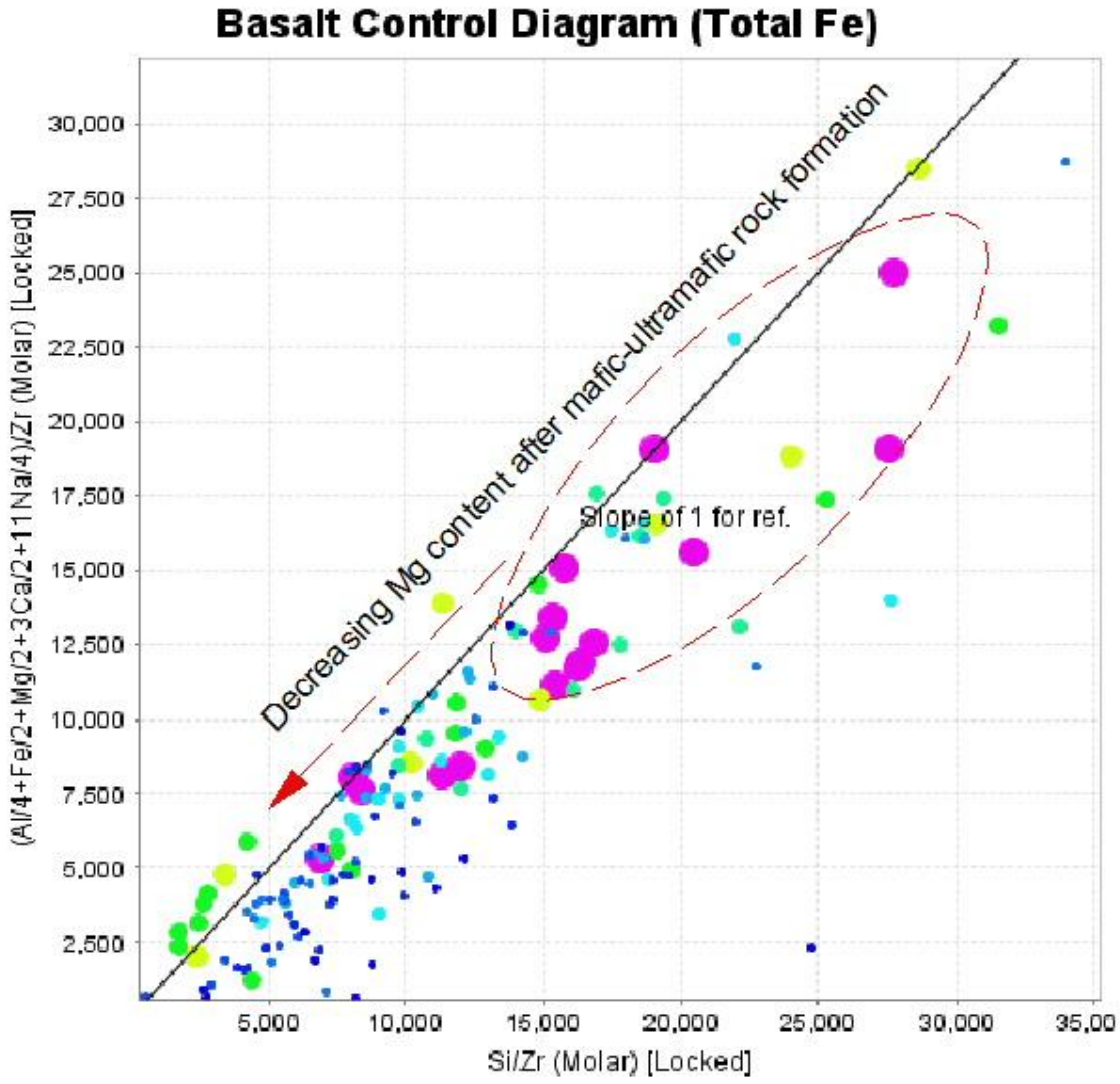
Basalt Control Diagram (Total Fe)
Decreasing Mg content after mafic-ultramafic rock formation
Slope of 1 for ref.
(Al/4+Fe/2+Mg/2+3Ca/2+11Na/4)/Zr (Molar) [Locked]
Si/Zr (Molar) [Locked]
30,000
27,500
25,000
22,500
20,000
17,500
15,000
12,500
10,000
7,500
5,000
2,500
5,000
10,000
15,000
20,000
25,000
30,000
35,00

C.)

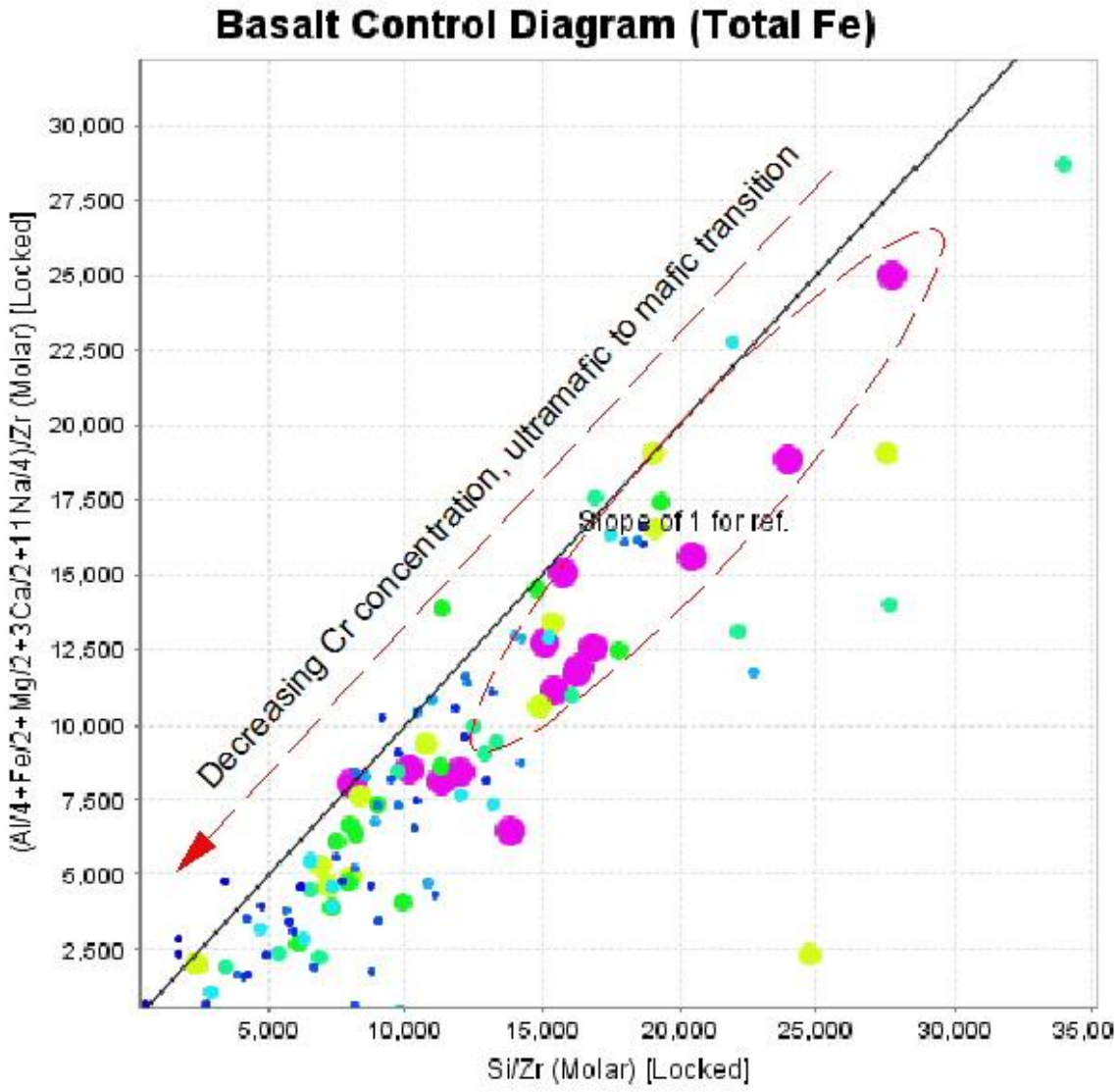
Basalt Control Diagram (Total Fe)
Decreasing Cr concentration, ultramafic to mafic transition
Slope of 1 for ref.
(Al/4+Fe/2+Mg/2+3Ca/2+11Na/4)/Zr (Molar) [Locked]
Si/Zr (Molar) [Locked]
30,000
27,500
25,000
22,500
20,000
17,500
15,000
12,500
10,000
7,500
5,000
2,500
5,000
10,000
15,000
20,000
25,000
30,000
35,00

D.)

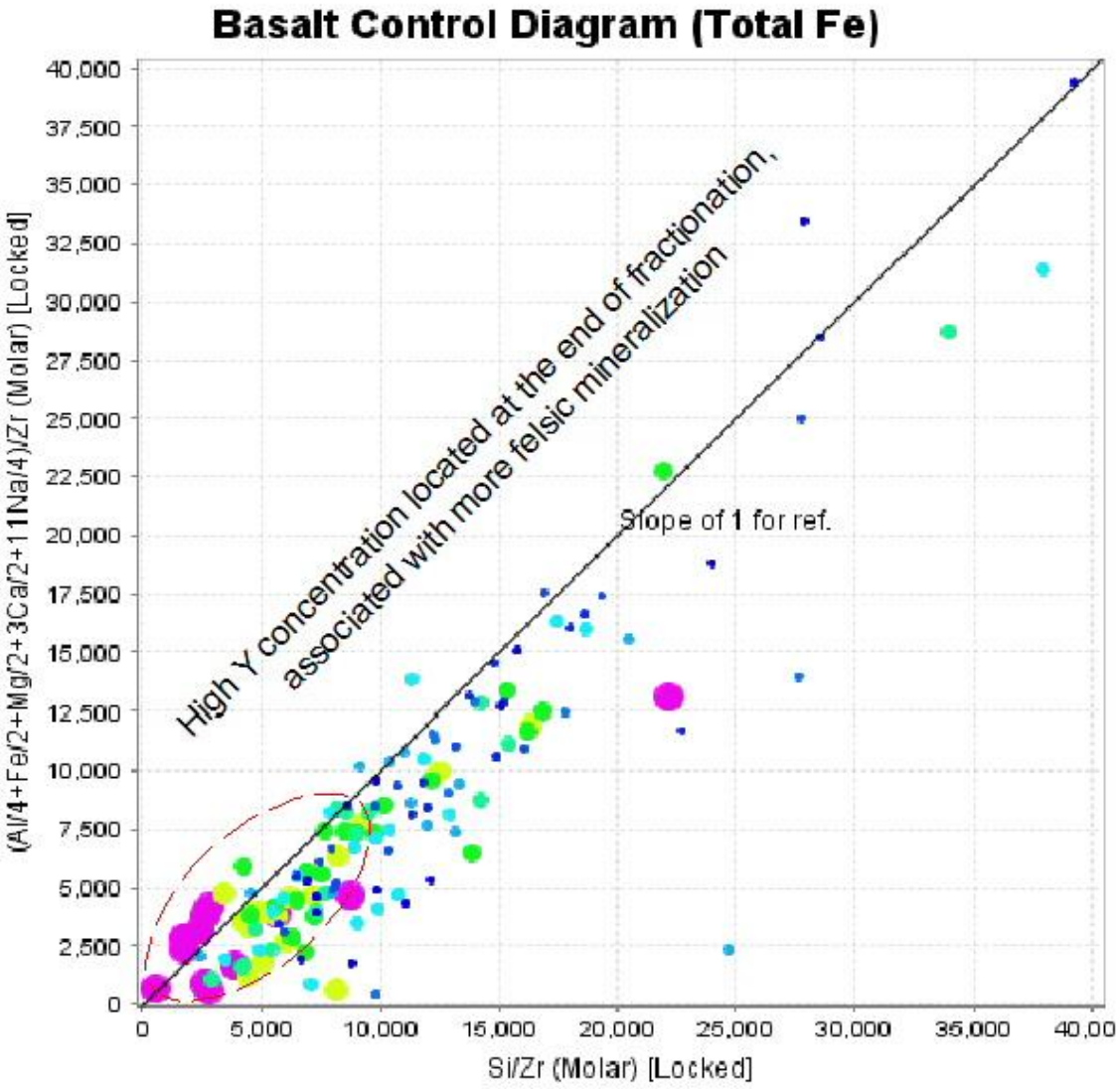

Figure 53 A through D, Basalt fractionation trends of the Tisdale mafic metavolcanic rocks, by plotting Si/Zr versus (Al/4+Fe/2+Mg/2+3Ca/2+11Na/4)/Zr (Molar) **A.)** Aluminum concentration is proportional to dot size, larger dots correpond to higher Al_2O_3 wt%. **B.)** Magnesium concentration is proportional to dot size, larger dots correspond to higher MgO wt%. **C.)** Chromium concentration is proportional to dot size, larger dots correspond to higher Cr ppm. **D.)** Yttrium concentration is proportional to dot size, larger dots correspond to higher Y ppm. Modified from Stanley and Madeisky 1996.

The concentration of the mobile sodium and potassiumcorresponds with rock type, as well as alteration type and intensity in rock units throughout the Porcupine Camp. Sodium is enriched by fractional crystallization and results in sodium concentrations being highest during later stages of crystallization (Fig. 54A). However, Na is deposited with calcium in the plagioclase solid solution series, so low concentrations are present in the earliest plagioclase formed. Potassium is also enriched in the final stages of fractional crystalization of a mafic magma and corresponds with the formation of alkali feldspar-ortholocase in the study area rocks (Fig. 54B). Both Na and K appear to behave according Bowen's Reactions Series and do not indicate that the mafic metavolcanic rock units have undergone strong alteration

A.)

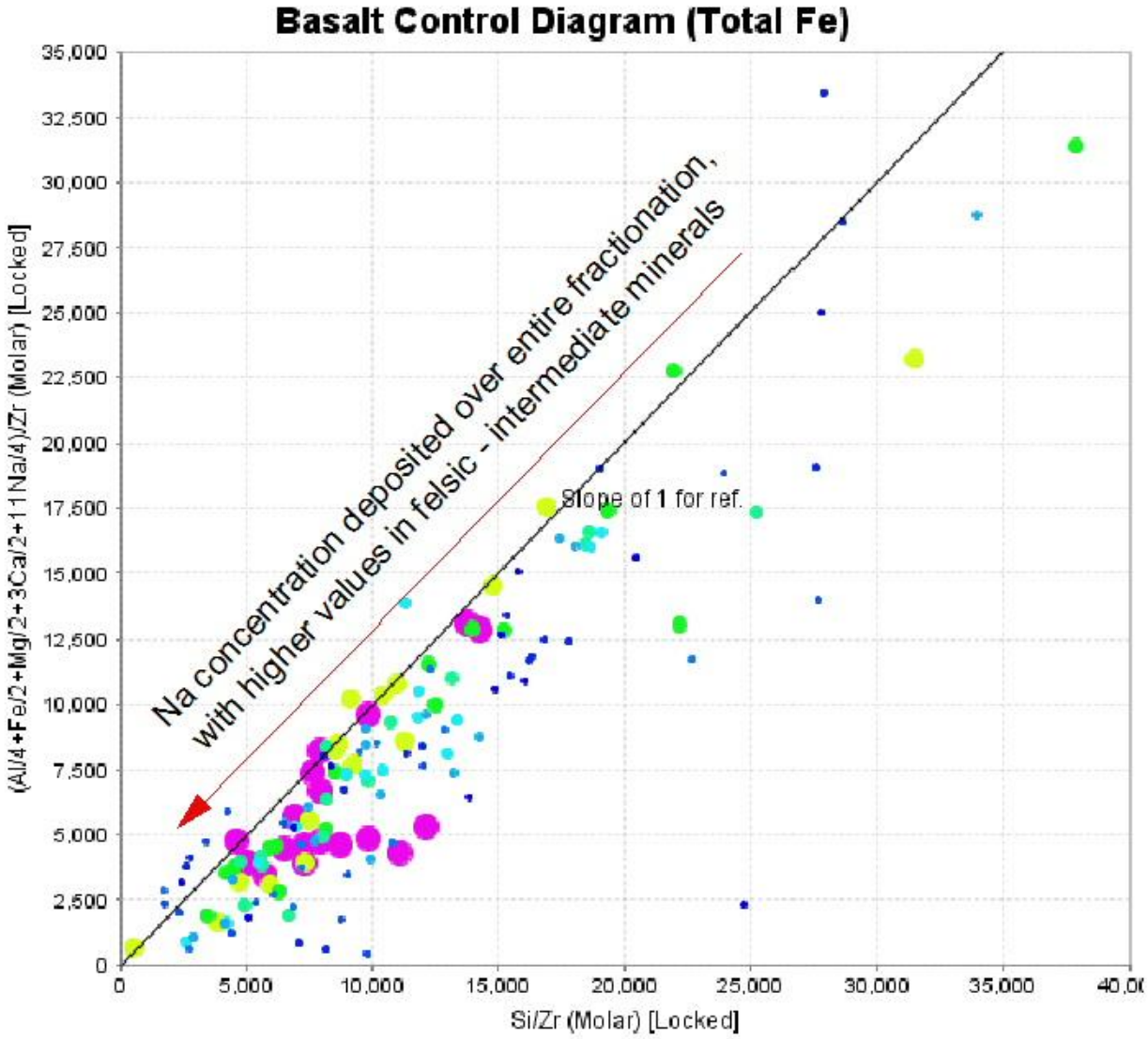
Basalt Control Diagram (Total Fe)
(Al/4+Fe/2+Mg/2+3Ca/2+11Na/4)/Zr (Molar) [Locked]
Si/Zr (Molar) [Locked]
Na concentration deposited over entire fractionation, with higher values in felsic - intermediate minerals
Slope of 1 for ref.
0
2,500
5,000
7,500
10,000
12,500
15,000
17,500
20,000
22,500
25,000
27,500
30,000
32,500
35,000
0
5,000
10,000
15,000
20,000
25,000
30,000
35,000

B.)

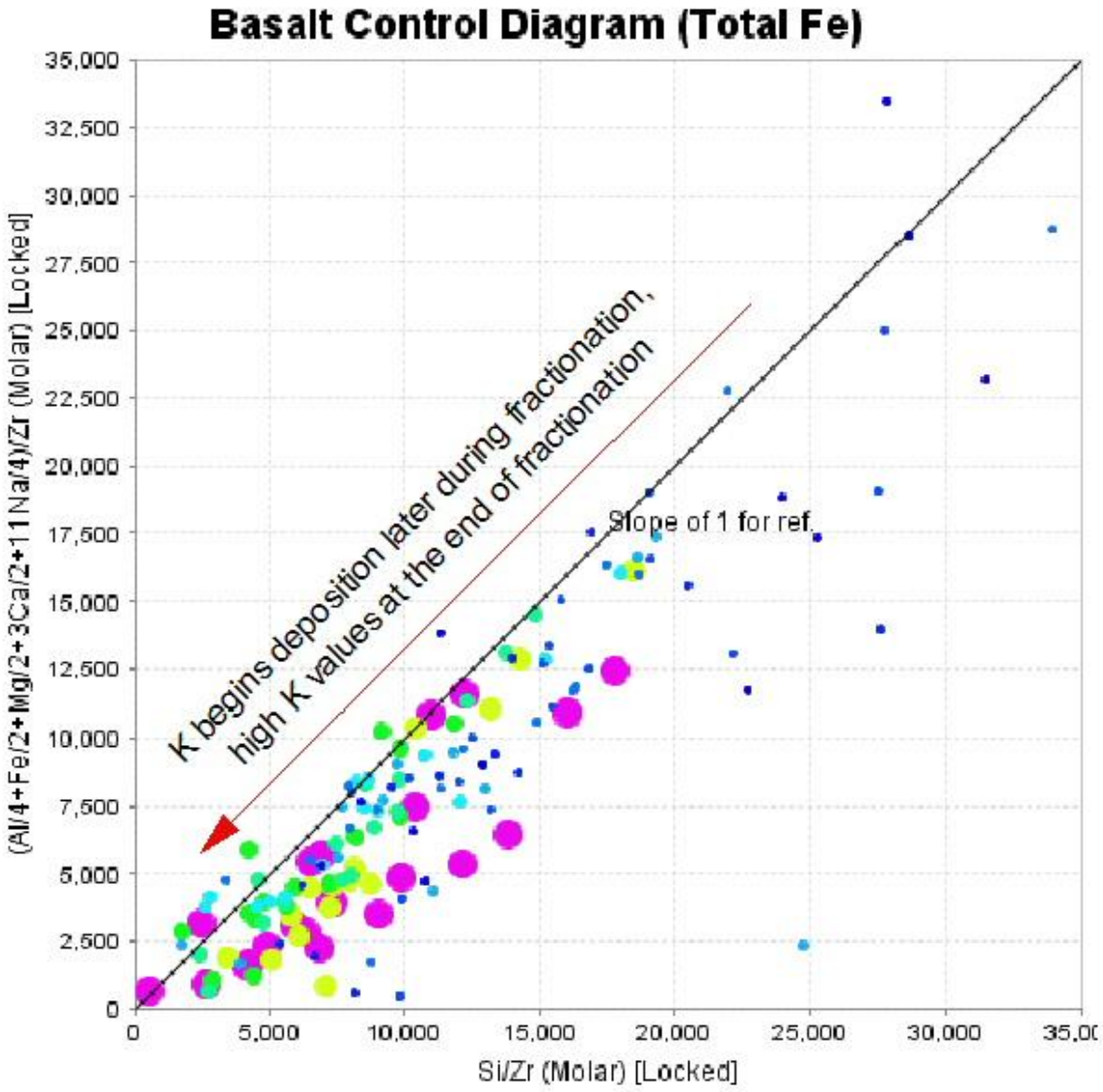

Figure 54 A and B, Basalt fractionation trend lines modified from the Stanley and Madeisky (1996), by plotting Si/Zr versus (Al/4+Fe/2+Mg/2+3Ca/2+11Na/4)/Zr (Molar) **A.)** Sodium concentration is proportional to dot size, larger dots correpond to higher Na_2O wt%. **B.)** Potassium concentration is proportional to dot size, larger dots correspond to higher K_2O wt%. Modified from Stanley and Madeisky 1996.

When interpreting the elements together, the samples appear to have experienced fractionation, supporting rhyolite-basalt type bimodal volcanism in the study area. The rock unit lacks strong carbonate hydrothermal alteration, and consequently the Tisdale mafic metavolcanic rocks have lower gold concentrations. The samples in the study area that have CO_2/CaO values above the 1.5 threshold contain higher gold concentrations. This range of values is similar to that found in metasedimentary rocks, where the target values lie between 1.5 and 2.0.

The mutual enrichment of barium, strontium, and phosphorus appear to be related to basalt fractionation and lacks the associated gold mineralization found in the metasedimentary rocks. Ba appears to have undergone weak mobility in the rock unit because some of the samples deviate from the fractionation trend line. The Ba concentrations increase with Si concentration suggesting that the rocks might have been silicified (Fig. 52 C). This association might indicate that hydrothermal alteration occurred without the carbonate and accompanying strontium and phosphorus that was seen in the metsedimentary rocks. This association could be explained in two possible ways: 1) It is low temperature alteration (possible on the periphery of a mineralized zone) that was able to mobilize Ba but not Sr and P; or 2) A different alteration type, with the Ba enriched rocks having undergone silicification, without addition of carbonate or chlorite.

4.5 Blake River and Kidd-Munro Felsic Metavolcanic Rocks

The felsic metavolcanic rocks of the Upper Blake River and Upper Kidd-Munro Assemblages underlie the northwestern corner of Bristol Township. The felsic rock

samples have been classified as a rhyolite-dacite dominantly of calc-alkaline affinity. The felsic metavolcanic rocks plot primarliy in the rhyolite-andesite of calc-alkaline composition with only minor tholeiitc rocks. Figure 55 plots data on a Jensen Cation Plot. The classification is best described by Thurston et al. (2008) interpretation with rocks being of the Lower Kidd-Munro and Upper Blake River Assemblages (Thurston et al. 2008).

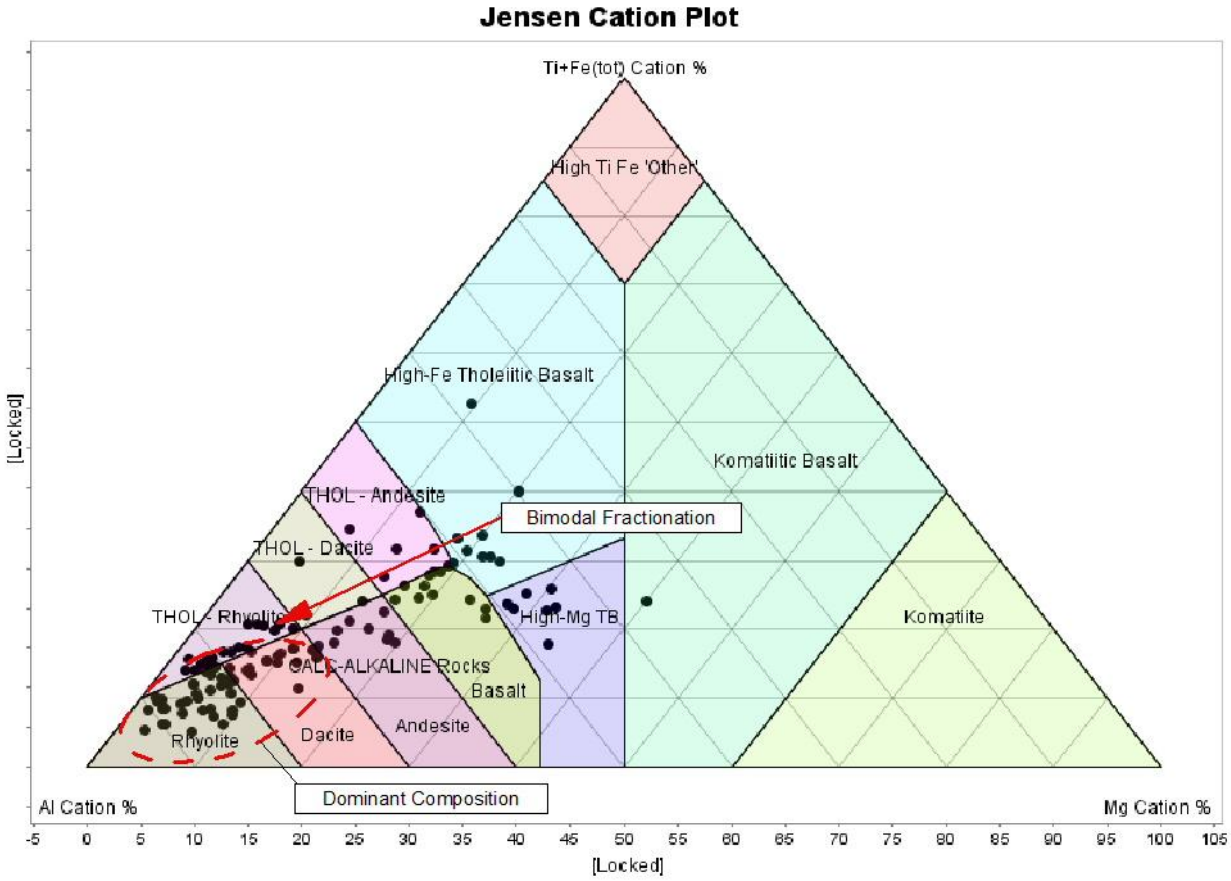

Figure 55 Jensen Cation Plot of the felsic metavolcanic rocks of Blake River and Kidd-Munro Assemblages in Bristol-Thorneloe Township. The data points plot primarily in the calc-alkaline rhyolite-basalt range with only a few samples plotting in the mafic tholeiitic field (Jensen 1976).

The calc-alkaline rhyolite-basalt rocks lack strong dolomite-ankerite carbonate alteration and have lower gold concentrations. There are only a few samples located in the dolomite-ankerite carbonate alteration field, with most plotting in the “least altered” zones (Fig. 56). Higher gold concentrations do appear to have an association with carbonate mineralization (Large et al. 2001) but there are too few samples to establish a conclusive relation. Additional gold assays of the samples that plot in the carbonate alteration field (Fig. 56) might provide evidence for a gold-carbonate association.

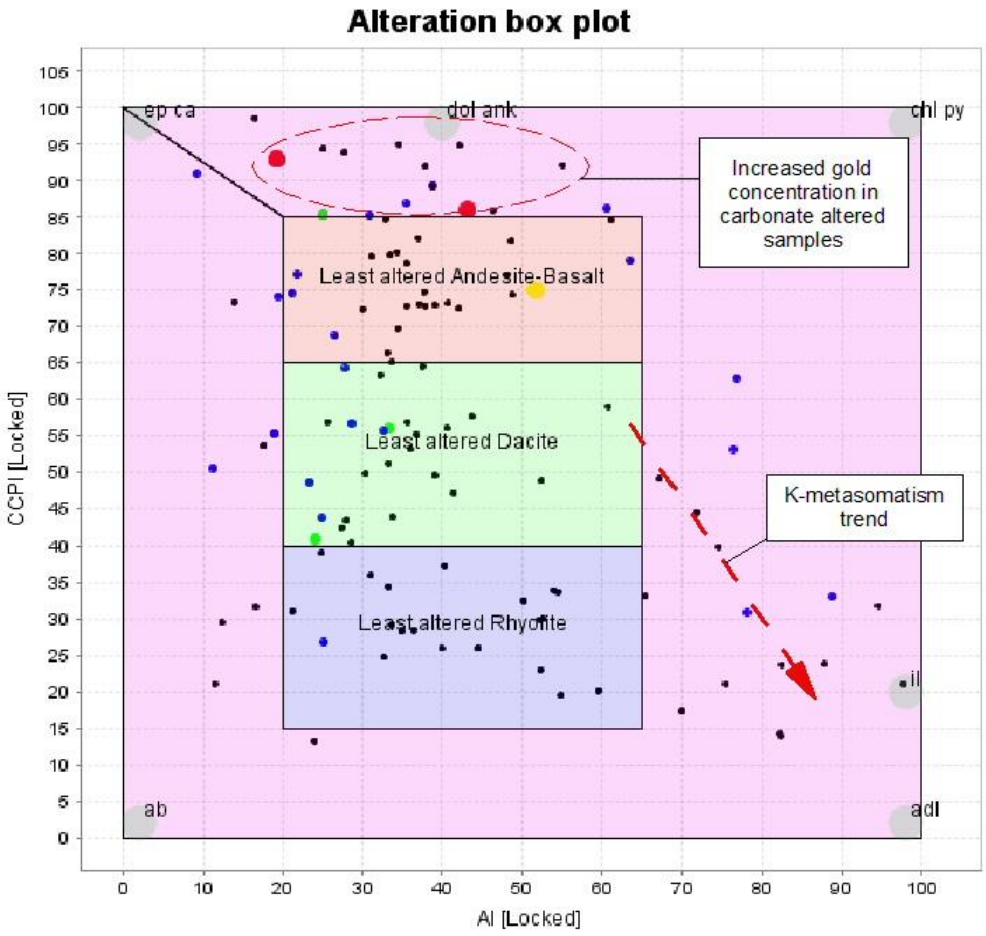

Figure 56 Alteration Box Plot of the felsic metavolcanic rocks of Blake River and Kidd-Munro Assembalges in Bristol-Thorneloe Township, red ovals envelop carbonate altered samples. Dot size and color correspond to gold concentration, Blue - < 5 ppb, Green – 5 to 30 ppb, Yellow 30 to 100 ppb, Red 100 to 500 ppb, Black – No Assay (Value), Modified from Large et al., 2001.

The alteration box plot contains a trend toward adularia formation. Adularia ($KAlSi_3O_8$) is deposited by low temperature hydrothermal fluids. This type of alteration is different from that found in the mafic metavolcanic and metasedimentary rocks, where alteration trends consist predominantly of carbonatization and chloritization. The dominant alteration type in felsic metavolcanic rocks is K-metasomatism with approximately two thirds of the rocks having K-enrichment (Fig. 57). Hydrothermal fluids

rich in potassium can either deposit K-feldspar or alter existing rocks to form serecite (K-rich mica). Deposition of K-spar is the dominant type of mineralization (~70%) in the felsic rocks of the study area (Fig. 58), with ~30% having compositions that are transitional to or being sericite-muscovite alteration (Stanley and Madiesky 1996). The abundant K-feldspar might have been deposited by fractional crystallization of the primary melt that formed the calc-alkaline rock units. The transition to and presence of muscovite-sericite alteration might be a later stage feature and not associated with the primary K-felspar in the rhyolite-dacite rocks.

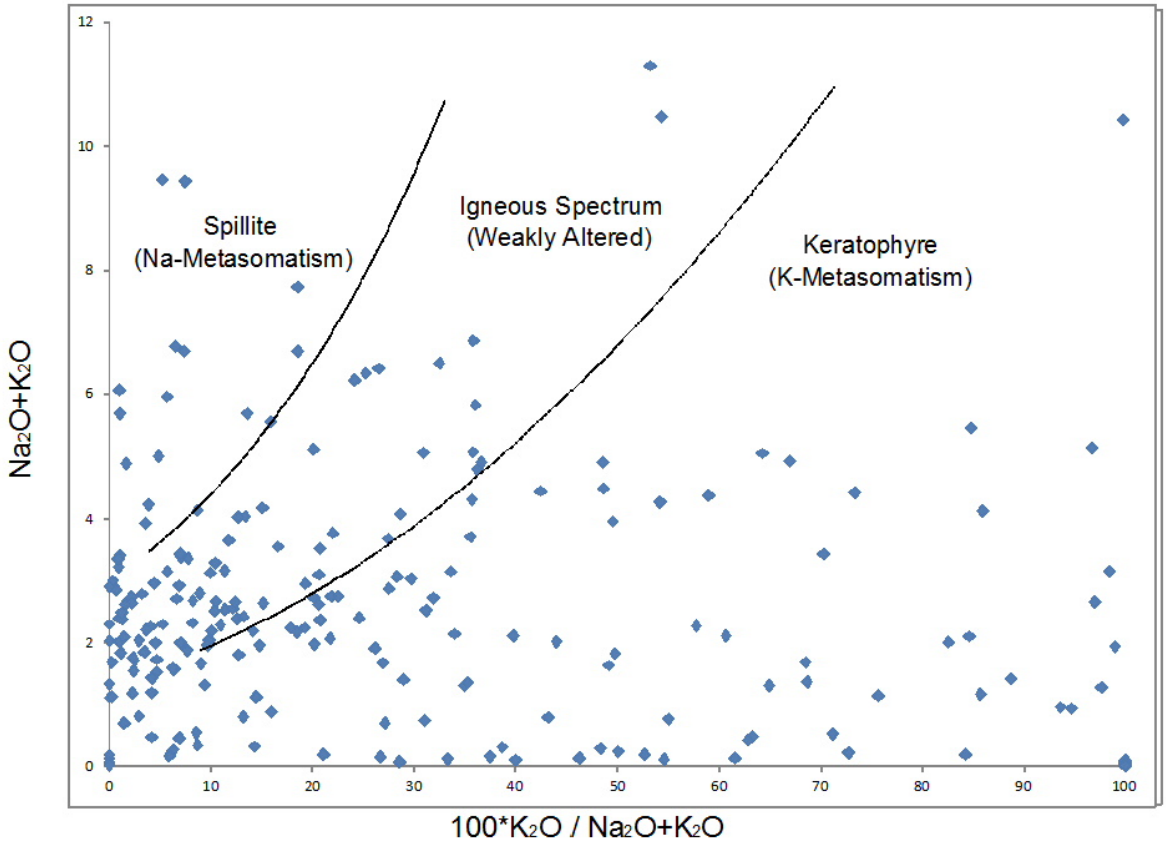

Figure 57 Alteration Type Discriminant Plot of the felsic metavolcanic rocks of Blake River and Kidd-Munro Assemblages in Bristol-Thorneloe Township, using major elements to analyze the type of metasomatic alteration. Modified from MacDonald 2005.

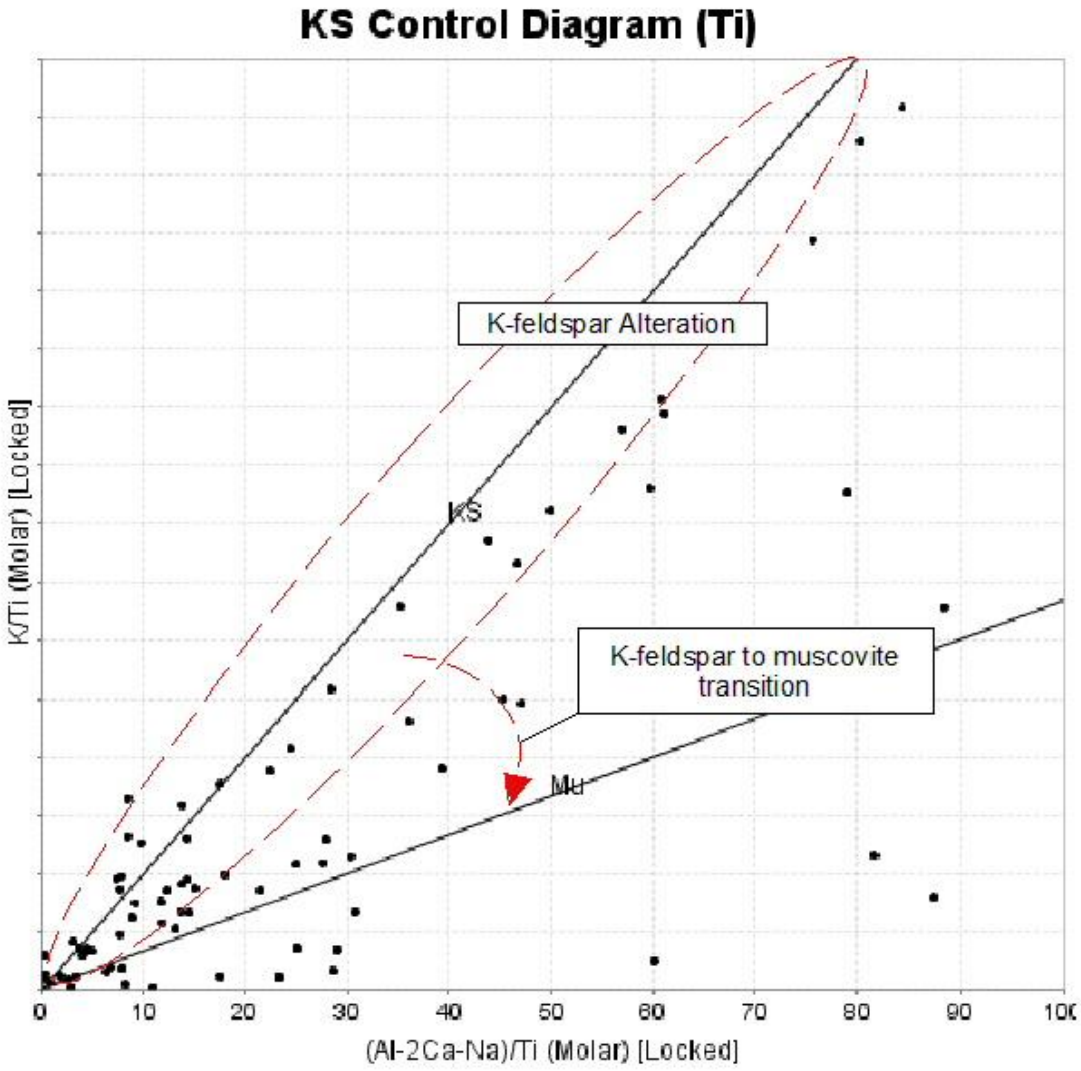

Figure 58 Potassium Alteration Type Diagram of the felsic metavolcanic rocks of Blake River and Kidd-Munro Assemblages in Bristol-Thorneloe Township, adularia to muscovite alteration. Modified from Stanley and Madiesky 1996.

Barium has also been mobilized in the calc-alkaline rhyolite-dacite rocks as indicated by higher Ba concentrations associated with higher alteration intensity (Ishikawa Index) (Fig. 59) and lower CCPI (Carbonate Chlorite Pyrite Index). Barium probably replaced K in the adularia ($KAlSi_3O_8$) by coupled substitution to form Celsian-cymrite ($BaAl_2Si_2O_8$) - ($BaAl_2Si_2O_8 \bullet H_2O$) or Hyalophane $(K,Ba)Al(Si,Al)Si_2O_8$. Barium replacement of Ca and

Na in alkali feldspars and plagioclase minerals, where K has been added can be seen in Fig. 60A and B and supports the formation of Celsian in the rhyolite – dacite rocks (Blundy and Wood 1991; Burzo 2007).

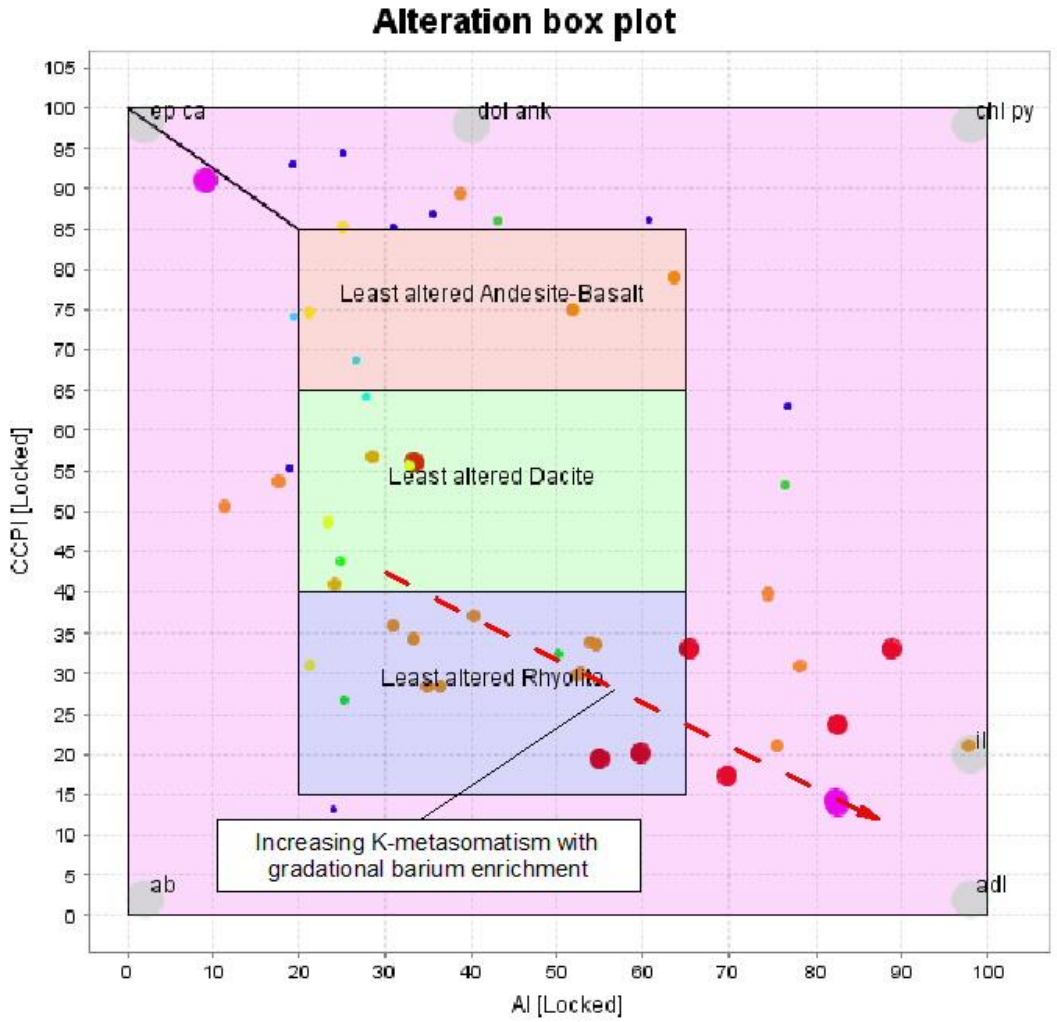

Figure 59 Alteration Box Plot of the felsic metavolcanic rocks of Blake River and Kidd-Munro Assemblages in Bristol-Thorneloe Township, dot size and color correspond to barium concentrations, Dark Blue - < 200 ppm, Light Blue – 200 to 300 ppm, Green – 300 to 400 ppm, Yellow – 400 to 500, Orange – 500 to 750 ppm, Red – 750 to 1,000 ppm, Purple - >1,000 ppm. Modified from Large et al., 2001.

A.)

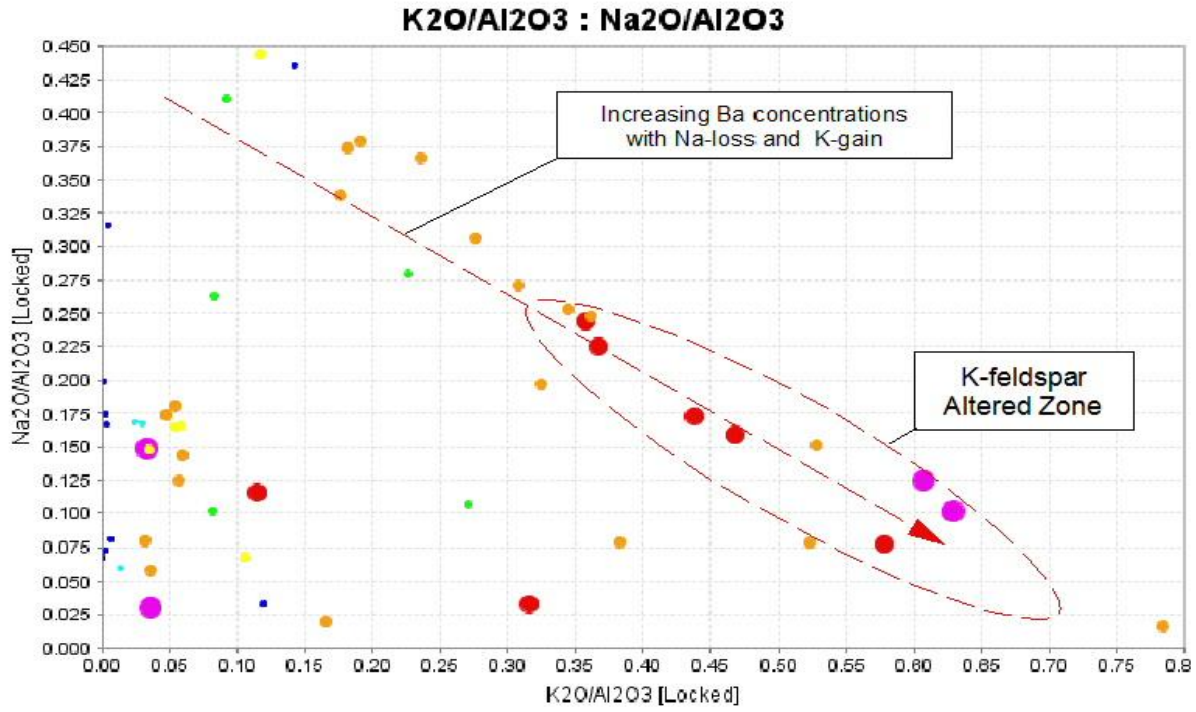
K2O/Al2O3 : Na2O/Al2O3
Increasing Ba concentrations with Na-loss and K-gain
K-feldspar Altered Zone
Na2O/Al2O3 [Locked]
K2O/Al2O3 [Locked]

B.)

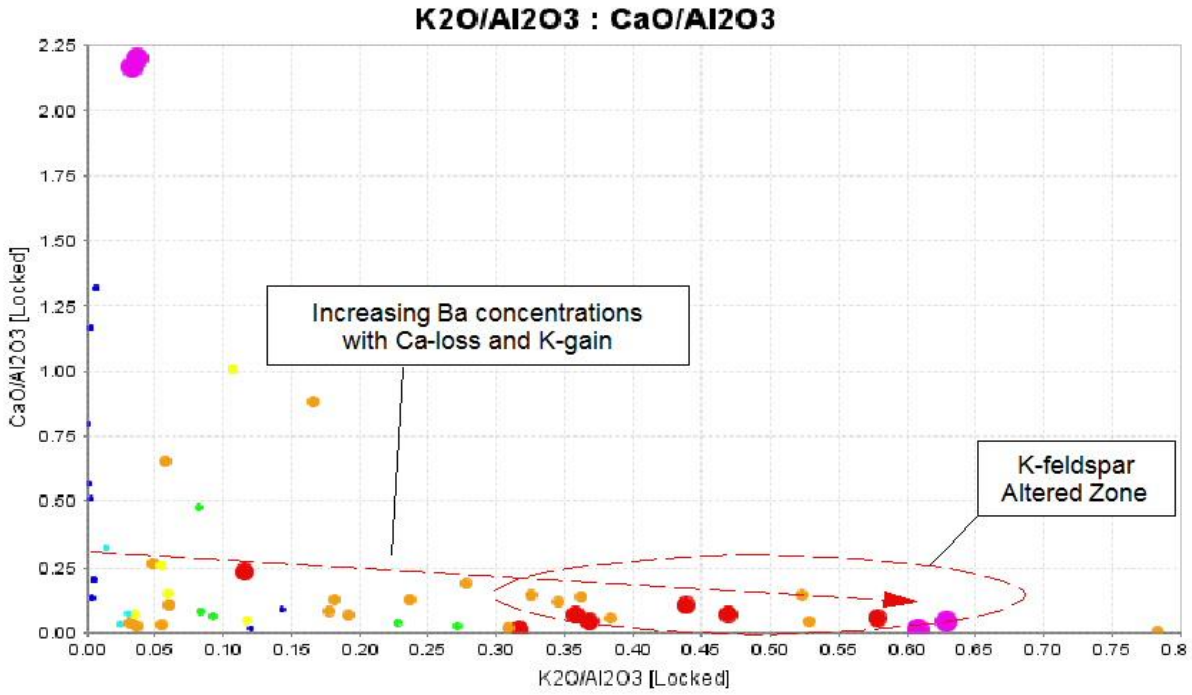
K2O/Al2O3 : CaO/Al2O3
Increasing Ba concentrations with Ca-loss and K-gain
K-feldspar Altered Zone
CaO/Al2O3 [Locked]
K2O/Al2O3 [Locked]

Figure 60 Barium enrichment plots; A) Barium in alkali feldspar formation - K_2O/Al_2O_3 vs. Na_2O/Al_2O_3, and B) Barium in plagioclase formation - K_2O/Al_2O_3 vs. CaO/Al_2O_3. Dot size and color correpond to barium concentraions, Dark Blue - < 200 ppm, Light Blue – 200 to 300 ppm, Green – 300 to 400 ppm, Yellow – 400 to 500, Orange – 500 to 750 ppm, Red – 750 to 1000 ppm, Purple - >1000 ppm.

Hydrothermal mobilization is the proposed method for Ba addition to the felsic metavolcanic rocks because barium is mobilized elsewhere in the Bristol-Thorneloe Study area. This alteration is thought to be caused by low temperature alteration that only weakly mobilizes barium to form celsian-cymrite minerals (Burzo 2007). The Ba concentrations found in K-metasomatic zone hosted by the felsic rocks are much lower than those found associated with gold mineralized samples collected from the metasedimentary and mafic metavolcanic rocks.

Strontium and phosphorus appear to be relatively immobile and have lower concentrations in rhyolite-dacite rocks. Typical values found in these rocks are <250 ppm Sr and <0.15 wt% P_2O_5. Higher concentrations of strontium and phosphorus are 250 to 500 ppm and 0.20 wt% to 0.50 wt%, respectively, in the Lower Kidd-Munro and Upper Blake River Assemblages in the andesitic to basaltic lens (Fig. 61A and B). These values are relatively low compared to other samples in the study area and are thought to be evidence of primary rock composition rather than a product of hydrothermal enrichment. Sr and P_2O_5 values plotted on Na_2O/Al_2O_3 versus K_2O/Al_2O_3 and CaO/Al_2O_3 versus K_2O/Al_2O_3 diagrams have higher values of each element plotting near the origin (Figs. 62 A - D) and is thought to be evidence that Sr and P_2O_5 are not related to Na or K metasomatism but are immobile and reflect initial concentrations in unaltered rocks.

A.)

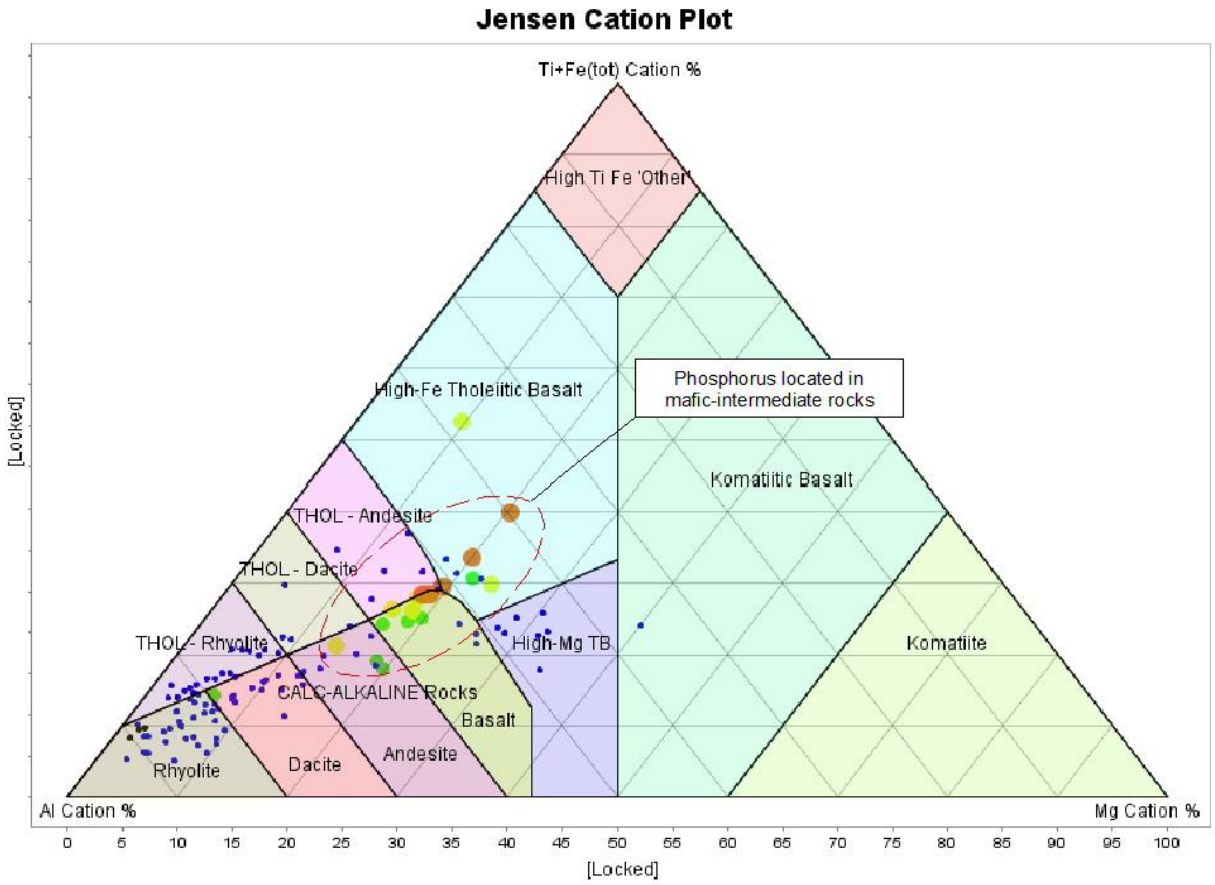
Jensen Cation Plot
Ti+Fe(tot) Cation %
High Ti Fe 'Other'
High-Fe Tholeiitic Basalt
Phosphorus located in mafic-intermediate rocks
Komatiitic Basalt
THOL - Andesite
THOL - Dacite
THOL - Rhyolite
High-Mg TB
Komatiite
CALC-ALKALINE Rocks
Basalt
Andesite
Dacite
Rhyolite
Al Cation %
Mg Cation %
[Locked]
[Locked]
0 5 10 15 20 25 30 35 40 45 50 55 60 65 70 75 80 85 90 95 100

B.)

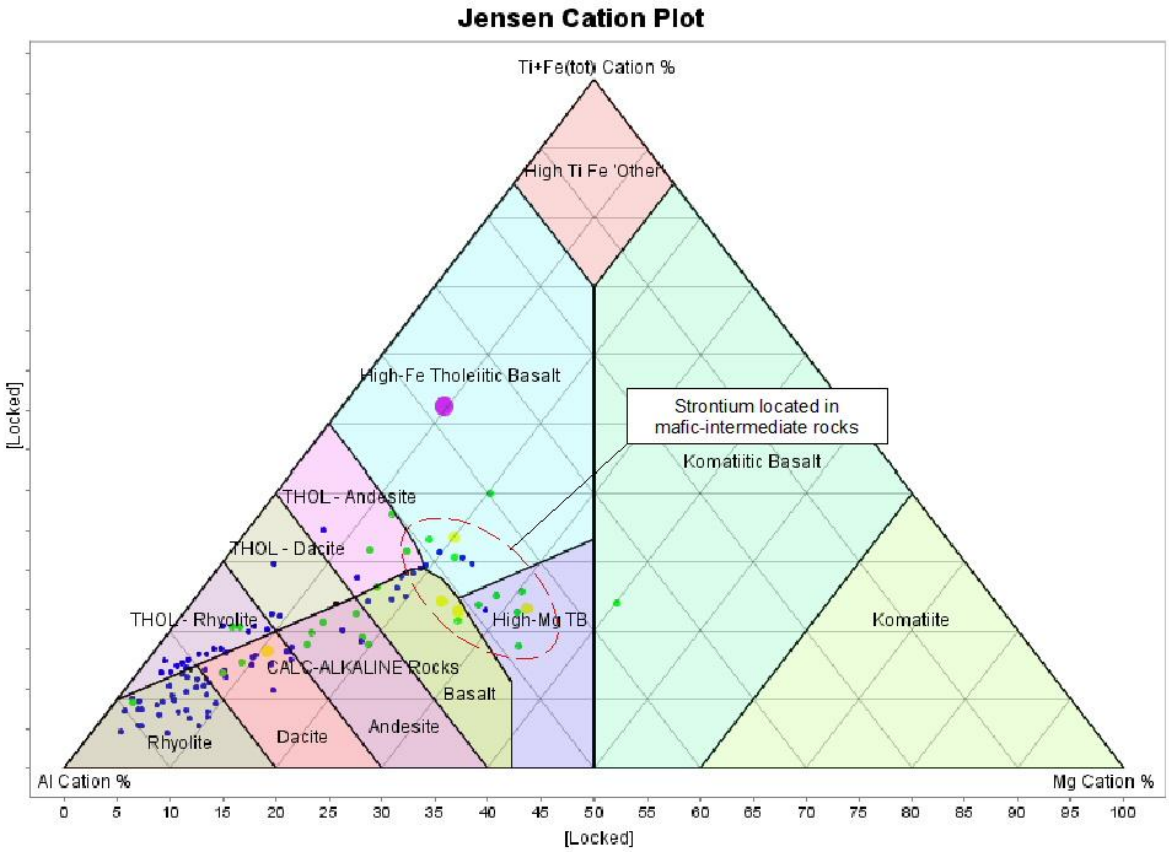

Figure 61 Jensen Cation Plot. **A.)** P_2O_5 wt% plotted against rock type, dot size and color correspond to P_2O_5 concentrations with Blue - < 0.15, Green – 0.15 to 0.20, Yellow – 0.20 to 0.25, Orange – 0.25 to 0.50, Purple - >0.75 wt%. **B.)** Sr ppm plotted relative to rock type, dot size and color correspond to Sr concentrations with Blue - < 100 ppm, Green – 100 ppm to 250 ppm, Purple - >1,000 ppm. Modified from Jensen, 1976.

A.)

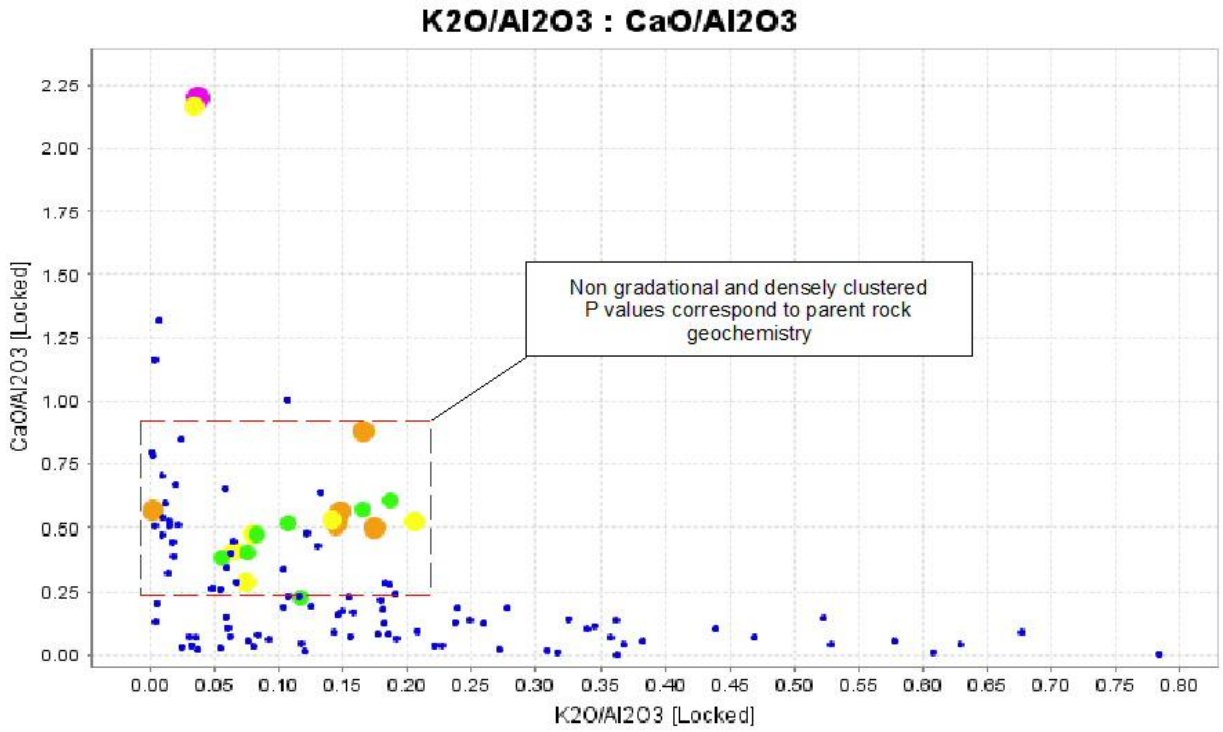
K2O/Al2O3 : CaO/Al2O3
CaO/Al2O3 [Locked]
K2O/Al2O3 [Locked]
Non gradational and densely clustered
P values correspond to parent rock
geochemistry
0.00
0.25
0.50
0.75
1.00
1.25
1.50
1.75
2.00
2.25
0.00
0.05
0.10
0.15
0.20
0.25
0.30
0.35
0.40
0.45
0.50
0.55
0.60
0.65
0.70
0.75
0.80

B.)

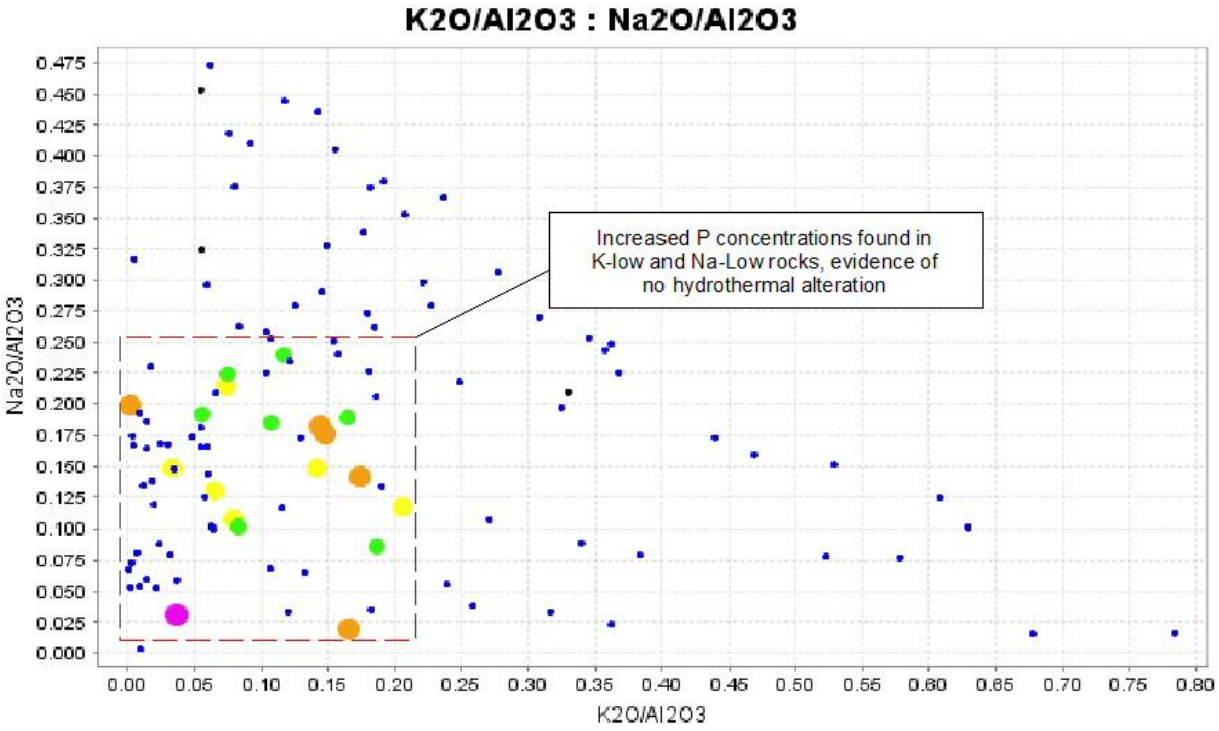
K2O/Al2O3 : Na2O/Al2O3
Increased P concentrations found in K-low and Na-Low rocks, evidence of no hydrothermal alteration
Na2O/Al2O3
K2O/Al2O3
0.475
0.450
0.425
0.400
0.375
0.350
0.325
0.300
0.275
0.250
0.225
0.200
0.175
0.150
0.125
0.100
0.075
0.050
0.025
0.000
0.00
0.05
0.10
0.15
0.20
0.25
0.30
0.35
0.40
0.45
0.50
0.55
0.60
0.65
0.70
0.75
0.80

C.)

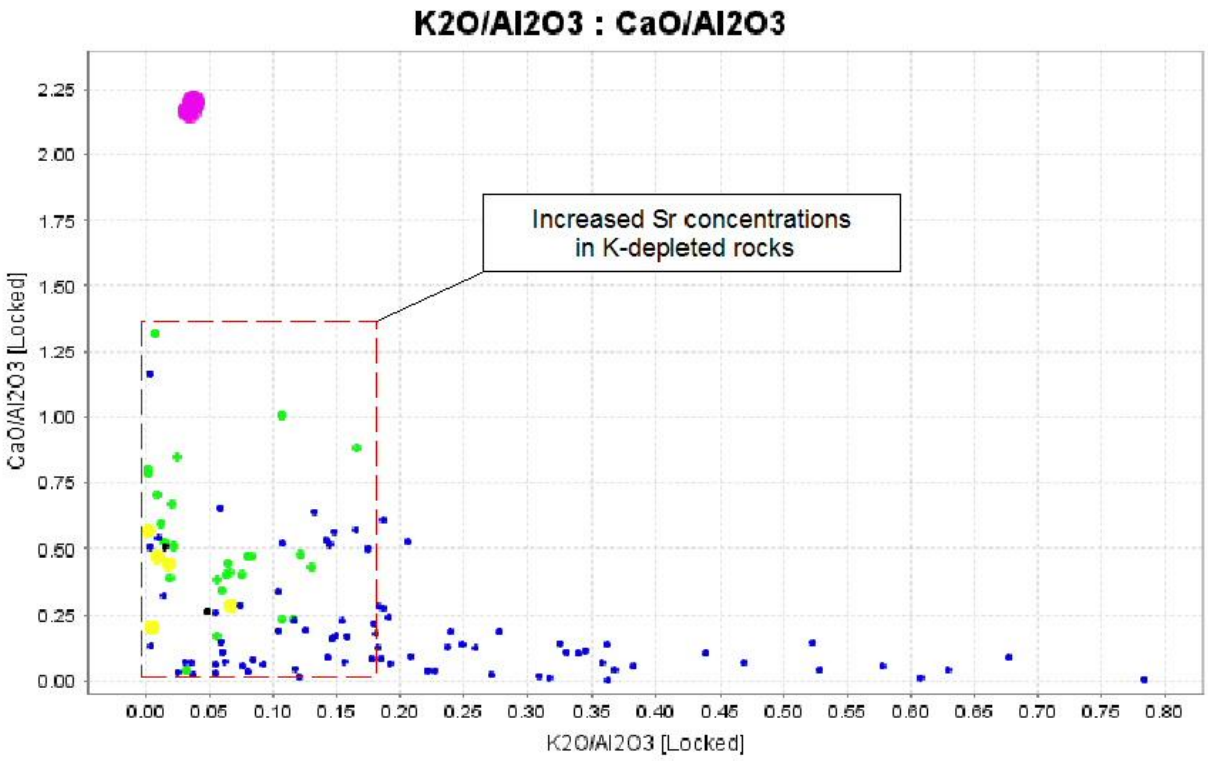
K2O/Al2O3 : CaO/Al2O3
Increased Sr concentrations
in K-depleted rocks
CaO/Al2O3 [Locked]
K2O/Al2O3 [Locked]
0.00
0.25
0.50
0.75
1.00
1.25
1.50
1.75
2.00
2.25
0.00
0.05
0.10
0.15
0.20
0.25
0.30
0.35
0.40
0.45
0.50
0.55
0.60
0.65
0.70
0.75
0.80

D.)

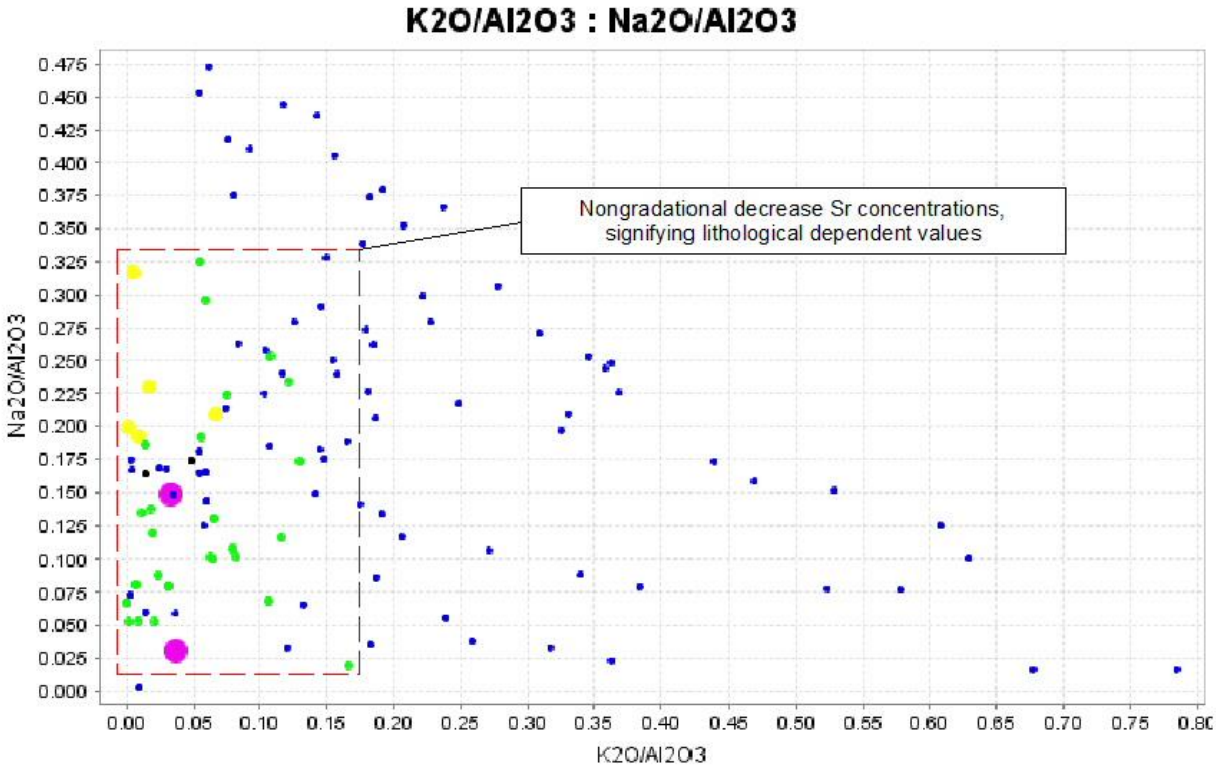

Figure 62 A through D Phosphorus and strontium plots for the felsic metavolcanic rocks of northwest Bristol Township: **A)** P_2O_5 concentrations plotted on CaO/Al_2O_3 versus K_2O/Al_2O_3 diagram, dot size and color correspond to P_2O_5 concentrations with Blue - < 0.15, Green – 0.15 to 0.20, Yellow – 0.20 to 0.25, Orange – 0.25 to 0.50, Purple - >0.75 wt%; **B)** P_2O_5 concentrations plotted on Na_2O/Al_2O_3 versus K_2O/Al_2O_3, dot concentrations are same as Figure 62 A; **C)** Sr ppm plotted on CaO/Al_2O_3 versus K_2O/Al_2O_3 diagram, dot size and color correspond to Sr concentrations with Blue - < 100 ppm, Green – 100 ppm to 250 ppm, Purple - > 1,000 ppm; **D)** Sr ppm plotted on Na_2O/Al_2O_3 versus K_2O/Al_2O_3 diagram, dot concentrations are same as Figure 62 C.

Two samples (EVH 16865 and EVH 16866) located in north-central Bristol Township have higher concentrations of Ba, Sr, and P that coincide with gold mineralization. The high values of these elements in these two samples are comparable to those found near the Lakeshore Gold Timmins West Mine. The concentrations and UTM coordinates are:

Table 2

Sample ID	Northing	Easting	P_2O_5 wt%	CO_2 wt%	Sr ppm	Ba ppm	Au ppb
EVH16865	5366450	460055	0.21	2.42	1227	1460	0
EVH16866	5366440	460067	3.39	2.00	1511	3328	135

The gold mineralization in sample EVH16866 is accompanied by higher concentrations of all the target mobile elements (Ba, Sr, P_2O_5) but not CO_2. The lower phosphorus and gold values in sample EVH 16865 might be explainable by either alteration intensity or original lithological differences.

4.6 Porphyry Suite Rocks

The Porphyry Suite consists of a series of felsic intrusive rocks, named the Bristol Township, Bristol Lake, and South Bristol Lake Porphyries, that occur in central and eastern Bristol Township. The intrusive bodies were grouped by MacDonald (2005) because they are chemically similar and are being treated in this study as single geochemical entity. The Porphyry Suite intrusive rocks have compositions that result in them plotting as tonalite–quartz monzonite on the R1-R2 Chemical Variation Diagram (Fig. 63).

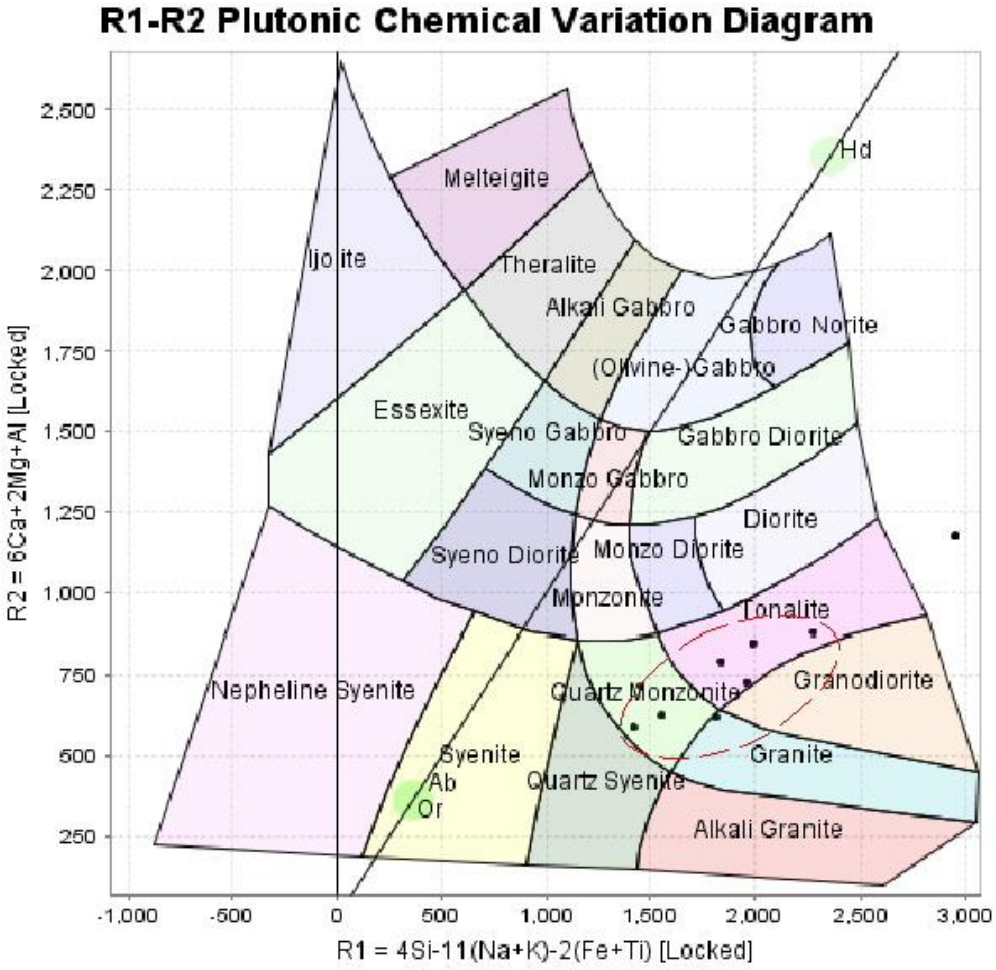

Figure 63 R1-R2 Chemical Variation Diagram for the Bristol Township, Bristol Lake and South Bristol Lake Porphyries in Bristol-Thorneloe Township. Modified from De La Roche et al., 1980.

A number of samples in this data set do not plot with the tonalite-quartz monozite intrusive rocks but are similar to the country rocks that host the intrusive rocks because they have geochemical compositions that plot in the calc-alkaline and tholeiitic andesite-basalt fields (Fig. 64). These andesite-basalt samples also contain high chromium (~300 ppm), nickel (>100 ppm) and CaO concentrations (> 5.00 wt%). It is likely that some of the samples analyzed by other workers and thought to belong to the porphyry

suite because of their location on geological maps are in fact altered basalt wallrocks that host the intrusive rather than a product of fractional crystallization in the felsic magma body. The results are interpreted this way because a number of samples collected from drill holes were projected vertically to surface and resulted in their plotting inside the intrusions near their edge.

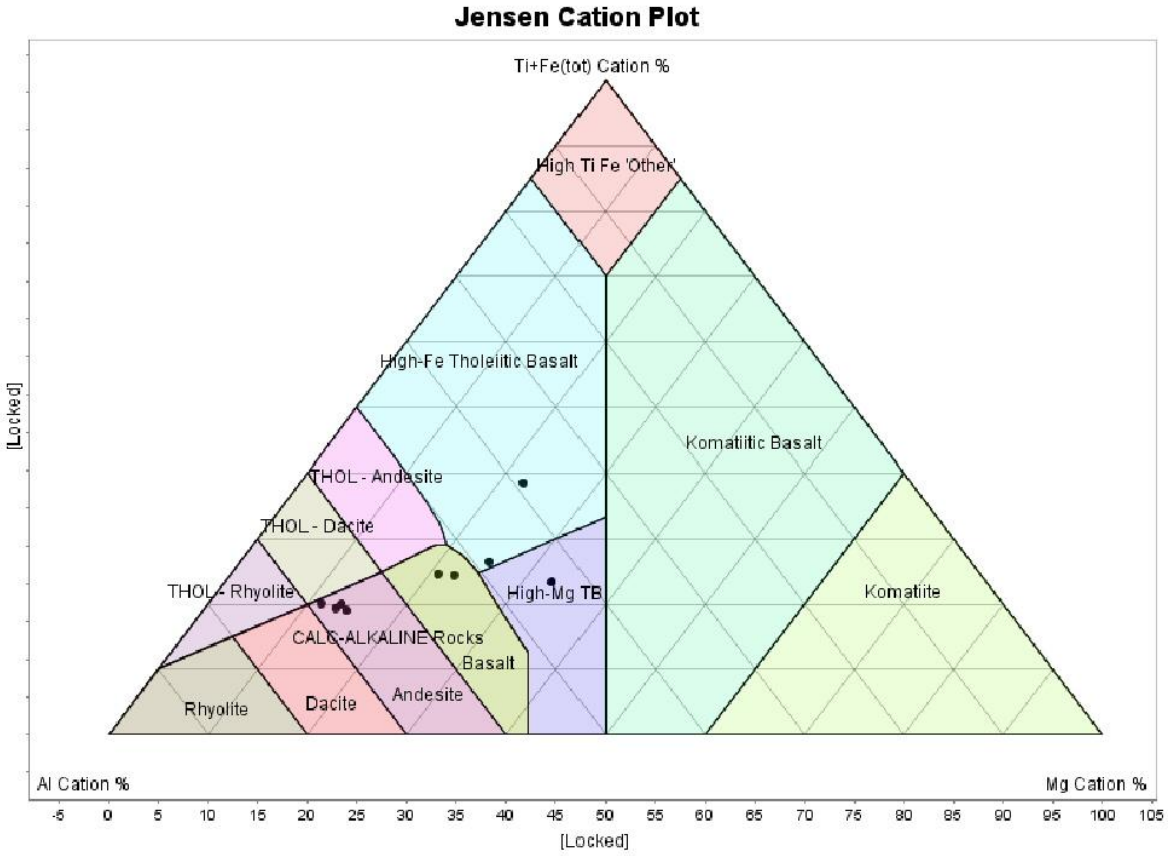

Figure 64 Jensen Cation Plot of the Porphyry Suite samples in Bristol-Thorneloe Township that did not plot on the R1-R2 Chemical Variation Diagram. Modified from Jensen, 1976.

Alteration type appears to vary in the two geochemically different types of rock. The tonalite-quartz monzonite intrusive rocks appear to have been subjected to Na-metasomatic alteration (Fig. 65 - red dots), and the intermediate-mafic rocks that plot in

the andesite-basalt field (Fig. 65 – blue dots) appear to have been weakly to moderately carbonatized (Large et al. 2001). MacDonald (2005) recognized both alteration types in the rock suite and came to the same conclusion that the Bristol Lake and South Bristol Lake porphyries had been albitized. The carbonate alteration consists primarily of partial to complete conversion of Ca-bearing silicates to calcite and two samples that contain a minor amount of Mg (Fig. 66). All the CO_2/CaO values fall below 1.5, the threshold for dolomite-ankerite formation, that is generally associated with the deposition of gold (Davies et al. 1982).

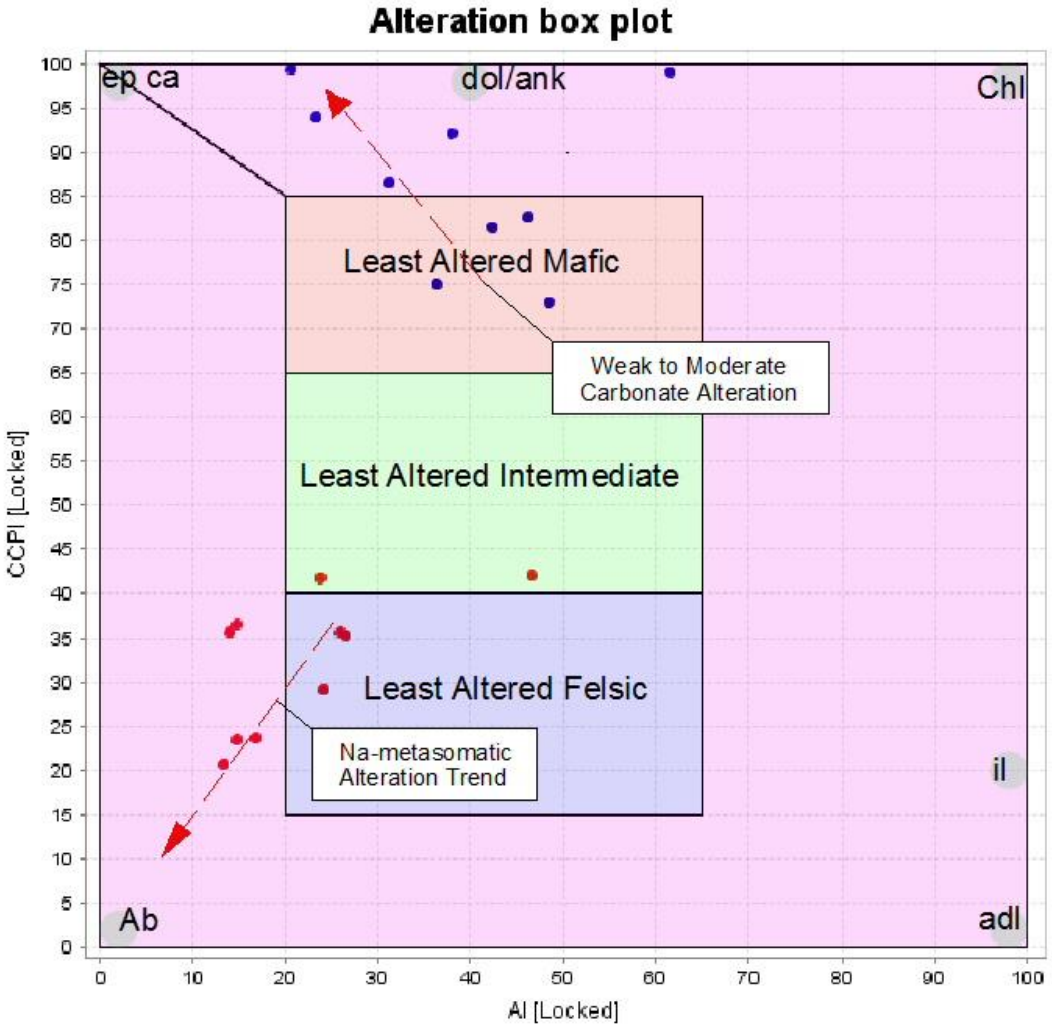

Figure 65 Alteration Box Plot for the Bristol Township, Bristol Lake, and South Bristol Lake Porphyries. Red dots indicate tonalite-quartz monzonite and blue dots indicate the intermediate-mafic rock unit that is interpreted to be andesite-basalt. Modified from Large et al., 2001.

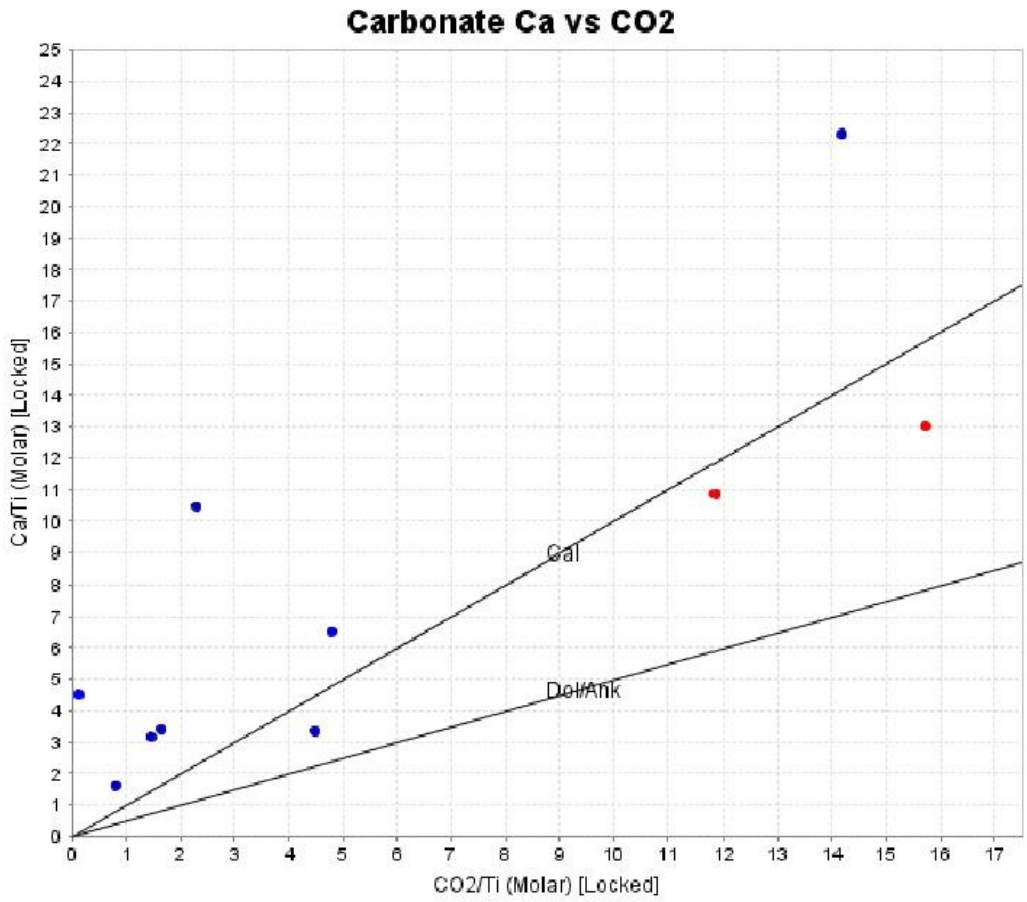

Figure 66 Ca/Ti vs. CO_2/Ti Carbonate Mineral-Alteration Plot for the Bristol Township, Bristol Lake, and South Bristol Lake Porphyries. Red dots indicate tonalite-quartz monzonite and blue dots indicate the intermediate-mafic rock unit that are interpreted to be andesite-basalt. Modified from Stanley and Madeisky, 1996.

The mobile constituents during alteration of the porphyry suite rocks are sodium, potassium, and barium. These rocks are characterized primarily by Na-addition and K-loss typically found in albite-muscovite alteration (Fig. 67). One sample (00-CMV-638a) differs from the others because it has K-addition and Na-depletion that typically occurs during Potassic Alteration (Fig. 67).

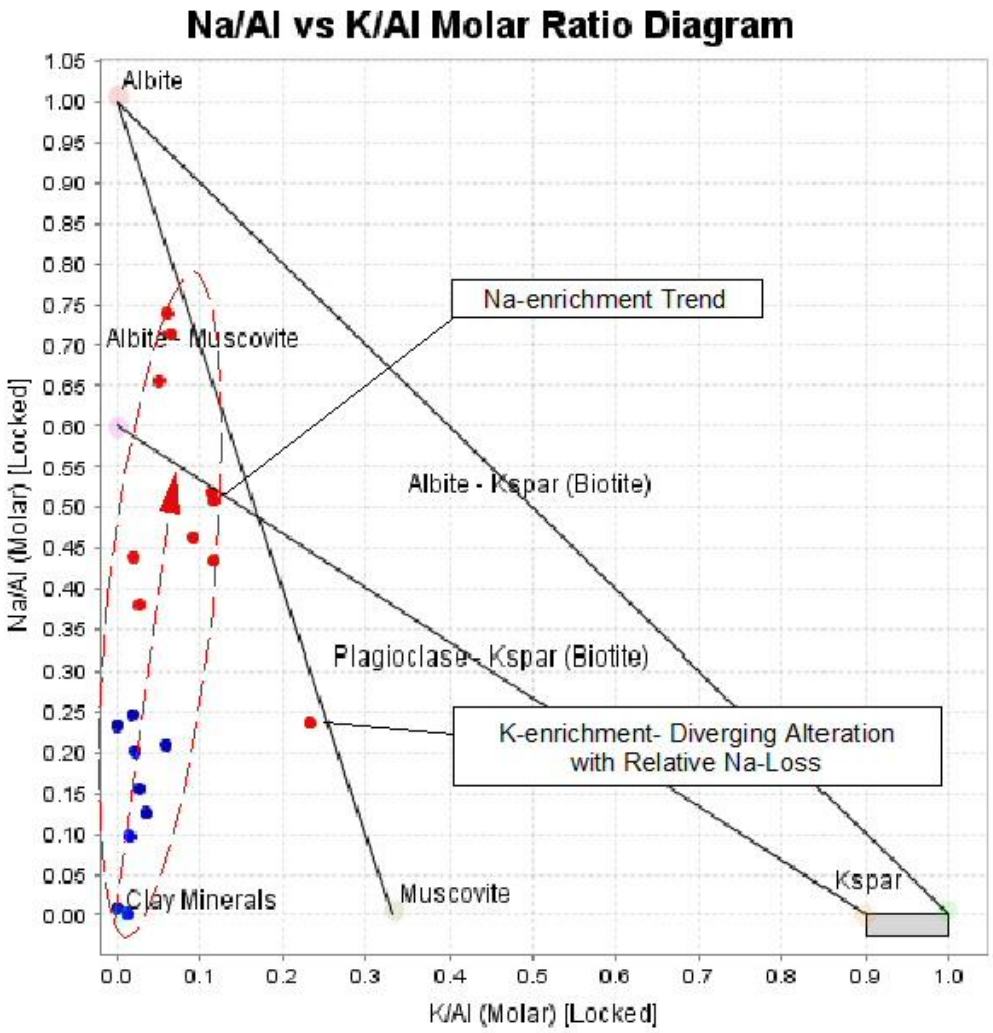

Figure 67 Alkali-Alumina Ratio Alteration Plot for the Bristol Township, Bristol Lake, and South Bristol Lake Porphyries. Red dots indicate tonalite-quartz monzonite and blue dots indicate the intermediate-mafic rock unit that is interpreted to be andesite-basalt. Modified from Davies and Whitehead, 2006.

Separate Na and K alteration types were documented by MacDonald (2005) and can be attributed to zonation caused by hydrothermal alteration, or possibly indicate that these rocks have been affected by two different fluids. Barium concentrations are scattered and appear to be independent of major element composition (felsic vs. mafic-intermediate rocks) and alteration type (Fig. 68). Higher barium concentrations might

correspond with the intensity of Na-metasomatic alteration. This possibility is evident in sample 04-PJM-256 that has both the strongest relative intensity of Na-alteration and highest Ba concentration (1,165 ppm). However, this possibility is based on just a single sample and additional results are necessary to form a positive association.

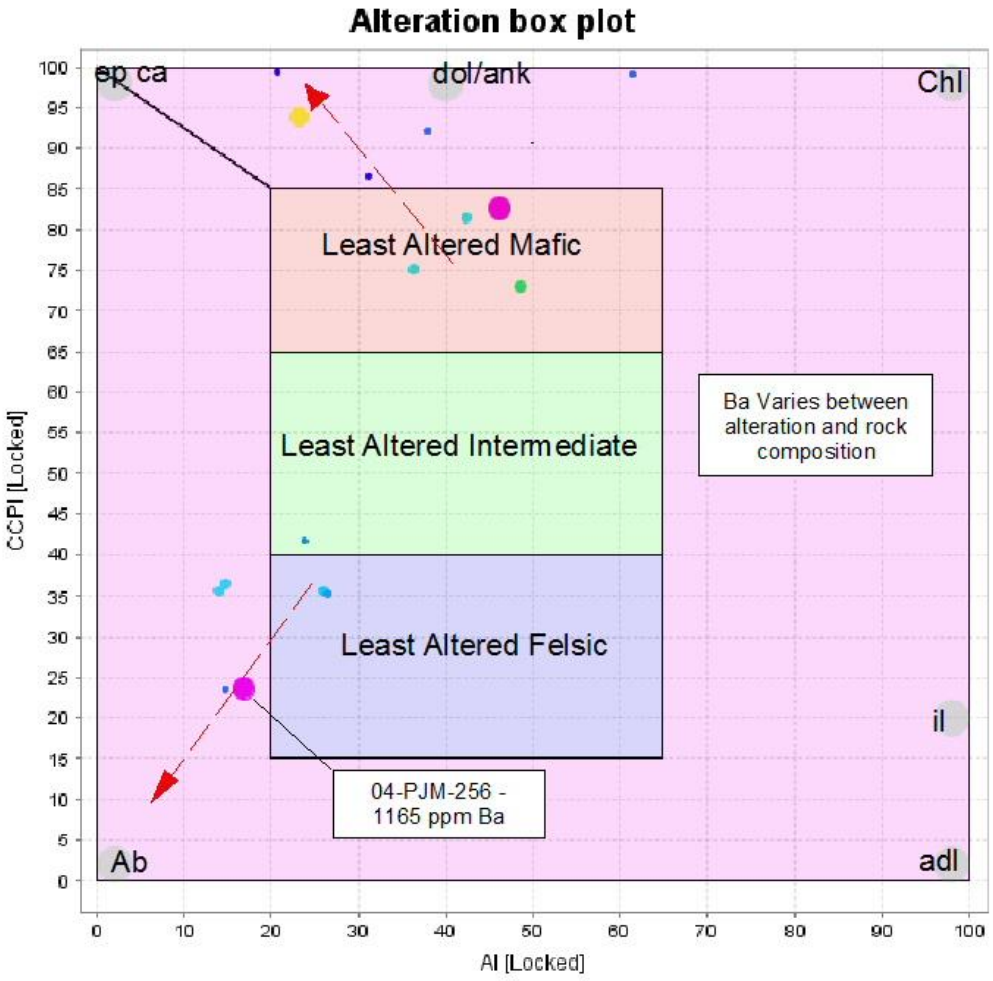

Figure 68 Alteration Box Plot considering Barium of the Porphry Suite in and Bristol-Thorneloe Township. Dot size and color correspond to barium concentrations; Dark Blue < 200 ppm, Light Blue – 200 to 300 ppm, Green – 300 to 400 ppm, Yellow – 400 to 500, Orange – 500 to 750 ppm, Red – 750 to 1,000 ppm, Purple >1,000 ppm. Modified from Large et al., 2001.

Strontium and phosphorus are immobile to weakly mobile elements that have concentrations typical for felsic to mafic rock units. Figure 69 and 70 show little to no variation in Sr and P in the mafic to intermediate rocks and the tonalite-quartz monzonite rocks. This lack of variation is interpreted to indicate immobile concentrations of each element in their respective rock units. This observation differs from those made by MacDonald (2005) who found that Sr was mobilized in the porphyries. The difference between this study and his might be attributable to MacDonald including the Holmer Porphyry and Thunder Creek syenite data with the Porphyry Suite rocks.

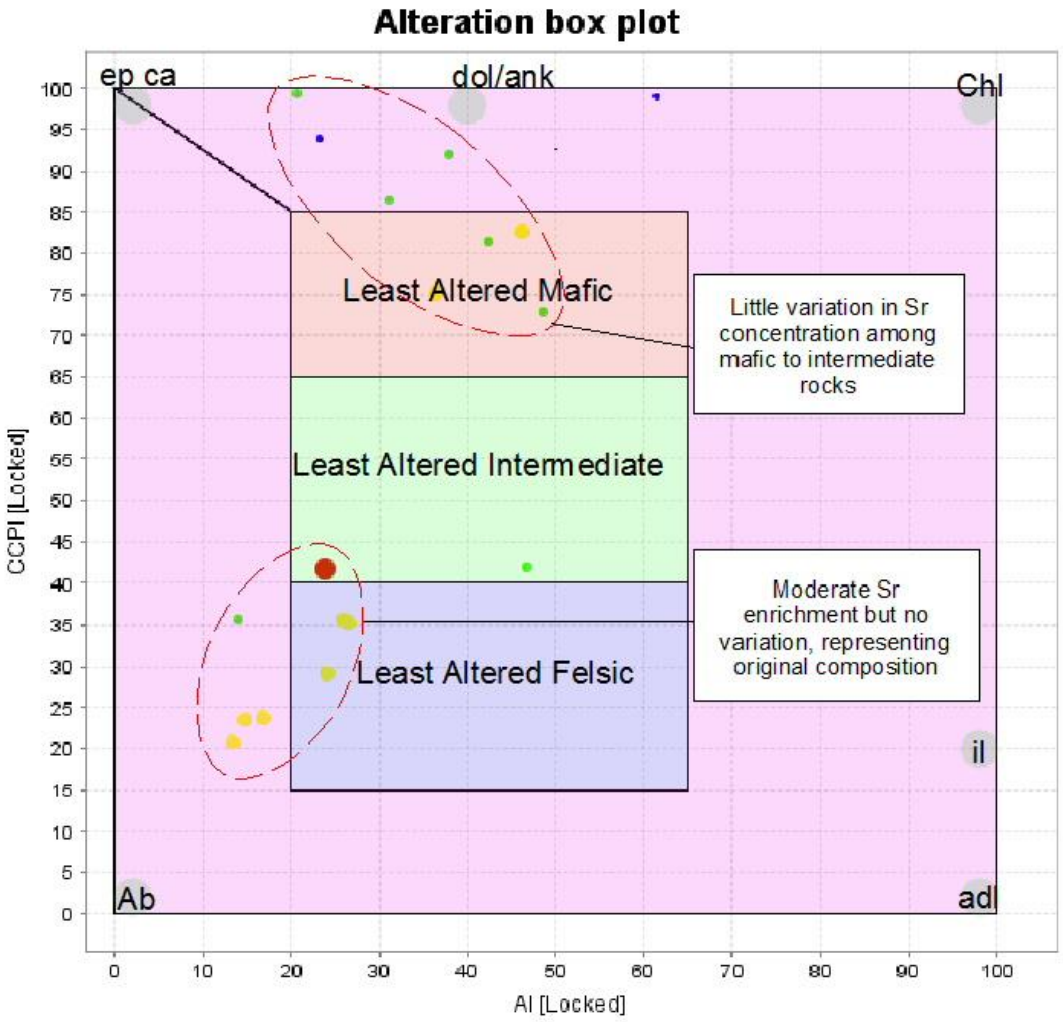

Figure 69 Alteration Box Plot considering Strontium of the Porphyry Suite in Bristol-Thornloe Township. Dot size and color correspond to strontium concentrations; Dark Blue < 100 ppm, Green – 100 to 250 ppm, Yellow – 250 to 500, Red – 500 to 750 ppm. Modified from Large et al., 2001.

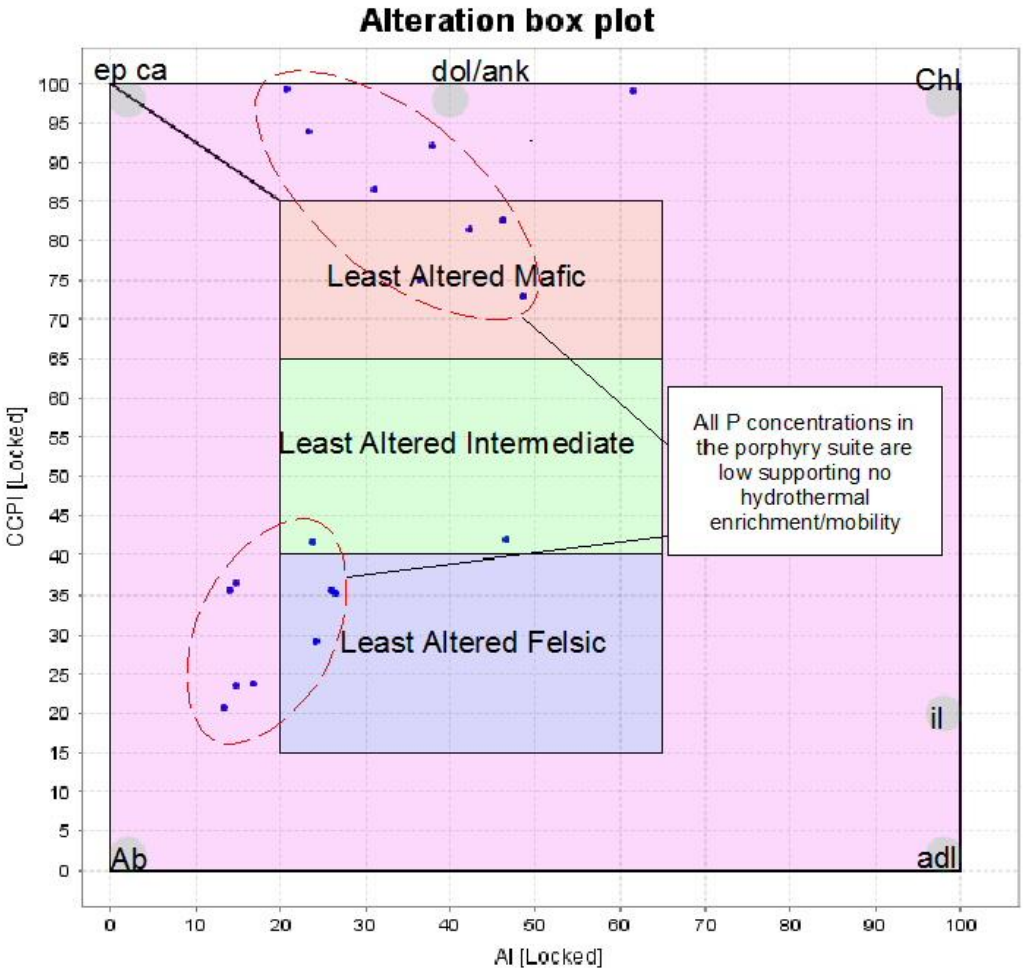

Figure 70 Alteration Box Plot considering Phosphorus of the Porhyry Suite in Bristol-Thorneloe Township. Dot size and color correspond to P_2O_5 wt% concentrations; Blue < 0.20 wt% (all samples). Modified from Large et al., 2001.

4.7 Alkalic and Intermediate Intrusives Rocks

A cluster of intrusive rocks that include the Thunder Creek Syenite, Southwest Bristol Syenite, Holmer Porphyry, and Intermediate-Mafic rocks, outcrop ~2.2 km southwest of the Porphyry Suite of rocks in southwestern Bristol Township. These intrusive units lie north of and along the contact between the Tisdale mafic metavolcanic and Porcupine metasedimentary rocks. These rocks were grouped together because of their close

spatial association with the Lake Shore Timmins West Gold Mine and their similar geological setting. The lithogeochemistry and alteration characteristics have previously been studied by MacDonald (2005).

Classification of the alkalic and related intrusive rocks using a R1-R2 Chemical Variation Diagram (Fig. 71) indicates that there are a syenite–quartz syenite (Southwest Bristol Syenite), a quartz syenite (Thunder Creek Syenite), a quartz monzonite (Holmer Porphyry), and tonalite-melteigite (intermediate to mafic intrusive rocks) (described as alkalic intrusive by others), present in southwest Bristol Township. Intrusive rocks in close proximity to Lake Shore Timmins West Gold Mine have different alteration trends (Fig. 72). The tonalite-melteigite is epidote-calcite altered, syenites (Southwest Bristol and Thunder Creek Syenite) are weakly K-Na altered, and the quartz-monzonite (Holmer Porphyry) is unaltered to weakly Na-altered (Fig. 72).

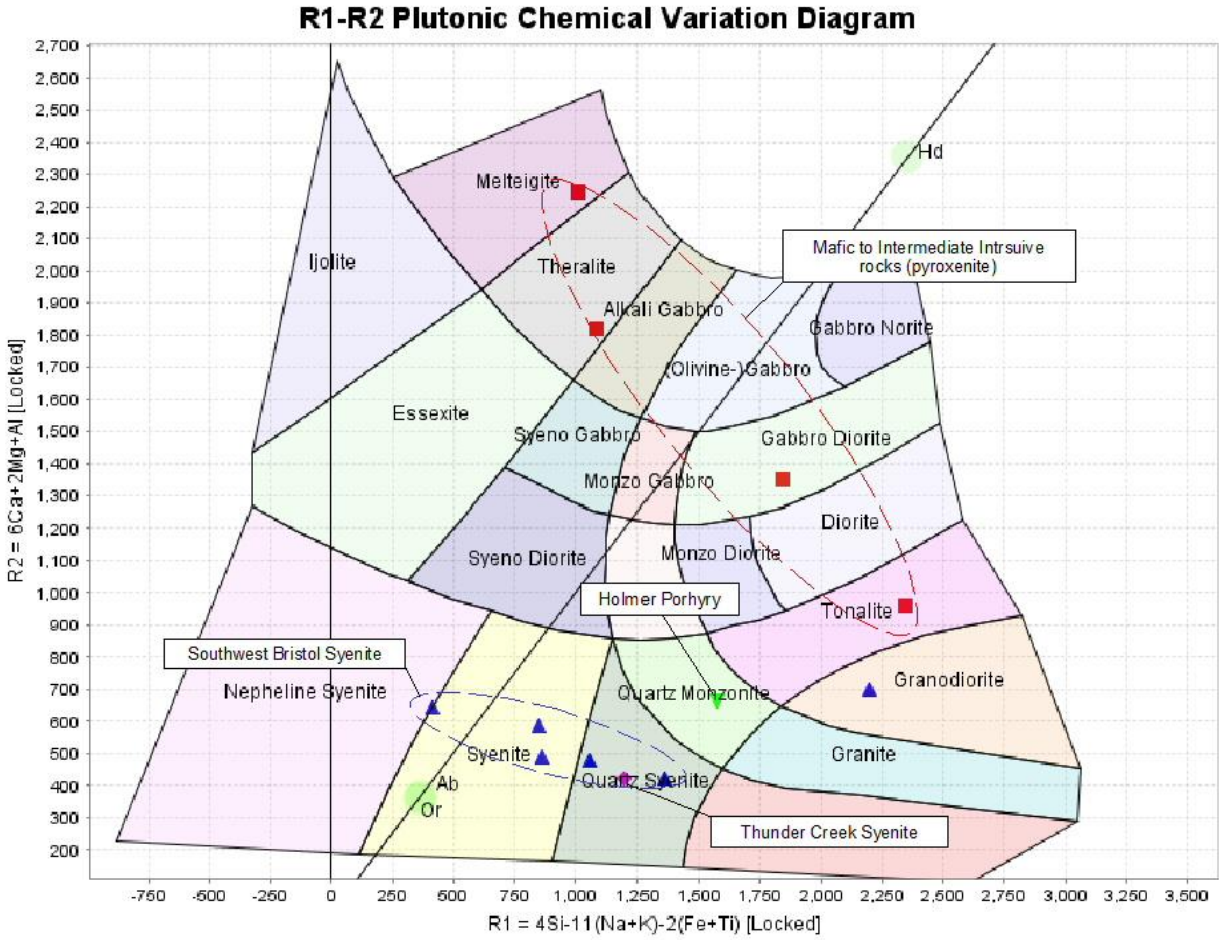

Figure 71 R1-R2 Chemical Variation Diagram for the Southwest Bristol Syenite, Thunder Creek Syenite, Holmer Porphyry, and Mafic to Intermediate Intrusive Rock (Alkalic intrusive). Modified from De La Roche et al., 1980.

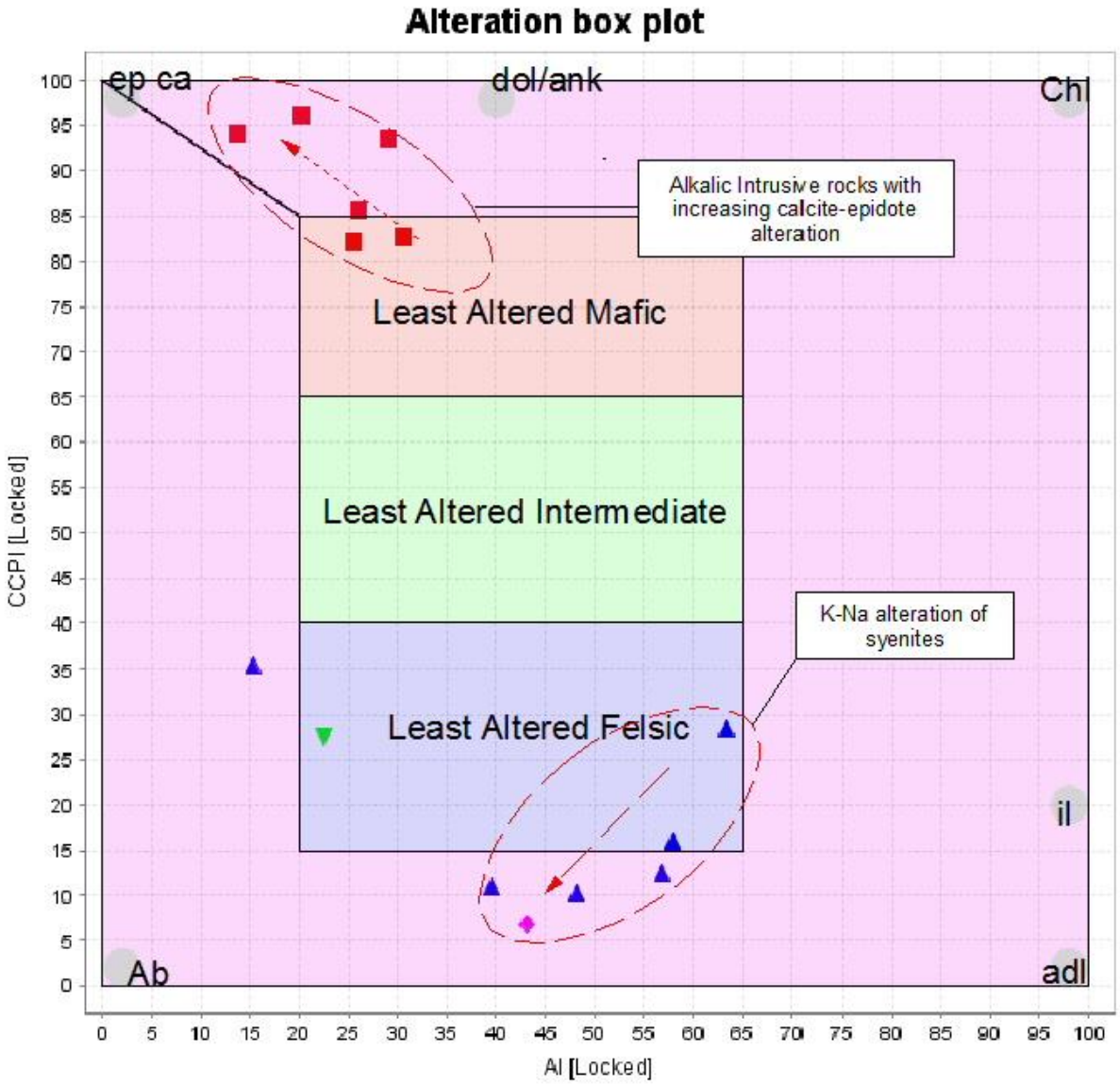

Figure 72 Alteration Box Plot for Southwest Bristol Syenite (Blue triangles), Thunder Creek Syenite (Purple diamond), Holmer Porphyry (Inverted green triangle), and Tonalite (Red square). Modified from Large et al., 2001.

Strontium, phosphorus, and barium all appear to be mobile in the study area, but the degree of mobility varies for each element. Strontium is enriched in the tonalite-melteigite (alkalic intrusive) unit and its concentration gradually increase with stronger calcite-epidote alteration (Fig. 73). Slightly higher Sr values also occur in the Na-K

metasomatically altered syenite samples, further supporting Sr mobility. Higher Sr concentrations are also associated with dolomite-ankerite type carbonate alteration (Fig. 74). The close association between Sr and carbonate that has been added to the country rocks also supports Sr mobility and that its concentration is independent of the host rock.

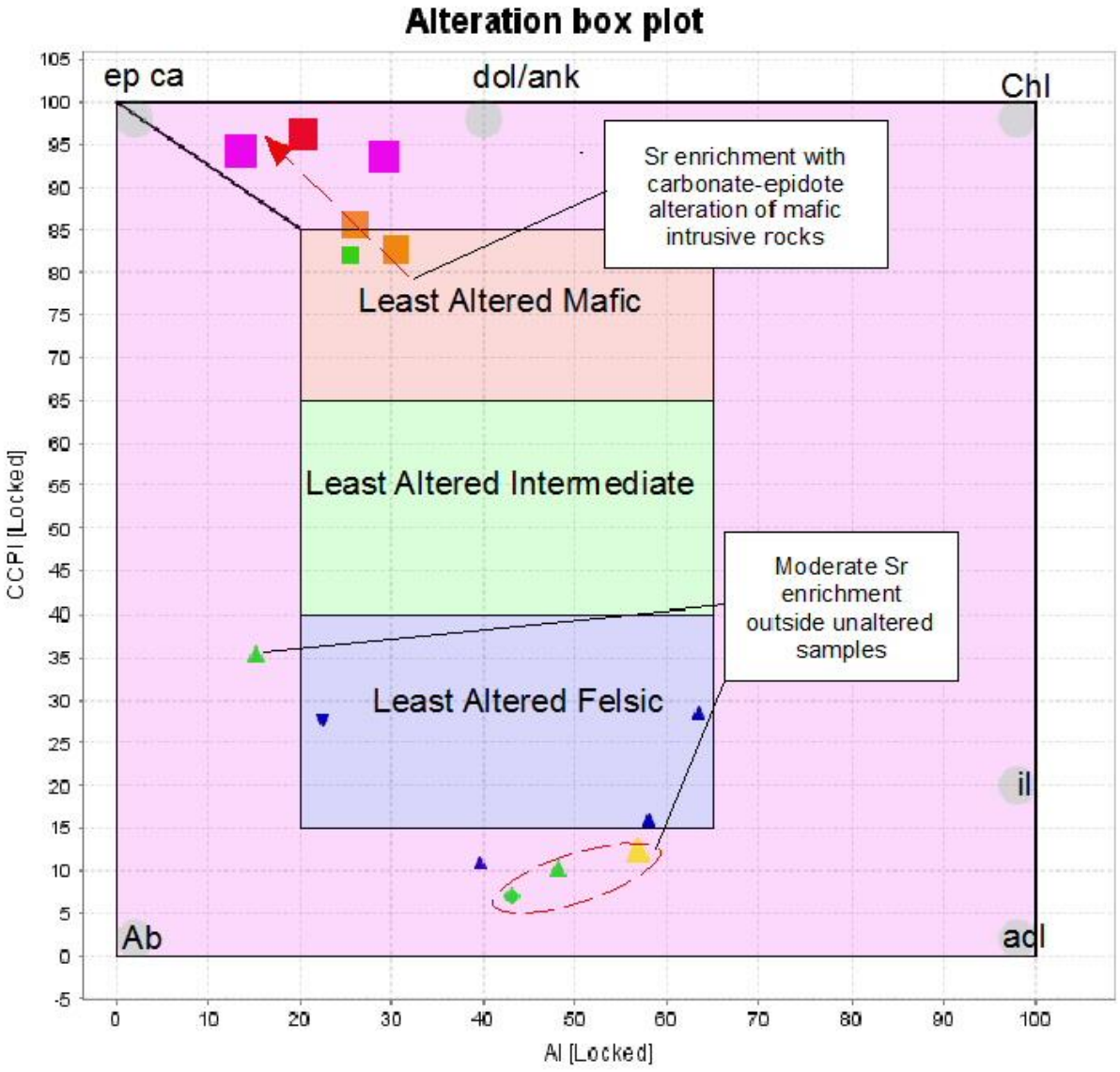

Figure 73 Alteration Box Plot for strontium mobility. Results indicate that carbonate altering fluids are mobilize Sr. Size and color correspond to Sr concentration, Blue < 500 ppm, Green – 500 to 750 ppm, Yellow – 750 to 1,000, Orange – 1,000 to 1,500 ppm, Red – 1,500 to 2,500 ppm, and Purple > 2,500 ppm. Southwest Bristol – Upright Triangle, Thunder Creek Syenite - Diamond, Holmer Porphyry - Inverted Triangle, and Tonalite-Melteigite (Alkalic intrusive) - Square. Modified from Large et al., 2001.

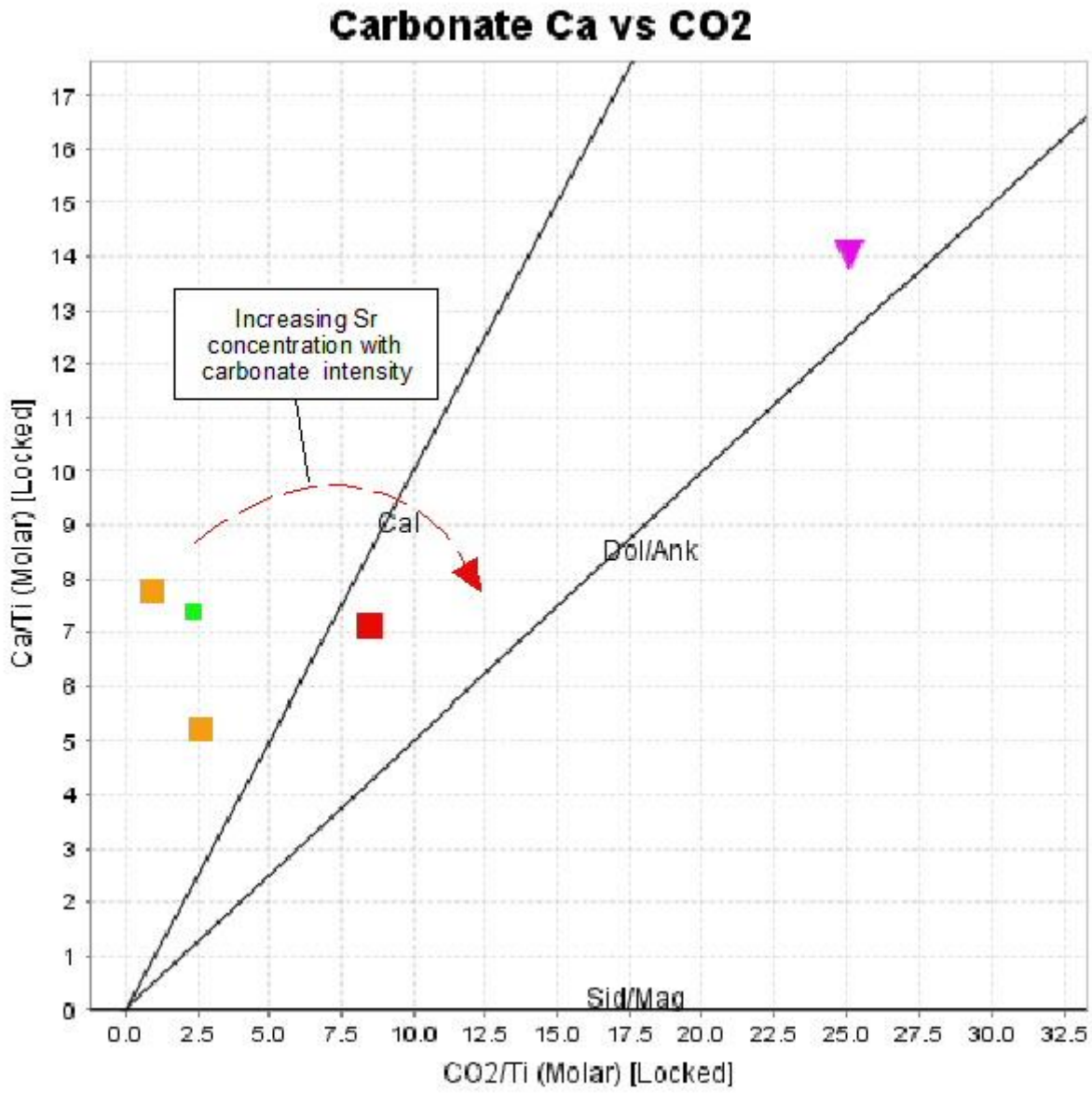

Figure 74 Carbonate alteration discriminant plot considerting Strontium of Southwest Bristol Porhyry, Thunder Creek Syenite, Holmer Porphyry, and Tonalite-Melteigite (Alkalic intrusive). Results indicate higher Sr concentration coincide with carbonate alteration type/intensity that is independent of host rock. Size and color correspond to Sr concentration, Blue < 500 ppm, Green – 500 to 750 ppm, Yellow – 750 to 1,000, Orange – 1,000 to 1,500 ppm, Red – 1,500 to 2,500 ppm, and Purple > 2,500 ppm. Southwest Bristol – Upright Triangle, Thunder Creek Syenite - Diamond, Holmer Porphyry - Inverted Triangle, and Tonalite-Melteigite (Alkalic intrusive) - Square. Modified from Stanley and Madeisky, 1996.

Phosphorus (P_2O_5) is similar to strontium in that it has higher concentrations in the tonalite-melteigite (alkalic intrusive) unit. Higher P_2O_5 concentrations associated with calcite-epidote and dolomite-ankerite type alteration are interpreted to have been added to these rocks. Low phosphorus concentrations in the syenites appear to be immobile and inherent to the rocks (Fig. 75).

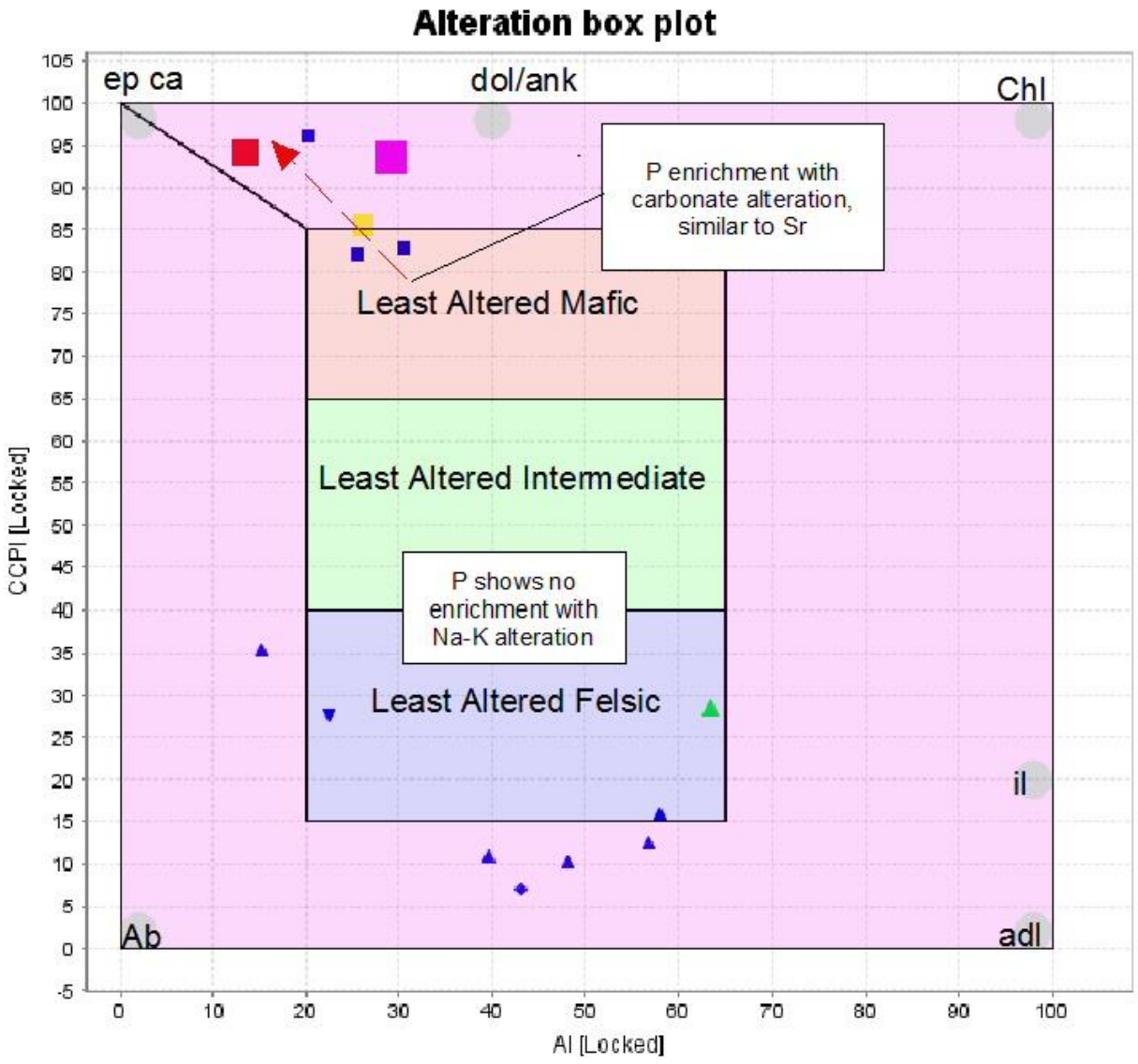

Figure 75 Alteration Box Plot considering phosphorus of the Southwest Bristol Porhyry, Thunder Creek Syenite, Holmer Porphyry, and Tonalite-Melteigite (Alkalic intrusive). Results indicate that P_2O_5 is mobilized in carbonate altering fluids and not in Na-K alteration. Size and color correspond to P_2O_5 wt% concentration, Blue < 0.20 wt%, Green – 0.20 to 0.25 wt%, Yellow – 0.25 to 0.50 wt%, Red – 0.50 to 0.75 wt%, and Purple >0.75 wt%. Southwest Bristol – Upright Triangle, Thunder Creek Syenite - Diamond, Holmer Porphyry - Inverted Triangle, and Tonalite-Melteigite (Alkalic intrusive) - Square. Modified from Large et al., 2001.

Barium concentrations are higher than strontium and phosphorus in all altered samples (Fig. 76) including samples with a lower overall intensity of alteration.

Figure 76 Alteration Box Plot considering barium of the Southwest Bristol Porhyry, Thunder Creek Syenite, Holmer Porphyry, and Tonalite-Melteigite (Alkalic intrusive). Results indicate that Ba is mobilized under all alteration conditions. Size and color correspond to Ba concentration, Blue < 200 ppm, Green – 200 to 300 ppm, Red – 300 to 1,000 ppm and Purple >1,000 ppm. Southwest Bristol – Upright Triangle, Thunder Creek Syenite - Diamond, Holmer Porphyry - Inverted Triangle, and Tonalite-Melteigite (Alkalic intrusive) - Square. Modified from Large et al., 2001.

4.8 Stable Isotope Analysis

The quartz-carbonate vein samples collected throughout the Bristol-Thorneloe study area have stable isotope values that provide information about the source and temperature of the mineralizing fluid, as well as help target locations with gold mineralization. The $\delta^{18}O_{qtz}$ values appear to be independent of host rock unit compositions and those samples with $\delta^{18}O_{qtz}$ values >13.5‰ are associated with gold mineralization (Fig. 77). Vein samples containing both quartz and tourmaline were collected from the Lake Shore Timmins West Gold Mine and the Allerston gold prospect in central Bristol Township (Fig. 77) so that the temperature of the gold-bearing fluid could be determined using the quartz-tourmaline $\delta^{18}O$ thermometer (Blamart 1991).

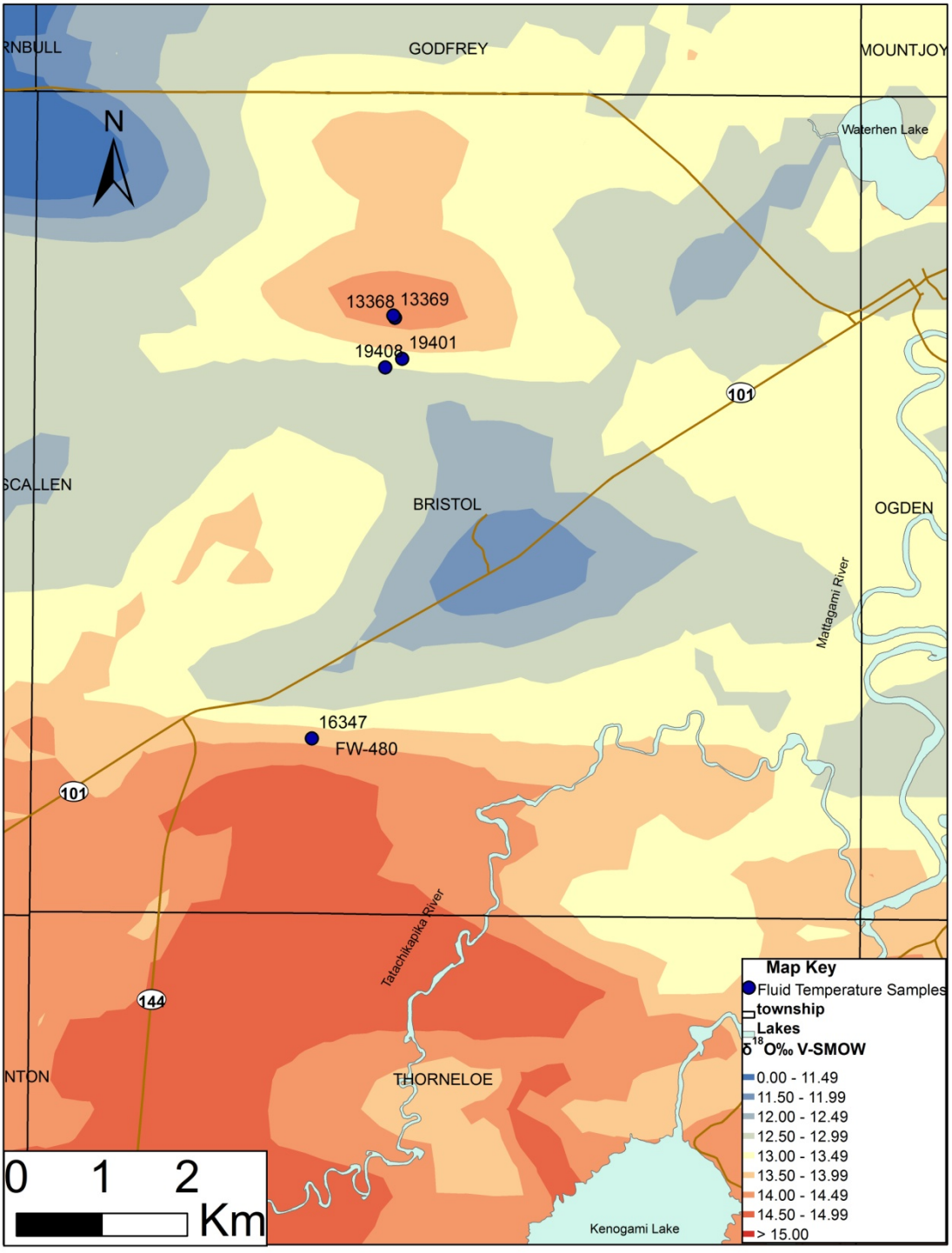

Figure 77 Bristol-Thorneloe study area temperature samples and their relation to the distribution of $\delta^{18}O_{qtz}$ values.

The quartz-tourmaline mineral pairs have isotopic compositions that indicate the mineralizing fluid had a temperature that ranged between 243° to 403°C (Table 3).

Table 3: Oxygen isotope values for quartz-tourmaline mineral pairs, calculated fluid temperature and $\sigma^{18}O_{fluid}$ composition.

Sample	$\delta^{18}O_{qtz}$ ‰	$\delta 18O_{tour}$ ‰	$\delta^{18}Oqtz-\delta^{18}O_{tour}$ ‰	$\delta^{18}O_{fluid}$ ‰	T (°C)
FW-480	14.5	9.6	4.9	8.3	338
16347	15.1	9.5	5.651	7.7	303
19401	13.7	6.4	7.291	4.0	243
13368	14.8	10.9	3.814	10.3	403
13369	16.2	10.6	5.642	8.8	303
19408	13.8	9.6	4.206	8.7	377

This temperature range is similar to other Canadian mesothermal gold deposits located in the Porcupine and Yellowknife Gold Camps (Fig. 78; (Kerrich and Hodder 1982; Washington 2008).

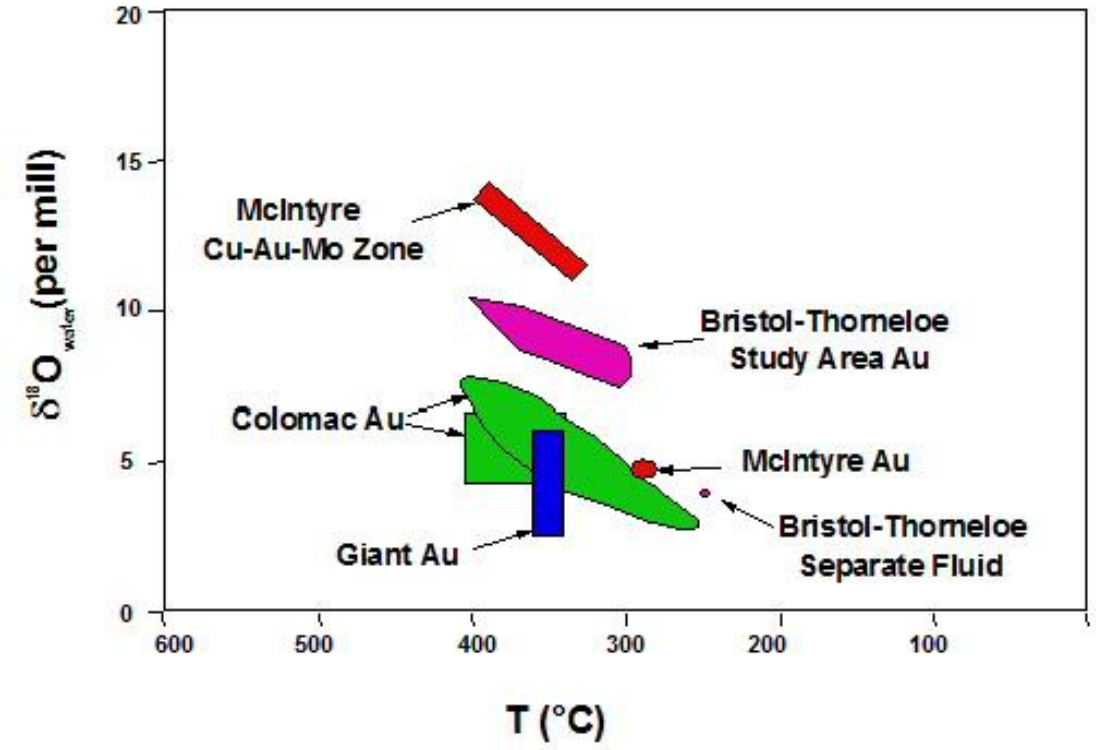

Figure 78 Plot of $\delta^{18}O_{fluid}$ vs. measured temperatures of Bristol-Thorneloe Township and other mesothermal gold deposits. Results indicate that gold mineralization in the Bristol-Thorneloe Township study area are mesothermal deposits with $\delta^{18}O_{fluid}$ compositions that are different than the nearby McIntyre Mine. Modified from Washington, 2008.

All the quartz samples had $\delta^{18}O_{qtz}$ values that are well above 13.5‰, indicating that they were deposited by a gold-bearing fluid (van Hees et al., 2000), except for one sample that has a calculated fluid temperature of 243°C and a $\delta^{18}O_{qtz}$ value of 13.7‰. This sample statistically falls on the boundary between gold-bearing and barren vein quartz (13.5‰) and has a temperature that is too low to transport gold as $Au(HS)_2^-$ (Barnes 1997). It is therefore interpreted to have been formed by an earlier, lower temperature fluid that was not gold-bearing, or the minerals were deposited separately and are out of equilibrium.

The mineralizing fluid that deposited the gold-bearing quartz-tourmaline veins in the Timmins West Gold Mine and Allerston prospect have $\delta^{18}O_{fluid}$ values that range from 7.7 to 10.3‰ (Table 3). These fluid compositions are a few per mill higher than those determined for the gold-bearing mesothermal veins in the McIntyre, Giant and Colomac gold mines but less than the fluid responsible for depositing the McIntyre Cu-Au-Mo mineralization (Fig. 78). Hydrothermal fluids with $\delta^{18}O_{fluid}$ values in this range are classified as metamorphic in origin (Taylor 1974).

The $\delta^{18}O_{qtz}$ values in the Bristol-Thorneloe Township study area identify hydrothermal fluids in gold-bearing and barren systems. Rocks containing anomalous concentrations of gold (Au ≥25 ppb) are all associated with $\delta^{18}O_{qtz}$ values of ≥13.5‰ (Fig. 79), as was found for gold deposits in the Porcupine and Yellowknife Gold Camps by van Hees et al., (2000). When analyzing the results on a smaller scale, the $\delta^{18}O_{qtz}$ values are commonly ≥14.0‰ in close proximity to host rocks that have gold concentrations ≥25 ppb. This close association between gold and higher $\delta^{18}O_{qtz}$ values was observed in the Dome Mine where auriferous gold veins were found to have $\delta^{18}O_{qtz}$ values of 14.0 to 15.2‰ (Kerrich and Hodder 1982). This higher threshold value might be useful for identifying better mineralized areas in more detailed studies. However, a 13.5‰ threshold is more conservative and better fit in larger, township-scale gold exploration projects similar to the Bristol-Thorneloe Study Area (van Hees et al. 2000).

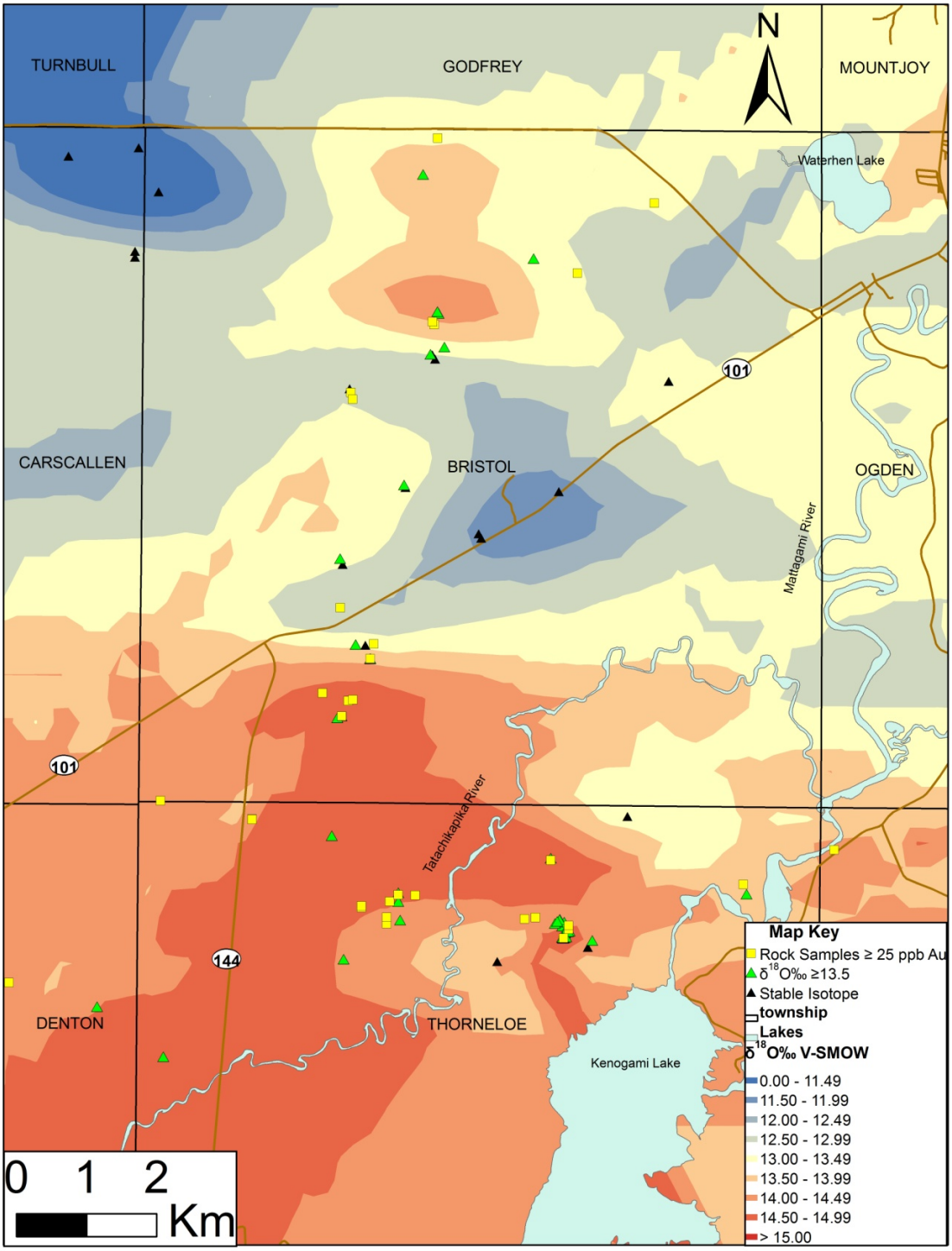

Figure 79 Plot of Bristol and Thorneloe Townships showing relation between anomalous gold (≥ 25 ppb-yellow squares) and $\delta^{18}O_{qtz}$ threshold (≥13.5‰-green triangles), and distant from < 13.5‰ (black triangle).

The close association between $\delta^{18}O_{qtz}$ values ≥13.5‰ and gold values ≥25 ppb (Fig. 79) supports that hydrothermal fluid characteristics are independent of the host rock. In Bristol and Thorneloe Townships regional metamorphism above lower greenschist facies (Upper Greenschist to Amphibolite) is closely association with $\delta^{18}O_{qtz}$ values ≥13.5‰ (Fig. 80). This association is supported by Thompson (2005) who found that higher-grade metamorphic facies were located near auriferous zones (Fig. 80). The metamorphic grade also appears to correspond with the higher isotope values and the extent of isotopic anomalies. Higher, more consistent $\delta^{18}O_{qtz}$ values are found near amphibolite grade metamorphism (Fig. 80). The close association of these regional metamorphic areas with the distribution of gold and higher $\delta^{18}O_{qtz}$ values suggests that they are a possible source for the auriferous fluids. Such an association is consistent with the isotopic classification of these fluids as being derived from a metamorphic source (Taylor 1974; Kerrich and Hodder 1982).

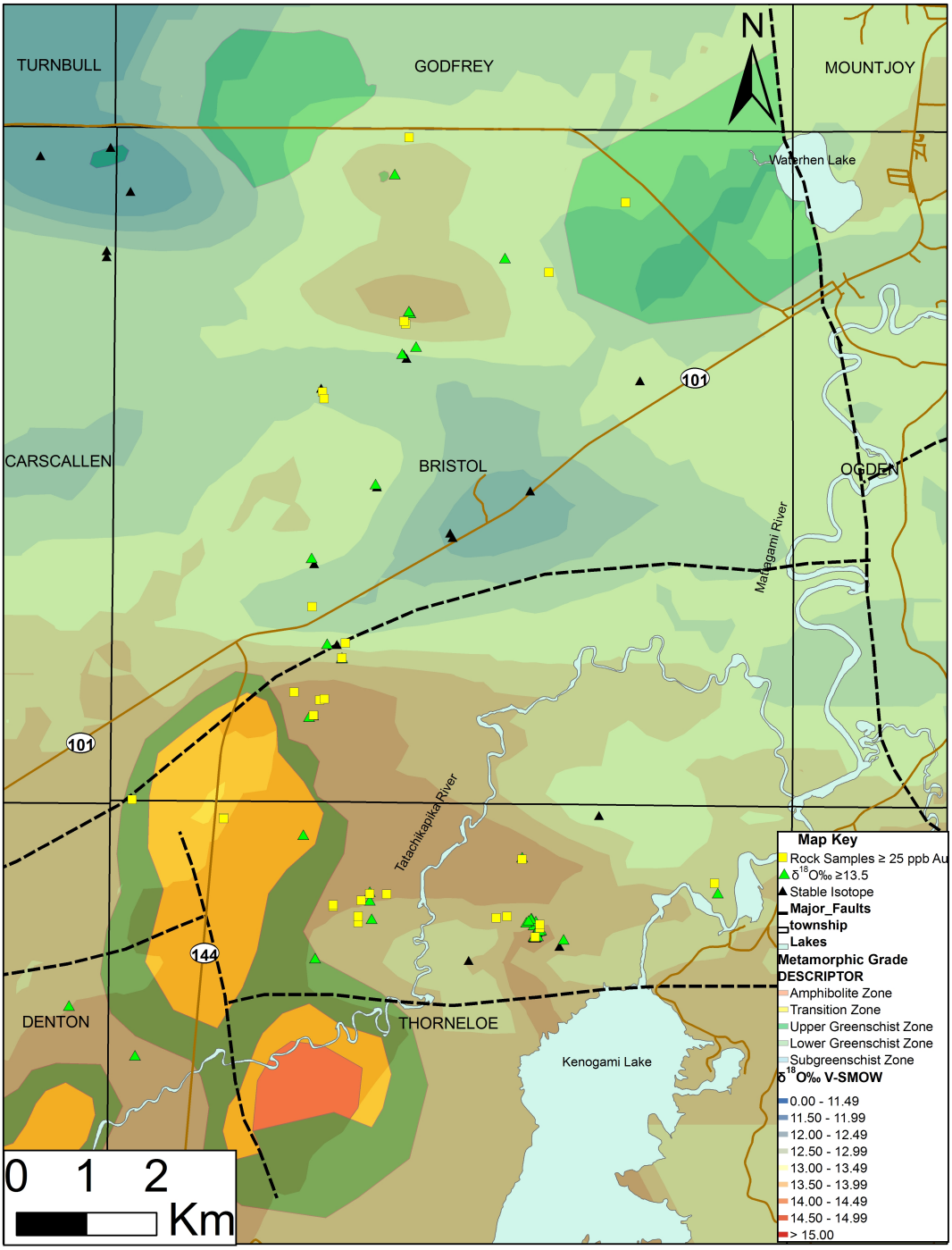

Figure 80 Bristol and Thorneloe Township plot of regional metamorphic grade overlain on $\delta^{18}O_{qtz}$ contour plot. Yellow squares are samples with Au ≥ 25 ppb, Green triangles are quartz veins with ≥13.5‰, and black triangles <13.5‰. Modified from Thompson 2005.

Chapter 5 Conclusion

The Bristol-Thorneloe Study Area appears to have been affected by different types and intensities of lithogeochemical alteration. The most obvious alteration in the study area is characterized by the enrichment or depletion of Na_2O and K_2O, and local addition of CO_2 to the country rocks. The observed variation in the concentration of Na_2O, K_2O, and CO_2 suggest that the study area has been affected by multiple fluids with different temperatures. CO_2 enrichment/addition to the country rocks is the major constituent most closely associated with the deposition of gold mineralization. The intensity of carbonate alteration in the country rocks was measured using the CO_2/CaO molar index and has anomalous values of between 1.5 to 2.0. This range of values is indicative of dolomite-ankerite alteration like that associated with gold-bearing deposits elsewhere in the Porcupine Camp. Index values of between 1.0 and 1.5 in the study area indicates the presence of calcite alteration and is interpreted as having been formed by lower temperature fluids that occur distal to gold deposits.

Gold concentrations greater than 25 ppb, or more than 5 times background, appear to have been added to the country rocks near all the gold deposits or prospects in the study area. The distribution of these anomalies are such that they are an excellent indicator of gold-bearing zones and are judged to be the best lithogeochemical indicator of gold exploration targets in the study area.

Evaluation of minor element concentrations in the country rocks indicated that barium, phosphorus and strontium are associated with gold-bearing zones and appear to also have been mobilized by gold-bearing fluids. Each of these elements has higher

concentrations in and around the Lake Shore Timmins West Gold Mine as well as at other localities in the study area. Barium deposition appears to be independent of lithology and probably occurs at lower temperatures. Barium appeared to be a product K-metasomatic alteration, where it is present as replacement for potassium. Replacement was found in the formation adularia and possibly sericite. Strontium and phosphorus are associated with intense dolomite/ankerite alteration. This relation is interpreted to indicate that Sr and P were mobilized by higher temperatures fluids like those that formed dolomite-ankerite mineralization. The addition/enrichment of these elements is linked to gold mineralizing fluids in the study area and appears to form halos with higher values in the country rocks that host the gold-bearing zones.

The stable isotope analysis of quartz-carbonate and quartz-carbonate-tourmaline vein samples was used to determine fluid origin, mineralizing temperature, and isotopic signature for gold mineralization. The auriferous fluids are classified as mesothermal because their measured temperatures range from 303° to 403°C. The $\delta^{18}O_{fluid}$ values of 7.7 to 10.3‰ measured on the same samples used to establish the temperature of the auriferous fluids is interpreted as indicating that the fluids are metamorphic in origin. A single sample had a fluid temperature of 243°C with an $\delta^{18}O$ that might be of magmatic origin. At this temperature it is unlikely that the fluid could mobilize gold, and might support the presence of a separate, barren, late stage hydrothermal fluid. Samples with $\delta^{18}O_{qtz}$ values ≥13.5‰ are spatially associated with anomalous gold concentrations (≥25 ppb). The ≥13.5‰ is used as a threshold value to determine gold-bearing fluids in the study area. After contouring these isotopic values it was found that, they have a close

spatial relation with higher grade regional metamorphism (Upper Greenschist to Amphibolite facies). This association also appears to support a metamorphic origin for the gold-bearing hydrothermal fluids.

APPENDIX A

GEOSTATISTICAL KRIGING PARAMETERS

Element	Model	Direction	Major Range	Minor Range	Sill	Nugget	Lag Size	Ellipse Direction	
Cr	spherical	330	31366.7	13244.7	6039.7	12262	2762.5	70	Anisotropy
NI	spherical	277	27605.5	10462.8	184010	63917	24726.7	70	Anisotropy
Zr	spherical	90	15021.1	6301.1	6101.3	13146	1319.5	70	Anisotropy
Cu	spherical	66.4	6684.3	3703.7	7494.9	4921.8	563.9	70	Anisotropy
Pb	spherical	49.7	27542.9	18839.6	26.9	35.94	2413	70	Anisotropy
Sr	spherical	83.9	15026.1	4938.4	88543	28180	1319.5	70	Anisotropy
Sc	spherical	85.1	22161.2	6146.8	169.1	85.136	2256.1	70	Anisotropy
Y	spherical	67.2	31409.8	20204.5	468.1	812.7	2762.5	70	Anisotropy
CO_2/Cao	spherical	65.6	8937.5	4514.8	0.744	0.273	761.81	70	Anisotropy
CCPI	spherical	89.3	31519.4	20181.1	100.26	451.6	2762.5	70	Anisotropy
K/Al	spherical	81.1	8739.37	3707.9	0.0085	0.018	759.09	70	Anisotropy
CSI	spherical	67.9	1241.2	672.7	62.2	67.9	104.71	70	Anisotropy
Chlorite Index	spherical	100.9	31415.4	14687.9	84.5	254.8	2762.5	70	Anisotropy
Ishikawa Index	spherical	70	31404.6	13306.8	350	120	2765.5	70	Anisotropy
Fe/Fe+Mg	spherical	65.8	25038.4	9356.8	0.02	0.013	2204.4	70	Anisotropy
Ba	spherical	85.4	20000	4016	200000	370780	2204.8	70	Anisotropy
Au	spherical	90	4016.5	4016.5	1000	1000	2204.8	70	Anisotropy
TiO_2	spherical	74.1	8793.2	366.87	0.112	0.146	759.1	70	Anisotropy
P_2O_5	spherical	70	8997.7	3015	0.65	0.23	759.1	70	Anisotropy
Na_2O	spherical	70	25688.9	28764.3	1.06	2.02	2426.7	70	Anisotropy
MnO	spherical	333.1	343.4	137.1	0.043	0.021	28.9	70	Anisotropy
MgO	spherical	277.2	31393.8	14667.8	36.9	14.5	2762.5	70	Anisotropy
K_2O	spherical	9	295.8	295.8	3.8	2.97	24.9	70	Anisotropy
Fe_2O_3	spherical	43.3	500	344.1	22.3	23.3	35.4	70	Anisotropy
CaO	spherical	74.4	15034.9	6110.64	9.2	10.3	1319.5	70	Anisotropy
Al_2O_3	spherical	90.3	31407	133.1.3	2.5	12	2762.5	70	Anisotropy
$\delta^{18}O$	spherical	97	3000	1500	1.9	1.2	1079.6	70	Anisotropy
$\delta^{13}C$	spherical	352.8	5290.6	2822.85	13.8	0.718	446.3	70	Anisotropy

APPENDIX B

WHOLE ROCK LITHOGEOCHEMICAL DATA

SampleNo	UTMNorth (m)	UTMEast (m)	Al_2O_3 (%)	CaO (%)	Fe_2O_3 (%)	K_2O (%)	MgO (%)	MnO (%)	Na_2O (%)	P_2O_5 (%)	SiO_2 (%)	TiO_2 (%)	LOI (%)	CO_2 (%)
00-CMV-001a	5361486	461629	18.21	3.02	1.53	0.84	0.74	0.02	7.26	0.08	64.26	0.14	-	-
00-CMV-015a	5365842	459910	14.36	4.13	14.19	1.06	5.76	0.15	3.07	0.21	50.48	0.14	-	-
00-CMV-016a	5366529	459759	9.97	2.82	9.79	1.82	3.18	0.24	0.35	0.03	68.56	0.14	-	-
00-CMV-017-A	5366597	459496	12.28	0.29	3.81	3.33	1.85	0.03	1.31	0.05	74.11	0.30	2.40	0.22
00-CMV-018a	5363277	459999	14.45	9.45	10.60	0.33	5.60	0.15	2.33	0.06	38.91	0.14	-	-
00-CMV-022	5363473	460330	14.56	10.83	15.04	0.48	5.21	0.29	0.88	0.07	38.80	0.82	12.80	9.04
00-CMV-022a	5363473	460330	14.34	14.09	11.94	0.50	4.14	0.28	1.41	0.06	37.20	0.14	-	-
00-CMV-023A	5366526	455879	14.17	3.23	9.73	1.31	2.37	0.10	4.38	0.15	59.94	0.14	-	-
00-CMV-029b	5362249	459737	14.29	10.59	9.30	0.20	6.56	0.13	2.72	0.06	54.24	0.14	-	-
00-CMV-032a	5361462	459631	13.04	12.00	10.32	0.80	7.10	0.17	0.83	0.05	42.60	0.14	-	-
00-CMV-041a2	5359811	458110	15.32	12.63	12.10	0.03	7.19	0.19	2.06	0.06	47.68	0.14	-	-
00-CMV-048a	5360256	457668	16.72	11.89	11.66	0.20	5.95	0.22	2.22	0.06	47.34	0.14	-	-
00-CMV-052a	5360037	457714	15.92	11.06	14.18	0.08	7.70	0.19	2.13	0.08	45.48	0.14	-	-
00-CMV-059a	5364759	463792	10.66	16.51	9.55	2.03	4.80	0.23	2.91	0.05	43.55	0.14	-	-
00-CMV-061a	5366302	464921	13.05	13.26	13.69	0.12	3.99	0.37	0.19	0.13	45.90	0.14	-	-
00-CMV-071-A	5358320	458872	11.77	11.91	12.94	0.59	6.31	0.27	3.84	0.14	48.57	1.31	1.90	1.17
00-CMV-075a4	5358109	458755	11.93	22.76	17.03	0.44	3.28	0.37	0.97	0.65	34.65	0.14	-	-
00-CMV-075a5	5358109	458755	3.27	21.10	20.04	1.82	6.93	0.16	0.24	6.53	25.04	0.14	-	-
00-CMV-087a	5365817	455860	15.04	6.22	10.66	0.34	3.56	0.11	5.62	0.25	47.78	0.14	-	-
00-CMV-088a	5365917	455801	12.76	0.33	1.84	0.44	0.90	0.02	6.33	0.01	75.39	0.14	-	-
00-CMV-088b2	5365917	455801	16.71	4.78	9.27	3.25	5.90	0.11	1.81	0.07	46.82	0.14	-	-
00-CMV-092a	5365773	455767	15.72	4.95	13.02	0.06	4.46	0.09	6.00	0.26	45.24	0.14	-	-
00-CMV-101a	5357497	458679	15.73	2.19	3.37	8.73	2.05	0.07	4.03	0.23	59.90	0.34	-	-
00-CMV-109a	5364581	459423	9.77	1.06	1.54	3.23	0.19	0.03	2.05	-	80.28	0.09	-	-
00-CMV-114a	5357215	458672	16.11	1.62	1.54	5.22	0.05	0.04	6.44	0.09	66.32	0.18	-	-
00-CMV-118a	5357966	457754	13.40	10.34	14.73	0.21	6.20	0.23	2.70	0.10	50.03	1.39	-	-
00-CMV-124a	5361457	458963	16.34	8.72	13.27	0.31	9.90	0.18	2.24	0.07	45.16	0.99	-	-
00-CMV-212a	5360008	475040	11.71	7.17	11.57	0.02	12.75	0.16	3.26	0.05	50.52	0.54	-	-
00-CMV-219-B	5361812	472286	16.62	1.69	2.78	2.77	0.48	0.06	3.85	0.12	67.86	0.34	3.30	1.35
00-CMV-220a2	5361881	472821	15.40	4.25	8.02	0.75	5.23	0.10	4.37	0.10	55.55	1.00	-	-
00-CMV-222a	5361240	472179	16.44	4.78	3.14	0.19	1.27	0.07	6.76	0.13	64.32	0.60	-	-
00-CMV-223a1	5361086	472021	2.18	-	8.83	-	38.96	0.05	-	-	37.49	0.10	-	-
00-CMV-241b	5364214	471930	14.52	9.81	12.32	0.02	4.84	0.20	2.00	0.08	49.52	1.13	-	-
00-CMV-243a	5363483	474901	6.38	8.60	15.63	0.01	20.56	0.25	0.35	0.08	43.35	0.86	-	-
00-CMV-252-A	5357553	465317	15.48	4.84	4.75	1.72	2.72	0.06	4.00	0.15	60.71	0.56	4.70	3.04
00-CMV-259a	5358549	455963	15.09	9.96	11.18	0.13	7.23	0.13	2.83	0.11	49.91	1.41	-	-
00-CMV-260a	5358837	456986	16.09	13.61	10.09	1.15	3.45	0.27	0.53	0.04	44.8	0.77	-	-
00-CMV-267-B	5358086	459880	15.02	5.28	6.73	0.03	4.14	0.10	5.03	0.36	58.66	1.34	3.00	0.77
00-CMV-274b1	5362697	471407	15.11	3.04	3.21	0.09	2.52	0.04	7.98	0.29	61.88	0.71	-	-
00-CMV-286a	5358599	459243	17.14	2.52	2.03	1.43	1.22	0.03	6.59	0.07	64.78	0.24	-	-
00-CMV-298a	5357183	459263	15.94	2.26	1.87	8.10	0.64	0.03	4.08	0.09	63.81	0.21	-	-
00-CMV-302b	5363506	474730	13.80	7.76	9.54	0.60	6.70	0.23	4.70	0.11	54.27	0.76	-	-
00-CMV-305a	5363305	473803	15.81	0.71	1.50	4.56	0.53	0.02	5.41	0.12	69.19	0.32	-	-
00-CMV-401a	5359223	475061	13.94	5.98	5.31	0.62	6.08	0.08	5.29	0.26	56.97	0.64	-	-
00-CMV-415a	5366510	455782	14.18	2.88	8.24	0.38	2.48	0.07	5.78	0.19	61.53	0.14	-	-

SampleNo	Cr (ppm)	Y (ppm)	Sc (ppm)	Sr (ppm)	Zr (ppm)	Au (ppb)	Ba (ppm)	Cu (ppm)	Ni (ppm)	Pb (ppm)	Zn (ppm)	Fe/Fe+Mg	CO_2/CaO	Ishikawa Index	Chlorite Index	SCI	CSI	K/Al	CCPI
00-CMV-001a	10	2	2	450	68	-	-	9	8	8	23	0.71	-	13	16	45	55	0.07	21
00-CMV-015a	10	30	39	44	126	-	-	152	67	2	87	0.74	-	49	69	41	59	0.12	82
00-CMV-016a	5	90	6	75	322	-	-	23	-	14	156	0.78	-	61	71	46	54	0.29	85
00-CMV-017-A	-	66	6	23	426	0	374	10	1	10	61	0.70	0.96	76	52	60	40	0.43	53
00-CMV-018a	175	17	31	109	50	-	-	143	197	1	68	0.69	-	33	56	38	62	0.04	85
00-CMV-022	151	17	29	66	48	2	115	76	163	1	66	0.77	1.06	33	61	35	65	0.05	93
00-CMV-022a	131	17	27	90	48	-	-	77	174	1	51	0.77	-	23	48	32	68	0.05	89
00-CMV-023A	15	37	20	153	224	-	-	102	26	4	47	0.83	-	33	55	37	63	0.15	66
00-CMV-029b	182	15	27	120	43	-	-	161	173	1	47	0.62	-	34	52	39	61	0.02	84
00-CMV-032a	177	15	31	92	47	-	-	84	116	0	59	0.63	-	38	55	41	59	0.10	91
00-CMV-041a2	290	18	36	329	53	-	-	94	100	1	65	0.66	-	33	55	37	63	0.00	90
00-CMV-048a	199	18	37	148	49	-	-	114	118	0	66	0.69	-	30	53	36	64	0.02	87
00-CMV-052a	105	23	40	148	64	-	-	121	104	1	75	0.68	-	37	61	38	62	0.01	90
00-CMV-059a	95	19	30	306	45	-	-	69	89	2	50	0.70	-	26	38	40	60	0.30	73
00-CMV-061a	18	27	37	333	101	-	-	82	64	2	83	0.80	-	23	55	30	70	0.01	98
00-CMV-071-A	205	25	41	1100	58	2	115	139	21	2	26	0.70	0.13	30	52	37	63	0.08	80
00-CMV-075a4	3	238	2	7301	2460	-	-	42	24	36	113	0.86	-	14	43	24	76	0.06	93
00-CMV-075a5	8	76	37	2670	165	-	-	28	38	30	115	0.77	-	29	52	36	64	0.87	92
00-CMV-087a	166	23	22	196	111	-	-	17	140	2	81	0.78	-	25	52	32	68	0.04	69
00-CMV-088a	8	72	1	80	154	-	-	3	-	2	9	0.70	-	17	26	39	61	0.05	27
00-CMV-088b2	187	25	26	123	57	-	-	10	199	4	50	0.65	-	58	59	50	50	0.31	74
00-CMV-092a	187	22	27	194	129	-	-	14	124	4	50	0.77	-	29	59	33	67	0.01	73
00-CMV-101a	67	19	8	450	218	-	-	7	43	21	113	0.66	-	63	25	71	29	0.87	28
00-CMV-109a	5	68	2	37	170	-	-	2		7	48	0.90	-	52	20	72	28	0.52	23
00-CMV-114a	16	9	3	450	113	-	-	12	8	21	51	0.97	-	40	10	80	20	0.51	11
00-CMV-118a	121	27	38	206	88	-	-	96	67	2	94	0.73	-	33	59	36	64	0.02	87
00-CMV-124a	217	19	34	138	53	-	-	32	191	0	67	0.61	-	48	66	42	58	0.03	90
00-CMV-212a	500	14	32	76	52	-	-	47	211	11	62	0.51	-	55	69	44	56	0.00	88
00-CMV-219-B	-	5	4	147	116	0	578	3	13	2	80	0.87	1.02	37	26	58	42	0.26	31
00-CMV-220a2	141	13	16	222	100	-	-	44	113	4	70	0.64	-	41	57	42	58	0.08	71
00-CMV-222a	78	22	14	202	152	-	-	5	29	5	34	0.74	-	11	26	30	70	0.02	37
00-CMV-223a1	500	2	8		8	-	-	-	1805	2	36	-	-	-	-	-	-	-	-
00-CMV-241b	125	30	48	165	72	-	-	132	160	1	79	0.75	-	29	57	34	66	0.00	89
00-CMV-243a	500	21	26	26	53	-	-	270	705	0	119	0.47	-	70	79	47	53	0.00	99
00-CMV-252-A	178	12	12	456	110	0	597	33	71	6	61	0.67	0.80	33	40	46	54	0.17	55
00-CMV-259a	216	26	44	121	91	-	-	98	64	10	88	0.64	-	37	57	39	61	0.01	85
00-CMV-260a	33	14	5	97	41	-	-	12	32	4	29	0.77	-	25	45	35	65	0.11	88
00-CMV-267-B	109	14	13	820	142	0	42	71	67	15	100	0.65	0.19	29	50	37	63	0.00	67
00-CMV-274b1	36	7	4	450	263	-	-	12	32	4	29	0.60	-	19	33	37	63	0.01	40
00-CMV-286a	32	3	4	450	65	-	-	13	20	8	59	0.66	-	23	22	50	50	0.13	28
00-CMV-298a	31	10	3	450	146	-	-	11	16	28	27	0.77	-	58	14	81	19	0.80	16
00-CMV-302b	268	17	27	174	91	-	-	129	84	1	57	0.62	-	37	54	41	59	0.07	74
00-CMV-305a	12	3	2	450	199	-	-	11		17	44	0.77	-	45	15	75	25	0.45	16
00-CMV-401a	248	15	11	450	143	-	-	29	191	14	45	0.50	-	37	48	44	56	0.07	65
00-CMV-415a	16	36	18	170	225	-	-	6	26	4	35	0.79	-	25	52	32	68	0.04	62

SampleNo	UTMNorth (m)	UTMEast (m)	Al_2O_3 (%)	CaO (%)	Fe_2O_3 (%)	K_2O (%)	MgO (%)	MnO (%)	Na_2O (%)	P_2O_5 (%)	SiO_2 (%)	TiO_2 (%)	LOI (%)	CO_2 (%)
00-CMV-429a	5365843	457771	13.14	1.12	1.62	2.43	0.60	0.03	3.44	0.01	74.17	0.13	-	-
00-CMV-431c	5357782	457422	9.81	9.33	23.50	0.88	3.08	0.35	4.67	0.44	44.6	2.34	-	-
00-CMV-434-A	5358303	457605	13.05	11.37	10.96	1.89	5.64	0.26	2.56	0.09	46.27	0.95	6.60	4.72
00-CMV-601a	5361953	464510	17.47	3.72	2.19	1.87	1.02	0.03	5.40	0.09	64.04	0.22	-	-
00-CMV-602a	5361825	464801	16.01	3.89	2.56	2.71	1.70	0.05	3.77	0.08	63.26	0.26	-	-
00-CMV-638a	5361897	464701	17.09	4.13	2.58	3.66	2.10	0.13	2.46	0.10	61.33	0.27	-	-
00-CMV-701a	5362178	473668	5.64	0.18	11.32	-	28.51	0.04	0.02	0.01	48.09	0.33	-	-
00-CMV-702b	5362230	473763	15.92	4.58	3.79	2.50	2.81	0.05	3.43	0.11	59.13	0.46	-	-
00-CMV-703-A	5362194	473574	8.04	10.37	8.68	0.02	7.11	0.32	0.57	0.05	51.9	0.40	11.60	8.31
00-CMV-705a	5362529	471517	8.26	-	12.50	-	27.68	0.04	0.03	0.04	43.6	0.46	-	-
00-CMV-706d	5362557	471617	10.10	10.34	5.04	0.05	3.50	0.14	3.41	0.07	57.05	0.34	-	-
00-CMV-708a	5362689	471794	16.44	2.41	0.76	2.02	0.27	-	4.72	0.11	69.53	0.38	-	-
00-CMV-709a	5362463	471694	16.59	3.55	3.57	1.82	2.12	0.04	5.70	0.10	64.18	0.41	-	-
00-CMV-807g	5363301	466926	13.94	8.87	10.44	0.03	7.08	0.19	3.33	0.05	51.3	0.72	-	-
00-CMV-809b	5362048	467253	14.18	4.38	4.61	1.19	2.20	0.11	3.92	0.13	61.48	0.68	-	-
01LAH-0002	5352910	456989	0.55	-	6.91	-	39.75	0.09	0.02	-	33.84	0.03	-	-
01LAH-0003A	5353708	448878	9.60	5.18	8.70	0.09	0.94	0.09	0.03	0.06	71.87	0.15	-	-
01LAH-0004A	5354272	449247	10.19	2.61	3.80	0.94	0.52	0.08	0.43	-	79.99	0.07	-	-
01LAH-0004B	5354270	449246	13.54	3.15	11.13	0.89	2.10	0.20	0.05	0.09	66.01	0.32	-	-
01LAH-0004C	5354274	449248	17.83	11.42	10.32	0.04	4.66	0.17	2.58	0.06	48.71	0.94	-	-
01LAH-0006	5352932	448939	19.10	9.65	11.05	0.03	3.65	0.19	1.94	0.05	49.87	0.92	-	-
01LAH-0008	5352989	448874	10.03	9.50	9.51	0.01	8.86	0.19	2.99	0.05	41.87	0.50	-	-
01LAH-0010	5352849	448794	15.98	10.69	8.96	0.18	6.40	0.20	2.53	0.04	44.1	0.61	-	-
01LAH-0012	5357236	451731	15.80	0.20	6.81	4.98	1.49	0.01	0.64	0.13	63.82	0.58	-	-
01LAH-0026	5360411	446573	13.81	7.77	14.99	0.61	6.67	0.22	3.69	0.08	50.65	1.22	-	-
01LAH-0029A	5361930	446394	17.06	8.59	12.32	1.18	3.28	0.24	2.37	0.09	49.6	1.08	-	-
01LAH-0029B	5361925	446396	12.30	2.05	4.52	1.98	0.42	0.08	3.36	0.07	72.59	0.48	-	-
01LAH-0032	5361140	446485	15.90	10.99	17.09	0.19	5.33	0.23	2.25	0.10	46.48	1.43	-	-
01LAH-0034	5361933	448649	14.60	5.33	9.76	0.94	4.84	0.24	3.53	0.09	53.39	0.62	-	-
01LAH-0041A	5358676	452645	17.21	0.76	2.86	4.98	1.77	0.04	0.17	0.06	68.96	0.90	-	-
01LAH-0041B	5358676	452645	0.60	0.08	12.87	0.02	1.68	0.19	-	-	85	0.01	-	-
01LAH-0041C	5358676	452645	14.79	2.39	18.54	0.45	7.71	0.43	1.22	0.06	49.25	0.97	-	-
01LAH-0042	5362164	448659	12.61	4.67	4.28	2.20	1.15	0.12	3.03	0.08	65.5	0.39	-	-
01LAH-0043A	5362249	448649	16.01	0.95	3.09	3.26	0.75	0.09	3.72	0.10	69.53	0.49	-	-
01LAH-0043B	5362255	448652	14.13	1.48	8.41	0.63	1.50	0.34	4.74	0.09	65.68	0.44	-	-
01LAH-0044A	5362551	448655	16.72	4.38	12.39	0.20	5.91	0.18	4.68	0.09	48.37	1.04	-	-
01LAH-0044B	5362555	448653	15.17	2.25	4.22	3.78	1.11	0.08	0.74	0.09	67.99	0.47	-	-
01LAH-0045A	5362831	448625	15.75	11.91	9.12	0.21	3.11	0.21	0.34	0.07	55.61	0.79	-	-
01LAH-0045B	5362831	448625	13.76	8.42	12.19	0.12	7.86	0.18	3.04	0.23	48.44	1.15	-	-
01LAH-0046	5362862	448560	13.31	2.33	3.91	2.60	1.00	0.08	0.46	-	75	0.11	-	-
01LAH-0048A	5362595	447882	11.42	2.13	3.73	1.98	0.99	0.06	2.25	0.04	73.36	0.12	-	-
01LAH-0048B	5362585	447875	15.04	4.30	5.75	1.56	2.68	0.10	3.80	0.09	64.17	0.50	-	-
01LAH-0051	5362520	447679	5.02	4.78	39.10	1.16	4.84	2.35	0.05	0.04	36.12	0.20	-	-
01LAH-0051B	5362515	447673	14.32	7.43	14.51	0.22	5.68	0.56	4.43	0.12	49.44	1.36	-	-
01LAH-0051C	5362522	447674	13.92	5.13	12.27	0.31	2.75	0.24	3.37	0.25	56.2	1.51	-	-

SampleNo	Cr (ppm)	Y (ppm)	Sc (ppm)	Sr (ppm)	Zr (ppm)	Au (ppb)	Ba (ppm)	Cu (ppm)	Ni (ppm)	Pb (ppm)	Zn (ppm)	Fe/Fe+Mg	CO_2/CaO	Ishikawa Index	Chlorite Index	SCI	CSI	K/Al	CCPI
00-CMV-429a	6	82	3	33	203	-	-			6	31	0.76	-	40	23	64	36	0.29	26
00-CMV-431c	13	44	7	1359	266	-	-	44	10	27	162	0.90	-	22	62	26	74	0.14	81
00-CMV-434-A	151	18	34	111	58	0	739	86	47	1	43	0.69	0.53	35	49	41	59	0.23	78
00-CMV-601a	16	2	2	450	65	-	-	4	8	2	16	0.71	-	24	21	53	47	0.17	29
00-CMV-602a	28	3	4	217	74	-	-	5	21	1	24	0.64	-	37	28	57	43	0.27	38
00-CMV-638a	36	4	5	153	73	-	-	9	26	2	72	0.59	-	47	30	61	39	0.34	42
00-CMV-701a	500	2	21	5	18	-	-	31	1196	2	51	0.32	-	99	99	50	50	0.00	100
00-CMV-702b	125	9	8	110	107	-	-	35	86	6	47	0.61	-	40	37	52	48	0.25	51
00-CMV-703-A	3147	10	29	84	20	0	3	64	2093	1	64	0.59	1.02	39	58	41	59	0.00	96
00-CMV-705a	500	6	22	9	20	-	-	35	875	3	55	0.34	-	100	100	50	50	0.00	100
00-CMV-706d	500	9	14	450	65	-	-	30	447	5	40	0.63	-	21	37	36	64	0.01	70
00-CMV-708a	57	6	5	333	128	-	-	24	32	8	33	0.77	-	24	9	72	28	0.19	12
00-CMV-709a	52	8	7	398	110	-	-	32	47	5	43	0.66	-	30	33	48	52	0.17	41
00-CMV-807g	135	17	49	149	42	-	-	129	87	1	66	0.63	-	37	57	39	61	0.00	83
00-CMV-809b	99	20	12	169	134	-	-	46	66	14	71	0.71	-	29	40	42	58	0.13	55
01LAH-0002	1553	1	-	1	-	-	-	-	-	-	-	0.17	-	100	100	50	50	0.00	100
01LAH-0003A	63	8	-	32	49	-	-	-	-	-	-	0.91	-	17	62	21	79	0.01	99
01LAH-0004A	10	65	-	151	142	-	-	-	-	-	-	0.89	-	32	50	39	61	0.14	74
01LAH-0004B	14	48	-	113	345	-	-	-	-	-	-	0.86	-	47	74	38	62	0.10	93
01LAH-0004C	415	19	-	253	61	-	-	-	-	-	-	0.72	-	25	50	34	66	0.00	84
01LAH-0006	178	18	-	167	55	-	-	-	-	-	-	0.78	-	24	54	31	69	0.00	87
01LAH-0008	1308	13	-	71	45	-	-	-	-	-	-	0.55	-	42	58	42	58	0.00	85
01LAH-0010	360	11	-	86	32	-	-	-	-	-	-	0.62	-	33	52	39	61	0.02	84
01LAH-0012	37	8	-	32	49	-	-	-	-	-	-	0.84	-	89	57	61	39	0.49	58
01LAH-0026	172	24	-	103	68	-	-	-	-	-	-	0.72	-	39	63	38	62	0.07	82
01LAH-0029A	297	19	-	178	65	-	-	-	-	-	-	0.81	-	29	54	35	65	0.11	80
01LAH-0029B	10	57	-	83	457	-	-	-	-	-	-	0.93	-	31	38	45	55	0.25	46
01LAH-0032	107	28	-	315	81	-	-	-	-	-	-	0.79	-	29	61	33	67	0.02	89
01LAH-0034	235	13	-	113	91	-	-	-	-	-	-	0.70	-	39	58	40	60	0.10	75
01LAH-0041A	45	19	-	35	212	-	-	-	-	-	-	0.65	-	88	42	67	33	0.45	46
01LAH-0041B	18	6	-	-	6	-	-	-	-	-	-	0.90	-	96	99	49	51	0.05	100
01LAH-0041C	410	11	-	46	48	-	-	-	-	-	-	0.74	-	69	86	45	55	0.05	94
01LAH-0042	11	38	-	70	274	-	-	-	-	-	-	0.81	-	30	34	47	53	0.27	49
01LAH-0043A	-	46	-	80	315	-	-	-	-	-	-	0.83	-	46	31	60	40	0.32	34
01LAH-0043B	14	45	-	106	262	-	-	-	-	-	-	0.87	-	26	57	31	69	0.07	63
01LAH-0044A	135	21	-	94	75	-	-	-	-	-	-	0.71	-	40	65	38	62	0.02	78
01LAH-0044B	12	48	-	48	280	-	-	-	-	-	-	0.82	-	62	42	60	40	0.39	52
01LAH-0045A	248	18	-	243	65	-	-	-	-	-	-	0.77	-	21	48	31	69	0.02	95
01LAH-0045B	592	19	-	529	82	-	-	-	-	-	-	0.64	-	41	62	40	60	0.01	86
01LAH-0046	11	129	-	75	260	-	-	-	-	-	-	0.82	-	56	46	55	45	0.31	60
01LAH-0048A	4	-	-	31	300	-	-	-	-	-	-	0.81	-	40	41	50	50	0.27	51
01LAH-0048B	105	20	-	157	168	-	-	-	-	-	-	0.71	-	34	45	43	57	0.16	59
01LAH-0051	101	14	-	60	37	-	-	-	-	-	-	0.90	-	55	87	39	61	0.36	97
01LAH-0051B	200	29	-	327	99	-	-	-	-	-	-	0.75	-	33	61	35	65	0.02	80
01LAH-0051C	37	36	-	255	182	-	-	-	-	-	-	0.84	-	26	61	30	70	0.03	79

SampleNo	UTMNorth (m)	UTMEast (m)	Al_2O_3 (%)	CaO (%)	Fe_2O_3 (%)	K_2O (%)	MgO (%)	MnO (%)	Na_2O (%)	P_2O_5 (%)	SiO_2 (%)	TiO_2 (%)	LOI (%)	CO_2 (%)
01LAH-0051D	5362522	447675	12.93	0.35	2.24	1.64	0.87	0.04	4.60	-	75.52	0.13	-	-
01LAH-0056A	5362586	446487	18.32	5.43	6.26	0.68	1.35	0.11	4.45	0.15	59.65	1.19	-	-
01LAH-0056B	5362580	446485	16.07	0.62	2.96	3.99	1.72	0.05	2.03	0.10	70.08	0.30	-	-
01LAH-0057	5362756	446494	13.81	7.90	22.86	0.71	4.58	1.00	2.52	0.08	44.53	0.56	-	-
01LAH-0059A	5362859	446436	12.24	1.08	2.27	2.56	0.24	0.04	2.31	0.02	76.97	0.20	-	-
01LAH-0059B	5362859	446438	15.87	0.60	2.96	3.99	1.70	0.05	2.02	0.10	69.22	0.29	-	-
01LAH-0060A	5362885	446456	12.24	0.89	3.23	5.30	0.40	0.05	0.34	0.02	73.93	0.20	-	-
01LAH-0060C	5362885	446456	15.33	4.28	6.31	0.73	3.77	0.17	5.44	0.09	58.63	0.63	-	-
01LAH-0061A	5363382	447054	17.42	6.24	4.66	1.31	1.12	0.13	3.21	0.15	62.87	1.15	-	-
01LAH-0061B	5363382	447054	1.32	0.98	15.27	0.03	2.22	0.71	0.03	0.02	78.93	0.03	-	-
01LAH-0065	5363245	447820	5.73	0.43	4.91	1.01	0.92	0.08	0.45	0.04	84.33	0.14	-	-
01LAH-0066	5363295	447598	0.59	3.00	20.57	0.06	2.05	0.20	0.06	0.06	74.01	0.02	-	-
01LAH-0069A	5353391	447962	15.82	11.14	11.05	0.14	8.60	0.18	0.85	0.05	46.34	0.75	-	-
01LAH-0069B	5353448	447924	16.25	12.72	11.11	0.03	7.15	0.18	0.86	0.05	47.08	0.73	-	-
01LAH-0069C	5353422	447891	13.67	2.37	2.18	0.75	0.21	0.02	4.44	-	75.99	0.07	-	-
01LAH-0069D	5353425	447895	14.37	5.61	5.78	0.26	0.97	0.09	1.98	0.10	68.53	0.32	-	-
01LAH-0074	5358589	452274	1.04	3.36	29.28	0.16	2.94	0.52	0.03	0.01	55.29	0.04	-	-
01LAH-0077A	5352162	455119	12.87	11.98	11.36	0.22	10.86	0.18	1.51	0.03	48.62	0.54	-	-
01LAH-0077B	5352160	455120	15.22	11.15	11.91	0.16	7.12	0.23	1.83	0.05	51.83	0.74	-	-
01LAH-0078	5352209	455049	15.06	10.95	12.29	0.31	7.42	0.26	1.88	0.04	49.85	0.68	-	-
01LAH-0081B	5354117	453722	16.43	3.96	15.04	0.29	3.81	0.19	6.15	0.16	45.06	2.16	-	-
01LAH-0083	5354764	449357	15.57	11.21	12.62	0.11	7.36	0.19	1.13	0.05	47.71	0.81	-	-
01LAH-0085	5354929	449575	14.73	4.59	9.43	0.69	1.89	0.12	2.60	0.09	62.36	0.58	-	-
01LAH-0092	5354190	448682	16.11	8.83	14.96	0.14	10.99	0.23	1.81	0.05	41.21	0.86	-	-
01LAH-0093	5356769	450233	16.99	3.27	3.00	1.62	1.16	0.04	5.60	0.10	65.65	0.37	-	-
01LAH-0096	5356455	442110	7.72	0.27	14.23	1.54	1.16	0.03	-	0.21	64.93	0.37	-	-
01LAH-0097	5356474	452172	16.58	2.54	3.41	4.11	1.27	0.03	1.86	0.11	65.77	0.44	-	-
01LAH-0102A	5354312	453783	6.15	7.67	10.54	-	24.20	0.15	0.04	0.01	45.56	0.27	-	-
01LAH-0102B	5354312	453783	15.00	7.73	16.02	0.03	6.84	0.20	3.50	0.14	46.22	1.91	-	-
01LAH-0103B	5357692	455628	13.52	3.62	13.63	0.29	7.39	0.23	1.67	0.09	53.42	1.29	-	-
01LAH-0105A	5355772	452214	18.31	0.09	3.85	4.62	0.99	0.01	0.83	0.05	67.02	0.48	-	-
01LAH-0105B	5355772	452214	7.63	0.91	10.17	0.79	0.96	0.04	2.08	0.06	72.41	0.24	-	-
01LAH-0105C	5355772	452214	13.31	9.24	13.28	0.91	5.93	0.26	0.92	0.09	44.26	1.01	-	-
01LAH-0107	5352193	453996	15.06	12.42	10.54	0.23	6.17	0.23	1.58	0.05	50.55	0.67	-	-
01LAH-0109	5351847	453996	6.17	5.61	10.30	0.01	27.76	0.14	0.20	0.02	41.61	0.33	-	-
01LAH-0111B	5350397	453702	15.39	8.35	14.36	0.71	6.73	0.20	4.14	0.15	49.2	0.70	-	-
01LAH-0111C	5350397	453702	14.11	8.34	15.12	1.02	7.11	0.26	3.29	0.06	49.7	1.27	-	-
01LAH-0111D	5350397	453702	13.81	3.79	3.00	0.03	2.25	0.04	8.49	0.06	66.1	0.37	-	-
01LAH-0111E	5350397	453702	14.87	0.93	0.43	4.53	0.04	0.02	5.00	-	73.82	0.03	-	-
01LAH-0113D	5349603	452928	14.84	5.76	6.80	2.77	4.98	0.10	4.53	0.48	56.4	0.67	-	-
01LAH-0114A	5349463	452583	15.99	2.23	2.86	3.02	1.87	0.05	5.11	0.15	67.15	0.33	-	-
01LAH-0115B	5349452	452447	16.87	2.70	1.27	1.77	0.52	0.02	5.93	0.07	69.7	0.20	-	-
01LAH-0119	5351149	450356	13.42	11.08	13.23	0.76	8.59	0.23	2.24	0.05	49.44	0.83	-	-
01LAH-0120A	5351578	450286	15.70	11.63	7.02	1.37	4.88	0.14	1.42	0.13	55.05	0.65	-	-
01LAH-0120B	5351578	450286	15.94	12.39	8.65	0.87	5.26	0.17	0.71	0.12	54.26	0.64	-	-

SampleNo	Cr (ppm)	Y (ppm)	Sc (ppm)	Sr (ppm)	Zr (ppm)	Au (ppb)	Ba (ppm)	Cu (ppm)	Ni (ppm)	Pb (ppm)	Zn (ppm)	Fe/Fe+Mg	CO_2/CaO	Ishikawa Index	Chlorite Index	SCI	CSI	K/Al	CCPI
01LAH-0051D	9	86	-	77	318	-	-	-	-	-	-	0.75	-	34	30	52	48	0.20	32
01LAH-0056A	208	19	-	197	99	-	-	-	-	-	-	0.84	-	17	40	30	70	0.06	58
01LAH-0056B	209	16	-	143	83	-	-	-	-	-	-	0.67	-	68	40	63	37	0.39	42
01LAH-0057	225	19	-	166	90	-	-	-	-	-	-	0.85	-	34	69	33	67	0.08	89
01LAH-0059A	9	36	-	98	264	-	-	-	-	-	-	0.92	-	45	28	62	38	0.33	32
01LAH-0059B	18	13	-	141	173	-	-	-	-	-	-	0.67	-	68	40	63	37	0.39	42
01LAH-0060A	4	41	-	26	277	-	-	-	-	-	-	0.90	-	82	34	71	29	0.68	37
01LAH-0060C	258	12	-	130	97	-	-	-	-	-	-	0.66	-	32	47	40	60	0.07	60
01LAH-0061A	8	19	-	195	142	-	-	-	-	-	-	0.83	-	20	33	38	62	0.12	54
01LAH-0061B	25	9	-	7	10	-	-	-	-	-	-	0.89	-	69	94	42	58	0.04	100
01LAH-0065	22	19	-	26	53	-	-	-	-	-	-	0.86	-	69	74	48	52	0.28	79
01LAH-0066	23	5	-	3	11	-	-	-	-	-	-	0.92	-	41	87	32	68	0.16	99
01LAH-0069A	255	18	-	186	48	-	-	-	-	-	-	0.60	-	42	60	41	59	0.01	95
01LAH-0069B	169	16	-	201	50	-	-	-	-	-	-	0.64	-	35	56	38	62	0.00	95
01LAH-0069C	9	82	-	108	169	-	-	-	-	-	-	0.92	-	12	22	36	64	0.09	29
01LAH-0069D	16	63	-	157	307	-	-	-	-	-	-	0.87	-	14	44	24	76	0.03	73
01LAH-0074	90	8	-	3	12	-	-	-	-	-	-	0.92	-	48	89	35	65	0.24	99
01LAH-0077A	721	15	-	80	31	-	-	-	-	-	-	0.55	-	45	61	43	57	0.03	92
01LAH-0077B	201	19	-	79	42	-	-	-	-	-	-	0.66	-	36	58	38	62	0.02	90
01LAH-0078	367	18	-	91	41	-	-	-	-	-	-	0.66	-	38	58	39	61	0.03	89
01LAH-0081B	115	29	-	75	130	-	-	-	-	-	-	0.82	-	29	63	32	68	0.03	73
01LAH-0083	390	18	-	127	36	-	-	-	-	-	-	0.67	-	38	60	39	61	0.01	94
01LAH-0085	13	25	-	123	126	-	-	-	-	-	-	0.85	-	26	57	32	68	0.07	76
01LAH-0092	472	18	-	150	45	-	-	-	-	-	-	0.61	-	51	69	42	58	0.01	93
01LAH-0093	20	8	-	422	119	-	-	-	-	-	-	0.75	-	24	27	47	53	0.15	35
01LAH-0096	25	7	-	24	104	-	-	-	-	-	-	0.93	-	91	89	51	49	0.31	90
01LAH-0097	18	5	-	73	127	-	-	-	-	-	-	0.76	-	55	34	62	38	0.39	42
01LAH-0102A	3153	5	-	6	12	-	-	-	-	-	-	0.34	-	76	81	48	52	0.00	100
01LAH-0102B	135	27	-	178	115	-	-	-	-	-	-	0.73	-	38	65	37	63	0.00	86
01LAH-0103B	255	20	-	37	77	-	-	-	-	-	-	0.68	-	59	78	43	57	0.03	91
01LAH-0105A	19	13	-	87	350	-	-	-	-	-	-	0.82	-	86	45	66	34	0.40	45
01LAH-0105B	54	9	-	71	77	-	-	-	-	-	-	0.92	-	37	73	34	66	0.16	78
01LAH-0105C	94	23	-	100	76	-	-	-	-	-	-	0.72	-	40	62	39	61	0.11	91
01LAH-0107	372	17	-	99	38	-	-	-	-	-	-	0.66	-	31	52	37	63	0.02	90
01LAH-0109	2411	8	-	22	19	-	-	-	-	-	-	0.30	-	83	86	49	51	0.00	99
01LAH-0111B	263	15	-	190	96	-	-	-	-	-	-	0.71	-	37	60	38	62	0.07	80
01LAH-0111C	75	20	-	248	50	-	-	-	-	-	-	0.71	-	41	62	40	60	0.11	83
01LAH-0111D	18	17	-	37	127	-	-	-	-	-	-	0.61	-	16	29	35	65	0.00	37
01LAH-0111E	6	4	-	139	42	-	-	-	-	-	-	0.93	-	44	4	92	8	0.48	4
01LAH-0113D	151	30	-	450	214	-	-	-	-	-	-	0.61	-	43	46	48	52	0.29	60
01LAH-0114A	22	11	-	450	133	-	-	-	-	-	-	0.64	-	40	30	57	43	0.30	35
01LAH-0115B	-	2	-	450	110	-	-	-	-	-	-	0.74	-	21	14	60	40	0.16	18
01LAH-0119	200	18	-	154	42	-	-	-	-	-	-	0.64	-	41	59	41	59	0.09	87
01LAH-0120A	674	12	-	260	86	-	-	-	-	-	-	0.63	-	32	44	43	57	0.14	80
01LAH-0120B	721	14	-	224	89	-	-	-	-	-	-	0.66	-	32	48	40	60	0.09	89

SampleNo	UTMNorth (m)	UTMEast (m)	Al_2O_3 (%)	CaO (%)	Fe_2O_3 (%)	K_2O (%)	MgO (%)	MnO (%)	Na_2O (%)	P_2O_5 (%)	SiO_2 (%)	TiO_2 (%)	LOI (%)	CO_2 (%)
01LAH-0122	5353631	452424	9.53	0.75	12.78	-	24.71	0.10	0.32	0.03	42	0.47	-	-
01LAH-0123	5353210	452640	19.81	0.28	7.23	1.75	2.73	0.03	2.71	0.14	60.97	0.81	-	-
01LAH-0124	5352837	452865	11.31	7.13	10.87	0.08	11.61	0.16	2.97	0.05	47.21	0.60	-	-
01LAH-0125	5352670	452855	15.32	5.57	4.25	2.57	1.56	0.06	1.92	0.15	61.7	0.49	-	-
01LAH-0126	5351880	449449	14.50	10.42	5.80	0.30	1.97	0.17	2.62	0.15	62.3	0.56	-	-
01LAH-0127	5351960	449421	10.25	19.33	12.64	0.09	6.34	0.39	0.23	0.15	48.24	1.04	-	-
01LAH-0130	5352638	448872	18.20	6.80	10.31	0.83	3.17	0.23	2.94	0.04	50.34	0.84	-	-
01LAH-0131	5352625	449015	19.93	6.65	11.04	0.73	3.57	0.21	2.79	0.05	50.88	0.97	-	-
01LAH-0133A	5352203	449081	16.40	7.33	6.84	1.54	3.48	0.11	2.12	0.14	59.95	0.70	-	-
01LAH-0133B	5352205	449080	16.32	3.23	2.49	0.99	1.28	0.03	5.36	0.10	69.77	0.31	-	-
01LAH-0139	5352051	448620	14.96	8.55	14.17	1.06	6.98	0.23	2.67	0.07	50.45	0.91	-	-
01LAH-0141	5352145	448385	17.02	3.69	3.30	2.52	2.31	0.05	5.23	0.17	63.17	0.33	-	-
01LAH-0143	5360193	448085	14.19	11.76	15.08	0.36	2.32	0.28	0.79	0.13	52.65	1.62	-	-
01LAH-0145A	5352604	452206	7.86	10.32	10.47	0.13	14.92	0.22	1.81	0.02	47.7	0.39	-	-
01LAH-0145B	5352604	452206	15.27	4.94	4.15	2.64	1.49	0.08	1.56	0.12	63.53	0.44	-	-
01LAH-0146	5352786	452222	15.52	2.64	2.27	2.11	1.17	0.05	5.50	0.08	66.11	0.32	-	-
01LAH-0147	5352786	452328	15.88	3.99	4.33	2.58	1.52	0.06	2.46	0.14	63.58	0.47	-	-
01LAH-0149	5351894	452025	6.20	7.08	10.67	-	26.73	0.16	0.22	0.01	41.54	0.33	-	-
01LAH-0150	5351882	452234	14.99	12.82	11.59	0.23	6.07	0.21	1.79	0.05	50.11	0.72	-	-
01LAH-0151	5351732	452351	6.59	6.77	11.53	0.04	25.35	0.14	0.50	0.02	41.64	0.34	-	-
01LAH-0152	5351450	452626	5.00	3.67	10.86	-	29.63	0.14	0.12	-	39.67	0.23	-	-
01LAH-0153	5351629	452777	14.69	3.10	2.57	1.20	1.06	0.04	4.50	0.07	71.09	0.27	-	-
01LAH-0154	5351862	452691	14.44	10.23	12.52	0.36	7.24	0.18	2.81	0.05	50.82	0.72	-	-
01LAH-0155	5351951	452579	14.92	4.51	4.42	0.77	2.91	0.06	4.91	0.22	63.98	0.55	-	-
01LAH-0160	5351937	452876	15.32	10.94	9.61	0.59	8.64	0.18	2.96	0.03	50.02	0.51	-	-
01LAH-0163	5351936	453196	15.02	11.08	11.16	0.19	6.81	0.23	1.77	0.05	51.19	0.67	-	-
01LAH-0167A	5349138	447243	15.38	6.23	9.20	0.36	5.37	0.19	4.03	0.07	52.77	1.03	-	-
01LAH-0167B	5349140	447242	15.37	6.84	7.97	2.43	5.14	0.14	4.97	0.54	52.95	0.87	-	-
01LAH-0171	5350886	446592	13.15	9.64	15.23	0.26	4.90	0.27	3.15	0.09	51.93	1.14	-	-
01LAH-0176	5352177	447483	14.51	3.57	7.38	0.63	0.59	0.13	5.71	0.14	65.77	0.44	-	-
01LAH-0182	5349389	447267	19.11	10.38	9.68	0.05	6.28	0.15	3.15	0.05	44.15	0.70	-	-
01LAH-0184	5349604	447422	16.30	4.58	8.98	0.03	3.94	0.15	3.68	0.16	58.32	1.07	-	-
01LAH-0186A	5350360	447665	15.63	5.13	15.28	0.03	3.58	0.34	4.33	0.10	49.22	0.86	-	-
01LAH-0186B	5350405	447712	17.44	5.58	12.37	0.56	7.20	0.11	2.82	0.05	42.34	0.82	-	-
01LAH-0186D	5350315	447695	16.08	11.15	10.44	0.02	7.96	0.18	2.08	0.05	47.58	0.73	-	-
01LAH-0187	5350431	447601	16.67	2.93	5.79	0.59	3.42	0.06	6.88	0.10	61.6	0.59	-	-
01LAH-0205	5349665	447351	16.63	4.69	6.59	1.13	2.60	0.13	1.63	0.15	59.43	0.85	-	-
01LAH-0211	5350781	447746	17.09	4.24	4.68	1.01	2.20	0.05	5.41	0.08	62.61	0.52	-	-
01LAH-0213	5354811	450017	15.88	6.43	8.86	0.65	2.92	0.18	3.92	0.26	58.26	1.76	-	-
01LAH-0214	5354106	450857	16.31	2.99	11.03	0.49	2.56	0.18	1.87	0.13	59.24	0.67	-	-
01LAH-0219A	5366329	455755	13.12	0.98	2.94	0.81	0.62	0.05	6.21	0.03	73.14	0.24	-	-
01LAH-0219B	5366329	455754	14.16	6.80	7.47	1.72	7.93	0.13	3.32	0.04	46.07	0.45	-	-
01LAH-0220	5366521	455869	14.79	5.14	8.60	1.18	2.71	0.10	4.22	0.15	59.9	0.90	-	-
01LAH-0221	5365874	455858	15.48	7.21	10.23	0.06	4.03	0.09	5.62	0.29	50.14	1.72	-	-
01LAH-0225	5365747	454147	12.30	1.17	2.88	2.55	0.25	0.06	4.34	0.03	74.45	0.20	-	-

SampleNo	Cr (ppm)	Y (ppm)	Sc (ppm)	Sr (ppm)	Zr (ppm)	Au (ppb)	Ba (ppm)	Cu (ppm)	Ni (ppm)	Pb (ppm)	Zn (ppm)	Fe/Fe+Mg	CO_2/CaO	Ishikawa Index	Chlorite Index	SCI	CSI	K/Al	CCPI
01LAH-0122	3833	7	-	7	32	-	-	-	-	-	-	0.37	-	96	97	50	50	0.00	99
01LAH-0123	246	13	-	379	150	-	-	-	-	-	-	0.75	-	60	66	48	52	0.14	67
01LAH-0124	1185	17	-	52	53	-	-	-	-	-	-	0.52	-	54	68	44	56	0.01	88
01LAH-0125	38	21	-	130	169	-	-	-	-	-	-	0.76	-	36	35	50	50	0.26	55
01LAH-0126	95	11	-	407	99	-	-	-	-	-	-	0.77	-	15	35	30	70	0.03	71
01LAH-0127	779	17	-	359	136	-	-	-	-	-	-	0.70	-	25	47	34	66	0.01	98
01LAH-0130	272	16	-	107	50	-	-	-	-	-	-	0.79	-	29	54	35	65	0.07	77
01LAH-0131	187	18	-	162	54	-	-	-	-	-	-	0.78	-	31	57	35	65	0.06	79
01LAH-0133A	246	13	-	342	109	-	-	-	-	-	-	0.70	-	35	47	43	57	0.15	72
01LAH-0133B	43	5	-	450	132	-	-	-	-	-	-	0.69	-	21	27	44	56	0.10	36
01LAH-0139	118	23	-	250	60	-	-	-	-	-	-	0.70	-	42	62	40	60	0.11	84
01LAH-0141	60	10	-	450	159	-	-	-	-	-	-	0.62	-	35	32	53	47	0.23	41
01LAH-0143	43	33	-	104	93	-	-	-	-	-	-	0.88	-	18	55	24	76	0.04	93
01LAH-0145A	2935	10	-	82	22	-	-	-	-	-	-	0.45	-	55	67	45	55	0.03	93
01LAH-0145B	32	17	-	152	152	-	-	-	-	-	-	0.76	-	39	36	52	48	0.27	55
01LAH-0146	34	5	-	134	101	-	-	-	-	-	-	0.69	-	29	24	55	45	0.21	30
01LAH-0147	30	19	-	144	164	-	-	-	-	-	-	0.77	-	39	37	51	49	0.25	52
01LAH-0149	2801	6	-	40	14	-	-	-	-	-	-	0.32	-	79	83	49	51	0.00	99
01LAH-0150	199	18	-	109	41	-	-	-	-	-	-	0.69	-	30	53	36	64	0.02	89
01LAH-0151	3101	8	-	15	18	-	-	-	-	-	-	0.35	-	78	83	48	52	0.01	99
01LAH-0152	2672	4	-	101	9	-	-	-	-	-	-	0.30	-	89	91	49	51	0.00	100
01LAH-0153	23	3	-	356	99	-	-	-	-	-	-	0.74	-	23	28	45	55	0.13	37
01LAH-0154	206	18	-	91	39	-	-	-	-	-	-	0.67	-	37	58	39	61	0.04	85
01LAH-0155	72	12	-	450	141	-	-	-	-	-	-	0.64	-	28	40	41	59	0.08	55
01LAH-0160	794	12	-	136	25	-	-	-	-	-	-	0.56	-	40	54	42	58	0.06	83
01LAH-0163	371	16	-	83	38	-	-	-	-	-	-	0.66	-	35	56	38	62	0.02	90
01LAH-0167A	147	17	-	266	55	-	-	-	-	-	-	0.67	-	36	56	39	61	0.04	76
01LAH-0167B	128	26	-	450	199	-	-	-	-	-	-	0.64	-	39	46	46	54	0.25	62
01LAH-0171	134	25	-	88	63	-	-	-	-	-	-	0.78	-	29	59	33	67	0.03	85
01LAH-0176	14	54	-	172	322	-	-	-	-	-	-	0.94	-	12	42	22	78	0.07	53
01LAH-0182	113	14	-	189	44	-	-	-	-	-	-	0.64	-	32	52	38	62	0.00	82
01LAH-0184	54	18	-	172	115	-	-	-	-	-	-	0.73	-	32	59	35	65	0.00	76
01LAH-0186A	85	18	-	51	79	-	-	-	-	-	-	0.83	-	28	65	30	70	0.00	80
01LAH-0186B	290	15	-	105	44	-	-	-	-	-	-	0.67	-	48	67	42	58	0.05	84
01LAH-0186D	516	15	-	175	45	-	-	-	-	-	-	0.60	-	38	57	40	60	0.00	89
01LAH-0187	93	12	-	227	113	-	-	-	-	-	-	0.66	-	29	45	39	61	0.06	54
01LAH-0205	85	16	-	178	131	-	-	-	-	-	-	0.75	-	37	53	41	59	0.11	76
01LAH-0211	266	10	-	190	90	-	-	-	-	-	-	0.71	-	25	38	40	60	0.09	50
01LAH-0213	8	23	-	155	122	-	-	-	-	-	-	0.78	-	26	50	34	66	0.06	70
01LAH-0214	363	18	-	156	111	-	-	-	-	-	-	0.83	-	39	70	36	64	0.05	84
01LAH-0219A	10	65	-	56	352	-	-	-	-	-	-	0.85	-	17	29	36	64	0.10	32
01LAH-0219B	513	15	-	112	61	-	-	-	-	-	-	0.52	-	49	55	47	53	0.19	74
01LAH-0220	34	36	-	273	205	-	-	-	-	-	-	0.79	-	29	50	37	63	0.13	66
01LAH-0221	225	25	-	364	121	-	-	-	-	-	-	0.75	-	24	51	32	68	0.01	70
01LAH-0225	7	67	-	68	363	-	-	-	-	-	-	0.93	-	34	26	56	44	0.33	29

SampleNo	UTMNorth (m)	UTMEast (m)	Al_2O_3 (%)	CaO (%)	Fe_2O_3 (%)	K_2O (%)	MgO (%)	MnO (%)	Na_2O (%)	P_2O_5 (%)	SiO_2 (%)	TiO_2 (%)	LOI (%)	CO_2 (%)
01LAH-0226	5365378	454202	11.39	2.16	4.20	1.18	1.64	0.07	2.94	0.03	73.56	0.18	-	-
01LAH-0501A	5353673	447987	13.66	0.89	1.86	0.74	0.18	0.03	6.19	-	75.31	0.07	-	-
01LAH-0501B	5353670	447989	15.30	10.26	11.49	0.30	7.36	0.19	1.82	0.07	49.63	0.88	-	-
01LAH-0504A	5353253	448292	16.18	10.35	10.60	2.14	3.02	0.34	1.06	0.14	43.48	0.86	-	-
01LAH-0504B	5353253	448292	16.01	7.13	9.85	0.27	5.69	0.16	3.68	0.15	54.02	1.11	-	-
01LAH-0504C	5353253	448292	16.30	4.71	9.67	1.08	6.46	0.14	3.41	0.15	53.32	1.03	-	-
01LAH-0504D	5353253	448292	17.43	8.91	18.47	0.37	3.40	0.46	0.92	0.09	43.62	0.96	-	-
01LAH-0504E	5353253	448292	18.12	7.31	14.68	1.13	3.35	0.30	1.84	0.10	51.82	0.96	-	-
01LAH-0517	5358425	451407	16.22	3.87	4.31	2.06	1.55	0.06	4.34	0.14	65.8	0.53	-	-
01LAH-0521B	5362870	449522	16.13	3.53	2.64	0.90	1.51	0.04	5.61	0.16	65.98	0.33	-	-
01LAH-0521C	5362870	449522	15.33	9.10	11.55	0.47	5.89	0.22	2.29	0.09	52.28	0.87	-	-
01LAH-0522A	5362905	449556	15.10	6.44	11.08	0.09	4.95	0.47	2.78	0.10	55.67	0.63	-	-
01LAH-0522B	5362905	449556	0.97	1.18	10.74	0.03	1.16	0.52	-	-	82.28	0.01	-	-
01LAH-0522C	5362905	449556	15.84	3.35	6.29	2.83	3.62	0.11	4.24	0.11	61.2	0.56	-	-
01LAH-0528	5363993	448893	13.87	0.10	4.04	4.09	0.25	0.05	0.23	0.06	73.52	0.35	-	-
01LAH-0533A	5364172	449518	16.05	8.54	10.47	1.49	7.91	0.19	2.02	0.02	51.25	0.43	-	-
01LAH-0533B	5364172	449518	14.54	3.65	4.54	1.70	1.00	0.05	3.90	0.08	69.23	0.46	-	-
01LAH-0544	5365040	449708	14.14	7.71	14.30	3.63	3.88	0.23	0.35	0.21	34.97	2.24	-	-
01LAH-0547	5363746	450430	9.83	3.34	3.63	2.14	1.24	0.05	0.89	0.06	74.98	0.25	-	-
01LAH-0548A	5363736	450509	15.32	10.72	12.02	0.07	7.00	0.22	1.58	0.06	49.45	0.83	-	-
01LAH-0548B	5363736	450509	13.07	1.54	4.83	1.63	0.55	0.05	4.08	0.09	70.1	0.52	-	-
01LAH-0554A	5364153	448891	12.25	0.73	2.25	3.09	0.72	0.05	0.84	0.01	78.14	0.18	-	-
01LAH-0574	5348524	449187	15.38	1.55	1.00	3.14	0.36	0.02	5.54	0.04	71.71	0.14	-	-
01LAH-0576A	5348694	449085	15.87	3.21	2.75	2.74	1.41	0.05	5.39	0.15	67.79	0.31	-	-
01LAH-0576B	5348694	449085	15.14	1.34	0.97	3.29	0.28	0.02	5.50	0.03	72.22	0.11	-	-
01LAH-0587	5350449	449106	16.14	3.68	3.01	1.97	1.83	0.05	5.45	0.13	66.14	0.34	-	-
01LAH-0599	5359546	455123	13.55	7.11	7.85	0.19	5.45	0.12	2.52	0.07	47.55	0.57	-	-
01LAH-0602A	5350362	452610	16.80	10.38	8.87	1.08	4.46	0.17	2.12	0.15	53.78	0.68	-	-
03-BHA-0098	5366763	453460	10.62	1.20	1.88	4.11	0.57	0.05	2.81	0.00	76.82	0.09	2.44	-
03-BHA-0099	5366914	453678	11.49	0.48	1.57	4.23	0.31	0.04	2.59	0.00	77.96	0.10	1.51	-
03-BHA-0102	5367130	453679	11.28	0.79	1.53	4.04	0.27	0.04	2.75	0.00	77.81	0.10	1.69	-
03-BHA-0105	5366857	453999	11.86	0.50	1.11	7.46	0.44	0.02	1.20	0.01	77.35	0.10	1.38	-
03-BHA-0122	5367060	458910	10.35	1.43	2.24	3.75	0.70	0.06	2.57	0.03	75.56	0.24	2.20	-
03-BHA-0125A	5367381	458678	13.36	0.88	2.43	2.56	0.85	0.03	5.07	0.07	74.08	0.35	1.52	-
03-BHA-0125B	5367382	458677	11.59	0.04	2.03	9.09	0.65	0.01	0.19	0.03	76.53	0.24	0.89	-
03-BHA-0128	5367123	458102	10.50	1.53	3.14	5.49	1.36	0.03	0.82	0.00	74.44	0.17	3.25	-
03-BHA-0131	5366635	458048	8.51	0.61	0.64	3.99	0.55	0.02	1.35	0.00	83.78	0.08	1.31	-
03-BHA-0144A	5367175	459536	11.78	0.65	2.08	6.81	0.53	0.04	0.91	0.00	76.04	0.14	1.50	-
03-BHA-0147	5367533	457798	11.06	1.29	2.42	3.82	0.65	0.03	2.80	0.02	76.39	0.22	0.00	-
03-BHA-0149	5367614	457551	10.96	1.15	2.62	4.81	0.96	0.04	1.90	0.02	74	0.19	2.54	-
03-BHA-0151	5368014	457544	10.94	1.56	2.38	5.06	0.80	0.03	1.22	0.03	76.08	0.25	2.45	-
03-BHA-0153	5367970	457303	11.28	1.62	2.45	3.67	0.83	0.04	2.22	0.01	75.56	0.18	2.60	-
03-BHA-0227A	5365830	459951	10.43	0.13	0.98	6.34	0.35	0.01	1.30	0.01	80.11	0.10	0.72	-
03-BHA-0229A	5365833	459673	9.86	0.41	1.31	5.21	0.61	0.04	1.49	0.00	80.18	0.11	1.17	-
03-BHA-0291	5365641	454301	12.00	1.53	2.81	2.84	0.34	0.07	4.40	0.03	73.48	0.22	2.66	-

SampleNo	Cr (ppm)	Y (ppm)	Sc (ppm)	Sr (ppm)	Zr (ppm)	Au (ppb)	Ba (ppm)	Cu (ppm)	Ni (ppm)	Pb (ppm)	Zn (ppm)	Fe/Fe+Mg	CO_2/CaO	Ishikawa Index	Chlorite Index	SCI	CSI	K/Al	CCPI
01LAH-0226	13	62	-	73	319	-	-	-	-	-	-	0.75	-	36	46	43	57	0.16	57
01LAH-0501A	12	68	-	62	150	-	-	-	-	-	-	0.92	-	12	19	38	62	0.08	21
01LAH-0501B	85	21	-	213	89	-	-	-	-	-	-	0.64	-	39	59	40	60	0.03	89
01LAH-0504A	74	18	-	95	83	-	-	-	-	-	-	0.80	-	31	48	39	61	0.21	80
01LAH-0504B	120	24	-	275	105	-	-	-	-	-	-	0.67	-	36	57	38	62	0.03	79
01LAH-0504C	154	23	-	265	112	-	-	-	-	-	-	0.63	-	48	62	44	56	0.10	77
01LAH-0504D	91	22	-	235	90	-	-	-	-	-	-	0.86	-	28	66	30	70	0.03	94
01LAH-0504E	225	19	-	127	90	-	-	-	-	-	-	0.84	-	33	62	35	65	0.10	85
01LAH-0517	17	15	-	420	180	-	-	-	-	-	-	0.76	-	31	35	47	53	0.20	46
01LAH-0521B	22	4	-	450	95	-	-	-	-	-	-	0.67	-	21	28	43	57	0.09	37
01LAH-0521C	211	23	-	275	96	-	-	-	-	-	-	0.69	-	36	58	38	62	0.05	86
01LAH-0522A	251	16	-	211	110	-	-	-	-	-	-	0.72	-	35	62	36	64	0.01	84
01LAH-0522B	21	4	-	4		-	-	-	-	-	-	0.91	-	50	90	36	64	0.05	100
01LAH-0522C	44	18	-	117	155	-	-	-	-	-	-	0.67	-	46	47	49	51	0.28	57
01LAH-0528	7	36	-	28	266	-	-	-	-	-	-	0.95	-	93	47	67	33	0.46	47
01LAH-0533A	161	12	-	139	28	-	-	-	-	-	-	0.61	-	47	59	44	56	0.15	83
01LAH-0533B	28	52	-	166	319	-	-	-	-	-	-	0.84	-	26	35	43	57	0.18	48
01LAH-0544	45	29	-	98	109	-	-	-	-	-	-	0.81	-	48	59	45	55	0.40	81
01LAH-0547	10	27	-	33	205	-	-	-	-	-	-	0.77	-	44	41	52	48	0.34	60
01LAH-0548A	135	21	-	225	58	-	-	-	-	-	-	0.67	-	36	59	38	62	0.01	92
01LAH-0548B	14	64	-	82	297	-	-	-	-	-	-	0.91	-	28	40	41	59	0.20	46
01LAH-0554A	11	126	-	48	401	-	-	-	-	-	-	0.78	-	71	37	66	34	0.40	41
01LAH-0574	5	5	-	450	70	-	-	-	-	-	-	0.76	-	33	11	75	25	0.32	13
01LAH-0576A	22	11	-	450	125	-	-	-	-	-	-	0.69	-	33	26	56	44	0.27	32
01LAH-0576B	-	4	-	450	68	-	-	-	-	-	-	0.80	-	34	10	77	23	0.34	12
01LAH-0587	67	9	-	450	146	-	-	-	-	-	-	0.66	-	29	29	50	50	0.19	38
01LAH-0599	378	25	-	166	130	-	-	-	-	-	-	0.63	-	37	56	40	60	0.02	82
01LAH-0602A	155	17	-	401	92	-	-	-	-	-	-	0.70	-	31	48	39	61	0.10	80
03-BHA-0098	-	79	2	43	174	-	810	0	4	-	39	-	-	-	-	-	-	-	-
03-BHA-0099	-	72	2	19	194	-	771	5	0	-	111	-	-	-	-	-	-	-	-
03-BHA-0102	-	64	2	26	177	-	776	0	0	-	83	-	-	-	-	-	-	-	-
03-BHA-0105	-	65	2	22	201	-	1085	0	3	-	41	-	-	-	-	-	-	-	-
03-BHA-0122	-	52	4	19	382	-	602	0	4	-	50	-	-	-	-	-	-	-	-
03-BHA-0125A	-	13	4	44	179	-	509	0	5	-	44	-	-	-	-	-	-	-	-
03-BHA-0125B	-	-	3	7	375	-	517	0	0	-	120	-	-	-	-	-	-	-	-
03-BHA-0128	-	104	2	30	340	-	699	0	5	-	65	-	-	-	-	-	-	-	-
03-BHA-0131	-	49	1	15	124	-	808	4	0	-	22	-	-	-	-	-	-	-	-
03-BHA-0144A	-	146	2	49	310	-	823	0	3	-	148	-	-	-	-	-	-	-	-
03-BHA-0147	-	54	4	23	342	-	527	0	3	-	59	-	-	-	-	-	-	-	-
03-BHA-0149	-	58	4	16	313	-	871	3	4	-	87	-	-	-	-	-	-	-	-
03-BHA-0151	-	49	5	10	375	-	417	8	3	-	52	-	-	-	-	-	-	-	-
03-BHA-0153	-	107	2	13	319	-	565	0	3	-	33	-	-	-	-	-	-	-	-
03-BHA-0227A	-	54	2	27	199	-	1042	6	0	-	65	-	-	-	-	-	-	-	-
03-BHA-0229A	-	52	2	30	199	-	721	0	4	-	56	-	-	-	-	-	-	-	-
03-BHA-0291	-	50	3	83	340	-	545	0	4	-	94	-	-	-	-	-	-	-	-

SampleNo	UTMNorth (m)	UTMEast (m)	Al_2O_3 (%)	CaO (%)	Fe_2O_3 (%)	K_2O (%)	MgO (%)	MnO (%)	Na_2O (%)	P_2O_5 (%)	SiO_2 (%)	TiO_2 (%)	LOI (%)	CO_2 (%)
03-BHA-0293	5365591	454161	11.68	2.19	3.78	3.24	0.65	0.08	3.58	0.03	72.19	0.20	2.28	-
03-BHA-0296	5365873	454416	12.47	0.22	3.56	3.85	0.46	0.02	3.37	0.02	74.79	0.17	1.31	-
03-BHA-0317	5365869	455858	14.09	7.87	11.21	0.04	3.88	0.12	5.14	0.28	47.14	1.60	8.71	-
03-BHA-0320	5365928	455602	15.76	9.24	13.22	0.02	4.36	0.19	2.29	0.30	51.01	1.66	3.23	-
03-BHA-0322	5366111	455986	13.12	1.10	3.45	2.32	0.44	0.03	4.44	0.04	72.37	0.26	2.64	-
03-BHA-0325A	5366260	455645	12.96	0.62	3.43	1.52	0.20	0.02	5.76	0.04	73.64	0.25	1.37	-
03-BHA-0326	5366128	455789	12.88	1.64	3.85	2.34	0.56	0.04	4.82	0.04	71.45	0.25	2.11	-
03-BHA-0332	5355457	456491	16.22	6.02	9.35	0.49	3.00	0.12	6.20	0.52	51.09	2.02	4.96	-
03-BHA-0363	5366499	459594	6.93	0.62	0.50	0.99	0.16	0.02	3.02	0.01	86.78	0.08	0.92	-
03-BHA-0365	5366357	458486	9.59	1.85	2.20	1.62	0.92	0.04	3.36	0.00	78.27	0.10	2.35	-
03-BHA-0368	5366012	457831	11.71	0.45	1.96	2.66	1.09	0.03	3.27	0.00	77.15	0.11	1.63	-
04-PJM-256	5361439	461664	15.75	2.21	1.69	0.93	0.89	0.03	6.83	0.08	61.87	0.21	9.87	-
04-PJM-257	5360896	462040	14.74	2.78	1.64	0.81	0.81	0.02	6.62	0.05	62.26	0.15	10.15	-
04-PJM-258	5358802	459498	16.12	3.94	5.22	0.12	3.18	0.09	6.97	0.69	53.35	0.56	11.09	-
04-PJM-259	5358799	459498	13.03	6.53	4.41	0.13	2.86	0.11	5.34	0.54	56.37	0.45	10.42	-
04-PJM-261a	5358148	458726	14.01	1.34	0.59	4.85	0.06	0.01	5.13	0.03	63.02	0.08	11.08	-
04-PJM-262	5359540	459056	18.72	0.75	2.41	0.70	1.13	0.03	8.74	0.14	56.5	0.31	10.72	-
04-PJM-263	5359540	459056	17.07	1.40	1.46	0.49	0.69	0.02	8.97	0.12	59.27	0.29	10.57	-
04-PJM-265	5357242	458687	17.24	3.12	2.62	0.81	0.56	0.05	4.51	0.13	61.18	0.28	10.02	-
04-PJM-275	5362031	464875	15.83	3.40	3.34	1.33	1.12	0.04	4.45	0.10	59.41	0.26	10.85	-
04-PJM-277	5362008	464871	15.82	2.47	3.02	1.65	0.96	0.04	4.98	0.08	61.02	0.22	10.08	-
04-PJM-294	5361719	464826	15.82	4.39	2.01	1.69	1.40	0.10	4.18	0.10	59.09	0.26	11.00	-
05-GPB-7238	5357243	458850	15.88	0.91	1.09	5.66	0.30	0.03	5.50	0.06	70.13	0.13	-	-
05-GPB-7239	5357410	458749	16.45	1.24	1.42	7.31	0.44	0.04	4.65	0.12	67.06	0.19	-	-
05-GPB-7327A	5358598	458957	4.29	20.08	11.90	1.66	11.10	0.18	0.35	4.61	35.44	1.35	-	-
05-GPB-7327B	5358598	458957	3.10	21.26	12.13	0.19	11.28	0.21	0.51	1.99	40.71	1.46	-	-
05-GPB-7327C	5358598	458957	11.80	22.10	11.45	1.01	1.99	0.35	2.67	0.53	40.21	1.63	-	-
05-GPB-7327D	5358598	458957	12.31	18.44	9.91	1.57	3.03	0.36	3.50	0.94	43.1	1.45	-	-
05-GPB-7328A	5359331	459212	2.56	22.52	10.99	0.14	11.54	0.14	0.38	4.39	38.09	1.38	-	-
05-GPB-7328B	5359331	459212	4.29	22.32	5.04	1.65	11.97	0.16	0.38	5.24	38.46	1.07	-	-
05-GPB-7328C	5359331	459212	5.78	19.04	6.13	1.37	12.41	0.19	0.26	3.12	40.57	1.24	-	-
05-GPB-7329A	5358010	457970	14.87	10.81	5.29	6.82	1.14	0.22	3.00	0.30	49.36	0.75	-	-
05-GPB-7329B	5358010	457970	8.28	21.09	11.13	1.70	3.28	0.35	2.50	1.17	44.42	1.56	-	-
AA10285	5364100	449000	10.79	0.45	4.79	2.58	0.72	0.03	0.77	0.02	75.94	0.13	2.62	-
AA10286	5364110	449000	10.19	0.65	0.98	2.76	0.35	0.01	0.45	0.01	82.09	0.12	1.39	-
AA10287	5364120	449100	11.66	0.22	1.75	3.01	0.54	0.01	0.58	0.03	79.06	0.19	2.00	-
AA10289	5364050	449600	15.08	6.95	8.91	1.04	3.60	0.14	2.73	0.12	58.34	0.78	1.77	-
AA10290	5364050	449600	13.78	3.57	4.50	0.94	1.16	0.04	4.37	0.09	69.67	0.48	1.39	-
AA10387	5362600	448140	0.42	1.31	6.70	0.01	0.32	0.04	0.02	0.06	87.4	0.01	2.00	-
AA10388	5362600	448140	11.80	2.46	1.85	2.11	0.40	0.04	3.29	0.04	74.78	0.23	2.16	-
AA10389	5362380	448460	11.43	1.68	3.25	2.54	0.29	0.06	0.81	0.02	77.2	0.19	1.77	-
AA10390	5362380	448460	13.27	1.10	1.59	2.49	0.46	0.02	3.16	0.02	75.42	0.12	1.70	-
AA10391	5363150	449020	12.66	1.43	3.42	3.32	1.39	0.03	1.50	0.03	71.79	0.43	2.70	-
AA10392	5362650	449460	12.92	3.21	5.86	1.28	0.78	0.23	4.40	0.09	67.02	0.42	2.93	-
AA10407	5362080	458030	10.44	7.78	10.81	1.31	3.30	0.17	0.96	0.21	51.94	1.23	11.54	-

SampleNo	Cr (ppm)	Y (ppm)	Sc (ppm)	Sr (ppm)	Zr (ppm)	Au (ppb)	Ba (ppm)	Cu (ppm)	Ni (ppm)	Pb (ppm)	Zn (ppm)	Fe/Fe+Mg	CO_2/CaO	Ishikawa Index	Chlorite Index	SCI	CSI	K/Al	CCPI
03-BHA-0293	-	52	3	61	328	-	521	3	5	-	189	-	-	-	-	-	-	-	-
03-BHA-0296	-	66	3	27	312	-	636	0	4	-	41	-	-	-	-	-	-	-	-
03-BHA-0317	-	18	17	255	111	-	43	0	100	-	62	-	-	-	-	-	-	-	-
03-BHA-0320	-	18	19	509	118	-	15	0	106	-	45	-	-	-	-	-	-	-	-
03-BHA-0322	-	56	4	51	382	-	726	0	6	-	28	-	-	-	-	-	-	-	-
03-BHA-0325A	-	56	4	53	383	-	485	51	5	-	15	-	-	-	-	-	-	-	-
03-BHA-0326	-	58	4	64	387	-	604	0	6	-	39	-	-	-	-	-	-	-	-
03-BHA-0332	-	18	18	279	169	-	298	0	126	-	80	-	-	-	-	-	-	-	-
03-BHA-0363	-	41	1	24	128	-	146	0	0	-	18	-	-	-	-	-	-	-	-
03-BHA-0365	-	56	2	33	149	-	274	17	4	-	125	-	-	-	-	-	-	-	-
03-BHA-0368	-	63	2	16	183	-	304	3	5	-	79	-	-	-	-	-	-	-	-
04-PJM-256	-	2	2	398	70	-	1165	66	11	-	4	-	-	-	-	-	-	-	-
04-PJM-257	-	2	2	284	51	-	205	9	8	-	0	-	-	-	-	-	-	-	-
04-PJM-258	-	33	10	1079	533	-	267	11	82	-	64	-	-	-	-	-	-	-	-
04-PJM-259	-	27	9	1200	381	-	361	15	73	-	45	-	-	-	-	-	-	-	-
04-PJM-261a	-	5	1	622	126	-	1400	4	0	-	0	-	-	-	-	-	-	-	-
04-PJM-262	-	3	3	442	87	-	168	3	22	-	0	-	-	-	-	-	-	-	-
04-PJM-263	-	8	3	169	65	-	107	0	19	-	0	-	-	-	-	-	-	-	-
04-PJM-265	-	17	5	504	249	-	1400	0	21	-	0	-	-	-	-	-	-	-	-
04-PJM-275	-	3	3	548	80	-	242	109	15	-	0	-	-	-	-	-	-	-	-
04-PJM-277	-	3	2	336	73	-	444	16	9	-	0	-	-	-	-	-	-	-	-
04-PJM-294	-	3	3	323	75	-	319	7	14	-	2	-	-	-	-	-	-	-	-
05-GPB-7238	17	6	2	656	115	-	-	-	-	-	-	-	-	-	-	-	-	-	-
05-GPB-7239	22	10	3	752	176	-	-	-	-	-	-	-	-	-	-	-	-	-	-
05-GPB-7327A	-	55	33	1241	163	-	-	-	-	-	-	-	-	-	-	-	-	-	-
05-GPB-7327B	324	31	37	940	180	-	-	-	-	-	-	-	-	-	-	-	-	-	-
05-GPB-7327C	-	128	3	5381	1165	-	-	-	-	-	-	-	-	-	-	-	-	-	-
05-GPB-7327D	-	124	5	3308	1046	-	-	-	-	-	-	-	-	-	-	-	-	-	-
05-GPB-7328A	195	47	42	1286	136	-	-	-	-	-	-	-	-	-	-	-	-	-	-
05-GPB-7328B	-	62	42	1627	267	-	-	-	-	-	-	-	-	-	-	-	-	-	-
05-GPB-7328C	213	50	52	1525	362	-	-	-	-	-	-	-	-	-	-	-	-	-	-
05-GPB-7329A	-	76	4	3972	570	-	-	-	-	-	-	-	-	-	-	-	-	-	-
05-GPB-7329B	8	196	12	2297	1619	-	-	-	-	-	-	-	-	-	-	-	-	-	-
AA10285	68	110	4	20	300	-	-	61	35	12	1600	0.89	-	73	57	56	44	0.38	60
AA10286	68	130	3	20	350	-	-	22	6	8	19	0.76	-	74	24	75	25	0.42	28
AA10287	68	110	4	60	310	-	-	26	23	12	220	0.79	-	82	36	70	30	0.40	37
AA10289	137	30	18	210	110	-	-	21	74	14	89	0.74	-	32	52	38	62	0.11	75
AA10290	68	60	8	170	330	-	-	18	23	12	33	0.82	-	21	37	36	64	0.11	50
AA10387	205	-	0	-	-	-	-	32	14	8	34	0.96	-	20	83	19	81	0.04	100
AA10388	68	60	7	50	190	-	-	10	7	12	34	0.84	-	30	21	59	41	0.28	28
AA10389	68	170	2	70	400	-	-	23	8	12	130	0.93	-	53	39	58	42	0.35	49
AA10390	68	80	1	60	360	-	-	63	6	12	53	0.80	-	41	22	65	35	0.29	25
AA10391	68	140	12	30	260	-	-	26	34	16	71	0.74	-	62	42	60	40	0.41	48
AA10392	-	70	10	150	290	-	-	17	11	14	97	0.90	-	21	41	34	66	0.16	52
AA10407	-	30	-	50	110	-	-	44	31	16	140	0.79	-	35	56	38	62	0.20	85

SampleNo	UTMNorth (m)	UTMEast (m)	Al_2O_3 (%)	CaO (%)	Fe_2O_3 (%)	K_2O (%)	MgO (%)	MnO (%)	Na_2O (%)	P_2O_5 (%)	SiO_2 (%)	TiO_2 (%)	LOI (%)	CO_2 (%)
AA10408	5362020	457910	11.08	4.70	5.12	1.96	0.80	0.11	2.00	0.14	69.78	0.62	4.08	-
AA13612	5361440	469220	16.18	0.52	3.48	1.75	2.52	0.03	5.40	0.12	66.41	0.38	2.70	-
AA13613	5361540	469220	15.87	3.20	3.72	0.92	1.91	0.05	6.07	0.09	65.15	0.36	3.08	-
AA13614	5361540	469220	15.50	3.15	3.38	1.10	1.69	0.04	5.70	0.09	64.76	0.35	3.39	-
AA13615	5361540	469220	14.81	4.11	2.95	1.35	2.11	0.08	4.91	0.09	63.59	0.33	6.47	-
AA13616	5361640	469220	11.10	8.47	11.59	1.15	6.66	0.25	0.94	0.06	46.28	0.53	12.47	-
AA13617	5361740	469220	15.04	10.45	11.66	0.27	7.52	0.18	1.91	0.06	47.95	0.77	3.16	-
AA13618	5361640	469120	16.48	3.37	8.43	0.12	4.93	0.09	4.46	0.19	56.04	0.88	3.62	-
AA13619	5361640	467020	11.65	12.06	10.53	0.97	6.29	0.26	1.24	0.05	42	0.53	14.62	-
AA13620	5361640	469020	16.10	6.76	8.79	0.17	7.58	0.18	1.77	0.05	45.7	0.41	13.23	-
AA13621	5361540	469020	14.38	7.77	8.21	1.47	3.35	0.11	2.99	0.22	53.24	0.61	8.39	-
AA13622	5361540	469020	15.77	6.45	6.60	2.43	2.44	0.10	2.92	0.21	54.93	0.67	7.47	-
AA13623	5361540	469020	16.72	3.45	6.67	2.78	2.42	0.07	2.69	0.23	60.02	0.72	4.93	-
AA13624	5361640	469320	16.42	3.96	4.07	2.70	2.42	0.04	2.68	0.17	62.04	0.47	5.70	-
AA13625	5361640	469020	12.14	8.20	11.22	0.88	7.14	0.24	1.61	0.08	45	0.61	12.85	-
AA13626	5361740	469420	15.97	0.49	7.31	1.97	4.84	0.10	2.72	0.24	61.04	0.90	3.62	-
AA13627	5361740	469420	16.20	3.07	8.31	2.10	5.41	0.09	2.25	0.23	55.96	0.91	6.00	-
AA13628	5361840	469420	17.35	1.17	2.67	1.18	1.04	0.03	7.22	0.11	67.02	0.32	1.85	-
AA13629	5361540	469420	15.63	3.14	3.74	0.85	2.37	0.05	5.64	0.09	65.42	0.42	3.16	-
AA13630	5361640	469520	17.70	4.60	4.76	0.41	3.13	0.11	6.24	0.03	55.4	0.39	8.08	-
AA13631	5361640	469620	16.67	10.17	12.20	0.06	9.20	0.16	1.58	0.06	44.56	0.81	3.54	-
AA13632	5361640	469620	17.37	10.14	13.76	0.05	9.87	0.17	1.27	0.06	41.73	0.81	3.93	-
AA13633	5361640	469620	16.51	11.37	11.85	0.04	8.53	0.16	1.39	0.06	45.29	0.80	3.08	-
AA13634	5361740	469620	13.97	8.94	8.58	1.36	3.63	0.12	2.49	0.21	51.24	0.59	9.23	-
AA13635	5361740	469620	16.05	4.51	4.53	1.78	3.05	0.05	4.09	0.12	61.41	0.49	4.16	-
AA13636	5361640	469420	13.35	8.89	7.94	1.60	6.09	0.20	0.58	0.07	48.32	0.74	13.00	-
AA13637	5361840	469620	13.40	10.13	10.22	0.04	7.07	0.23	2.28	0.06	52.22	0.66	3.31	-
AA13638	5361840	469620	14.33	9.19	12.77	0.24	6.01	0.20	2.06	0.09	48.61	1.25	5.39	-
AA15361	5362340	468520	10.54	8.12	12.19	0.86	6.97	0.26	1.71	0.09	45	1.08	13.93	-
AA15362	5362340	468820	17.26	1.93	4.28	2.32	0.80	0.03	2.67	0.11	65.6	0.64	4.00	-
AA15363	5362040	469120	14.69	4.86	4.14	2.31	2.14	0.06	3.35	0.17	65.13	0.34	1.70	-
AA15364	5362000	469420	5.84	10.76	9.85	0.14	22.11	0.17	0.16	0.03	40.29	0.31	10.16	-
AA15365	5362340	469520	4.89	8.49	9.34	0.03	20.00	0.16	0.12	0.03	38.13	0.24	19.08	-
AA15366	5362440	469820	16.88	1.40	3.47	1.28	2.01	0.04	5.66	0.09	65.32	0.39	2.08	-
AA15367	5362640	469820	13.61	9.85	12.17	0.14	7.32	0.17	1.86	0.06	49.81	0.73	3.47	-
AA15368	5362240	469920	14.45	9.47	14.79	0.84	5.05	0.20	2.24	0.14	48.48	1.30	2.00	-
AA15369	5362040	469820	5.52	11.65	9.71	0.08	20.97	0.19	0.18	0.03	40.95	0.26	9.77	-
AA15370	5361840	470220	17.48	1.71	6.28	0.08	2.65	0.06	8.07	0.10	58.96	0.79	3.08	-
AA15371	5361820	470020	5.19	6.89	10.35	0.05	24.16	0.17	0.19	0.03	46.17	0.39	5.85	-
AA15372	5361440	469820	8.55	10.14	11.93	0.34	15.04	0.18	0.93	0.08	42.25	0.69	9.70	-
AA15373	5361440	469620	6.44	11.25	11.08	0.04	18.92	0.15	0.22	0.03	39.13	0.31	12.54	-
AA15374	5361440	469420	15.74	2.89	7.02	0.09	5.13	0.08	5.07	0.19	58.24	0.92	3.70	-
AA15375	5361440	469220	14.06	5.55	8.49	0.30	5.19	0.11	3.81	0.15	55.88	1.02	5.62	-
AA15376	5361440	469220	16.34	0.73	3.33	2.45	2.07	0.04	4.58	0.13	65.81	0.40	2.62	-
AA15377	5361440	468820	15.52	4.17	3.33	1.56	2.17	0.03	4.31	0.09	64.69	0.34	3.77	-

SampleNo	Cr (ppm)	Y (ppm)	Sc (ppm)	Sr (ppm)	Zr (ppm)	Au (ppb)	Ba (ppm)	Cu (ppm)	Ni (ppm)	Pb (ppm)	Zn (ppm)	Fe/Fe+Mg	CO_2/CaO	Ishikawa Index	Chlorite Index	SCI	CSI	K/Al	CCPI
AA10408	-	70	-	50	400	-	-	12	7	14	100	0.88	-	29	38	43	57	0.28	58
AA13612	68	0	-	150	110	-	-	9	44	0	62	0.62	-	42	42	50	50	0.17	44
AA13613	-	0	-	440	100	-	-	10	31	0	60	0.69	-	23	34	41	59	0.09	43
AA13614	-	0	-	410	90	-	-	9	30	0	53	0.70	-	24	32	43	57	0.11	41
AA13615	-	0	-	390	90	-	-	8	26	0	43	0.62	-	28	31	47	53	0.14	43
AA13616	1232	0	-	110	40	-	-	74	800	0	87	0.67	-	45	62	42	58	0.16	89
AA13617	137	0	-	130	-	-	-	130	140	0	67	0.64	-	39	59	40	60	0.03	89
AA13618	342	0	-	480	120	-	-	41	150	0	92	0.66	-	39	61	39	61	0.01	73
AA13619	889	0	-	170	20	-	-	88	650	0	90	0.66	-	35	52	40	60	0.13	88
AA13620	137	0	-	120	20	-	-	150	100	0	98	0.57	-	48	64	43	57	0.02	89
AA13621	137	0	-	330	90	-	-	950	140	0	88	0.74	-	31	47	40	60	0.16	71
AA13622	137	0	-	330	110	-	-	170	110	0	82	0.76	-	34	42	45	55	0.24	61
AA13623	205	0	-	260	120	-	-	76	110	0	74	0.76	-	46	49	49	51	0.26	61
AA13624	-	0	-	280	120	-	-	5	51	0	60	0.66	-	44	39	52	48	0.26	53
AA13625	1095	0	-	150	40	-	-	88	630	0	88	0.65	-	45	62	42	58	0.11	87
AA13626	205	0	-	80	110	-	-	21	85	0	92	0.64	-	68	69	50	50	0.19	71
AA13627	137	0	-	180	130	-	-	58	99	0	100	0.64	-	59	63	48	52	0.20	75
AA13628	68	0	-	530	90	-	-	27	54	0	57	0.75	-	21	26	44	56	0.11	29
AA13629	68	0	-	400	100	-	-	12	46	0	56	0.65	-	27	37	42	58	0.09	47
AA13630	616	0	-	70	10	-	-	43	270	0	79	0.64	-	25	40	38	62	0.04	53
AA13631	-	0	-	110	20	-	-	130	170	0	57	0.61	-	44	63	41	59	0.01	92
AA13632	-	0	-	170	20	-	-	160	220	0	71	0.62	-	47	66	41	59	0.00	94
AA13633	-	0	-	180	20	-	-	140	170	0	51	0.62	-	40	60	40	60	0.00	93
AA13634	137	0	-	240	70	-	-	1300	140	0	87	0.73	-	30	47	39	61	0.15	75
AA13635	68	0	-	520	110	-	-	43	61	0	58	0.63	-	36	41	47	53	0.17	55
AA13636	68	0	-	70	30	-	-	120	49	0	65	0.60	-	45	54	45	55	0.19	86
AA13637	137	0	-	70	30	-	-	97	66	0	53	0.63	-	36	57	39	61	0.00	88
AA13638	68	0	-	110	50	-	-	120	91	0	82	0.71	-	36	60	37	63	0.03	88
AA15361	479	0	-	50	20	-	-	210	260	0	90	0.67	-	44	63	41	59	0.13	87
AA15362	68	0	-	140	80	-	-	32	38	0	51	0.86	-	40	40	50	50	0.21	48
AA15363	68	0	-	100	50	-	-	32	32	0	46	0.69	-	35	36	50	50	0.25	51
AA15364	1984	0	-	0	10	-	-	0	0	0	0	0.34	-	67	74	48	52	0.04	99
AA15365	1437	0	-	10	-	-	-	39	260	0	19	0.35	-	70	77	48	52	0.01	99
AA15366	68	0	-	100	30	-	-	17	27	0	62	0.67	-	32	38	45	55	0.12	43
AA15367	68	0	-	30	-	-	-	120	44	0	46	0.66	-	39	61	39	61	0.02	90
AA15368	68	0	-	90	30	-	-	140	30	0	77	0.77	-	33	59	36	64	0.09	86
AA15369	1642	0	-	10	-	-	-	49	880	0	33	0.35	-	64	71	47	53	0.02	99
AA15370	137	0	-	150	-	-	-	53	100	0	66	0.73	-	22	46	32	68	0.01	50
AA15371	2463	0	-	10	10	-	-	31	930	0	39	0.33	-	77	82	48	52	0.02	99
AA15372	1368	0	-	40	10	-	-	57	280	0	31	0.48	-	58	69	46	54	0.06	95
AA15373	2121	0	-	0	10	-	-	44	310	0	27	0.40	-	62	72	47	53	0.01	99
AA15374	137	0	-	130	0	-	-	11	70	0	59	0.61	-	40	59	40	60	0.01	69
AA15375	137	0	-	80	20	-	-	30	85	0	64	0.65	-	37	57	39	61	0.03	76
AA15376	68	0	-	110	80	-	-	18	41	0	41	0.65	-	46	39	54	46	0.24	42
AA15377	68	0	-	100	40	-	-	27	25	0	32	0.64	-	31	34	47	53	0.16	47

SampleNo	UTMNorth (m)	UTMEast (m)	Al_2O_3 (%)	CaO (%)	Fe_2O_3 (%)	K_2O (%)	MgO (%)	MnO (%)	Na_2O (%)	P_2O_5 (%)	SiO_2 (%)	TiO_2 (%)	LOI (%)	CO_2 (%)
AA21212	5362050	458800	12.90	8.24	14.20	0.55	4.66	0.23	2.18	0.14	51.1	1.47	3.77	-
AA21213	5361900	459650	16.20	10.70	11.00	0.28	4.71	0.23	2.39	0.07	50	0.92	3.39	-
AA21214	5363000	459050	17.10	5.92	13.50	2.31	5.91	0.21	1.96	0.11	47.5	1.32	3.70	-
AA21223	5359960	457710	15.70	12.80	12.20	0.29	4.82	0.21	1.67	0.07	46.8	0.83	3.93	-
AA21224	5357690	457460	13.30	9.44	13.80	0.40	5.93	0.25	1.84	0.11	50	1.31	2.23	-
AA21225	5357550	456910	15.10	10.30	13.20	0.59	8.03	0.19	1.81	0.09	45.9	1.04	2.85	-
AA21226	5359660	457000	13.30	0.65	1.92	1.43	0.67	0.02	6.29	0.02	74.1	0.09	0.77	-
AA21227	5358840	456540	15.80	10.50	10.70	1.06	7.73	0.16	2.09	0.07	48.4	0.78	2.39	-
AA21228	5359290	458600	16.40	10.60	11.00	0.09	6.11	0.15	2.70	0.07	43.5	0.87	8.62	-
AA21229	5359370	457295	14.90	11.50	12.00	0.19	6.70	0.17	2.13	0.09	49.3	1.00	2.23	-
AA21230	5358370	456770	13.60	3.94	1.76	3.60	0.67	0.01	1.92	0.02	73.3	0.10	1.31	-
AA21231	5358750	456500	10.10	5.07	3.73	0.24	2.49	0.04	3.15	0.03	73.7	0.18	0.77	-
AA21232	5361790	458410	11.70	10.50	10.10	0.06	12.00	0.15	1.98	0.06	50.1	0.59	2.54	-
AA21242	5366220	458250	11.30	0.26	1.89	3.55	0.77	0.01	2.71	0.02	78.3	0.10	1.08	-
AA21248	5357040	458600	15.60	1.02	1.65	6.15	0.62	0.03	5.52	0.09	67.5	0.15	1.00	-
AA21249	5357380	458070	15.80	11.50	15.30	0.15	6.44	0.21	1.51	0.11	44.4	1.27	2.85	-
AA21250	5364560	457410	12.80	0.74	3.35	0.97	1.04	0.05	5.35	0.04	73.6	0.19	1.54	-
AA21258	5365660	458390	12.30	1.27	2.66	4.18	1.83	0.04	1.09	0.03	73.3	0.17	3.00	-
AA21259	5366240	458960	11.00	0.92	1.07	9.28	0.59	0.02	0.14	0.02	74.8	0.09	1.62	-
AA21272	5363250	457480	12.80	7.61	11.90	0.15	11.30	0.19	1.72	0.09	46.5	0.92	5.93	-
AA21273	5363250	457480	16.30	7.70	12.00	0.14	9.24	0.17	3.14	0.07	46.4	0.77	3.93	-
AA21292	5363490	458000	13.60	0.55	2.00	3.01	0.68	0.01	4.06	0.06	74.3	0.31	1.70	-
AA21327	5360830	459850	15.30	9.85	10.50	0.11	8.42	0.14	2.64	0.07	47.9	0.85	2.54	-
AA21331	5366230	459740	8.91	0.15	0.49	6.09	0.32	0.00	0.58	0.03	81.7	0.08	0.47	-
AA21332	5361810	459950	14.10	8.42	6.51	0.49	5.31	0.10	5.33	0.26	57.4	0.63	1.77	-
AA21347	5365860	458490	11.60	0.03	1.17	4.21	1.04	0.01	0.27	0.02	79.2	0.10	1.93	-
AA21348	5365670	458400	13.90	0.48	5.85	1.11	2.79	0.02	5.22	0.13	67.6	0.62	2.16	-
AA21350	5365650	459860	12.80	1.79	4.26	3.18	1.85	0.06	2.78	0.08	69.7	0.38	2.93	-
AA21353	5365810	457720	11.90	0.86	1.44	1.85	0.91	0.03	4.83	0.02	76.6	0.10	1.93	-
AA21357	5365490	459610	10.60	0.97	1.49	7.18	0.96	0.02	0.17	0.02	76.1	0.10	1.74	-
AA21655	5361740	469520	15.20	3.27	5.59	1.56	5.03	0.07	4.22	0.17	61.5	0.61	2.62	-
AA21656	5361790	469520	11.10	4.78	11.80	0.13	10.80	0.18	0.66	0.06	50.9	0.70	8.70	-
AA21657	5361840	469520	16.10	3.77	2.33	1.73	0.69	0.02	5.41	0.10	66.2	0.33	3.12	-
AA21658	5361890	469520	4.01	5.51	8.49	0.05	27.30	0.12	-0.01	0.02	38.6	0.23	14.00	-
AA21659	5361940	469520	5.33	5.81	10.60	0.07	25.70	0.17	0.03	0.03	42.3	0.36	7.62	-
AA21660	5362040	469520	15.10	5.31	11.10	0.34	6.02	0.19	3.27	0.06	52.7	0.88	3.46	-
AA21661	5362040	469620	14.50	6.22	9.08	0.08	7.10	0.17	4.03	0.06	49.6	0.84	7.85	-
AA21662	5362140	469620	16.90	1.59	4.18	1.92	2.11	0.04	3.16	0.11	65.6	0.51	2.77	-
AA21663	5361940	469620	11.70	10.50	12.70	0.12	11.20	0.23	2.24	0.04	43.7	0.62	5.85	-
AA21664	5361890	469620	13.40	8.91	15.50	0.94	4.81	0.22	2.23	0.17	49.6	1.58	1.16	-
AA21665	5361790	469620	15.70	5.97	4.75	2.22	3.22	0.07	2.07	0.12	58.9	0.49	6.66	-
AA21666	5361740	469720	14.10	7.65	7.89	1.54	4.45	0.11	2.59	0.23	52.6	0.82	8.23	-
AA21667	5361790	469720	16.00	4.19	3.87	2.49	2.07	0.04	2.60	0.19	62.6	0.49	5.31	-
AA21668	5361840	469720	10.70	9.36	10.30	0.14	9.22	0.21	1.48	0.05	46.6	0.55	9.54	-
AA21669	5361890	469720	14.50	2.68	2.82	0.92	1.24	0.04	6.14	0.10	69.2	0.34	2.08	-

SampleNo	Cr (ppm)	Y (ppm)	Sc (ppm)	Sr (ppm)	Zr (ppm)	Au (ppb)	Ba (ppm)	Cu (ppm)	Ni (ppm)	Pb (ppm)	Zn (ppm)	Fe/Fe+Mg	CO_2/CaO	Ishikawa Index	Chlorite Index	SCI	CSI	K/Al	CCPI
AA21212	-	20	-	120	80	-	-	-	-	-	0	0.78	-	33	61	35	65	0.07	86
AA21213	205	10	-	110	50	-	-	-	-	-	150	0.73	-	28	52	35	65	0.03	85
AA21214	68	20	-	90	70	-	-	-	-	-	270	0.73	-	51	64	44	56	0.21	81
AA21223	137	10	-	170	40	-	-	-	-	-	170	0.75	-	26	52	34	66	0.03	89
AA21224	137	30	-	160	80	-	-	-	-	-	0	0.73	-	36	61	37	63	0.05	89
AA21225	68	20	-	160	60	-	-	-	-	-	0	0.66	-	42	61	41	59	0.06	89
AA21226	68	70	-	50	130	-	-	-	-	-	40	0.77	-	23	22	51	49	0.17	24
AA21227	137	-	-	240	40	-	-	-	-	-	170	0.62	-	41	56	42	58	0.11	85
AA21228	205	30	-	240	30	-	-	-	-	-	0	0.68	-	32	54	37	63	0.01	85
AA21229	68	10	-	120	40	-	-	-	-	-	0	0.68	-	34	56	38	62	0.02	88
AA21230	68	50	-	290	120	-	-	-	-	-	40	0.75	-	42	19	69	31	0.42	29
AA21231	137	90	-	110	290	-	-	-	-	-	60	0.63	-	25	41	38	62	0.04	63
AA21232	889	-	-	60	40	-	-	-	-	-	170	0.49	-	49	63	44	56	0.01	91
AA21242	-	100	-	20	160	-	-	-	-	-	100	0.74	-	59	27	68	32	0.49	28
AA21248	-	-	-	690	110	-	-	-	-	-	0	0.76	-	51	14	78	22	0.62	15
AA21249	68	-	-	350	70	-	-	-	-	-	80	0.73	-	34	61	36	64	0.01	92
AA21250	68	60	-	20	380	-	-	-	-	-	80	0.79	-	25	36	40	60	0.12	39
AA21258	-	100	-	0	220	-	-	-	-	-	0	0.63	-	72	39	65	35	0.53	44
AA21259	274	60	-	10	160	-	-	-	-	-	0	0.68	-	90	13	87	13	1.32	14
AA21272	342	10	-	140	30	-	-	-	-	-	200	0.55	-	55	70	44	56	0.02	92
AA21273	205	10	-	280	10	-	-	-	-	-	0	0.60	-	46	65	42	58	0.01	86
AA21292	68	30	-	60	170	-	-	-	-	-	0	0.77	-	44	25	64	36	0.35	26
AA21327	274	30	-	80	30	-	-	-	-	-	90	0.59	-	41	59	41	59	0.01	87
AA21331	68	60	-	30	150	-	-	-	-	-	0	0.64	-	90	10	90	10	1.07	10
AA21332	137	10	-	300	60	-	-	-	-	-	0	0.59	-	30	44	40	60	0.05	66
AA21347	-	90	-	0	180	-	-	-	-	-	50	0.57	-	95	32	75	25	0.57	32
AA21348	-	30	-	50	260	-	-	-	-	-	90	0.71	-	41	54	43	57	0.13	56
AA21350	-	40	-	10	260	-	-	-	-	-	60	0.73	-	52	42	55	45	0.39	49
AA21353	-	130	-	20	210	-	-	-	-	-	0	0.65	-	33	23	59	41	0.24	25
AA21357	-	70	-	0	160	-	-	-	-	-	70	0.64	-	88	22	80	20	1.06	24
AA21655	205	10	-	360	120	-	-	59	180	-	82	0.56	-	47	53	47	53	0.16	64
AA21656	821	10	-	80	20	-	-	89	600	-	120	0.56	-	67	79	46	54	0.02	96
AA21657	-	-	-	560	100	-	-	21	41	-	66	0.80	-	21	20	51	49	0.17	28
AA21658	1574	-	-	60	-	-	-	13	1300	-	66	0.27	-	83	86	49	51	0.02	100
AA21659	2531	10	-	0	-	-	-	18	1300	-	76	0.32	-	82	86	49	51	0.02	100
AA21660	68	40	-	140	30	-	-	180	91	-	120	0.68	-	43	64	40	60	0.04	82
AA21661	68	30	-	30	20	-	-	170	120	-	110	0.60	-	41	60	41	59	0.01	79
AA21662	68	30	-	260	130	-	-	59	120	-	110	0.70	-	46	47	50	50	0.18	54
AA21663	889	20	-	60	-	-	-	49	340	-	130	0.57	-	47	64	42	58	0.02	91
AA21664	68	30	-	150	140	-	-	190	74	-	180	0.79	-	34	61	36	64	0.11	86
AA21665	68	10	-	390	90	-	-	40	150	-	110	0.63	-	40	42	49	51	0.22	64
AA21666	68	30	-	150	110	-	-	51	140	-	110	0.67	-	37	50	43	57	0.17	74
AA21667	-	20	-	380	110	-	-	450	60	-	110	0.68	-	40	37	52	48	0.24	52
AA21668	958	20	-	210	10	-	-	120	660	-	110	0.56	-	46	63	42	58	0.02	92
AA21669	68	0	-	270	120	-	-	18	26	-	42	0.73	-	20	28	41	59	0.10	35

SampleNo	UTMNorth (m)	UTMEast (m)	Al_2O_3 (%)	CaO (%)	Fe_2O_3 (%)	K_2O (%)	MgO (%)	MnO (%)	Na_2O (%)	P_2O_5 (%)	SiO_2 (%)	TiO_2 (%)	LOI (%)	CO_2 (%)
AA21670	5361940	469720	3.29	3.73	8.48	0.06	29.60	0.16	-0.01	0.02	41.6	0.19	11.39	-
AA21671	5362040	469720	14.40	10.30	9.67	0.07	5.11	0.21	1.99	0.06	52.9	0.76	4.16	-
AA21672	5361640	469070	16.80	4.25	5.44	1.32	5.02	0.07	4.01	0.13	56.8	0.57	4.77	-
AA21673	5361690	469020	11.10	8.97	10.50	0.07	7.36	0.23	1.35	0.06	49.2	0.55	10.31	-
AA21675	5361690	469120	12.00	8.84	9.64	0.35	6.60	0.22	2.04	0.08	49.4	0.57	10.00	-
AB01307	5362240	449380	15.40	3.27	6.79	0.75	3.29	0.13	5.82	0.12	61.8	0.58	2.00	-
AB01308	5362740	449310	11.90	0.63	6.28	1.73	0.63	0.04	4.19	0.05	71.2	0.27	3.00	-
AB01801	5359290	456570	12.80	6.60	8.08	0.62	5.23	0.14	2.13	0.08	47.6	0.61	15.62	-
AB01802	5359810	457610	14.70	11.90	12.20	0.09	5.28	0.21	1.91	0.08	48.7	1.03	3.39	-
AB01803	5359730	457530	16.40	9.92	13.70	0.10	5.67	0.23	1.47	0.07	47.8	1.08	3.31	-
AB01804	5359760	457410	13.10	9.35	14.00	0.30	3.94	0.24	2.09	0.16	50.6	1.78	3.85	-
AB01805	5359730	457410	12.60	10.10	13.50	0.31	5.10	0.23	2.82	0.12	49	1.38	3.39	-
AB01806	5359700	457310	16.80	12.30	12.70	0.08	6.34	0.21	1.65	0.08	45.3	0.99	2.85	-
AB01807	5359730	457380	13.10	7.32	15.10	0.40	3.96	0.26	2.24	0.16	49.9	1.88	4.08	-
AB01808	5359960	457470	12.50	7.73	16.00	0.57	5.21	0.28	2.38	0.14	49.4	1.71	2.77	-
AB01809	5359760	457430	13.20	8.90	15.30	0.25	5.15	0.27	2.04	0.12	48.9	1.49	2.93	-
AB01810	5359910	457380	12.80	8.26	16.80	0.43	4.51	0.24	1.81	0.15	49.7	1.75	2.77	-
AB01811	5360710	457330	14.10	11.20	15.20	0.10	5.36	0.20	1.49	0.15	45.7	1.79	3.23	-
AB01814	5359690	456550	8.60	8.01	10.90	0.01	18.80	0.18	0.69	0.06	46.1	0.50	4.85	-
AB01815	5359845	456270	10.60	6.20	10.80	0.03	14.90	0.17	2.46	0.05	47.9	0.57	4.31	-
AB01816	5359800	456250	8.32	13.00	0.56	10.40	2.54	0.15	0.02	0.17	10.9	0.05	10.00	-
AB01817	5359510	456470	12.00	9.10	9.87	0.51	9.60	0.21	3.52	0.23	47.7	0.57	5.62	-
AB04016	5366323	446780	14.50	13.90	7.11	0.09	11.20	0.15	1.27	0.02	48.5	0.20	2.70	-
AB04019	5362615	449463	16.10	1.97	3.22	1.10	1.84	0.04	5.78	0.15	67.4	0.36	2.23	-
AB04020	5364000	450612	12.20	2.56	4.81	2.20	1.14	0.05	2.39	0.12	70.5	0.64	2.77	-
AB04021	5363508	449571	10.50	7.90	14.20	2.15	3.40	0.24	0.23	0.14	48.5	1.47	11.39	-
AB04025	5365748	446336	18.20	9.18	8.13	0.10	7.41	0.17	2.58	0.02	50.3	0.15	3.39	-
AB04026	5365735	446336	17.00	9.88	8.63	0.09	7.82	0.18	1.70	0.02	50.4	0.15	3.77	-
AB04027	5365628	446304	1.86	2.18	15.60	-0.01	28.40	0.10	0.02	0.02	38	0.09	10.93	-
AB04028	5365577	446304	20.90	10.50	6.17	0.01	13.40	0.10	0.75	0.02	41	0.02	5.77	-
AB04029	5365114	446716	24.80	4.24	5.59	1.64	11.30	0.07	1.95	0.02	42.9	0.08	6.54	-
AB04076	5356269	451837	14.60	3.08	4.55	1.61	1.45	0.07	4.51	0.15	66.8	0.59	1.31	-
AB04077	5363862	448716	13.70	0.12	4.53	4.09	0.88	0.03	0.40	0.03	71.1	0.20	3.00	-
AB04078	5363805	448672	5.99	15.40	11.60	0.40	11.60	0.31	0.05	0.02	29.2	0.29	23.43	-
AB04079	5362983	447821	18.50	12.50	10.10	0.10	6.73	0.12	1.77	0.02	45.8	0.41	3.46	-
AB04080	5362193	446390	12.80	6.23	12.80	0.54	2.43	0.60	3.26	0.09	59.6	0.56	0.39	-
AB04081	5362444	446390	2.86	0.32	38.00	0.62	0.92	0.06	0.08	0.03	40.1	0.11	16.77	-
AB04082	5362533	447260	12.60	5.27	14.70	0.20	4.63	0.74	2.85	0.09	51.5	0.56	5.39	-
AB04083	5362520	447266	8.93	3.12	34.90	0.47	5.01	1.15	0.37	0.08	40.5	0.42	5.31	-
AB04084	5362495	447266	13.50	7.22	14.60	0.25	4.87	0.36	1.50	0.13	51.2	1.24	3.77	-
AB04085	5363000	447422	0.57	2.69	24.10	0.03	1.88	0.20	0.08	0.05	70.1	0.04	0.31	-
AB04106	5364888	446561	21.50	11.80	6.29	0.03	12.70	0.10	0.69	0.02	39.9	0.05	5.77	-
AB04107	5364869	446564	14.60	8.24	9.07	0.01	20.20	0.13	0.18	0.02	37.6	0.04	8.62	-
AB04111	5362368	446479	14.00	7.15	19.00	0.13	3.96	0.63	1.30	0.10	48.5	0.63	4.62	-
AB04112	5363000	447146	15.50	8.11	7.78	0.79	3.26	0.24	3.29	0.19	58	1.07	1.70	-

SampleNo	Cr (ppm)	Y (ppm)	Sc (ppm)	Sr (ppm)	Zr (ppm)	Au (ppb)	Ba (ppm)	Cu (ppm)	Ni (ppm)	Pb (ppm)	Zn (ppm)	Fe/Fe+Mg	CO_2/CaO	Ishikawa Index	Chlorite Index	SCI	CSI	K/Al	CCPI
AA21670	1642	0	-	40	-	-	-	7	2000	-	78	0.25	-	89	91	49	51	0.03	100
AA21671	137	20	-	90	20	-	-	150	130	-	110	0.69	-	30	53	36	64	0.01	87
AA21672	68	10	-	400	80	-	-	25	140	-	88	0.56	-	43	51	46	54	0.12	65
AA21673	821	20	-	110	50	-	-	79	500	-	100	0.62	-	42	62	40	60	0.01	92
AA21675	684	20	-	130	50	-	-	83	470	-	100	0.63	-	39	58	40	60	0.05	86
AB01307	68	10	-	150	160	-	-	23	46	12	130	0.71	-	31	49	39	61	0.08	59
AB01308	-	30	9	80	290	-	-	33	7	14	210	0.92	-	33	49	40	60	0.23	51
AB01801	137	40	0	70	130	-	-	48	120	14	63	0.64	-	40	57	41	59	0.08	82
AB01802	68	20	0	190	40	-	-	99	64	8	51	0.73	-	28	54	34	66	0.01	89
AB01803	68	30	0	210	60	-	-	64	110	6	73	0.74	-	34	61	36	64	0.01	92
AB01804	-	30	0	180	140	-	-	42	33	10	110	0.80	-	27	58	32	68	0.04	87
AB01805	-	30	0	120	90	-	-	65	40	8	64	0.75	-	30	57	34	66	0.04	85
AB01806	205	20	0	140	40	-	-	110	84	4	55	0.70	-	32	56	36	64	0.01	91
AB01807	-	60	0	120	140	-	-	22	31	10	130	0.82	-	31	64	33	67	0.05	87
AB01808	-	20	0	70	130	-	-	34	28	8	120	0.78	-	36	65	36	64	0.07	87
AB01809	-	10	0	130	110	-	-	67	40	8	98	0.78	-	33	63	34	66	0.03	89
AB01810	-	20	0	130	140	-	-	46	31	10	110	0.81	-	33	65	34	66	0.05	90
AB01811	205	10	0	390	110	-	-	85	120	8	100	0.77	-	30	60	33	67	0.01	92
AB01814	1505	0	0	0	30	-	-	12	340	4	38	0.40	-	68	77	47	53	0.00	98
AB01815	1368	20	0	0	20	-	-	160	180	4	33	0.46	-	63	74	46	54	0.00	91
AB01816	21620	30	0	0	60	-	-	32	0	0	210	0.20	-	50	12	81	19	1.96	23
AB01817	547	10	0	110	50	-	-	5	110	14	53	0.54	-	44	58	43	57	0.07	82
AB04016	547	-	0	90	-	-	-	-	-	-	-	0.42	-	43	54	44	56	0.01	93
AB04019	68	10	0	500	90	-	-	-	-	-	-	0.67	-	28	35	44	56	0.11	41
AB04020	-	40	0	70	280	-	-	-	-	-	-	0.83	-	40	43	48	52	0.28	54
AB04021	-	20	0	90	90	-	-	-	-	-	-	0.83	-	41	61	40	60	0.32	87
AB04025	68	0	0	170	-	-	-	-	-	-	-	0.56	-	39	55	41	59	0.01	85
AB04026	68	10	0	150	-	-	-	-	-	-	-	0.56	-	41	57	42	58	0.01	90
AB04027	137	0	0	0	-	-	-	2000	3200	10	36	0.39	-	93	95	49	51	-	100
AB04028	-	0	0	110	-	-	-	-	-	-	-	0.35	-	54	63	46	54	0.00	96
AB04029	-	10	0	190	-	-	-	-	-	-	-	0.36	-	68	68	50	50	0.10	82
AB04076	68	40	-	500	210	-	-	-	-	-	-	0.78	-	29	38	43	57	0.17	48
AB04077	68	50	3	10	370	-	-	37	9	16	75	0.86	-	91	52	64	36	0.47	52
AB04078	1642	-	18	330	20	-	-	6	1000	20	260	0.54	-	44	58	43	57	0.10	98
AB04079	342	10	29	110	-	-	-	280	240	20	77	0.64	-	32	52	38	62	0.01	89
AB04080	137	10	17	80	80	-	-	14	65	18	88	0.86	-	24	58	29	71	0.07	79
AB04081	68	-	3	0	-	-	-	120	26	18	310	0.98	-	79	97	45	55	0.34	98
AB04082	137	10	19	90	90	-	-	5	99	14	94	0.79	-	37	68	35	65	0.02	85
AB04083	68	-	14	0	60	-	-	75	60	14	120	0.89	-	61	90	40	60	0.08	98
AB04084	68	10	44	310	100	-	-	26	63	20	97	0.78	-	37	67	36	64	0.03	91
AB04085	68	10	2	0	-	-	-	17	62	10	120	0.94	-	41	89	31	69	0.08	100
AB04106	-	0	0	120	-	-	-	-	-	-	-	0.36	-	50	59	46	54	0.00	96
AB04107	137	0	0	20	-	-	-	-	-	-	-	0.34	-	71	77	48	52	0.00	99
AB04111	137	10	27	220	120	-	-	38	120	32	170	0.85	-	33	71	31	69	0.01	94
AB04112	-	0	21	180	90	-	-	6	47	30	84	0.73	-	26	46	36	64	0.08	72

SampleNo	UTMNorth (m)	UTMEast (m)	Al_2O_3 (%)	CaO (%)	Fe_2O_3 (%)	K_2O (%)	MgO (%)	MnO (%)	Na_2O (%)	P_2O_5 (%)	SiO_2 (%)	TiO_2 (%)	LOI (%)	CO_2 (%)
AB04113	5362989	447146	6.29	4.93	0.12	39.60	0.17	0.00	0.09	1.43	1.85	0.05	0.00	-
AB06971	5357023	456102	14.70	7.92	16.60	0.25	4.27	0.23	2.55	0.24	47.9	2.29	3.00	-
AB06972	5357021	456111	7.28	9.28	11.00	-0.01	20.60	0.17	0.07	0.04	43.6	0.45	5.93	-
AB06973	5356995	456125	6.43	8.12	10.50	0.01	22.40	0.16	0.16	0.04	44.8	0.38	5.77	-
AB06974	5356972	456145	13.40	6.18	14.10	0.24	5.80	0.24	4.77	0.13	49.8	1.18	3.54	-
AB06975	5356970	456149	4.98	15.80	8.54	0.00	17.50	0.19	0.18	0.03	35.9	0.28	15.77	-
AB06976	5356965	456152	6.12	11.90	9.83	0.00	18.30	0.15	0.07	0.03	38.3	0.35	13.31	-
AB06977	5356960	456155	4.75	5.33	10.40	0.00	26.40	0.16	0.04	0.03	39.4	0.26	11.31	-
AB06978	5356955	456160	5.03	11.70	9.49	0.00	20.10	0.19	0.06	0.03	44.5	0.27	6.93	-
AB06979	5356950	456165	10.70	7.56	13.50	0.22	9.01	0.28	1.97	0.14	44.9	1.37	8.62	-
AB06980	5356945	456168	9.19	9.88	14.00	0.00	17.40	0.28	0.13	0.07	36.2	0.65	10.70	-
AB06981	5356942	456170	14.80	6.41	14.80	0.08	3.96	0.19	4.81	0.17	45.4	1.98	5.93	-
AB06982	5356928	456180	14.20	9.63	13.10	0.26	4.94	0.29	3.10	0.13	44.8	1.48	7.39	-
AD05253	5360750	455470	15.10	6.09	5.96	1.13	3.56	0.00	3.39	0.17	57	0.79	6.70	-
AD05254	5360750	455470	16.80	7.54	8.28	1.08	3.55	0.00	1.68	0.09	47.8	0.86	12.54	-
AD05255	5360750	455470	14.00	11.90	11.60	0.33	7.67	0.20	1.23	0.06	33.2	0.79	19.40	-
AD05256	5360810	455270	15.00	5.82	5.35	0.83	3.75	0.00	2.88	0.17	53.8	0.89	11.47	-
AD05257	5360810	455270	14.50	5.97	5.53	0.94	2.44	0.00	1.89	0.23	56.4	1.14	10.85	-
AD05258	5360810	455270	14.40	6.87	8.49	1.14	3.26	0.16	1.55	0.24	50.3	1.13	12.54	-
AD05259	5360810	455270	15.40	5.36	5.24	0.91	2.50	0.00	4.56	0.14	57	0.69	8.39	-
AD05260	5360970	455070	14.50	6.26	5.88	1.88	2.30	0.00	2.51	0.11	56.5	0.51	9.62	-
AD05261	5360970	455070	14.80	5.03	5.93	1.53	3.50	0.00	3.33	0.11	57	0.53	8.31	-
AD05262	5360970	455070	14.40	3.35	3.12	1.54	1.17	0.00	3.64	0.11	66.6	0.53	5.31	-
AM07406	5352739	455754	0.82	1.07	5.94	0.04	34.16	0.09	0.08	0.04	28.45	0.04	27.60	-
AM07407	5352727	455755	14.52	4.38	5.12	3.30	2.80	0.07	1.63	0.20	61.19	0.54	5.92	-
AM07408	5352726	455755	6.64	7.28	9.33	0.10	20.94	0.17	0.09	0.06	46.62	0.30	8.78	-
AM07409	5352722	455755	14.38	4.82	5.12	1.74	2.80	0.08	3.06	0.18	61.34	0.49	5.64	-
AM07410	5352707	455756	11.61	4.70	11.69	0.54	8.93	0.29	2.08	0.12	53.79	0.65	5.52	-
AM07411	5352701	455756	0.59	1.97	5.87	0.00	33.97	0.08	0.05	0.02	28.81	0.03	26.44	-
AM07412	5352694	455757	14.90	3.86	8.63	0.54	6.29	0.14	3.50	0.22	55.57	0.71	6.35	-
AM07413	5352687	455758	14.54	4.27	4.58	2.58	1.98	0.09	1.80	0.22	61.64	0.56	7.26	-
AM07414	5352683	455758	3.59	4.40	8.27	0.06	27.18	0.13	0.05	0.04	35.87	0.16	18.33	-
AM07415	5352677	455758	15.49	4.73	5.16	2.18	2.65	0.07	2.31	0.22	59.95	0.54	6.44	-
AM07416	5352674	455759	1.07	6.72	4.48	0.06	26.11	0.09	0.07	0.02	46.78	0.04	14.14	-
AM07417	5352669	455759	13.42	6.59	8.67	0.14	6.75	0.13	3.79	0.12	51.73	0.56	8.40	-
AM07418	5352657	455760	7.14	4.40	10.54	0.06	23.54	0.12	0.07	0.04	44.51	0.37	9.42	-
AM07419	5352632	455762	15.88	4.60	3.22	1.50	2.83	0.04	4.72	0.14	65.24	0.32	2.17	-
AM07420	5352628	455763	15.52	10.85	11.67	0.32	7.44	0.22	2.10	0.08	49.86	0.65	1.65	-
AM07421	5352609	455764	15.37	11.09	12.64	0.40	7.77	0.25	1.58	0.08	47.77	0.66	2.60	-
AM07422	5352593	455765	15.10	10.35	12.29	0.40	6.81	0.23	1.77	0.08	49.11	0.64	3.19	-
AM07424	5352869	456002	9.06	0.46	9.31	-0.02	7.80	0.06	0.61	0.06	67.88	0.44	4.61	-
AM07425	5352861	456002	16.87	3.18	3.03	1.66	1.76	0.04	5.68	0.12	63.7	0.34	3.73	-
AM07426	5352847	456001	14.77	4.40	7.80	0.18	5.48	0.10	5.86	0.20	57.08	0.89	4.18	-
AM07427	5352808	456000	16.32	2.04	4.53	1.60	3.43	0.04	4.73	0.18	63.5	0.44	3.68	-
AM07428	5352803	456000	2.40	8.34	7.38	0.04	26.44	0.15	0.08	0.00	36.21	0.12	17.94	-

SampleNo	Cr (ppm)	Y (ppm)	Sc (ppm)	Sr (ppm)	Zr (ppm)	Au (ppb)	Ba (ppm)	Cu (ppm)	Ni (ppm)	Pb (ppm)	Zn (ppm)	Fe/Fe+Mg	CO_2/CaO	Ishikawa Index	Chlorite Index	SCI	CSI	K/Al	CCPI
AB04113	7937	0	0	0	-	-	-	190	50	0	73	0.45	-	89	1	99	1	-	1
AB06971	-	30	0	220	160	-	-	58	18	4	160	0.82	-	30	64	32	68	0.03	87
AB06972	-	20	0	10	10	-	-	120	1400	2	87	0.38	-	69	77	47	53	-	100
AB06973	-	10	0	20	-	-	-	6	1200	2	61	0.35	-	73	79	48	52	0.00	99
AB06974	-	30	39	140	100	10	-	120	91	6	98	0.74	-	36	62	36	64	0.03	79
AB06975	-	0	20	90	20	-	-	40	1000	2	65	0.36	-	52	61	46	54	-	99
AB06976	-	10	24	60	-	60	-	46	1100	2	83	0.38	-	60	69	47	53	-	100
AB06977	-	0	20	20	-	-	-	4	1600	-	49	0.31	-	83	87	49	51	-	100
AB06978	-	0	22	30	-	-	-	10	1200	4	99	0.35	-	63	71	47	53	-	100
AB06979	-	10	0	50	60	-	-	100	210	10	130	0.63	-	49	68	42	58	0.03	91
AB06980	-	10	28	40	20	10	-	50	950	2	130	0.48	-	63	75	46	54	-	100
AB06981	-	20	0	70	90	-	-	75	89	2	130	0.81	-	26	60	30	70	0.01	78
AB06982	-	10	48	130	80	-	-	50	50	4	95	0.75	-	29	56	34	66	0.03	83
AD05253	-	-	-	140	150	-	-	65	69	-	130	0.66	-	33	46	42	58	0.12	66
AD05254	-	20	-	180	70	-	-	86	140	-	230	0.73	-	33	52	39	61	0.10	80
AD05255	-	10	-	150	30	-	-	26	130	-	230	0.64	-	38	57	40	60	0.04	92
AD05256	-	50	-	140	130	-	-	64	81	-	160	0.62	-	34	47	42	58	0.09	70
AD05257	-	30	-	190	160	-	-	73	41	-	160	0.72	-	30	46	40	60	0.10	72
AD05258	-	30	-	130	200	-	-	72	41	-	120	0.75	-	34	53	39	61	0.12	80
AD05259	-	20	-	120	120	-	-	28	31	-	68	0.71	-	26	40	39	61	0.09	57
AD05260	-	10	-	150	120	-	-	25	49	-	99	0.75	-	32	42	44	56	0.20	63
AD05261	-	20	-	100	120	-	-	49	49	-	64	0.66	-	38	47	44	56	0.16	65
AD05262	-	30	-	110	190	-	-	35	14	-	71	0.76	-	28	32	47	53	0.17	43
AM07406	958	-	-	-	24	-	-	80	2520	-	0	0.17	-	97	97	50	50	0.08	100
AM07407	68	22	-	-	226	-	-	30	120	-	35	0.68	-	50	44	53	47	0.36	60
AM07408	2121	10	-	-	62	-	-	15	1270	-	0	0.34	-	74	80	48	52	0.02	99
AM07409	68	14	-	-	158	-	-	20	50	-	40	0.68	-	37	44	46	54	0.19	61
AM07410	616	16	-	-	102	-	-	30	360	-	60	0.60	-	58	73	45	55	0.07	88
AM07411	958	0	-	-	12	-	-	-	2420	-	0	0.17	-	94	95	50	50	-	100
AM07412	205	22	-	-	176	-	-	10	230	-	45	0.61	-	48	64	43	57	0.06	78
AM07413	68	24	-	-	222	-	-	35	20	-	50	0.73	-	43	41	51	49	0.28	58
AM07414	3010	2	-	-	38	-	-	25	1850	-	0	0.26	-	86	88	49	51	0.03	100
AM07415	68	20	-	-	186	-	-	20	60	-	60	0.69	-	41	44	48	52	0.22	62
AM07416	958	-	-	-	26	-	-	65	2160	-	0	0.17	-	79	81	49	51	0.09	100
AM07417	342	16	-	-	98	-	-	55	180	-	25	0.60	-	40	58	41	59	0.02	79
AM07418	2326	8	-	-	56	-	-	10	1260	-	0	0.34	-	84	88	49	51	0.01	100
AM07419	205	6	-	-	134	-	-	20	120	-	30	0.57	-	32	35	48	52	0.15	48
AM07420	616	16	-	-	70	-	-	110	110	-	60	0.65	-	37	57	39	61	0.03	88
AM07421	274	16	-	-	74	-	-	115	70	-	25	0.65	-	39	59	40	60	0.04	91
AM07422	411	16	-	-	100	-	-	125	100	-	50	0.68	-	37	59	39	61	0.04	89
AM07424	3147	8	-	-	94	-	-	15	1060	-	55	0.58	-	88	94	48	52	-	96
AM07425	205	6	-	-	142	-	-	-	40	-	15	0.67	-	28	30	48	52	0.15	38
AM07426	274	10	-	-	206	-	-	35	110	-	60	0.62	-	36	54	39	61	0.02	67
AM07427	68	8	-	-	166	-	-	20	60	-	45	0.60	-	43	47	47	53	0.15	54
AM07428	1232	-	-	-	70	-	-	0	2140	-	0	0.24	-	76	80	49	51	0.03	100

SampleNo	UTMNorth (m)	UTMEast (m)	Al_2O_3 (%)	CaO (%)	Fe_2O_3 (%)	K_2O (%)	MgO (%)	MnO (%)	Na_2O (%)	P_2O_5 (%)	SiO_2 (%)	TiO_2 (%)	LOI (%)	CO_2 (%)
AM07429	5352793	455999	1.73	0.54	7.23	-0.02	32.77	0.05	0.02	0.00	35.38	0.09	20.27	-
AM07430	5352784	455999	2.12	2.99	7.44	-0.02	30.70	0.08	-0.01	0.00	34.01	0.11	20.46	-
AM07431	5352778	455999	16.11	1.92	3.19	2.46	2.78	0.05	4.40	0.12	64.78	0.32	4.15	-
AM07432	5352746	455998	0.65	0.18	6.05	0.04	35.79	0.07	0.06	-0.02	30.08	0.03	25.97	-
AM07433	5352737	455999	0.37	0.45	6.27	-0.02	37.46	0.11	0.02	-0.02	33.42	0.02	21.17	-
AM07434	5352718	455999	15.21	4.67	6.63	1.54	3.67	0.12	2.77	0.20	58.33	0.71	7.04	-
AM07436	5352813	456000	9.61	8.98	10.62	0.08	14.23	0.12	0.05	0.04	43.42	0.48	10.67	-
AN00001	5351990	453935	13.39	8.06	15.68	0.24	5.17	0.24	3.20	0.14	52.84	1.31	0.21	-
AN00002	5351927	454018	14.90	11.75	10.92	0.22	7.18	0.22	2.46	0.08	50.72	0.62	0.72	-
AN00004	5352040	453385	13.83	10.04	16.30	0.14	5.93	0.24	1.86	0.10	50.54	1.35	0.54	-
AN01932	5352768	454355	6.34	4.32	10.15	0.12	24.12	0.13	0.12	0.00	40.6	0.27	11.42	-
AN01933	5352749	454356	7.74	4.96	7.96	0.06	17.69	0.11	1.37	0.02	37.9	0.35	19.61	-
AN01934	5352732	454357	6.13	5.19	9.93	0.04	22.60	0.13	0.11	0.00	39.8	0.29	13.41	-
AN01935	5352724	454358	14.89	2.42	4.56	1.24	4.50	0.05	5.45	0.20	62.1	0.42	4.57	-
AN01936	5352719	454359	4.73	1.87	7.61	0.04	28.51	0.10	0.15	0.00	38.4	0.22	16.03	-
AN01937	5352714	454359	5.47	3.40	8.83	0.06	27.88	0.11	0.10	0.02	34.02	0.30	17.41	-
AN01938	5352699	454361	14.63	4.69	4.41	2.38	1.91	0.07	2.53	0.16	64.1	0.45	5.56	-
AN01940	5352736	455497	1.13	5.15	6.11	0.04	29.55	0.10	0.00	0.00	34.3	0.04	21.28	-
AN01941	5352729	455497	15.20	4.95	3.91	1.82	2.69	0.07	3.26	0.16	62.63	0.41	5.76	-
AN01942	5352720	455497	0.69	2.55	6.99	0.16	1.00	0.43	0.06	0.00	85.36	0.05	3.28	-
AN01943	5352718	455497	10.60	8.08	11.08	0.84	6.38	0.41	1.27	0.08	49.71	0.52	11.50	-
AN01944	5352714	455497	1.96	1.53	7.29	0.02	30.42	0.11	0.05	0.00	35.58	0.08	20.75	-
AN01945	5352700	455496	12.84	6.18	9.68	1.28	3.68	0.26	0.83	0.16	55.04	0.64	9.09	-
AN01946	5352697	455496	14.63	4.07	4.57	3.24	2.08	0.11	1.18	0.16	62.77	0.45	7.22	-
AN01947	5352667	455495	6.56	6.80	10.16	0.14	22.00	0.15	0.15	0.00	44.72	0.31	6.71	-
AN01948	5352644	455494	15.02	3.88	3.58	1.70	2.88	0.05	4.71	0.20	66.58	0.38	1.70	-
AN01949	5352623	455492	14.98	10.46	9.30	0.60	6.53	0.17	2.15	0.26	52.7	0.66	2.02	-
AP08501	5362694	449553	0.80	0.76	20.72	0.08	0.99	0.52	0.03	0.00	69.99	0.04	5.92	-
AP08502	5362694	449556	15.21	3.25	6.92	3.62	3.52	0.15	2.76	0.14	62.08	0.53	2.28	-
AP08503	5362686	449549	14.40	5.87	9.39	0.62	4.47	0.38	4.35	0.12	56.83	0.58	3.59	-
AP08504	5362623	449524	14.94	9.47	10.66	0.46	5.70	0.19	2.41	0.12	51.08	0.84	2.49	-
AP08530	5362759	449432	13.13	4.02	14.23	0.50	4.57	0.52	2.76	0.10	54.5	0.51	5.20	-
AP08531	5362779	449407	12.66	6.60	15.92	1.04	4.53	0.50	2.33	0.06	53.02	0.53	2.78	-
AP08532	5363159	449739	15.45	5.45	8.79	0.88	2.24	0.15	3.75	0.24	54.67	0.87	8.19	-
AP08533	5363197	449712	15.37	4.83	7.86	0.84	2.71	0.11	3.85	0.26	59.72	0.98	4.42	-
AP08534	5362890	449614	15.30	4.92	7.55	1.62	2.88	0.10	4.00	0.16	57.5	0.81	5.94	-
AP08535	5363103	449731	14.97	1.60	2.26	1.30	0.17	0.04	3.75	0.14	73.66	0.49	2.58	-
AP08536	5362823	449582	13.72	3.02	2.43	1.66	0.98	0.05	4.63	0.12	67.58	0.41	3.14	-
AP08545	5362791	446897	14.38	10.83	9.64	1.22	3.41	0.20	1.46	0.22	55.38	1.01	1.58	-
AP08546	5362792	446950	13.46	2.89	5.51	1.20	1.00	0.08	4.36	0.12	68.78	0.44	1.03	-
AP08547	5362621	446893	11.95	0.34	4.83	1.14	2.94	0.03	4.11	0.10	72.5	0.43	2.05	-
AP08549	5362476	446834	16.53	10.39	12.17	0.22	7.54	0.29	2.27	0.08	47.85	0.88	2.62	-
AP08550	5362244	446746	15.88	11.70	15.44	0.80	3.99	0.44	2.69	0.08	47.2	0.65	1.86	-
AP08551	5362249	446751	9.09	2.36	4.18	1.20	0.93	0.09	3.35	0.00	76.54	0.12	1.20	-
AP08552	5362210	446745	16.58	8.88	10.61	0.58	4.86	0.19	3.68	0.12	53.95	0.79	0.74	-

SampleNo	Cr (ppm)	Y (ppm)	Sc (ppm)	Sr (ppm)	Zr (ppm)	Au (ppb)	Ba (ppm)	Cu (ppm)	Ni (ppm)	Pb (ppm)	Zn (ppm)	Fe/Fe+Mg	CO_2/CaO	Ishikawa Index	Chlorite Index	SCI	CSI	K/Al	CCPI
AM07429	1095	4	-	-	82	-	-	0	2360	-	0	0.20	-	98	99	50	50	-	100
AM07430	1505	-	-	-	60	-	-	0	2060	-	0	0.22	-	91	93	50	50	-	100
AM07431	547	6	-	-	134	-	-	0	60	-	35	0.57	-	45	39	54	46	0.24	45
AM07432	1163	2	-	-	30	-	-	0	2440	-	0	0.16	-	99	99	50	50	0.10	100
AM07433	1095	-	-	-	62	-	-	0	2260	-	0	0.16	-	99	99	50	50	-	100
AM07434	274	20	-	-	254	-	-	20	40	-	70	0.68	-	41	52	44	56	0.16	69
AM07436	958	8	-	-	46	-	-	35	460	-	10	0.46	-	61	72	46	54	0.01	99
AN00001	-	40	-	-	86	-	-	15	40	-	85	0.78	-	32	63	34	66	0.03	85
AN00002	342	14	-	-	40	-	-	110	80	-	65	0.64	-	34	54	39	61	0.02	86
AN00004	342	28	-	-	84	-	-	70	60	-	120	0.76	-	34	63	35	65	0.02	91
AN01932	2053	32	-	-	40	-	-	35	1370	-	165	0.33	-	85	88	49	51	0.03	99
AN01933	1505	26	-	-	60	-	-	30	1120	-	75	0.34	-	74	80	48	52	0.01	95
AN01934	2053	28	-	-	38	-	-	45	1240	-	115	0.34	-	81	86	49	51	0.01	100
AN01935	274	28	-	-	144	-	-	25	40	-	60	0.54	-	42	49	46	54	0.13	56
AN01936	1163	24	-	-	40	-	-	45	1980	-	70	0.24	-	93	94	50	50	0.01	99
AN01937	1095	26	-	-	36	-	-	120	4000	-	50	0.27	-	89	91	49	51	0.02	100
AN01938	205	26	-	-	152	-	-	25	140	-	150	0.73	-	37	38	50	50	0.26	54
AN01940	1163	16	-	-	20	-	-	0	2720	-	220	0.19	-	85	87	49	51	0.06	100
AN01941	205	24	-	-	128	-	-	10	160	-	85	0.63	-	35	38	48	52	0.19	55
AN01942	1095	18	-	-	52	-	-	10	130	-	60	0.89	-	31	72	30	70	0.36	97
AN01943	616	40	-	-	104	-	-	20	460	-	90	0.67	-	44	62	41	59	0.12	89
AN01944	1505	18	-	-	28	-	-	15	2370	-	160	0.22	-	95	96	50	50	0.02	100
AN01945	342	40	-	-	138	-	-	25	230	-	85	0.75	-	41	60	41	59	0.16	85
AN01946	274	30	-	-	138	-	-	25	90	-	85	0.72	-	50	42	54	46	0.35	58
AN01947	1847	30	-	-	44	-	-	60	1300	-	5	0.35	-	76	81	48	52	0.03	99
AN01948	342	18	-	-	126	-	-	15	130	-	50	0.59	-	35	37	48	52	0.18	49
AN01949	342	38	-	-	98	-	-	60	210	-	40	0.62	-	36	53	41	59	0.06	84
AP08501	1300	6	-	-	16	-	-	25	10	-	750	0.96	-	58	96	38	62	0.16	99
AP08502	411	18	-	-	132	-	-	0	40	-	75	0.70	-	54	50	52	48	0.37	60
AP08503	342	14	-	-	100	-	-	0	95	-	145	0.71	-	33	54	38	62	0.07	72
AP08504	616	20	-	-	94	-	-	20	65	-	80	0.68	-	34	55	38	62	0.05	84
AP08530	411	16	-	-	94	-	-	0	65	-	105	0.78	-	43	70	38	62	0.06	84
AP08531	616	12	-	-	90	-	-	0	45	-	70	0.80	-	38	65	37	63	0.13	85
AP08532	479	20	-	-	132	-	-	0	50	-	85	0.82	-	25	50	34	66	0.09	69
AP08533	342	22	-	-	158	-	-	45	45	-	95	0.77	-	29	51	36	64	0.09	68
AP08534	205	10	-	-	84	-	-	10	45	-	75	0.75	-	34	48	41	59	0.17	63
AP08535	889	44	-	-	422	-	-	15	25	-	95	0.94	-	22	25	46	54	0.14	30
AP08536	479	46	-	-	256	-	-	0	25	-	40	0.74	-	26	25	50	50	0.19	33
AP08545	616	26	-	-	122	-	-	10	30	-	105	0.77	-	27	47	37	63	0.13	82
AP08546	821	42	-	-	264	-	-	5	20	-	60	0.86	-	23	41	36	64	0.14	52
AP08547	616	42	-	-	272	-	-	40	30	-	25	0.66	-	48	57	46	54	0.15	58
AP08549	547	18	-	-	56	-	-	15	135	-	120	0.65	-	38	59	39	61	0.02	88
AP08550	547	22	-	-	66	-	-	30	125	-	90	0.82	-	25	54	32	68	0.08	84
AP08551	1779	60	-	-	182	-	-	95	35	-	55	0.84	-	27	40	40	60	0.21	51
AP08552	821	20	-	-	82	-	-	95	80	-	85	0.72	-	30	52	37	63	0.05	77

SampleNo	UTMNorth (m)	UTMEast (m)	Al_2O_3 (%)	CaO (%)	Fe_2O_3 (%)	K_2O (%)	MgO (%)	MnO (%)	Na_2O (%)	P_2O_5 (%)	SiO_2 (%)	TiO_2 (%)	LOI (%)	CO_2 (%)
AP08553	5362125	446616	18.37	6.43	7.83	1.38	1.82	0.14	3.10	0.20	57.49	1.15	2.09	-
AP08554	5362479	446734	15.06	6.96	13.47	1.06	3.35	0.38	2.98	0.14	56.2	0.65	0.69	-
AP08555	5362586	446792	10.36	0.47	2.34	2.58	0.58	0.04	1.18	0.02	78.36	0.13	1.80	-
AP08556	5362625	446789	11.79	5.35	9.24	0.34	3.13	0.40	4.31	0.08	58.41	0.47	6.66	-
AP08557	5362800	446866	14.05	8.84	13.85	0.90	6.50	0.27	2.14	0.10	49.7	1.08	3.15	-
AP08558	5362791	446868	13.23	3.19	5.82	0.58	1.14	0.10	4.67	0.10	67.2	0.44	1.20	-
AP08559	5362814	446892	17.38	6.04	10.92	1.52	3.07	0.18	3.08	0.26	55.1	1.27	2.06	-
AP08560	5362800	446942	13.30	2.73	5.70	1.20	0.98	0.07	3.72	0.10	67.8	0.47	1.46	-
AP08561	5361904	448674	12.56	1.84	4.15	2.30	0.69	0.08	3.15	0.10	72.5	0.40	3.07	-
AP08562	5361911	448648	10.30	0.27	2.89	1.50	1.98	0.03	1.22	0.00	77.45	0.13	2.04	-
AP08563	5361766	448584	13.79	4.06	11.49	1.26	3.03	0.30	2.90	0.12	57.15	0.57	6.17	-
AP08564	5361638	448567	14.61	4.66	15.28	0.56	3.04	0.43	2.65	0.06	52.45	0.69	6.53	-
AP08565	5362007	448476	13.09	1.68	5.43	2.06	0.63	0.14	4.15	0.12	70.2	0.43	2.61	-
AP08566	5361996	448477	11.26	0.87	4.30	1.92	0.94	0.06	2.99	0.06	72.48	0.37	2.38	-
AP08567	5361992	448474	15.06	8.12	14.72	2.76	4.59	0.29	1.81	0.08	39.17	1.41	12.58	-
AP08568	5361717	448264	15.45	4.32	4.57	1.74	1.02	0.14	2.99	0.10	66.85	0.74	3.03	-
AP08569	5361923	448334	1.81	6.92	34.10	0.54	2.43	1.68	0.17	0.00	42.13	0.09	10.20	-
AP08570	5362105	446716	15.91	7.97	8.41	0.64	2.82	0.29	3.32	0.14	58.29	0.61	2.29	-
AP08571	5362101	448071	12.77	1.69	4.79	2.40	0.71	0.14	3.68	0.10	71.12	0.43	2.01	-
AP08572	5362082	448058	14.75	4.23	11.67	0.52	5.76	0.18	3.23	0.10	53.44	1.04	6.06	-
AP08573	5362086	448061	12.92	1.32	4.24	0.94	1.17	0.07	4.41	0.08	73.45	0.46	1.41	-
AP08574	5361943	448041	13.73	5.61	9.09	0.32	3.23	0.31	4.00	0.10	56.79	0.58	6.70	-
AP08575	5361928	448010	14.45	8.39	14.56	0.16	3.87	0.50	1.45	0.10	51.91	0.61	4.34	-
AP08576	5361919	448013	15.90	4.43	6.36	2.84	2.95	0.14	1.22	0.10	59.95	0.66	5.99	-
AP08577	5361831	447988	17.12	7.69	7.92	0.56	3.78	0.19	2.57	0.16	54.4	1.04	5.24	-
AP08578	5361859	447895	15.97	4.93	6.04	0.80	2.43	0.16	4.01	0.18	62.4	1.02	2.97	-
AP08580	5361924	447947	15.57	6.97	15.26	0.60	3.79	0.45	2.14	0.08	50.7	0.70	3.88	-
AP08581	5362189	447953	10.36	0.47	2.26	2.54	0.57	0.04	1.15	0.02	78.28	0.14	1.89	-
AP08587	5363308	446240	15.88	8.39	6.50	0.68	2.06	0.12	1.97	0.14	62.4	0.76	1.97	-
AP08588	5362670	446275	16.10	6.39	5.32	1.50	1.82	0.12	2.60	0.10	64.36	0.67	1.99	-
AP08589	5362741	446295	8.59	10.05	9.06	0.10	15.15	0.26	0.22	0.04	39.36	0.40	17.72	-
AP08592	5363292	446483	19.24	3.87	6.81	2.62	1.45	0.21	3.68	0.18	59.1	1.52	2.19	-
AP08593	5363277	446578	13.24	2.54	5.45	1.64	1.24	0.08	3.59	0.12	70.1	0.49	1.39	-
AP08594	5363500	446660	11.92	8.81	23.84	0.06	5.43	0.42	0.14	0.06	43.01	3.07	4.23	-
AP08595	5363600	446705	13.73	2.24	4.03	2.86	0.83	0.07	3.89	0.08	70.54	0.38	1.10	-
AP08596	5363399	446626	12.33	9.42	18.81	1.02	5.76	0.27	2.23	0.24	48	2.16	0.75	-
AP08597	5363080	447151	15.41	6.66	13.58	0.30	4.29	0.26	2.60	0.26	53.05	1.32	3.27	-
AP08598	5363106	447165	16.43	6.76	9.77	1.30	2.61	0.21	2.19	0.20	57.9	1.14	2.44	-
AP08599	5363251	447209	15.65	4.32	14.72	0.26	3.46	0.42	4.36	0.22	53.45	1.35	2.79	-
AP08600	5363437	447252	13.21	6.29	11.25	0.78	4.25	0.20	2.41	0.08	59.2	0.85	2.06	-
AP09302	5362765	447033	13.06	1.88	4.98	1.22	0.89	0.08	4.78	0.10	72.15	0.44	1.30	-
AP09303	5363112	447168	15.89	6.71	8.44	1.36	2.43	0.13	2.37	0.28	60.04	1.11	2.18	-
AP09304	5362883	447074	15.61	3.72	8.54	0.92	2.84	0.14	5.55	0.24	59.55	1.15	1.69	-
AP09305	5363310	447230	3.79	5.68	23.95	0.44	6.06	0.24	0.41	0.20	55.08	0.25	4.22	-
AP09306	5362853	447084	15.31	5.66	7.99	1.10	2.81	0.14	3.93	0.24	59.99	1.13	1.61	-

SampleNo	Cr (ppm)	Y (ppm)	Sc (ppm)	Sr (ppm)	Zr (ppm)	Au (ppb)	Ba (ppm)	Cu (ppm)	Ni (ppm)	Pb (ppm)	Zn (ppm)	Fe/Fe+Mg	CO_2/CaO	Ishikawa Index	Chlorite Index	SCI	CSI	K/Al	CCPI
AP08553	821	16	-	-	92	-	-	40	110	-	110	0.83	-	25	45	36	64	0.12	66
AP08554	616	10	-	-	100	-	-	45	80	-	60	0.82	-	31	58	34	66	0.11	79
AP08555	547	126	-	-	332	-	-	0	5	-	35	0.82	-	66	39	63	37	0.39	42
AP08556	342	12	-	-	78	-	-	10	100	-	125	0.77	-	26	53	33	67	0.05	71
AP08557	342	28	-	-	82	-	-	40	55	-	220	0.71	-	40	61	40	60	0.10	86
AP08558	1163	40	-	-	200	-	-	0	20	-	65	0.86	-	18	43	29	71	0.07	55
AP08559	274	24	-	-	148	-	-	40	20	-	115	0.80	-	33	55	38	62	0.14	74
AP08560	1163	36	-	-	238	-	-	30	20	-	50	0.87	-	25	44	36	64	0.14	55
AP08561	547	42	-	-	244	-	-	5	15	-	35	0.87	-	37	38	50	50	0.29	45
AP08562	479	80	-	-	240	-	-	0	0	-	75	0.63	-	70	61	54	46	0.23	63
AP08563	547	14	-	-	94	-	-	20	55	-	55	0.81	-	38	62	38	62	0.14	76
AP08564	274	14	-	-	56	-	-	20	100	-	70	0.85	-	33	68	33	67	0.06	84
AP08565	547	46	-	-	248	-	-	0	10	-	85	0.91	-	32	41	43	57	0.25	47
AP08566	1095	46	-	-	238	-	-	10	25	-	80	0.84	-	43	45	48	52	0.27	49
AP08567	205	30	-	-	86	-	-	45	80	-	155	0.79	-	43	58	42	58	0.29	80
AP08568	1026	14	-	-	58	-	-	145	90	-	2835	0.84	-	27	36	43	57	0.18	52
AP08569	274	4	-	-	54	-	-	40	-	-	135	0.94	-	30	81	27	73	0.47	98
AP08570	684	12	-	-	86	-	-	35	85	-	150	0.78	-	23	47	34	66	0.06	72
AP08571	411	44	-	-	246	-	-	10	15	-	35	0.89	-	37	39	48	52	0.29	45
AP08572	205	26	-	-	104	-	-	35	65	-	105	0.70	-	46	67	41	59	0.06	81
AP08573	342	64	-	-	266	-	-	10	10	-	30	0.81	-	27	43	39	61	0.11	48
AP08574	274	18	-	-	74	-	-	25	95	-	1800	0.77	-	27	53	34	66	0.04	73
AP08575	411	18	-	-	122	-	-	25	105	-	70	0.81	-	29	63	32	68	0.02	91
AP08576	342	18	-	-	98	-	-	45	100	-	35	0.71	-	51	51	50	50	0.28	68
AP08577	274	16	-	-	80	-	-	35	85	-	70	0.71	-	30	50	37	63	0.05	78
AP08578	342	18	-	-	98	-	-	40	60	-	50	0.74	-	27	45	37	63	0.08	62
AP08580	411	14	-	-	78	-	-	30	135	-	60	0.82	-	33	64	34	66	0.06	86
AP08581	547	126	-	-	332	-	-	0	5	-	35	0.82	-	66	38	63	37	0.38	41
AP08587	821	12	-	-	88	-	-	15	95	-	45	0.79	-	21	42	33	67	0.07	75
AP08588	616	10	-	-	60	-	-	35	90	-	70	0.77	-	27	39	41	59	0.15	62
AP08589	1916	6	-	-	34	-	-	0	1010	-	145	0.41	-	60	69	46	54	0.02	99
AP08592	547	18	-	-	112	-	-	10	100	-	60	0.84	-	35	43	45	55	0.21	55
AP08593	958	44	-	-	272	-	-	0	20	-	35	0.84	-	32	44	42	58	0.19	54
AP08594	205	24	-	-	78	-	-	60	45	-	90	0.84	-	38	75	34	66	0.01	99
AP08595	547	44	-	-	150	-	-	5	10	-	25	0.85	-	38	33	53	47	0.33	40
AP08596	274	42	-	-	138	-	-	135	55	-	135	0.79	-	37	64	36	64	0.13	87
AP08597	205	26	-	-	134	-	-	20	30	-	80	0.79	-	33	63	34	66	0.03	85
AP08598	547	18	-	-	118	-	-	55	30	-	80	0.81	-	30	53	37	63	0.12	77
AP08599	137	16	-	-	98	-	-	15	65	-	90	0.83	-	30	65	32	68	0.03	78
AP08600	411	30	-	-	102	-	-	25	30	-	95	0.75	-	37	60	38	62	0.09	82
AP09302	684	40	-	-	272	-	-	15	10	-	60	0.87	-	24	41	37	63	0.15	47
AP09303	1163	22	-	-	128	-	-	10	35	-	75	0.80	-	29	49	38	62	0.13	73
AP09304	616	24	-	-	130	-	-	40	35	-	75	0.78	-	29	51	36	64	0.09	62
AP09305	616	8	-	-	40	-	-	340	5	-	255	0.82	-	52	81	39	61	0.18	97
AP09306	411	20	-	-	124	-	-	40	25	-	70	0.77	-	29	48	37	63	0.11	67

SampleNo	UTMNorth (m)	UTMEast (m)	Al_2O_3 (%)	CaO (%)	Fe_2O_3 (%)	K_2O (%)	MgO (%)	MnO (%)	Na_2O (%)	P_2O_5 (%)	SiO_2 (%)	TiO_2 (%)	LOI (%)	CO_2 (%)
AP09307	5362547	446924	11.56	0.49	2.34	3.36	0.51	0.04	0.33	0.04	79.5	0.17	1.84	-
AP09308	5363275	447328	14.15	2.99	3.52	2.58	0.83	0.06	3.49	0.10	71.3	0.34	1.26	-
AP09309	5362765	447152	13.95	6.94	4.98	0.56	1.08	0.08	3.65	0.20	66.77	0.99	1.48	-
AP09310	5362557	447069	8.51	0.70	5.45	0.64	1.91	0.06	2.47	0.06	78.42	0.35	1.90	-
AP09311	5362547	447061	13.08	2.69	5.50	1.84	0.75	0.08	3.22	0.10	71.31	0.42	1.75	-
AP09312	5363476	447361	15.39	10.98	11.18	0.16	8.41	0.18	2.76	0.12	48.1	0.85	2.54	-
AP09313	5362672	447112	16.48	4.08	9.38	1.08	2.42	0.14	4.68	0.24	59.15	1.28	1.64	-
AP09314	5362816	447158	12.59	2.31	4.43	2.56	0.50	0.10	2.59	0.08	72.76	0.29	2.23	-
AP09315	5362508	447019	11.64	0.42	2.03	2.66	0.29	0.04	1.26	0.02	80.6	0.14	1.45	-
AP09316	5363238	447309	14.42	1.60	17.15	0.84	2.27	0.33	3.41	0.18	54.5	1.08	4.53	-
AP09318	5363215	447302	15.79	8.15	6.59	1.26	2.27	0.12	1.06	0.12	61.9	0.55	2.39	-
AP09319	5362929	447292	16.18	8.97	11.08	0.54	3.28	0.25	2.59	0.20	54.2	0.86	2.73	-
AP09320	5363081	447263	17.40	6.87	10.31	2.22	1.65	0.28	2.09	0.20	52.61	0.84	5.32	-
AP09321	5362847	447285	13.16	10.72	25.83	0.40	5.19	1.00	0.97	0.14	41.05	0.75	1.70	-
AP09322	5362546	447273	15.67	4.68	9.10	1.44	2.17	0.20	3.96	0.24	59.41	1.14	2.34	-
AP09323	5362342	447849	12.20	1.79	8.86	0.44	3.76	0.10	1.17	0.04	66.55	0.21	4.56	-
AP09324	5363500	446337	15.11	2.09	3.19	1.32	1.11	0.04	4.82	0.12	71.45	0.34	1.30	-
AP09325	5363230	446279	14.70	9.65	13.37	0.72	3.58	0.41	1.93	0.16	54.2	0.66	1.49	-
AP09326	5363939	448841	12.05	0.20	2.10	3.38	0.84	0.04	0.47	0.04	76.95	0.16	1.66	-
AP09329	5363936	448825	11.14	0.07	1.06	3.56	0.43	0.01	0.34	0.04	79.39	0.14	1.47	-
AP09331	5364003	448824	11.56	0.11	3.01	3.24	0.53	0.02	0.29	0.06	77.51	0.15	2.29	-
AP09332	5363977	448874	13.96	0.72	7.62	1.36	0.98	0.20	3.66	0.06	69.53	0.35	1.49	-
AP09333	5362262	447671	12.60	7.07	18.37	0.38	4.75	0.76	1.74	0.10	50.42	0.51	4.28	-
AP09334	5362462	447653	13.96	10.80	13.49	0.04	6.29	0.26	0.10	0.12	47.3	1.03	7.61	-
AP09335	5362310	447656	12.13	0.12	23.92	0.04	6.32	0.64	0.04	0.08	51.22	0.55	5.94	-
AP09336	5362214	447602	12.36	8.22	23.89	0.20	5.79	0.96	0.75	0.08	44.3	0.54	3.87	-
AP09338	5362908	449522	13.42	1.40	5.45	2.12	0.46	0.13	3.54	0.12	69.84	0.50	1.98	-
AP09339	5363539	449728	13.67	0.26	3.26	3.10	0.56	0.03	1.52	0.08	73.84	0.41	1.90	-
AP09341	5363635	449673	14.55	2.41	4.96	3.80	0.83	0.07	2.32	0.10	68.75	0.44	2.61	-
AP09342	5363655	449667	11.42	3.06	5.94	1.92	0.61	0.10	2.52	0.08	70.39	0.35	3.38	-
AP09343	5363233	449452	15.50	2.34	13.74	0.62	5.51	0.10	2.58	0.14	53.12	1.23	5.99	-
AP09344	5363222	449439	14.75	1.91	3.33	1.62	0.27	0.09	3.76	0.14	70.49	0.48	2.82	-
AP09345	5363236	449442	15.95	1.35	6.40	1.76	0.59	0.10	3.76	0.14	67.21	0.56	2.95	-
AP09346	5363226	449429	15.45	2.30	4.69	1.50	0.34	0.10	4.09	0.14	68.12	0.55	3.67	-
AP09347	5363237	449442	16.00	1.72	3.38	1.74	0.35	0.08	4.65	0.14	69.45	0.56	2.73	-
AP09348	5363248	449433	14.67	3.20	13.71	0.46	4.53	0.15	3.38	0.14	52.4	1.35	5.84	-
AP09349	5363250	449429	14.05	0.88	1.89	2.22	0.47	0.04	3.69	0.08	74.65	0.56	1.74	-
AP09350	5363554	449751	13.52	6.53	12.39	0.70	5.14	0.20	2.71	0.12	50.24	1.06	8.33	-
AP09351	5363553	449751	12.99	2.63	4.46	0.94	1.22	0.07	5.10	0.12	70.4	0.46	2.58	-
AP09352	5363248	449650	13.90	0.59	1.09	2.54	0.20	0.02	3.44	0.10	76.9	0.57	1.46	-
AP09353	5362985	449556	13.07	0.97	3.16	1.58	0.39	0.06	4.57	0.10	74.92	0.45	1.68	-
AP09354	5362831	449501	12.00	0.99	5.76	1.54	0.88	0.07	3.21	0.10	73.05	0.42	1.92	-
AP09355	5363857	449627	12.43	1.52	2.83	3.82	0.56	0.04	1.76	0.08	73.85	0.42	1.69	-
AP09356	5363863	449628	15.38	3.82	14.88	2.12	6.60	0.20	1.03	0.08	51.1	0.96	4.74	-
AP09357	5363275	449414	13.74	0.43	5.57	2.64	0.77	0.11	2.64	0.12	72.21	0.50	1.96	-

SampleNo	Cr (ppm)	Y (ppm)	Sc (ppm)	Sr (ppm)	Zr (ppm)	Au (ppb)	Ba (ppm)	Cu (ppm)	Ni (ppm)	Pb (ppm)	Zn (ppm)	Fe/Fe+Mg	CO_2/CaO	Ishikawa Index	Chlorite Index	SCI	CSI	K/Al	CCPI
AP09307	889	116	-	-	292	-	-	20	15	-	40	0.84	-	83	38	68	32	0.46	41
AP09308	479	32	-	-	154	-	-	0	10	-	35	0.83	-	34	31	53	47	0.29	40
AP09309	684	18	-	-	116	-	-	35	15	-	40	0.84	-	13	33	29	71	0.06	57
AP09310	1710	16	-	-	134	-	-	10	45	-	35	0.77	-	45	64	41	59	0.12	69
AP09311	616	42	-	-	254	-	-	5	10	-	55	0.89	-	30	42	42	58	0.22	53
AP09312	479	18	-	-	40	-	-	95	105	-	70	0.61	-	38	57	40	60	0.02	86
AP09313	753	20	-	-	140	-	-	50	40	-	75	0.82	-	29	52	35	65	0.10	65
AP09314	821	42	-	-	252	-	-	10	10	-	75	0.91	-	38	38	51	49	0.32	47
AP09315	411	80	-	-	254	-	-	10	5	-	60	0.89	-	64	33	66	34	0.36	35
AP09316	753	16	-	-	110	-	-	215	25	-	115	0.90	-	38	75	34	66	0.09	81
AP09318	958	22	-	-	88	-	-	50	50	-	80	0.77	-	28	44	39	61	0.13	78
AP09319	547	22	-	-	122	-	-	45	35	-	50	0.80	-	25	52	32	68	0.05	81
AP09320	342	18	-	-	96	-	-	15	25	-	70	0.88	-	30	49	38	62	0.20	72
AP09321	274	18	-	-	80	-	-	60	40	-	80	0.85	-	32	70	32	68	0.05	95
AP09322	274	20	-	-	130	-	-	40	15	-	75	0.83	-	29	51	37	63	0.14	66
AP09323	274	200	-	-	934	-	-	20	0	-	335	0.73	-	59	78	43	57	0.06	88
AP09324	274	16	-	-	166	-	-	20	5	-	40	0.77	-	26	33	44	56	0.14	39
AP09325	684	14	-	-	96	-	-	10	85	-	75	0.81	-	27	56	33	67	0.08	85
AP09326	958	66	-	-	306	-	-	5	5	-	30	0.74	-	86	40	68	32	0.44	41
AP09329	616	58	-	-	282	-	-	5	15	-	5	0.74	-	91	26	78	22	0.50	26
AP09331	1026	62	-	-	306	-	-	45	25	-	85	0.87	-	90	47	66	34	0.44	48
AP09332	1095	40	-	-	164	-	-	35	25	-	55	0.90	-	35	58	38	62	0.15	61
AP09333	342	12	-	-	120	-	-	60	60	-	35	0.82	-	37	70	35	65	0.05	91
AP09334	274	24	-	-	84	-	-	40	95	-	95	0.71	-	37	63	37	63	0.00	99
AP09335	274	14	-	-	76	-	-	10	50	-	85	0.81	-	98	99	50	50	0.01	100
AP09336	205	18	-	-	88	-	-	45	75	-	55	0.83	-	40	75	35	65	0.03	97
AP09338	889	44	-	-	262	-	-	30	5	-	30	0.93	-	34	43	44	56	0.25	49
AP09339	889	50	-	-	280	-	-	5	30	-	30	0.87	-	67	42	62	38	0.36	43
AP09341	889	48	-	-	238	-	-	10	20	-	30	0.87	-	49	38	56	44	0.41	46
AP09342	1368	34	-	-	266	-	-	20	25	-	75	0.92	-	31	44	41	59	0.26	57
AP09343	342	28	-	-	90	-	-	25	90	-	95	0.74	-	55	76	42	58	0.06	85
AP09344	616	14	-	-	134	-	-	10	25	-	25	0.93	-	25	31	45	55	0.17	38
AP09345	411	22	-	-	154	-	-	20	50	-	45	0.93	-	32	48	40	60	0.17	53
AP09346	411	22	-	-	148	-	-	5	30	-	25	0.94	-	22	37	38	62	0.15	45
AP09347	342	18	-	-	148	-	-	40	35	-	10	0.92	-	25	29	46	54	0.17	35
AP09348	205	30	-	-	118	-	-	25	65	-	90	0.78	-	43	71	38	62	0.05	81
AP09349	205	16	-	-	140	-	-	0	20	-	-	0.82	-	37	24	60	40	0.25	27
AP09350	205	18	-	-	88	-	-	50	45	-	165	0.74	-	39	62	38	62	0.08	83
AP09351	616	44	-	-	260	-	-	10	20	-	60	0.81	-	22	38	37	63	0.11	46
AP09352	342	34	-	-	258	-	-	0	0	-	20	0.86	-	40	15	73	27	0.29	16
AP09353	411	42	-	-	258	-	-	0	0	-	50	0.90	-	26	31	46	54	0.19	34
AP09354	274	44	-	-	250	-	-	10	0	-	55	0.88	-	37	51	42	58	0.20	56
AP09355	958	38	-	-	180	-	-	0	0	-	10	0.85	-	57	30	65	35	0.48	36
AP09356	479	42	-	-	92	-	-	40	75	-	135	0.72	-	64	74	46	54	0.22	86
AP09357	342	54	-	-	258	-	-	0	0	-	60	0.89	-	53	50	51	49	0.30	52

SampleNo	UTMNorth (m)	UTMEast (m)	Al_2O_3 (%)	CaO (%)	Fe_2O_3 (%)	K_2O (%)	MgO (%)	MnO (%)	Na_2O (%)	P_2O_5 (%)	SiO_2 (%)	TiO_2 (%)	LOI (%)	CO_2 (%)
AP09358	5364035	449687	15.55	9.69	10.02	2.90	9.01	0.21	0.80	0.08	48.9	0.55	2.91	-
AP09359	5362034	448479	17.37	1.39	2.67	3.66	0.26	0.04	3.63	0.14	67.11	0.29	2.42	-
AP09360	5362067	448382	13.28	1.68	4.74	3.22	0.77	0.06	2.65	0.10	71.4	0.43	2.44	-
AP09361	5362692	448599	17.88	11.35	11.65	0.38	8.60	0.14	1.49	0.08	44.44	0.38	4.52	-
AP09362	5362511	447479	9.48	0.56	1.11	2.32	0.59	0.03	2.43	0.04	79.95	0.15	0.97	-
AP09364	5362426	447244	12.87	2.38	4.17	1.08	1.19	0.06	3.62	0.10	71.75	0.40	1.48	-
AP09365	5362951	447529	15.38	6.75	10.71	1.00	4.19	0.24	3.57	0.10	56.3	0.84	1.83	-
AP09366	5362230	447152	15.43	8.33	12.66	0.94	6.52	0.29	3.13	0.14	51.02	0.82	1.52	-
AP09367	5362438	447135	13.13	3.78	7.00	2.00	1.47	0.13	0.54	0.12	67.84	0.42	2.30	-
AP09368	5362707	447449	16.06	3.25	9.12	1.42	2.95	0.14	4.34	0.20	59.7	1.05	2.46	-
AP09369	5362290	447187	12.05	0.51	3.16	0.54	0.65	0.05	5.83	0.00	74.06	0.18	0.61	-
AP09370	5362624	447523	13.58	0.12	2.82	3.58	0.44	0.03	1.73	0.04	76.3	0.14	2.04	-
AP09371	5362286	447196	12.22	6.60	24.95	0.62	5.96	0.94	1.61	0.08	44.76	0.47	2.42	-
AP09372	5362468	447359	13.61	0.52	2.74	2.64	1.25	0.11	1.96	0.02	76.04	0.17	1.87	-
AP09373	5362570	447409	11.78	0.27	3.27	2.98	0.76	0.07	0.90	0.02	75.65	0.16	1.84	-
AP09374	5362406	447460	12.52	5.15	20.76	0.88	4.99	0.89	1.42	0.12	49.73	0.51	3.12	-
AP09375	5362587	447411	11.96	0.33	5.82	2.34	0.46	0.07	2.59	0.06	74.65	0.31	2.36	-
AP09385	5363904	449341	11.01	0.45	7.26	1.30	0.88	0.06	3.55	0.06	68.82	0.26	3.95	-
AP09386	5362434	446929	11.63	0.54	2.69	2.22	0.68	0.02	0.93	0.04	79.74	0.16	1.89	-
AP09387	5363319	448971	12.57	0.08	2.55	3.98	0.17	0.03	2.15	0.02	77.3	0.14	1.48	-
AP09389	5363896	449445	11.43	0.12	2.09	2.88	0.44	0.02	0.83	0.00	81.19	0.17	1.57	-
AP09390	5363184	449087	13.77	1.72	2.36	2.38	0.23	0.07	3.69	0.12	71.81	0.41	2.20	-
AP09391	5363379	448869	15.24	1.67	10.00	1.06	2.29	0.39	3.62	0.14	62.45	0.50	3.07	-
AP09392	5364002	449376	14.26	8.41	12.85	0.40	6.79	0.21	1.58	0.10	51.7	1.03	3.58	-
AP09393	5363836	449441	15.09	2.14	4.03	2.78	1.37	0.06	2.40	0.12	70.5	0.55	1.87	-
AP09394	5363999	449377	12.98	0.39	2.29	3.04	0.81	0.03	1.99	0.02	76.76	0.21	1.72	-
AP09395	5363884	449466	12.60	0.06	2.07	3.16	0.60	0.02	0.74	0.02	79.7	0.18	1.78	-
AP09396	5362608	446657	10.89	0.22	2.94	6.92	0.56	0.03	1.30	0.06	73.5	0.24	1.08	-
AP09397	5362630	448559	11.07	0.42	1.89	3.42	0.49	0.03	0.38	0.04	79.79	0.12	1.83	-
AP09398	5362217	448747	12.13	6.25	11.31	0.28	2.80	0.16	2.98	0.22	56.92	1.28	6.31	-
AP09399	5362411	448846	13.41	7.07	10.10	0.04	3.11	0.28	3.42	0.20	55.78	1.07	4.79	-
AP09400	5362040	448600	12.70	4.02	6.43	1.32	1.08	0.24	3.36	0.10	66.5	0.42	3.45	-
AP09601	5362027	448687	9.54	2.93	17.56	0.08	3.86	0.60	0.20	0.00	59.11	0.15	5.73	-
AP09602	5362335	448823	15.17	7.29	12.25	0.92	3.18	0.26	2.46	0.20	53.8	1.23	4.10	-
AP09603	5363979	449263	13.34	1.18	4.08	2.72	0.78	0.05	2.78	0.12	72.57	0.49	2.42	-
AP09604	5363631	449150	14.05	5.17	11.14	0.66	5.92	0.14	2.39	0.10	52.16	0.91	7.91	-
AP09605	5362269	447610	14.89	10.56	12.80	0.54	7.08	0.21	2.33	0.10	49.05	1.00	2.42	-
AP09606	5362100	447544	12.30	10.44	23.60	0.28	5.58	0.86	1.13	0.12	42.58	0.58	3.19	-
AP09607	5362278	447714	12.95	5.51	10.90	0.16	3.18	0.44	4.66	0.12	55.67	0.56	5.48	-
AP09608	5362450	447650	11.73	2.52	3.86	0.30	1.10	0.08	0.98	0.10	74.5	0.38	2.12	-
AP09609	5361607	446221	10.38	8.33	11.07	0.58	13.88	0.19	1.30	0.06	50.8	0.55	3.22	-
AP09610	5361532	446636	14.90	5.58	11.68	1.48	3.01	0.20	3.30	0.24	55.76	1.36	1.09	-
AP09612	5361373	446620	15.03	5.51	13.52	0.34	2.60	0.20	3.87	0.24	56.25	1.32	0.89	-
AP09613	5361470	446485	6.44	12.20	33.56	0.10	6.27	0.89	0.62	0.02	34.11	0.33	6.05	-
AP09614	5361222	446616	15.88	10.90	13.29	0.24	8.57	0.24	2.48	0.08	46.75	0.75	1.64	-

SampleNo	Cr (ppm)	Y (ppm)	Sc (ppm)	Sr (ppm)	Zr (ppm)	Au (ppb)	Ba (ppm)	Cu (ppm)	Ni (ppm)	Pb (ppm)	Zn (ppm)	Fe/Fe+Mg	CO_2/CaO	Ishikawa Index	Chlorite Index	SCI	CSI	K/Al	CCPI
AP09358	479	16	-	-	60	-	-	10	175	-	65	0.56	-	53	57	48	52	0.29	83
AP09359	205	4	-	-	64	-	-	0	25	-	40	0.92	-	44	23	65	35	0.33	27
AP09360	342	40	-	-	252	-	-	0	-	-	55	0.88	-	48	40	55	45	0.38	46
AP09361	479	4	-	-	28	-	-	420	320	-	50	0.61	-	41	59	41	59	0.03	91
AP09362	547	84	-	-	354	-	-	5	10	-	20	0.69	-	49	23	68	32	0.38	25
AP09364	958	38	-	-	270	-	-	25	5	-	25	0.80	-	27	41	40	60	0.13	51
AP09365	547	20	-	-	98	-	-	50	125	-	70	0.75	-	33	55	38	62	0.10	75
AP09366	342	16	-	-	98	-	-	105	135	-	60	0.69	-	39	59	40	60	0.10	81
AP09367	753	50	-	-	248	-	-	20	5	-	45	0.85	-	45	55	45	55	0.24	75
AP09368	274	22	-	-	148	-	-	0	30	-	25	0.78	-	37	55	40	60	0.14	66
AP09369	1574	98	-	-	292	-	-	0	35	-	10	0.85	-	16	34	32	68	0.07	35
AP09370	479	134	-	-	372	-	-	10	5	-	50	0.88	-	68	35	66	34	0.41	36
AP09371	205	18	-	-	96	-	-	90	80	-	55	0.83	-	44	76	37	63	0.08	93
AP09372	342	66	-	-	350	-	-	10	0	-	25	0.72	-	61	42	59	41	0.30	45
AP09373	479	72	-	-	272	-	-	0	20	-	50	0.83	-	76	47	62	38	0.40	49
AP09374	342	20	-	-	152	-	-	10	75	-	155	0.83	-	47	76	38	62	0.11	91
AP09375	205	40	-	-	402	-	-	20	15	-	25	0.94	-	49	52	48	52	0.31	54
AP09385	1300	28	-	-	248	-	-	10	10	-	115	0.91	-	35	58	38	62	0.19	60
AP09386	889	42	-	-	394	-	-	10	5	-	30	0.82	-	66	46	59	41	0.30	50
AP09387	547	110	-	-	338	-	-	10	10	-	55	0.95	-	65	28	70	30	0.50	29
AP09389	821	38	-	-	236	-	-	0	25	-	20	0.85	-	78	38	67	33	0.40	38
AP09390	616	52	-	-	282	-	-	0	10	-	20	0.92	-	33	23	58	42	0.27	28
AP09391	274	62	-	-	326	-	-	0	10	-	100	0.84	-	39	64	38	62	0.11	71
AP09392	274	34	-	-	86	-	-	70	85	-	90	0.69	-	42	64	40	60	0.04	90
AP09393	342	36	-	-	236	-	-	15	20	-	70	0.77	-	48	41	54	46	0.29	49
AP09394	342	46	-	-	250	-	-	5	15	-	150	0.77	-	62	35	64	36	0.37	36
AP09395	479	46	-	-	232	-	-	0	0	-	25	0.80	-	82	38	68	32	0.39	39
AP09396	342	120	-	-	292	-	-	30	55	-	85	0.86	-	83	28	75	25	1.00	28
AP09397	274	56	-	-	262	-	-	0	0	-	35	0.82	-	83	34	71	29	0.48	37
AP09398	68	36	-	-	182	-	-	20	20	-	60	0.82	-	25	58	30	70	0.04	80
AP09399	137	16	-	-	102	-	-	30	30	-	40	0.79	-	23	54	30	70	0.00	78
AP09400	342	44	-	-	332	-	-	20	50	-	95	0.87	-	25	44	36	64	0.16	59
AP09601	137	46	-	-	284	-	-	-	5	-	215	0.84	-	56	86	39	61	0.01	99
AP09602	68	20	-	-	136	-	-	15	25	-	80	0.82	-	30	57	34	66	0.10	81
AP09603	342	46	-	-	284	-	-	5	15	-	15	0.86	-	47	40	54	46	0.32	45
AP09604	274	28	-	-	98	-	-	60	65	-	110	0.69	-	47	66	41	59	0.07	84
AP09605	274	22	-	-	84	-	-	65	105	-	65	0.68	-	37	58	39	61	0.06	87
AP09606	205	26	-	-	80	-	-	135	125	-	105	0.83	-	34	69	33	67	0.04	95
AP09607	342	12	-	-	82	-	-	25	125	-	30	0.80	-	25	56	31	69	0.02	73
AP09608	547	28	-	-	256	-	-	0	0	-	20	0.80	-	29	55	34	66	0.04	78
AP09609	1300	12	-	-	62	-	-	30	390	-	30	0.48	-	60	70	46	54	0.09	93
AP09610	274	26	-	-	120	-	-	5	35	-	65	0.82	-	34	57	37	63	0.16	74
AP09612	411	30	-	-	138	-	-	20	25	-	115	0.86	-	24	60	28	72	0.04	78
AP09613	68	18	-	-	84	-	-	10	20	-	80	0.86	-	33	74	31	69	0.02	98
AP09614	411	16	-	-	48	-	-	105	170	-	70	0.64	-	40	60	40	60	0.02	88

SampleNo	UTMNorth (m)	UTMEast (m)	Al_2O_3 (%)	CaO (%)	Fe_2O_3 (%)	K_2O (%)	MgO (%)	MnO (%)	Na_2O (%)	P_2O_5 (%)	SiO_2 (%)	TiO_2 (%)	LOI (%)	CO_2 (%)
AP09615	5361820	446388	13.11	6.44	8.54	0.80	10.14	0.14	2.74	0.08	54.02	0.59	2.46	-
AP09618	5361657	446451	14.77	7.82	26.03	0.78	4.02	1.15	1.56	0.10	42.4	0.65	0.96	-
AP09621	5361758	446140	14.07	10.78	14.58	0.50	6.55	0.25	1.73	0.12	49.7	0.96	1.78	-
AP09623	5362537	446451	8.51	7.40	40.22	0.72	4.99	2.14	1.01	0.08	34.15	0.37	0.45	-
AP09624	5362683	446450	14.13	6.90	21.69	0.12	4.21	0.80	0.85	0.10	47.88	0.55	3.75	-
AP09625	5363238	446782	16.80	11.58	9.05	0.76	2.40	0.22	1.36	0.28	54.58	1.16	2.36	-
AP09626	5362645	446658	13.64	7.17	14.67	0.28	4.38	0.47	1.96	0.12	54.85	0.64	2.66	-
AP09627	5363097	446832	17.10	5.42	9.12	1.66	2.21	0.20	3.18	0.22	58.97	1.22	1.66	-
AP09628	5363475	447181	14.82	9.17	15.63	0.22	7.28	0.26	2.36	0.08	47.15	1.11	2.69	-
AP09629	5363176	446971	13.05	8.12	23.21	0.36	4.06	0.39	0.90	0.14	41.8	0.85	6.63	-
AP09630	5363650	447025	20.75	11.36	9.17	0.22	10.31	0.14	1.05	0.04	43.1	0.31	4.43	-
AP09631	5362343	446575	15.99	9.72	11.15	1.06	7.95	0.20	2.05	0.08	49.45	0.84	2.15	-
AP09632	5362609	446659	14.95	3.37	13.94	1.48	7.46	0.31	1.09	0.10	50.08	1.05	6.31	-
AP09633	5362289	446562	17.15	6.69	13.01	0.50	4.47	0.32	3.15	0.10	52.16	0.75	2.06	-
AP09634	5362612	446660	13.96	7.97	15.12	0.34	7.58	0.24	2.73	0.10	50.54	1.10	1.32	-
AP09635	5361837	446291	15.63	5.55	9.63	1.16	2.88	0.21	2.65	0.22	58.18	0.96	2.00	-
AP09636	5362621	446569	16.20	2.36	5.45	3.04	1.51	0.09	3.70	0.10	62.4	0.53	2.17	-
AP09637	5361870	446299	17.06	4.68	8.13	1.34	2.69	0.13	3.66	0.10	60.06	0.48	1.90	-
AP09638	5362533	446686	13.37	5.96	13.06	0.70	4.03	0.41	2.42	0.12	59.1	0.56	1.16	-
AP09639	5362609	446660	10.49	1.07	4.50	0.94	1.21	0.09	3.51	0.04	74.38	0.21	1.58	-
AP09640	5362512	446650	14.90	5.38	12.23	1.24	2.97	0.53	2.32	0.12	58.51	0.59	1.91	-
AP09641	5362246	446295	14.12	2.14	6.91	0.58	1.43	0.11	4.15	0.08	67.58	0.45	1.54	-
AP09642	5362442	446403	14.60	8.06	8.69	1.02	3.86	0.24	2.90	0.12	56.1	0.58	1.57	-
AP09643	5363345	446707	16.74	8.27	9.13	0.94	4.02	0.16	3.79	0.20	52.32	1.16	1.73	-
AP09644	5363646	449168	13.23	0.58	4.04	2.96	1.19	0.05	0.82	0.04	72.35	0.25	2.18	-
AP09645	5363738	449071	12.66	-0.01	1.70	3.86	0.56	0.01	0.21	0.04	76.6	0.11	1.80	-
AP09646	5363603	449235	12.59	1.36	2.07	1.84	0.33	0.05	4.24	0.06	72.85	0.22	1.95	-
AP09650	5362100	446760	15.07	4.44	11.40	1.12	2.90	0.17	3.72	0.18	58.28	0.64	2.72	-
AP09801	5363013	449756	15.61	2.91	5.16	2.14	1.70	0.09	2.45	0.14	65.32	0.53	4.11	-
AP09802	5363012	449757	14.94	3.75	5.32	1.30	0.88	0.10	3.73	0.10	65.05	0.48	4.48	-
AP09803	5363089	449744	15.86	0.24	2.35	1.68	0.13	0.04	4.41	0.10	70.2	0.52	2.18	-
AP09845	5362318	446157	13.13	2.88	6.78	2.38	1.08	0.15	2.75	0.22	68.1	0.67	2.85	-
AP09905	5364002	448836	9.72	1.48	16.29	0.10	8.54	0.22	0.18	0.06	53.39	0.26	8.29	-
AP09906	5364000	448830	11.60	1.23	2.29	2.50	0.86	0.04	0.87	0.02	76.66	0.32	1.49	-
AP09909	5363943	448820	12.41	0.73	3.69	0.80	0.76	0.06	4.84	0.10	74.11	0.42	1.25	-
AP09910	5363938	448816	10.28	0.09	1.73	0.32	0.51	0.03	5.19	0.02	81.2	0.10	0.47	-
AP09911	5363938	448816	12.90	0.09	3.92	2.78	1.49	0.06	1.19	0.02	74.74	0.12	2.11	-
AP09915	5361831	447984	15.35	9.96	8.76	0.44	3.60	0.21	2.39	0.16	52.11	0.87	5.81	-
AP09931	5362915	447394	17.63	5.26	7.38	1.66	1.97	0.15	4.50	0.28	58.27	0.82	1.74	-
AP09932	5362913	447395	16.74	6.19	8.30	0.84	2.45	0.18	3.97	0.22	57.54	0.82	2.44	-
AP09933	5362958	447340	12.10	9.95	26.68	0.46	6.48	0.96	1.01	0.12	39.35	0.63	2.08	-
AP09934	5362410	447331	11.90	0.71	3.63	3.34	0.87	0.10	0.78	0.04	76.72	0.17	1.70	-
AP09935	5362974	447400	17.67	6.24	7.00	1.32	2.54	0.12	2.63	0.16	58.98	0.79	2.41	-
AR01383	5362363	447629	1.49	2.34	19.30	0.14	3.11	0.96	0.10	0.00	62.35	0.10	8.35	-
AR01384	5362360	447632	13.16	7.96	16.30	0.18	5.10	0.46	2.37	0.18	51.08	1.46	2.53	-

SampleNo	Cr (ppm)	Y (ppm)	Sc (ppm)	Sr (ppm)	Zr (ppm)	Au (ppb)	Ba (ppm)	Cu (ppm)	Ni (ppm)	Pb (ppm)	Zn (ppm)	Fe/Fe+Mg	CO_2/CaO	Ishikawa Index	Chlorite Index	SCI	CSI	K/Al	CCPI
AP09615	616	10	-	-	60	-	-	15	320	-	20	0.49	-	54	64	46	54	0.10	83
AP09618	342	28	-	-	90	-	-	35	125	-	115	0.88	-	34	73	32	68	0.08	92
AP09621	547	22	-	-	70	-	-	25	65	-	85	0.72	-	36	60	37	63	0.06	90
AP09623	205	14	-	-	98	-	-	0	60	-	110	0.90	-	40	82	33	67	0.13	96
AP09624	205	16	-	-	96	-	-	0	80	-	125	0.86	-	36	75	32	68	0.01	96
AP09625	411	32	-	-	162	-	-	10	40	-	375	0.81	-	20	43	31	69	0.07	83
AP09626	616	14	-	-	100	-	-	25	110	-	255	0.80	-	34	65	34	66	0.03	89
AP09627	411	22	-	-	132	-	-	20	30	-	55	0.83	-	31	50	38	62	0.15	68
AP09628	205	22	-	-	54	-	-	25	75	-	180	0.71	-	39	64	38	62	0.02	89
AP09629	411	22	-	-	92	-	-	120	65	-	190	0.87	-	33	73	31	69	0.04	95
AP09630	137	4	-	-	22	-	-	50	340	-	105	0.51	-	46	60	44	56	0.02	94
AP09631	342	20	-	-	68	-	-	45	180	-	35	0.62	-	43	58	43	57	0.10	85
AP09632	342	24	-	-	78	-	-	40	105	-	205	0.68	-	67	77	46	54	0.16	89
AP09633	479	14	-	-	72	-	-	135	150	-	90	0.77	-	34	61	35	65	0.05	82
AP09634	342	20	-	-	70	-	-	160	70	-	85	0.70	-	43	66	39	61	0.04	87
AP09635	616	22	-	-	200	-	-	35	110	-	65	0.79	-	33	55	37	63	0.12	75
AP09636	958	58	-	-	478	-	-	25	25	-	55	0.81	-	43	41	51	49	0.29	49
AP09637	411	14	-	-	92	-	-	45	130	-	40	0.78	-	33	51	39	61	0.12	67
AP09638	821	14	-	-	98	-	-	35	100	-	60	0.79	-	36	63	36	64	0.08	83
AP09639	1300	40	-	-	178	-	-	40	35	-	765	0.81	-	32	49	40	60	0.14	54
AP09640	547	16	-	-	108	-	-	20	75	-	60	0.83	-	35	61	37	63	0.13	80
AP09641	616	8	-	-	82	-	-	10	30	-	45	0.85	-	24	53	31	69	0.06	62
AP09642	616	12	-	-	86	-	-	20	120	-	60	0.72	-	31	49	38	62	0.11	75
AP09643	205	22	-	-	128	-	-	15	115	-	55	0.72	-	29	48	38	62	0.09	72
AP09644	821	48	-	-	238	-	-	10	35	-	65	0.80	-	75	53	59	41	0.35	56
AP09645	616	40	-	-	240	-	-	5	10	-	45	0.78	-	96	34	74	26	0.48	34
AP09646	342	46	-	-	330	-	-	20	-	-	110	0.88	-	28	23	55	45	0.23	27
AP09650	342	20	-	-	116	-	-	0	50	-	60	0.82	-	33	59	36	64	0.12	73
AP09801	274	22	-	-	156	-	-	30	30	-	70	0.78	-	42	46	48	52	0.22	58
AP09802	342	24	-	-	156	-	-	0	30	-	85	0.88	-	23	39	37	63	0.14	53
AP09803	616	24	-	-	156	-	-	0	15	-	40	0.95	-	28	26	52	48	0.17	27
AP09845	274	66	-	-	450	-	-	130	10	-	65	0.88	-	38	47	45	55	0.28	58
AP09905	411	70	-	-	338	-	-	65	15	-	850	0.69	-	84	93	47	53	0.02	99
AP09906	821	58	-	-	380	-	-	15	35	-	50	0.76	-	62	39	61	39	0.34	46
AP09909	1232	44	-	-	186	-	-	265	20	-	40	0.85	-	22	39	36	64	0.10	42
AP09910	1163	52	-	-	176	-	-	20	15	-	15	0.80	-	14	27	34	66	0.05	27
AP09911	616	88	-	-	258	-	-	0	25	-	50	0.75	-	77	55	58	42	0.34	56
AP09915	547	20	-	-	80	-	-	50	75	-	285	0.74	-	25	47	34	66	0.04	80
AP09931	1026	28	-	-	114	-	-	500	35	-	190	0.81	-	27	43	39	61	0.15	58
AP09932	684	28	-	-	108	-	-	90	50	-	200	0.80	-	24	47	34	66	0.08	67
AP09933	274	20	-	-	94	-	-	45	40	-	120	0.83	-	39	73	35	65	0.06	95
AP09934	547	94	-	-	298	-	-	15	20	-	30	0.83	-	74	46	62	38	0.44	50
AP09935	547	24	-	-	96	-	-	75	45	-	110	0.76	-	30	46	39	61	0.12	69
AR01383	547	8	-	-	56	-	-	30	40	-	10	0.88	-	57	89	39	61	0.15	99
AR01384	274	26	-	-	102	-	-	0	50	-	40	0.79	-	34	65	34	66	0.02	89

SampleNo	UTMNorth (m)	UTMEast (m)	Al_2O_3 (%)	CaO (%)	Fe_2O_3 (%)	K_2O (%)	MgO (%)	MnO (%)	Na_2O (%)	P_2O_5 (%)	SiO_2 (%)	TiO_2 (%)	LOI (%)	CO_2 (%)
AR01385	5362344	447623	11.65	6.73	23.11	0.66	5.32	1.23	1.52	0.10	47.71	0.51	1.93	-
AR01386	5362346	447627	15.27	2.02	15.91	0.28	4.31	0.80	4.02	0.16	53.71	0.67	3.04	-
AR01387	5362350	447627	7.67	5.37	29.77	0.52	4.55	1.01	0.71	0.06	45.13	0.34	5.61	-
AR01389	5362293	447654	14.18	4.34	15.94	0.16	3.90	0.70	3.54	0.12	53.27	0.58	3.97	-
AR01390	5362292	447654	11.51	2.14	24.57	0.76	3.45	0.77	2.06	0.12	50.06	0.55	4.97	-
AR01391	5362297	447658	4.51	1.82	52.56	0.58	4.18	1.37	0.11	0.04	26.2	0.22	9.10	-
AR01392	5362303	447660	12.00	1.53	18.10	0.24	5.06	0.80	1.95	0.12	53.72	0.81	5.44	-
AT04301	5363208	453878	15.12	3.46	3.38	1.76	0.92	0.08	3.63	0.16	63.95	0.54	6.30	-
AT04302	5363227	453877	11.39	2.14	3.60	2.72	1.59	0.07	0.63	0.12	71.96	0.42	6.16	-
AT04303	5363233	453876	12.28	1.56	2.83	3.18	0.98	0.05	0.47	0.12	72.55	0.38	4.83	-
AT04304	5363239	453876	13.23	6.96	8.63	2.72	3.46	0.15	1.54	0.22	47.74	1.22	14.19	-
AT04305	5363257	453875	13.32	6.67	8.80	2.32	3.56	0.13	1.88	0.26	48.7	1.38	13.84	-
AT04306	5363276	453874	12.30	6.94	8.99	1.82	3.69	0.14	2.16	0.26	49.18	1.31	14.13	-
AT04307	5363282	453874	11.42	2.60	4.31	1.76	0.96	0.06	2.86	0.12	70.32	0.51	5.40	-
AT04308	5363285	453874	11.33	2.75	4.28	2.16	1.15	0.06	1.51	0.14	67.85	0.47	6.42	-
AT04309	5363290	453873	13.20	8.02	6.97	2.46	3.42	0.11	1.14	0.18	46.71	1.20	14.59	-
AT04310	5363303	453873	10.95	3.05	4.72	2.04	1.04	0.07	2.26	0.12	69.48	0.51	6.12	-
AT04311	5363309	453873	13.93	7.93	6.81	2.30	3.07	0.11	2.63	0.18	49.34	1.30	13.38	-
AT04312	5363329	453872	13.82	7.18	7.68	1.48	3.90	0.12	2.56	0.20	49.53	1.30	12.50	-
AT04313	5363333	453872	11.18	2.18	3.98	1.40	0.91	0.06	3.12	0.12	70.54	0.49	4.75	-
AT04314	5363340	453872	13.05	6.93	7.63	1.84	3.40	0.12	1.94	0.22	48.16	1.22	13.77	-
AT04315	5363346	453872	12.28	2.23	3.48	2.22	1.32	0.06	2.78	0.06	70.51	0.24	5.36	-
AT04316	5363366	453871	11.81	2.05	3.58	1.76	0.61	0.07	3.87	0.06	71.77	0.21	4.47	-
AT04318	5363460	453879	12.34	6.36	8.19	1.78	3.46	0.14	2.25	0.28	49.57	1.33	13.21	-
AT04319	5363472	453879	10.73	1.71	4.63	1.56	1.15	0.07	3.12	0.12	69.25	0.49	5.19	-
AT04320	5363505	453879	11.92	2.03	3.79	1.88	1.25	0.06	2.86	0.06	68.94	0.22	5.60	-
AT04321	5363525	453879	11.72	2.55	3.68	2.10	0.83	0.05	3.20	0.06	70.64	0.22	5.31	-
EVH13102	5355211	459375	15.04	3.19	3.98	0.22	1.33	0.04	2.93	0.27	-	0.58	-	-
EVH13104	5355303	459375	14.80	3.21	5.83	0.41	2.54	0.10	1.58	1.52	-	1.45	-	-
EVH13106	5355331	459375	16.94	1.70	6.43	1.41	2.61	0.08	0.90	0.14	-	0.66	-	-
EVH13110	5355272	459375	12.62	9.12	4.25	0.29	2.42	0.09	0.86	0.40	-	0.50	-	-
EVH13112	5355527	459418	13.35	4.34	3.20	0.27	1.32	0.05	2.40	0.40	-	0.65	-	-
EVH13114	5355608	459418	15.93	3.89	3.14	0.83	1.55	0.04	1.95	0.14	-	0.40	-	-
EVH13116	5355633	459418	10.83	7.05	4.22	0.40	1.90	0.05	1.73	0.59	-	1.10	-	-
EVH13120	5355298	461496	11.24	6.65	11.38	0.22	4.78	0.25	0.29	0.09	-	1.13	-	-
EVH13121	5356704	457455	14.52	2.25	2.37	2.41	0.27	0.03	1.02	0.36	-	0.20	-	-
EVH13123	5356696	457455	8.96	26.97	21.44	0.87	1.55	0.30	1.85	0.62	-	2.54	-	-
EVH13124	5356634	457455	4.65	19.00	16.03	0.16	10.42	0.41	0.97	0.95	-	2.35	-	-
EVH13126	5360070	458868	16.75	3.16	7.49	0.73	3.49	0.07	1.41	0.38	-	1.10	2.97	0.39
EVH13140	5364177	457475	11.27	0.78	1.99	0.39	0.79	0.01	1.66	0.07	-	0.38	-	-
EVH13144	5364148	457644	9.19	2.38	5.98	0.50	0.54	0.05	1.52	0.08	-	0.35	-	-
EVH13151	5354070	455222	12.87	15.46	7.62	0.41	2.56	0.29	1.00	0.05	-	0.57	-	-
EVH13152	5354029	455246	10.40	8.74	0.00	0.12	6.02	0.47	1.19	0.11	42.45	1.63	12.45	16.42
EVH13153	5354373	453993	16.64	4.25	4.80	2.07	0.69	0.06	0.42	0.06	57.62	0.43	9.09	3.87
EVH13154	5354415	453968	12.63	8.06	13.80	0.03	3.07	0.21	0.70	0.13	46.82	1.60	9.09	3.87

SampleNo	Cr (ppm)	Y (ppm)	Sc (ppm)	Sr (ppm)	Zr (ppm)	Au (ppb)	Ba (ppm)	Cu (ppm)	Ni (ppm)	Pb (ppm)	Zn (ppm)	Fe/Fe+Mg	CO_2/CaO	Ishikawa Index	Chlorite Index	SCI	CSI	K/Al	CCPI
AR01385	205	14	-	-	104	-	-	0	55	-	20	0.83	-	42	75	36	64	0.09	92
AR01386	274	16	-	-	104	-	-	0	65	-	25	0.81	-	43	75	37	63	0.03	81
AR01387	205	14	-	-	78	-	-	45	30	-	20	0.88	-	45	83	36	64	0.11	96
AR01389	205	18	-	-	102	-	-	0	80	-	10	0.83	-	34	69	33	67	0.02	83
AR01390	137	16	-	-	96	-	-	45	20	-	-	0.89	-	50	84	37	63	0.10	90
AR01391	68	12	-	-	80	-	-	45	10	-	-	0.94	-	71	95	43	57	0.20	99
AR01392	205	20	-	-	84	-	-	0	40	-	45	0.81	-	60	85	41	59	0.03	91
AT04301	205	16	13	-	142	-	-	110	30	-	15	0.81	-	27	31	47	53	0.18	42
AT04302	-	46	11	-	254	-	-	10	30	-	65	0.72	-	61	47	57	43	0.37	59
AT04303	-	40	8	-	234	-	-	5	-	-	45	0.77	-	67	40	62	38	0.41	49
AT04304	205	26	22	-	158	-	-	20	75	-	105	0.74	-	42	50	46	54	0.32	72
AT04305	137	30	19	-	190	-	-	35	55	-	120	0.74	-	41	51	44	56	0.27	73
AT04306	137	30	18	-	186	-	-	40	45	-	55	0.74	-	38	52	42	58	0.23	75
AT04307	205	60	10	-	300	-	-	10	5	-	35	0.84	-	33	40	45	55	0.24	51
AT04308	68	48	10	-	284	-	-	0	10	-	45	0.81	-	44	44	50	50	0.30	58
AT04309	274	20	25	-	122	-	-	50	80	-	65	0.70	-	39	45	46	54	0.29	73
AT04310	205	58	11	-	274	-	-	10	10	-	50	0.84	-	37	42	47	53	0.29	55
AT04311	205	24	25	-	136	-	-	70	85	-	60	0.72	-	34	42	45	55	0.26	65
AT04312	205	24	26	-	134	-	-	35	105	-	85	0.70	-	36	49	42	58	0.17	73
AT04313	205	62	11	-	298	-	-	5	25	-	70	0.84	-	30	40	43	57	0.20	50
AT04314	205	24	23	-	142	-	-	30	60	-	75	0.72	-	37	49	43	57	0.22	73
AT04315	205	76	5	-	354	-	-	0	25	-	75	0.75	-	41	38	52	48	0.28	47
AT04316	205	70	4	-	348	-	-	10	30	-	35	0.87	-	29	33	46	54	0.23	40
AT04318	68	32	18	-	212	-	-	25	45	-	155	0.73	-	38	51	43	57	0.23	73
AT04319	274	62	9	-	304	-	-	5	15	-	60	0.82	-	36	45	44	56	0.23	53
AT04320	205	78	5	-	394	-	-	10	15	-	75	0.78	-	39	41	49	51	0.25	50
AT04321	205	76	4	-	376	-	-	10	25	-	110	0.84	-	34	35	49	51	0.28	44
EVH13102	50	0	-3	39	212	136	785	8	0	0	16	0.78	-	20	44	32	68	0.68	61
EVH13104	152	15	11	60	154	54	444	7	63	2	36	0.73	-	38	60	39	61	0.22	80
EVH13106	89	0	18	69	171	0	643	17	14	19	49	0.74	-	61	68	47	53	8.06	78
EVH13110	50	0	10	43	89	0	420	11	0	25	20	0.67	-	21	38	36	64	0.60	84
EVH13112	61	0	0	33	115	217	579	12	0	4	16	0.74	-	19	37	34	66	0.56	61
EVH13114	-	-	8	-	-	0	404	8	0	0	7	0.70	-	29	40	42	58	5.06	61
EVH13116	203	0	3	46	92	0	379	5	17	4	32	0.72	-	21	38	35	65	0.56	73
EVH13120	73	7	36	129	50	381	202	22	41	7	54	0.73	-	42	68	38	62	2.08	97
EVH13121	25	44	0	2	496	69	2396	3	0	1	9	0.91	-	45	30	60	40	5.50	41
EVH13123	5	29	18	236	241	51	802	23	0	10	62	0.94	-	8	41	16	84	1.17	88
EVH13124	2	21	9	196	157	0	408	3	0	5	207	0.64	-	35	55	39	61	0.14	96
EVH13126	101	2	19	82	226	0	813	18	10	32	60	0.71	0.16	41	60	41	59	0.07	74
EVH13140	59	0	0	17	148	0	358	2	0	0	11	0.74	-	33	48	41	59	0.05	56
EVH13144	45	47	6	64	210	0	472	6	0	25	54	0.93	-	21	57	27	73	0.08	75
EVH13151	165	19	37	104	24	0	246	14	105	13	59	0.78	-	15	35	30	70	0.05	83
EVH13152	81	32	49	175	170	0	178	19	24	16	57	-	2.39	39	38	51	49	0.02	85
EVH13153	162	13	31	114	121	195	762	43	197	0	77	0.89	1.16	35	41	46	54	0.19	63
EVH13154	-	-	55	-	-	0	195	5	0	11	50	0.84	0.61	23	60	28	72	0.00	86

SampleNo	UTMNorth (m)	UTMEast (m)	Al_2O_3 (%)	CaO (%)	Fe_2O_3 (%)	K_2O (%)	MgO (%)	MnO (%)	Na_2O (%)	P_2O_5 (%)	SiO_2 (%)	TiO_2 (%)	LOI (%)	CO_2 (%)
EVH13155	5355365	454538	17.79	10.10	18.14	0.12	4.64	0.22	2.18	0.08	36.77	2.74	7.13	0.10
EVH13156	5355308	454571	15.11	7.02	2.37	0.04	2.24	0.23	1.68	0.08	64.86	0.74	4.32	1.31
EVH13157	5366069	454763	13.31	7.53	12.09	0.02	4.54	0.11	2.65	0.36	44.74	1.81	7.92	4.91
EVH13158	5366153	454847	14.94	7.59	13.37	0.04	5.59	0.17	2.61	0.07	39.69	1.11	9.06	5.76
EVH13159	5352960	454366	10.84	5.25	11.45	0.01	11.61	0.15	1.35	0.08	54.16	0.55	4.27	0.30
EVH13160	5352960	454366	10.19	1.83	2.49	0.41	1.55	0.08	0.98	0.07	74.53	0.36	4.58	2.94
EVH13161	5355465	459016	13.88	3.61	2.50	0.73	1.68	0.07	3.54	0.18	58.17	0.30	9.98	5.37
EVH13162	5355440	459016	14.78	3.20	5.30	0.87	1.43	0.04	1.98	0.08	60.51	0.44	5.53	5.85
EVH13163	5355394	459016	9.87	6.00	4.33	0.19	2.87	0.07	0.69	0.08	-	0.32	11.11	-
EVH13164	5356203	465751	8.53	4.43	16.03	0.02	5.76	0.46	1.66	0.02	61.14	0.46	1.04	0.46
EVH13165	5356298	465751	16.04	0.88	4.72	0.28	1.75	0.04	4.57	0.20	69.56	0.59	1.39	-
EVH13166	5356264	465751	16.71	0.59	6.16	0.50	2.48	0.05	1.00	0.16	-	0.63	3.35	0.31
EVH13167	5360825	460654	13.49	5.10	10.18	0.15	8.04	0.14	0.01	0.04	51.32	0.67	7.93	2.94
EVH13168	5360819	460657	14.42	8.70	9.24	0.00	4.86	0.17	2.04	0.05	54.87	0.71	3.44	1.50
EVH13169	5360800	460668	15.22	2.38	6.15	0.37	2.44	0.07	1.44	0.13	63.92	0.61	4.77	2.50
EVH13170	5360762	460690	10.48	6.87	14.07	0.21	4.78	0.21	1.28	0.18	58.45	1.30	2.05	0.14
EVH13171	5360727	460710	14.17	0.98	5.64	0.77	1.86	0.07	1.80	0.10	70.82	0.52	2.88	0.38
EVH13172	5360683	460735	14.72	2.19	5.66	0.24	2.27	0.06	2.21	0.13	68.29	0.59	2.86	0.79
EVH13173	5360655	460752	17.97	2.91	6.87	0.58	3.09	0.08	1.37	0.19	61.71	0.73	3.41	1.10
EVH13174	5355664	464522	12.91	2.26	2.32	0.69	0.60	0.02	0.30	0.11	62.08	0.31	6.12	12.28
EVH13175	5355586	464477	12.78	4.51	4.49	0.61	1.67	0.07	1.91	0.16	63.10	0.43	6.01	4.27
EVH13176	5355542	464451	14.10	2.76	5.64	0.33	2.50	0.06	2.59	0.09	66.38	0.56	3.63	1.35
EVH13177	5355005	461896	15.99	1.87	4.07	0.23	1.96	0.04	1.43	0.08	65.19	0.54	5.25	3.37
EVH13178	5355743	464440	11.17	1.92	1.73	0.30	0.98	0.04	3.73	0.08	73.64	0.10	3.23	3.08
EVH13179	5355748	464443	12.49	3.10	4.52	0.64	1.72	0.07	2.22	0.11	61.70	0.41	7.45	5.57
EVH13180	5355771	464456	12.31	4.36	5.83	0.35	2.27	0.06	2.80	0.13	58.70	0.49	6.13	6.56
EVH13181	5356697	462792	11.01	7.28	12.06	0.12	4.54	0.17	1.29	0.08	61.07	0.85	1.46	0.07
EVH13182	5356801	462830	13.39	3.26	6.13	0.40	2.33	0.08	1.62	0.10	64.07	0.54	5.00	3.08
EVH13183	5356918	462872	12.85	1.00	4.10	1.02	2.11	0.03	1.03	0.19	74.01	0.35	2.95	0.36
EVH13184	5361503	459599	15.32	5.64	19.32	0.00	14.02	0.15	2.03	0.10	30.08	0.91	8.04	4.38
EVH13185	5361462	459623	13.65	9.01	12.13	0.02	6.11	0.15	1.82	0.06	51.91	0.85	3.36	0.95
EVH13186	5361418	459648	15.96	4.46	13.60	0.04	6.25	0.21	3.37	0.06	51.90	0.88	3.23	0.05
EVH13187	5363416	460203	13.30	10.35	9.71	0.07	4.39	0.22	1.45	0.08	23.47	0.79	18.01	18.15
EVH13188	5355029	462304	12.49	2.34	8.57	0.03	3.69	0.09	0.52	0.08	61.75	0.62	6.23	3.59
EVH13189	5354937	462304	12.97	2.51	6.14	0.40	1.84	0.07	1.17	0.08	64.95	0.51	5.48	3.88
EVH13190	5355184	461966	13.19	5.86	7.79	0.24	4.65	0.10	0.92	0.11	57.30	0.49	5.48	3.88
EVH13191	5355132	461966	12.82	3.20	5.62	0.23	2.19	0.08	1.45	0.09	60.76	0.54	6.90	6.10
EVH13192	5363307	460010	9.11	6.48	10.86	0.02	3.77	0.21	0.46	0.06	31.21	0.54	17.94	19.34
EVH13193	5363360	459979	13.07	6.55	0.00	0.01	19.73	0.16	0.00	0.05	40.51	0.80	11.32	7.80
EVH13194	5363372	459973	13.70	7.32	13.86	0.06	4.71	0.18	2.59	0.06	41.67	0.88	8.68	6.29
EVH13195	5363437	460452	12.01	14.87	7.98	0.03	2.52	0.23	1.16	0.04	28.08	0.59	16.00	16.49
EVH13196	5363303	460156	16.49	15.34	15.64	0.14	8.31	0.24	1.74	0.03	-	0.92	-	-
EVH13197	5363358	460249	10.60	2.73	3.98	0.46	0.74	0.07	0.85	0.07	40.46	0.51	19.08	20.45
EVH13198	5364269	459217	12.66	1.39	3.17	0.76	0.52	0.04	1.81	0.06	73.84	0.23	3.37	2.15
EVH13199	5364250	459222	12.14	1.83	2.37	0.72	0.45	0.03	2.01	0.04	73.88	0.21	3.67	2.66

SampleNo	Cr (ppm)	Y (ppm)	Sc (ppm)	Sr (ppm)	Zr (ppm)	Au (ppb)	Ba (ppm)	Cu (ppm)	Ni (ppm)	Pb (ppm)	Zn (ppm)	Fe/Fe+Mg	CO_2/CaO	Ishikawa Index	Chlorite Index	SCI	CSI	K/Al	CCPI
EVH13155	1018	37	65	232	265	0	196	12	66	0	45	0.82	0.01	28	63	31	69	0.01	91
EVH13156	226	21	42	195	90	0	6	21	107	0	72	0.55	0.24	21	33	38	62	0.00	71
EVH13157	-	-	26	-	-	0	70	4	22	0	28	0.76	0.83	37	66	36	64	0.00	98
EVH13158	87	83	44	31	106	0	64	30	0	0	102	0.74	0.97	40	67	37	63	0.00	94
EVH13159	783	0	29	178	75	0	20	12	117	6	36	0.53	0.07	62	75	45	55	0.00	92
EVH13160	96	17	8	46	246	0	165	2	0	11	20	0.65	2.04	41	54	43	57	0.06	73
EVH13161	29	24	9	144	97	892	784	8	0	0	146	0.63	-	32	41	44	56	0.08	65
EVH13162	85	13	16	72	223	925	342	7	0	0	33	0.81	2.33	35	55	39	61	0.09	77
EVH13163	-	-	11	-	-	-	269	2	0	0	15	0.64	-	30	48	38	62	0.03	83
EVH13164	3059	16	38	209	38	-	149	6	565	1	28	0.76	0.13	54	81	40	60	0.00	98
EVH13165	-	-	29	-	-	-	351	5	0	0	58	0.76	-	56	76	42	58	0.03	86
EVH13166	-	-	22	-	-	248	780	1	19	0	48	0.74	0.66	52	71	42	58	0.05	75
EVH13167	-	-	32	-	-	0	218	10	101	0	27	0.59	0.73	55	71	43	57	0.02	90
EVH13168	236	20	32	108	96	0	10	47	100	0	37	0.69	0.22	30	54	36	64	0.00	83
EVH13169	121	18	23	88	272	7	391	9	0	6	24	0.75	1.34	36	60	38	62	0.04	73
EVH13170	28	27	28	227	187	7	649	89	0	0	70	0.77	0.03	38	67	36	64	0.03	92
EVH13171	104	20	16	63	248	0	560	10	0	0	37	0.78	0.50	57	72	44	56	0.09	80
EVH13172	169	15	12	71	243	0	364	13	0	4	29	0.74	0.46	30	55	36	64	0.03	66
EVH13173	103	0	17	72	232	0	810	23	17	9	26	0.72	0.48	43	63	41	59	0.05	78
EVH13174	-	-	8	-	-	-	723	30	0	0	336	0.82	6.92	30	42	42	58	0.08	66
EVH13175	-	-	14	-	-	0	591	10	0	18	59	0.76	1.21	27	46	37	63	0.07	72
EVH13176	-	-	28	-	-	0	281	5	23	0	58	0.72	0.62	28	50	36	64	0.04	61
EVH13177	116	41	6	211	217	167	701	131	0	0	22	0.71	2.29	43	64	40	60	0.02	82
EVH13178	36	50	2	516	276	0	1887	9	0	0	48	0.67	2.04	40	53	43	57	0.04	89
EVH13179	-	-	11	-	-	0	613	9	0	1	41	0.75	2.28	31	50	39	61	0.08	68
EVH13180	-	-	12	-	-	134	329	7	0	0	45	0.75	1.91	31	55	36	64	0.05	81
EVH13181	-	-	41	-	-	12	213	41	0	0	42	0.75	0.01	35	64	36	64	0.02	92
EVH13182	184	12	16	84	148	0	255	24	22	0	43	0.75	1.20	35	59	37	63	0.05	78
EVH13183	-	-	8	-	-	0	620	4	0	11	34	0.69	0.46	49	58	46	54	0.12	64
EVH13184	388	23	32	181	58	6	10	45	110	0	55	0.62	0.99	67	82	45	55	0.00	96
EVH13185	-	-	30	-	-	0	11	36	51	0	51	0.70	0.13	40	65	38	62	0.00	98
EVH13186	153	49	42	25	68	0	18	26	103	9	99	0.72	0.01	50	74	40	60	0.00	90
EVH13187	-	-	39	-	-	7	41	44	55	0	49	0.72	2.23	26	50	34	66	0.01	83
EVH13188	206	34	19	95	118	5	423	3	131	0	26	0.73	1.95	50	75	40	60	0.00	89
EVH13189	-	-	10	-	-	16	611	9	0	0	55	0.79	1.97	26	53	33	67	0.05	64
EVH13190	-	-	24	-	-	27	458	4	2	14	12	0.66	0.84	38	58	39	61	0.03	83
EVH13191	127	45	10	89	178	134	250	10	5	15	23	0.75	2.43	29	54	35	65	0.03	71
EVH13192	-	-	57	-	-	5	54	33	142	1	89	0.77	3.80	33	63	34	66	0.00	91
EVH13193	-	-	33	-	-	7	57	20	29	8	29	-	1.51	71	71	50	50	0.00	92
EVH13194	-	-	45	-	-	0	42	116	47	0	94	0.77	1.09	36	67	35	65	0.01	94
EVH13195	58	27	21	105	92	24	141	15	58	0	37	0.79	1.41	13	36	26	74	0.00	82
EVH13196	-	-	32	-	-	0	178	48	104	0	73	0.69	-	33	56	37	63	0.01	92
EVH13197	21	128	12	30	303	6	753	1	0	6	29	0.86	9.55	16	40	29	71	0.07	53
EVH13198	-	-	6	-	-	0	679	7	0	0	25	0.88	1.97	31	48	39	61	0.09	60
EVH13199	32	213	7	28	531	0	451	13	0	0	38	0.86	1.85	33	46	42	58	0.09	68

SampleNo	UTMNorth (m)	UTMEast (m)	Al_2O_3 (%)	CaO (%)	Fe_2O_3 (%)	K_2O (%)	MgO (%)	MnO (%)	Na_2O (%)	P_2O_5 (%)	SiO_2 (%)	TiO_2 (%)	LOI (%)	CO_2 (%)
EVH13200	5362945	458817	13.85	7.70	7.94	0.03	6.67	0.12	0.32	0.04	44.99	0.51	11.07	6.76
EVH13201	5362888	458832	14.50	6.97	0.00	0.06	10.17	0.16	1.79	0.06	29.58	0.93	17.49	18.29
EVH13202	5362780	458865	10.95	21.56	9.93	0.03	10.53	0.26	0.43	0.61	-	0.97	29.07	32.06
EVH13203	5362687	458890	12.30	9.27	0.00	0.09	22.34	0.15	0.00	0.07	20.14	0.69	16.78	18.16
EVH13204	5361155	459680	13.28	2.39	1.68	0.03	1.12	0.02	2.36	0.07	74.00	0.26	3.02	1.77
EVH13205	5361130	459695	13.55	3.07	3.07	0.11	1.02	0.03	0.69	0.08	70.90	0.28	4.74	2.46
EVH13206	5361065	459732	13.69	10.23	0.00	0.06	24.68	0.19	0.00	0.06	47.58	0.68	2.67	0.16
EVH13207	5360132	457930	13.87	4.36	9.49	0.00	4.99	0.13	1.33	0.04	55.75	0.60	6.57	2.87
EVH13208	5360016	458021	13.10	7.72	0.00	0.05	9.33	0.15	0.50	0.05	63.16	0.86	3.97	1.11
EVH13209	5360441	458695	14.89	9.70	11.14	0.00	7.94	0.14	1.11	0.04	51.18	0.75	2.97	0.14
EVH13210	5360070	458868	3.94	0.34	1.33	0.05	0.60	0.02	0.28	0.04	89.90	0.14	2.97	0.39
EVH13211	5360075	458866	6.63	12.81	10.23	0.42	12.73	0.15	0.34	0.38	36.66	2.58	9.34	7.73
EVH13212	5361311	460927	2.78	1.87	3.34	0.02	0.42	0.06	0.25	0.05	89.98	0.42	0.72	0.08
EVH13213	5361333	460912	16.00	7.53	11.83	0.02	7.94	0.16	2.38	0.13	37.71	0.70	10.11	5.49
EVH13214	5361422	460849	15.56	8.53	6.52	0.00	4.67	0.12	1.13	0.03	58.15	0.43	4.40	0.46
EVH13215	5363749	460051	12.15	14.15	9.69	0.03	3.55	0.18	0.88	0.06	49.17	0.62	5.18	4.35
EVH13216	5363788	460028	18.61	0.71	4.95	0.59	1.77	0.04	1.48	0.14	63.36	0.60	4.28	3.47
EVH13217	5354738	460951	15.01	1.43	4.68	0.17	1.99	0.05	1.61	0.14	63.83	0.50	6.09	4.51
EVH13218	5354690	460951	14.75	2.07	1.73	0.31	0.87	0.03	2.15	0.16	73.44	0.33	4.17	-
EVH13219	5354639	460951	12.70	2.47	4.21	0.15	1.57	0.07	2.95	0.14	65.40	0.62	5.39	4.35
EVH13220	5355280	461341	12.36	7.56	0.95	0.99	3.11	0.12	1.86	0.45	49.91	0.72	10.68	11.31
EVH13221	5355224	461341	16.18	6.92	7.48	0.47	3.33	0.10	1.10	0.11	53.75	0.60	9.98	-
EVH13303	5362696	458850	15.06	13.51	0.00	0.09	10.82	0.21	2.17	0.05	19.74	0.80	18.78	18.77
EVH13307	5362861	458601	16.08	2.15	10.81	0.06	7.40	0.14	2.68	0.08	53.43	0.67	5.49	1.01
EVH13375	5360830	460650	15.73	2.99	4.19	0.00	2.62	0.34	0.58	0.09	64.80	1.94	6.49	0.23
EVH16155	5365707	457048	5.83	0.19	2.43	0.14	0.28	0.03	0.98	0.02	-	0.06	-	0.56
EVH16159	5365885	459900	7.09	0.51	2.30	0.21	0.44	0.04	1.19	0.04	-	0.14	-	0.36
EVH16160	5365888	459898	8.78	0.10	1.32	2.78	0.33	0.01	0.29	0.02	-	0.09	-	0.15
EVH16161	5364365	460042	9.78	0.15	2.39	1.18	0.40	0.01	0.33	0.03	74.50	0.10	5.77	5.37
EVH16162	5365641	456120	15.93	4.40	8.81	0.90	3.57	0.12	0.06	0.31	-	1.61	-	6.16
EVH16164	5366263	455843	11.63	0.31	2.62	0.34	0.20	0.01	2.95	0.04	-	0.21	-	1.20
EVH16165	5359594	458291	13.80	9.14	9.96	0.05	6.91	0.14	1.15	0.06	-	0.73	-	0.30
EVH16166	5355597	459271	12.82	2.87	2.92	0.09	1.02	0.03	1.04	0.10	66.86	1.17	5.70	5.38
EVH16168	5364740	455788	11.70	0.33	1.96	0.63	0.14	0.01	2.12	0.01	78.84	0.08	2.26	1.91
EVH16171	5364309	456101	11.20	0.90	2.96	0.93	0.34	0.03	2.94	0.02	77.91	0.14	1.81	0.80
EVH16172	5364771	455901	9.14	5.96	1.48	0.53	0.38	0.09	1.14	0.04	68.41	0.08	6.44	6.31
EVH16175	5365481	463189	13.63	6.47	11.84	1.12	4.85	0.17	1.39	0.15	46.24	1.11	7.83	5.20
EVH16177	5364687	461467	10.57	2.79	2.48	0.51	0.48	0.05	1.84	0.04	-	0.29	-	-
EVH16178	5365621	463171	13.49	6.87	6.42	0.19	2.34	0.18	2.21	0.14	-	1.04	-	-
EVH16179	5365639	463171	-	-	0.00	-	-	-	-	-	-	-	4.88	2.21
EVH16181	5361832	455489	14.00	4.55	2.06	0.19	1.10	0.07	0.84	0.12	58.95	0.49	8.99	8.64
EVH16184	5356399	466493	11.88	9.09	7.59	0.06	5.78	0.14	0.43	0.05	50.15	0.53	8.22	6.09
EVH16187	5354324	462431	15.48	3.49	0.00	0.81	0.93	0.03	4.01	0.09	66.45	0.21	4.72	3.77
EVH16189	5358628	459251	8.77	15.77	0.00	0.33	9.43	0.25	2.17	2.35	19.15	0.96	18.72	22.11
EVH16193	5358729	454018	13.42	8.56	11.03	0.34	7.01	0.15	0.45	0.07	38.53	0.86	11.82	7.76

SampleNo	Cr (ppm)	Y (ppm)	Sc (ppm)	Sr (ppm)	Zr (ppm)	Au (ppb)	Ba (ppm)	Cu (ppm)	Ni (ppm)	Pb (ppm)	Zn (ppm)	Fe/Fe+Mg	CO_2/CaO	Ishikawa Index	Chlorite Index	SCI	CSI	K/Al	CCPI
EVH13200	241	17	25	131	32	8	678	5	111	0	23	0.58	1.12	43	61	41	59	0.00	92
EVH13201	-	-	48	-	-	7	45	33	3	0	39	-	3.34	56	56	50	50	0.01	91
EVH13202	242	71	37	227	79	202	382	238	124	0	35	0.52	1.89	31	46	41	59	0.00	93
EVH13203	59	43	31	69	8	91	243	14	162	0	35	-	2.49	70	69	50	50	0.01	98
EVH13204	-	-	6	-	-	0	143	0	0	0	15	0.64	0.94	32	52	38	62	0.00	99
EVH13205	-	-	6	-	-	10	500	3	0	0	11	0.78	1.02	17	40	30	70	0.01	58
EVH13206	129	33	30	88	48	0	40	57	106	10	72	-	0.02	68	68	50	50	0.01	95
EVH13207	71	58	27	27	85	0	49	4	76	0	27	0.69	0.84	45	69	40	60	0.00	89
EVH13208	97	52	32	34	70	0	15	14	55	0	47	-	0.18	52	52	50	50	0.01	91
EVH13209	290	16	42	142	76	6	22	13	125	0	24	0.62	0.02	41	61	40	60	0.00	91
EVH13210	-	-	19	-	-	0	372	91	12	2	52	0.72	1.46	22	43	33	67	0.02	47
EVH13211	-	-	30	-	-	0	3948	70	250	0	57	0.48	0.77	50	62	45	55	0.10	97
EVH13212	-	-	45	-	-	0	259	48	0	0	57	0.90	0.05	11	48	18	82	0.01	65
EVH13213	-	-	24	-	-	0	31	9	149	2	59	0.63	0.93	50	70	42	58	0.00	98
EVH13214	116	10	42	124	44	0	19	28	329	14	37	0.62	0.07	35	55	39	61	0.00	100
EVH13215	41	46	26	37	58	196	133	9	73	0	32	0.76	0.39	18	43	30	70	0.00	84
EVH13216	12	84	13	53	651	46	584	6	0	0	45	0.76	6.17	63	76	45	55	0.05	83
EVH13217	166	22	10	69	149	6	636	14	35	3	34	0.73	4.01	60	80	43	57	0.02	97
EVH13218	11	6	4	11	224	-	1080	3	0	0	21	0.70	-	26	40	39	61	0.03	60
EVH13219	191	23	9	62	211	0	159	17	0	10	55	0.76	2.24	37	63	37	63	0.02	89
EVH13220	28	55	10	191	222	390	438	29	0	0	100	0.26	1.91	32	29	52	48	0.13	65
EVH13221	154	36	21	55	522	-	2340	6	0	0	13	0.72	-	35	57	38	62	0.05	93
EVH13303	125	23	39	161	42	23	133	46	91	0	58	-	1.77	44	44	50	50	0.01	96
EVH13307	161	42	27	136	40	0	63	1	174	0	41	0.63	0.60	76	87	46	54	0.01	98
EVH13375	11	38	67	399	221	8	7	383	0	0	84	0.65	-	33	54	38	62	0.00	73
EVH16155	-	-	3	-	-	0	355	5	0	0	8	0.91	3.65	24	63	28	72	0.04	66
EVH16159	53	71	2	24	460	0	170	8	0	0	11	0.86	0.89	32	61	34	66	0.05	70
EVH16160	46	145	2	8	167	5	769	5	0	0	31	0.82	1.86	66	26	72	28	0.50	26
EVH16161	18	77	3	25	294	0	471	0	0	0	75	0.87	45.28	47	47	50	50	0.19	48
EVH16162	127	38	29	111	208	0	565	2	35	0	28	0.74	1.78	41	61	40	60	0.09	79
EVH16164	37	179	4	17	431	13	485	2	0	0	15	0.94	4.83	14	42	26	74	0.05	44
EVH16165	-	-	34	-	-	9	19	24	88	0	39	0.63	0.04	39	59	40	60	0.01	89
EVH16166	-	-	7	-	-	0	54	53	0	5	55	0.77	2.39	22	47	32	68	0.01	75
EVH16168	-	-	6	-	-	10	645	4	0	0	26	0.94	7.43	24	38	38	62	0.09	40
EVH16171	19	13	4	27	152	0	327	2	0	0	13	0.91	1.13	26	40	40	60	0.13	45
EVH16172	21	73	4	63	45	0	518	2	0	0	36	0.82	1.35	12	19	38	62	0.09	61
EVH16175	88	47	38	166	269	138	388	78	0	0	107	0.74	1.02	44	64	41	59	0.13	88
EVH16177	-	-	4	-	-	-	573	35	0	0	90	0.86	-	20	38	35	65	0.08	62
EVH16178	-	-	27	-	-	0	-	-	-	-	-	0.76	-	26	52	33	67	0.02	94
EVH16179	136	35	29	97	92	0	15	6	8	0	47	-	-	-	-	-	-	-	-
EVH16181	49	16	14	48	215	0	291	47	0	0	15	0.68	2.42	21	37	36	64	0.02	85
EVH16184	211	16	47	114	38	0	8	10	34	6	28	0.60	0.85	39	58	40	60	0.01	99
EVH16187	45	0	2	107	128	12	2845	2	0	0	24	-	1.38	21	11	65	35	0.08	20
EVH16189	11	157	22	1714	595	23	1196	32	0	0	136	-	1.79	37	35	51	49	0.06	86
EVH16193	138	23	55	158	82	10	261	45	117	4	63	0.65	1.15	43	63	41	59	0.04	92

SampleNo	UTMNorth (m)	UTMEast (m)	Al_2O_3 (%)	CaO (%)	Fe_2O_3 (%)	K_2O (%)	MgO (%)	MnO (%)	Na_2O (%)	P_2O_5 (%)	SiO_2 (%)	TiO_2 (%)	LOI (%)	CO_2 (%)
EVH16196	5360064	460542	14.93	2.18	3.94	0.25	2.28	0.04	5.57	0.07	65.42	0.67	3.12	1.53
EVH16198	5361369	461827	11.69	15.63	9.24	0.16	4.79	0.15	0.69	0.03	-	0.46	-	-
EVH16199	5361730	462468	14.76	17.09	9.33	0.00	4.47	0.15	0.08	0.06	38.20	0.65	6.68	8.53
EVH16851	5358385	458827	13.10	14.27	12.50	0.11	3.35	0.23	1.20	0.36	45.76	0.93	4.31	3.89
EVH16852	5358404	458891	14.03	5.86	5.00	0.20	0.81	0.11	3.09	0.18	61.98	0.47	4.37	3.90
EVH16853	5358405	458890	12.66	13.94	10.89	0.34	3.33	0.20	1.02	0.08	47.64	0.91	5.03	3.96
EVH16854	5361469	459611	12.01	9.55	8.54	0.04	2.26	0.16	1.72	0.06	55.13	0.85	5.73	3.96
EVH16855	5363258	460065	13.45	13.42	10.93	0.02	5.40	0.16	0.79	0.05	10.01	0.67	21.93	23.15
EVH16856	5359181	459071	12.62	13.25	0.00	0.09	17.17	0.19	0.00	0.09	50.73	0.93	3.00	1.94
EVH16857	5359219	459071	13.83	1.96	1.22	0.16	0.38	0.01	4.07	0.02	73.74	0.17	2.42	2.01
EVH16858	5362940	463394	12.98	4.92	13.20	0.01	4.92	0.14	2.51	0.09	48.10	0.93	7.68	4.52
EVH16859	5364483	462094	10.12	3.36	4.76	1.00	0.71	0.08	0.17	0.10	67.78	0.51	6.16	5.25
EVH16860	5355261	459566	-	-	-	-	-	-	-	-	-	-	6.77	4.88
EVH16861	5354969	458761	14.58	1.93	4.27	0.88	1.86	0.07	2.22	0.10	65.34	0.42	5.14	3.19
EVH16862	5354696	458761	13.51	1.96	4.40	0.76	2.18	0.05	2.02	0.07	66.55	0.34	4.98	3.18
EVH16863	5354664	463021	13.45	2.09	5.72	0.25	2.00	0.05	0.90	0.12	66.48	0.44	5.37	3.14
EVH16864	5354404	464653	4.12	4.36	9.44	0.68	11.93	0.11	0.03	0.02	15.77	0.22	25.32	28.00
EVH16865	5366409	460101	7.71	16.72	14.15	0.26	1.54	0.33	1.15	0.21	50.42	1.58	3.52	2.42
EVH16866	5366409	460101	5.80	12.76	0.00	0.21	14.12	0.18	0.18	3.39	56.87	1.47	3.02	2.00
EVH16868	5359186	458931	14.05	5.82	13.59	0.20	6.24	0.18	1.84	0.08	52.17	1.05	4.40	0.39
EVH16869	5359186	458931	10.91	14.91	7.47	0.38	2.04	0.27	0.15	0.07	20.53	1.00	20.27	22.01
EVH16870	5359186	458931	-	-	-	-	-	-	-	-	-	-	9.52	6.14
EVH16871	5358133	458682	12.77	8.72	11.43	0.59	3.42	0.17	3.02	0.08	53.75	1.01	2.85	2.18
EVH16872	5366452	461078	13.93	3.25	3.63	1.61	0.83	0.05	1.61	0.14	71.27	1.48	2.04	0.16
EVH16873	5366396	461101	14.73	0.32	4.18	0.54	1.53	0.03	0.87	0.08	73.83	0.51	2.90	0.48
EVH16874	5356626	462181	14.46	0.43	5.19	0.58	0.55	0.04	0.67	0.12	72.33	0.47	4.71	0.44
EVH16875	5356571	462181	20.17	0.79	7.44	0.65	2.35	0.05	2.32	0.10	60.82	0.81	3.70	0.81
EVH16876	5359137	459191	11.74	6.53	16.06	0.10	4.39	0.21	1.17	0.15	56.74	1.30	1.39	0.24
EVH16877	5359200	459191	12.50	5.80	12.30	0.00	3.84	0.17	1.87	0.13	49.93	1.97	6.24	5.23
EVH16878	5359230	459191	15.20	0.81	7.17	0.60	1.24	0.06	1.27	0.11	69.24	0.61	3.44	0.24
EVH16879	5359230	459191	17.14	11.17	3.91	0.02	2.38	0.15	1.57	0.03	44.62	0.26	10.39	8.37
EVH16880	5361439	461468	13.76	2.40	1.58	0.24	0.75	0.02	3.68	0.07	72.00	0.16	3.08	2.27
EVH16881	5361379	461496	14.42	2.61	1.61	0.35	0.68	0.03	3.33	0.09	71.28	0.21	3.16	2.24
EVH16882	5355314	460857	15.51	3.65	5.59	0.31	2.02	0.08	1.82	0.18	56.86	0.59	7.43	5.97
EVH16883	5355404	460863	12.87	7.35	7.26	0.62	3.40	0.19	0.82	0.10	40.09	1.08	13.34	12.89
EVH16884	5355434	460865	12.07	5.65	10.69	0.00	5.20	0.11	1.59	0.06	51.09	0.64	8.77	4.13
EVH16885	5355453	460866	7.15	10.61	12.11	0.45	6.53	0.30	0.30	0.08	25.24	0.80	17.95	18.47
EVH16886	5353290	456191	12.82	5.02	2.94	0.64	1.63	0.07	2.01	0.19	61.68	0.59	7.50	4.92
EVH16887	5358166	458739	9.43	17.17	16.50	0.08	4.50	0.33	0.87	0.19	18.99	2.06	13.84	16.05
EVH16888	5358168	458735	13.70	5.27	10.93	0.12	2.59	0.12	2.44	0.40	56.14	0.86	5.32	2.09
EVH16889	5358988	459142	15.19	11.18	12.21	1.78	3.93	0.25	0.32	0.33	20.43	1.08	15.85	17.45
EVH16890	5358941	459142	11.23	7.95	13.98	0.04	5.03	0.21	1.51	0.08	51.32	1.07	4.94	2.64
EVH16891	5358908	459142	10.43	10.45	8.61	0.00	3.33	0.15	1.68	0.06	45.45	0.75	10.17	8.91
EVH16892	5355628	459271	28.59	1.31	4.52	0.60	1.59	0.05	1.33	0.22	46.53	1.07	8.55	5.64
EVH16894	5355515	459271	15.29	1.90	4.70	0.90	1.98	0.06	1.57	0.11	60.48	0.50	7.02	5.48

SampleNo	Cr (ppm)	Y (ppm)	Sc (ppm)	Sr (ppm)	Zr (ppm)	Au (ppb)	Ba (ppm)	Cu (ppm)	Ni (ppm)	Pb (ppm)	Zn (ppm)	Fe/Fe+Mg	CO_2/CaO	Ishikawa Index	Chlorite Index	SCI	CSI	K/Al	CCPI
EVH16196	-	-	11	-	-	15	145	12	0	0	49	0.67	0.89	37	56	40	60	0.03	71
EVH16198	-	-	27	-	-	-	592	77	7	0	18	0.69	-	21	41	34	66	0.02	81
EVH16199	145	39	31	44	52	9	23	68	82	15	34	0.71	-	20	41	32	68	0.00	92
EVH16851	10	54	22	169	460	267	2013	35	14	0	117	0.81	0.35	18	48	27	73	0.01	91
EVH16852	36	43	3	734	83	138	8168	4	0	4	53	0.88	0.85	12	40	22	78	0.02	72
EVH16853	34	44	37	590	73	0	765	26	64	0	64	0.79	0.36	19	44	29	71	0.04	84
EVH16854	158	18	40	144	85	0	21	59	43	10	55	0.81	0.53	18	49	27	73	0.01	92
EVH16855	114	20	28	155	17	0	235	15	123	0	22	0.70	2.20	28	52	35	65	0.00	97
EVH16856	-	-	36	-	-	0	189	115	26	4	71	-	0.19	50	50	50	50	0.01	81
EVH16857	-	-	3	-	-	21	307	10	0	14	17	0.79	1.31	12	26	31	69	0.02	39
EVH16858	23	35	38	182	107	0	52	1	0	5	59	0.76	1.17	48	76	39	61	0.00	97
EVH16859	14	156	11	23	368	47	540	11	0	2	55	0.89	1.99	16	33	32	68	0.16	43
EVH16860	124	0	22	74	232	0	410	11	15	0	20	-	-	-	-	-	-	-	-
EVH16861	-	-	14	-	-	0	363	13	0	0	55	0.73	2.10	51	62	45	55	0.10	78
EVH16862	-	-	8	-	-	0	466	16	73	0	36	0.70	2.06	59	69	46	54	0.09	88
EVH16863	60	36	16	151	80	-	490	7	26	0	16	0.77	1.92	41	67	38	62	0.03	83
EVH16864	115	338	26	34	14	6	301	48	879	7	58	0.48	8.18	63	72	47	53	0.26	84
EVH16865	12	162	2	218	2488	0	1460	51	0	0	68	0.91	0.18	9	44	17	83	0.05	92
EVH16866	4	48	43	263	125	135	3328	6	36	0	106	-	0.20	50	49	50	50	0.06	88
EVH16868	20	59	27	97	75	0	36	158	62	0	79	0.72	0.09	49	73	40	60	0.02	95
EVH16869	126	24	29	169	111	0	256	23	5	0	38	0.81	1.88	14	36	28	72	0.05	96
EVH16870	-	-	-	-	-	0	-	-	-	-	-	-	-	-	-	-	-	-	-
EVH16871	-	-	34	-	-	0	169	22	42	0	84	0.79	0.32	24	51	32	68	0.07	75
EVH16872	118	148	57	45	219	8	785	6	0	0	107	0.84	0.06	30	36	45	55	0.18	50
EVH16873	34	34	15	56	121	0	565	20	0	0	39	0.76	1.95	81	84	49	51	0.06	88
EVH16874	73	21	18	57	128	0	733	10	27	0	49	0.92	1.30	30	62	33	67	0.06	65
EVH16875	-	-	25	-	-	0	530	10	27	0	22	0.79	1.30	51	72	42	58	0.05	77
EVH16876	103	46	42	220	256	0	285	37	13	0	64	0.81	0.05	38	71	35	65	0.01	95
EVH16877	12	40	40	181	225	538	15	46	0	0	79	0.79	1.15	40	72	36	64	0.00	100
EVH16878	136	0	27	108	199	0	425	12	46	0	58	0.87	0.37	49	75	39	61	0.06	81
EVH16879	225	13	44	48	31	0	51	9	160	0	46	0.66	0.95	17	34	34	66	0.00	97
EVH16880	40	2	1	110	70	0	406	1	0	2	386	0.71	1.21	19	33	37	63	0.03	51
EVH16881	-	-	3	-	-	0	467	10	0	5	24	0.73	1.09	27	41	40	60	0.04	81
EVH16882	-	-	13	-	-	0	532	77	0	0	21	0.76	2.08	26	50	34	66	0.03	68
EVH16883	-	-	37	-	-	0	267	36	0	0	52	0.71	2.23	31	51	38	62	0.08	82
EVH16884	72	19	36	154	80	0	9	53	8	0	48	0.70	-	44	69	39	61	0.00	94
EVH16885	2607	20	60	164	74	9	340	221	561	0	138	0.68	2.22	38	60	39	61	0.10	94
EVH16886	163	15	23	68	164	5	304	18	30	1	73	0.68	1.25	24	35	40	60	0.08	59
EVH16887	141	96	58	895	202	2300	759	46	264	0	68	0.81	1.19	20	51	28	72	0.01	94
EVH16888	-	-	4	-	-	190	3816	5	0	0	37	0.83	0.50	28	63	30	70	0.01	86
EVH16889	137	12	54	176	112	217	636	159	22	15	92	0.78	1.99	31	51	38	62	0.18	83
EVH16890	-	-	45	-	-	0	122	35	25	0	61	0.76	0.42	35	65	35	65	0.01	92
EVH16891	-	-	33	-	-	0	43	17	19	0	49	0.75	1.09	19	44	30	70	0.00	75
EVH16892	251	22	27	63	503	0	1257	2	64	0	31	0.77	5.47	32	52	38	62	0.03	59
EVH16894	103	21	15	75	216	0	587	42	0	4	57	0.73	3.66	44	57	43	57	0.09	70

SampleNo	UTMNorth (m)	UTMEast (m)	Al_2O_3 (%)	CaO (%)	Fe_2O_3 (%)	K_2O (%)	MgO (%)	MnO (%)	Na_2O (%)	P_2O_5 (%)	SiO_2 (%)	TiO_2 (%)	LOI (%)	CO_2 (%)
EVH16895	5355685	459781	12.81	2.56	2.01	0.03	1.05	0.06	1.98	0.10	73.20	0.40	3.62	2.19
EVH16896	5355615	459781	12.82	5.54	3.50	0.17	2.11	0.08	2.10	0.11	55.24	0.43	9.02	8.87
EVH16897	5355596	459781	12.62	2.41	4.46	0.70	2.45	0.07	2.68	0.10	58.44	0.43	7.58	8.06
EVH16898	5355556	459781	12.25	4.48	4.19	0.64	1.80	0.06	1.24	0.08	54.82	0.42	10.02	9.99
EVH16899	5355250	461461	14.33	1.81	5.85	0.25	1.39	0.02	1.04	0.10	66.70	0.36	4.79	3.36
EVH16900	5356146	461712	14.72	1.97	2.65	0.02	1.27	0.05	4.07	0.12	72.32	0.27	-	2.54
EVH19451	5356115	461712	18.89	4.66	2.58	0.87	0.33	0.03	3.62	0.14	60.57	0.36	4.21	3.75
EVH19452	5354886	462801	13.76	9.38	12.70	0.08	6.93	0.18	1.13	0.03	29.62	0.71	13.96	11.54
EVH19453	5354771	462801	15.87	1.78	5.14	0.85	2.07	0.04	3.02	0.18	63.24	0.54	4.67	2.60
EVH19454	5354778	462801	13.46	2.87	5.52	0.52	1.96	0.07	1.50	0.11	61.96	0.58	6.22	5.24
EVH19455	5356466	458591	12.67	1.98	5.75	0.31	2.71	0.05	2.30	0.10	70.17	0.48	2.99	0.49
EVH19456	5363868	460139	3.28	0.67	1.02	0.02	0.38	0.01	1.04	0.03	74.06	0.11	10.48	8.90
EVH19457	5363915	460107	12.29	12.35	10.41	1.31	3.10	0.22	0.83	0.06	19.92	0.82	17.85	20.84
EVH19458	5363964	460074	11.73	15.44	0.00	0.08	4.29	0.25	0.95	0.06	42.69	0.72	12.78	11.02
EVH19459	5364000	460050	12.62	10.05	11.97	0.01	3.64	0.17	0.85	0.08	38.38	0.90	6.49	14.83
EVH19460	5355722	459541	13.61	3.40	4.48	0.69	2.01	0.05	1.59	0.11	58.34	0.47	7.98	7.27
EVH19461	5355623	459541	15.41	1.36	1.86	0.13	0.55	0.02	4.33	0.13	70.50	0.38	3.23	2.11
EVH19462	5355524	459541	12.96	5.77	7.52	0.14	3.67	0.12	0.78	0.12	43.98	0.45	12.20	12.29
KK-11	5364050	449500	12.99	2.30	9.07	3.11	1.29	0.27	1.50	0.11	68.95	0.41	4.06	-
KK-7	5359400	458550	15.20	10.51	12.59	3.11	7.39	0.20	0.05	0.09	49.86	0.99	3.04	-
KK-8	5359750	458050	15.41	10.99	13.05	2.58	7.19	0.20	0.08	0.09	49.41	1.01	2.30	-
KK13	5370300	458950	13.41	7.20	9.78	2.92	2.39	0.49	1.32	0.54	60.13	1.81	10.19	-
LKS041	5358498	458460	15.55	9.27	11.90	2.10	5.72	0.28	3.72	0.08	48.50	1.08	1.50	0.11
LKS042	5358498	458460	14.68	11.91	11.81	1.17	6.28	0.18	2.91	0.09	47.60	1.09	1.70	0.44
LKS045	5358498	458460	14.76	13.69	12.19	0.63	3.91	0.20	3.55	0.11	46.77	1.14	2.70	1.76
LKS047	5358498	458460	12.09	17.04	12.67	1.80	3.42	0.36	3.11	1.57	42.30	1.74	2.40	1.54
LKS054	5358498	458460	3.38	20.63	21.20	0.23	8.92	0.31	0.51	2.38	37.14	1.83	2.70	2.23
LKS056	5358498	458460	3.20	20.68	20.13	0.89	7.98	0.27	1.13	3.73	31.32	1.74	7.90	7.80
LKS064	5358498	458460	15.72	0.74	0.99	6.01	0.13	0.01	5.29	0.07	69.31	0.11	1.20	0.55
LKS068	5358498	458460	14.40	0.56	1.38	5.68	0.22	0.02	4.79	0.02	71.20	0.08	1.30	0.70
LKS073	5358498	458460	12.47	8.49	8.82	2.11	1.28	0.25	4.38	0.17	54.18	1.74	5.90	5.42
LKS083	5359716	458716	14.42	8.15	15.97	0.79	4.48	0.21	1.74	0.20	48.32	2.16	3.20	0.26
LKS086	5359716	458716	14.58	6.47	12.14	0.36	3.04	0.24	3.78	0.25	53.12	2.16	3.60	0.84
LKS094	5359716	458716	2.64	18.05	15.12	0.31	9.27	0.13	0.18	4.39	29.60	1.33	18.40	18.63
LKS101	5359716	458716	2.33	19.85	13.21	0.27	8.36	0.12	0.16	4.47	29.48	1.05	20.10	19.73
LKS106	5359716	458716	2.50	16.54	20.06	0.85	9.00	0.25	0.46	2.08	31.14	1.35	15.30	11.86
LKS107	5359716	458716	2.84	19.05	14.80	1.92	9.23	0.17	0.02	3.13	33.08	1.37	13.70	12.41
LKS112	5359716	458716	2.64	16.33	25.28	0.14	10.54	0.18	0.74	2.67	33.87	1.85	5.20	4.50
LKS116	5359716	458716	12.72	14.34	11.59	0.29	2.94	0.24	2.25	0.14	44.03	1.17	10.10	8.56
LKS120	5358088	458537	15.41	8.95	13.11	0.42	8.52	0.19	3.23	0.12	45.57	1.21	2.90	0.15
MON004	5370838	463818	9.37	0.26	0.60	1.44	0.26	<0.01	3.05	0.10	83.39	0.19	1.20	0.15
MON005	5370838	463818	10.60	8.59	8.51	2.41	6.16	0.20	0.63	0.35	47.38	0.66	14.10	12.04
MON007	5370838	463818	11.09	2.39	4.99	1.43	0.98	0.09	3.92	0.06	70.73	0.44	3.70	2.89
MON008	5370838	463818	9.38	1.08	0.89	2.59	0.19	0.02	3.27	0.03	81.04	0.19	1.10	1.17
MON015	5370838	463818	12.04	2.76	4.68	2.51	1.19	0.09	2.78	0.12	68.30	0.71	4.60	3.88

SampleNo	Cr (ppm)	Y (ppm)	Sc (ppm)	Sr (ppm)	Zr (ppm)	Au (ppb)	Ba (ppm)	Cu (ppm)	Ni (ppm)	Pb (ppm)	Zn (ppm)	Fe/Fe+Mg	CO_2/CaO	Ishikawa Index	Chlorite Index	SCI	CSI	K/Al	CCPI
EVH16895	62	25	9	164	57	0	203	14	10	0	12	0.69	1.09	24	46	35	65	0.00	77
EVH16896	136	34	9	282	123	311	390	3	32	0	29	0.66	2.04	24	42	37	63	0.02	75
EVH16897	63	34	10	158	157	10	425	9	0	0	92	0.68	4.26	54	65	45	55	0.09	87
EVH16898	170	13	10	57	176	8	343	8	16	17	62	0.73	2.84	27	44	38	62	0.08	68
EVH16899	-	-	11	-	-	7	543	4	38	10	15	0.83	2.37	38	69	35	65	0.03	86
EVH16900	38	14	5	145	126	0	174	3	0	0	28	0.71	1.64	23	45	33	67	0.00	60
EVH19451	-	-	6	-	-	132	599	5	0	9	16	0.90	1.02	19	31	38	62	0.07	69
EVH19452	32	45	37	49	39	14	153	21	0	0	37	0.68	1.57	39	63	38	62	0.01	92
EVH19453	72	46	16	154	140	0	530	53	15	8	70	0.74	1.86	46	61	43	57	0.08	73
EVH19454	333	15	16	105	152	0	664	23	48	0	97	0.77	2.32	37	60	38	62	0.06	79
EVH19455	297	15	20	83	141	15	312	12	89	11	49	0.71	0.32	46	67	41	59	0.04	81
EVH19456	-	-	14	-	-	0	56	7	2	0	20	0.76	16.97	13	33	28	72	0.01	40
EVH19457	55	53	27	65	73	14	158	22	1	0	51	0.80	2.15	23	44	35	65	0.17	79
EVH19458	108	33	27	51	53	0	60	37	50	5	40	-	0.91	19	19	50	50	0.01	61
EVH19459	-	-	37	-	-	-	108	15	62	0	47	0.79	1.88	24	56	30	70	0.00	92
EVH19460	125	0	9	64	162	0	465	12	13	0	33	0.72	2.72	38	54	41	59	0.08	78
EVH19461	-	-	2	-	-	134	551	13	0	2	9	0.80	1.98	11	29	28	72	0.01	35
EVH19462	100	19	14	101	180	0	361	115	23	5	50	0.70	2.71	29	52	36	64	0.02	74
KK-11	7	21	10	83	275	-	253	0	0	4	0	0.89	-	56	59	49	51	0.38	69
KK-7	297	16	39	102	44	-	25	0	0	3	0	0.66	-	47	55	46	54	0.32	80
KK-8	365	16	39	93	40	-	23	72	133	0	86	0.68	-	42	54	44	56	0.26	80
KK13	138	33	21	113	238	-	234	25	2	3	103	0.83	-	34	46	43	57	0.34	65
LKS041	164	19	37	512	68	2	290	47	72	2	67	0.71	0.02	38	52	42	58	0.21	74
LKS042	144	19	36	1342	70	1	1527	85	48	4	51	0.69	0.05	33	51	39	61	0.13	81
LKS045	68	20	30	1119	78	2	489	95	45	1	21	0.78	0.16	21	45	31	69	0.07	78
LKS047	27	151	7	3053	1275	0	3038	39	19	26	199	0.81	0.11	21	40	34	66	0.23	75
LKS054	21	58	39	1559	331	0	172	28	11	6	24	0.73	0.14	30	57	35	65	0.11	97
LKS056	21	68	37	2138	285	0	2057	18	16	12	53	0.75	0.48	29	53	35	65	0.44	93
LKS064	-	5	0	1461	107	27	2033	2	3	11	32	0.90	0.94	50	8	87	13	0.60	8
LKS068	-	5	0	574	89	10674	2254	7	3	41	15	0.88	1.58	52	12	82	18	0.62	12
LKS073	-	26	23	346	119	3	386	45	10	15	80	0.89	0.81	21	38	35	65	0.27	59
LKS083	-	33	30	382	166	0	793	39	4	1	146	0.81	0.04	35	64	35	65	0.09	88
LKS086	-	34	30	304	161	2	116	52	5	2	154	0.82	0.17	25	57	30	70	0.04	77
LKS094	-	50	64	1122	174	115	61	34	13	9	81	0.65	1.31	34	55	38	62	0.18	98
LKS101	-	51	44	1354	163	14	234	5	17	7	82	0.65	1.26	30	50	38	62	0.18	98
LKS106	-	27	45	1212	114	2	207	2	15	5	91	0.72	0.91	37	60	38	62	0.53	95
LKS107	-	52	41	1793	211	0	486	2	13	8	65	0.65	0.83	37	52	42	58	1.06	92
LKS112	21	39	53	600	154	0	52	6	26	5	42	0.74	0.35	38	66	37	63	0.08	97
LKS116	157	22	33	174	82	1	124	82	67	0	94	0.82	0.76	16	44	27	73	0.04	84
LKS120	68	23	33	706	92	0	137	99	77	2	55	0.64	0.02	42	62	41	59	0.04	85
MON004	21	122	3	48	255	1	366	1	5	1	86	0.73	0.72	34	14	70	30	0.24	15
MON005	465	24	22	308	118	0	592	47	85	2	127	0.62	1.78	48	54	47	53	0.36	82
MON007	21	88	8	104	303	2	298	39	8	5	126	0.86	1.54	28	41	40	60	0.20	51
MON008	34	86	3	100	233	0	665	10	2	2	124	0.84	1.38	39	12	76	24	0.43	14
MON015	-	71	12	150	252	5	571	13	7	5	75	0.82	1.79	40	40	50	50	0.33	51

SampleNo	UTMNorth (m)	UTMEast (m)	Al_2O_3 (%)	CaO (%)	Fe_2O_3 (%)	K_2O (%)	MgO (%)	MnO (%)	Na_2O (%)	P_2O_5 (%)	SiO_2 (%)	TiO_2 (%)	LOI (%)	CO_2 (%)
MON021	5370838	463818	10.84	1.00	1.49	0.66	0.39	0.03	5.20	0.04	78.56	0.25	1.40	1.24
MON023	5370838	463818	17.23	4.71	4.41	2.74	1.77	0.11	5.27	0.18	55.81	0.39	7.10	6.48
MON025	5370838	463818	13.50	2.44	2.22	0.78	1.14	0.05	5.96	0.14	70.58	0.48	2.60	1.68
MON031	5370838	463818	12.47	5.29	10.73	0.41	2.90	0.12	3.72	0.17	57.02	1.39	5.60	3.62
MON035	5370838	463818	13.39	7.89	11.86	0.24	6.36	0.15	3.77	0.23	49.67	1.49	4.60	1.83
MON038	5370838	463818	15.70	3.92	4.19	2.09	1.71	0.08	5.64	0.23	61.69	0.36	4.10	2.85
MON039	5370838	463818	13.50	3.39	12.13	0.21	2.95	0.05	5.07	0.20	56.51	1.59	4.20	2.34
MON044	5370838	463818	12.37	8.28	7.02	1.25	3.29	0.10	4.43	0.27	49.52	1.78	11.40	11.31
MON048	5370838	463818	14.15	7.07	12.23	1.36	7.31	0.15	2.55	0.14	40.61	0.89	13.20	10.65
MON154	5373144	462298	17.26	8.50	8.90	1.03	3.96	0.20	4.09	0.05	51.75	0.97	3.00	1.21
MON159	5375750	464721	12.55	0.66	3.57	2.80	0.27	0.09	4.45	0.02	73.38	0.19	1.80	0.88
PA00048	5360199	457217	11.10	12.40	1.30	-0.10	9.00	0.18	2.90	0.07	51.50	0.94	0.00	-
PA00049	5360206	457286	12.10	12.10	1.50	-0.10	8.60	0.19	2.30	0.08	50.50	1.60	0.00	-
SM09008	5370449	458683	13.02	9.11	17.76	0.87	4.96	0.24	2.20	0.28	48.39	2.08	0.80	0.40
SM09009	5370377	458777	12.05	0.96	23.30	1.25	4.39	0.26	0.03	0.19	48.17	1.76	7.30	0.22
SM09010	5370341	458860	13.01	8.80	17.16	0.64	4.77	0.23	2.46	0.23	48.77	1.81	1.80	0.11
SM09011	5370412	458889	14.39	2.93	12.18	3.55	6.11	0.29	0.58	0.12	54.53	1.41	3.40	0.81
SM09012	5370267	458819	8.88	0.25	5.62	1.26	4.12	0.04	0.16	0.15	75.39	0.72	3.20	0.00
SM09013	5370220	458809	13.19	0.68	7.64	0.87	9.89	0.04	0.28	0.48	59.60	1.71	5.30	0.18
SM09014	5370233	458854	14.32	3.90	13.36	0.18	8.88	0.14	2.97	0.14	50.79	1.35	3.70	0.33
TB09019	5363447	475260	12.85	6.16	8.62	1.22	6.60	0.14	2.87	0.12	49.15	0.78	11.20	9.92
TB09020	5363330	474824	4.18	7.94	7.59	0.04	19.18	0.17	0.71	0.00	32.61	0.19	26.70	28.18
TB09023	5356950	457345	13.61	10.37	14.51	0.43	5.59	0.30	3.22	0.11	48.71	1.36	1.50	0.33
TB09024	5357977	457496	13.61	10.30	12.77	0.38	6.13	0.25	3.18	0.12	50.09	1.34	1.50	0.48
TB09025	5358792	457786	12.46	8.72	12.00	0.26	5.92	0.18	2.26	0.11	47.16	1.25	9.40	6.30
TB09026	5359366	458287	15.78	11.13	9.93	0.03	7.59	0.16	3.20	0.06	46.95	0.85	4.00	1.39
TB09027	5359466	458608	16.48	11.37	12.80	0.03	8.82	0.17	1.75	0.07	43.70	1.05	3.40	0.11
TB09029	5375128	459756	10.98	0.55	1.13	8.64	0.24	0.02	0.40	0.04	76.76	0.24	0.80	0.37
TB09030	5375868	459031	13.70	4.13	12.11	0.84	5.85	0.29	4.21	0.16	54.01	1.50	2.90	0.51
TB09035	5375895	458563	10.94	0.07	4.34	3.33	1.93	0.03	0.05	0.03	76.22	0.16	2.70	0.18
TB09037	5375704	458643	10.14	0.08	0.93	3.37	0.35	0.00	0.07	0.02	83.32	0.16	1.40	0.15
TB09038	5375767	458610	13.24	5.77	17.26	0.95	5.69	0.23	1.19	0.43	44.79	2.21	7.90	4.21
TB09039	5375756	458503	12.12	4.73	12.30	0.16	4.73	0.17	4.15	0.21	55.18	1.71	4.30	1.65
TI0032	5365989	473211	16.93	1.60	5.85	2.20	3.03	0.06	3.73	0.17	62.39	0.60	3.20	0.92
TI0033	5364039	474941	13.95	9.64	10.93	0.03	6.81	0.18	2.23	0.05	50.80	0.70	4.50	0.33
TI0262	5353559	450002	14.28	7.35	4.84	1.32	3.93	0.11	2.39	0.13	52.37	0.62	12.50	10.83
TI0389	5373524	471961	16.31	3.54	5.12	2.46	2.87	0.07	3.16	0.17	61.95	0.61	3.50	1.43
TI0436	5369249	457922	14.34	8.80	11.50	0.17	8.03	0.15	1.33	0.10	47.88	0.98	6.50	2.42
TI0478	5372169	469231	16.08	5.48	1.57	1.22	1.06	0.04	6.21	0.08	61.79	0.23	6.10	5.31
TI1408	5370579	454336	12.36	0.68	1.57	4.74	1.15	0.02	0.98	0.02	76.00	0.11	2.20	0.70
TI1431	5375251	467024	17.03	10.31	11.18	0.14	6.71	0.16	2.33	0.11	47.71	0.83	3.30	0.44
TI1613	5358249	458611	14.44	16.33	10.39	0.86	3.44	0.30	3.48	0.37	43.77	1.02	4.90	4.28
TI1842_1	5370199	454666	11.22	9.88	14.58	1.86	4.53	0.17	0.22	0.33	42.70	1.87	12.30	9.48
TI1842_2	5370199	454666	13.25	0.86	1.71	1.22	0.90	0.02	5.44	0.05	74.28	0.22	1.90	0.77
TI2023	5352689	448802	15.59	9.90	10.33	0.90	3.78	0.23	2.13	0.07	45.78	0.86	10.20	7.17

SampleNo	Cr (ppm)	Y (ppm)	Sc (ppm)	Sr (ppm)	Zr (ppm)	Au (ppb)	Ba (ppm)	Cu (ppm)	Ni (ppm)	Pb (ppm)	Zn (ppm)	Fe/Fe+Mg	CO_2/CaO	Ishikawa Index	Chlorite Index	SCI	CSI	K/Al	CCPI
MON021	21	96	3	94	285	0	232	9	3	2	88	0.82	1.58	14	20	42	58	0.10	23
MON023	41	19	9	513	171	1	798	30	10	8	43	0.74	1.75	31	31	50	50	0.25	42
MON025	21	25	7	195	234	1	314	1	10	2	25	0.69	0.88	19	25	42	58	0.09	32
MON031	-	51	28	266	191	0	242	38	11	4	34	0.81	0.87	27	57	32	68	0.05	75
MON035	205	22	20	345	110	1	141	59	103	1	77	0.68	0.30	36	59	38	62	0.03	81
MON038	34	17	8	379	158	1	1064	22	9	5	39	0.74	0.93	28	32	47	53	0.21	41
MON039	27	58	32	277	180	1	96	3	12	2	17	0.83	0.88	27	62	31	69	0.02	72
MON044	-	68	39	349	170	0	344	2	17	1	18	0.71	1.74	26	41	39	61	0.16	63
MON048	171	21	28	520	52	1	361	6	127	2	78	0.66	1.92	47	63	43	57	0.15	82
MON154	185	22	49	153	55	0	347	100	102	1	70	0.72	0.18	28	47	38	62	0.09	70
MON159	-	112	2	75	373	0	390	12	2	7	162	0.94	1.69	38	31	55	45	0.35	32
PA00048	-	-	0	120	30	-	-	100	68	1	65	0.14	-	40	43	48	52	-	92
PA00049	-	-	0	170	37	-	-	84	89	1	100	0.17	-	40	44	48	52	-	93
SM09008	62	41	44	132	156	2	251	168	23	4	100	0.81	0.06	34	63	35	65	0.10	87
SM09009	-	35	40	15	145	42	219	284	11	47	507	0.86	0.29	85	92	48	52	0.16	95
SM09010	96	42	42	114	177	1	183	169	28	3	76	0.81	0.02	32	63	34	66	0.08	87
SM09011	89	21	49	28	93	12	1980	456	46	1	206	0.70	0.35	73	71	51	49	0.39	81
SM09012	-	21	15	8	162	13	293	41	10	10	320	0.61	-	93	85	52	48	0.22	87
SM09013	-	39	28	17	207	4	206	26	2	2	76	0.47	0.34	92	90	50	50	0.10	94
SM09014	89	28	51	149	103	1	91	104	33	1	85	0.64	0.11	57	75	43	57	0.02	87
TB09019	164	15	29	158	71	3	346	58	52	2	109	0.60	2.05	46	58	44	56	0.15	78
TB09020	1238	5	15	218	10	13	19	4	558	2	47	0.31	4.52	69	75	48	52	0.02	97
TB09023	171	24	43	311	87	1	160	64	14	1	34	0.75	0.04	31	57	35	65	0.05	84
TB09024	212	24	43	183	86	0	123	35	13	1	27	0.71	0.06	33	56	37	63	0.04	83
TB09025	144	22	38	88	80	0	137	40	40	1	79	0.70	0.92	36	60	38	62	0.03	87
TB09026	308	14	34	127	42	1	10	115	106	0	36	0.60	0.16	35	54	39	61	0.00	84
TB09027	328	17	41	172	53	1	6	90	94	0	44	0.63	0.01	40	61	40	60	0.00	92
TB09029	27	103	3	11	257	0	779	2	2	2	7	0.85	0.85	90	12	89	11	1.23	12
TB09030	-	32	44	37	121	0	321	84	18	2	99	0.71	0.16	45	65	41	59	0.10	77
TB09035	-	108	2	2	318	0	441	117	1	4	244	0.72	3.33	98	63	61	39	0.48	63
TB09037	-	100	2	3	295	0	373	5	1	1	23	0.75	2.33	96	25	79	21	0.52	26
TB09038	130	43	35	65	247	1	224	53	68	3	152	0.78	0.93	49	73	40	60	0.11	91
TB09039	-	32	41	57	143	0	75	37	12	3	155	0.75	0.44	36	64	36	64	0.02	79
TI0032	185	12	15	354	116	1	565	49	78	17	79	0.69	0.73	50	52	49	51	0.20	58
TI0033	123	17	48	136	42	1	14	91	32	0	47	0.65	0.04	37	58	39	61	0.00	88
TI0262	130	14	17	155	98	0	317	46	82	1	42	0.59	1.88	37	43	45	55	0.14	69
TI0389	151	12	14	313	136	1	840	75	76	10	62	0.67	0.51	37	45	50	50	0.24	57
TI0436	82	18	40	147	63	1	44	76	47	0	55	0.62	0.35	37	64	41	59	0.02	92
TI0478	-	2	3	123	59	1	358	4	8	1	37	0.63	1.23	37	16	50	50	0.12	25
TI1408	-	75	3	18	188	0	542	5	0	5	18	0.61	1.30	37	29	73	27	0.60	31
TI1431	41	17	28	198	60	1	37	58	82	0	50	0.66	0.05	37	57	38	62	0.01	87
TI1613	164	46	22	2284	425	1	648	116	32	18	112	0.78	0.33	37	38	32	68	0.09	75
TI1842_1	103	39	38	104	177	3	510	49	59	2	178	0.79	1.22	37	60	39	61	0.26	89
TI1842_2	-	74	4	62	383	0	323	4	1	1	17	0.69	1.14	37	24	51	49	0.14	27
TI2023	116	15	33	94	53	2	161	102	147	0	80	0.76	0.92	37	50	36	64	0.09	81

SampleNo	UTMNorth (m)	UTMEast (m)	Al_2O_3 (%)	CaO (%)	Fe_2O_3 (%)	K_2O (%)	MgO (%)	MnO (%)	Na_2O (%)	P_2O_5 (%)	SiO_2 (%)	TiO_2 (%)	LOI (%)	CO_2 (%)
TI2640	5364789	455541	12.58	2.82	4.55	1.96	1.27	0.07	2.54	0.05	69.78	0.24	4.00	2.05
TI2726	5354319	451402	12.06	7.94	11.11	0.45	2.89	0.18	1.62	0.12	50.19	1.00	12.30	10.03
TI2728	5354549	451412	12.78	5.84	15.62	0.02	3.54	0.24	2.83	0.15	49.48	1.74	7.60	4.83
TI3289	5376579	460321	11.88	0.71	2.95	4.36	0.50	0.08	2.62	0.06	74.32	0.39	1.90	1.10
TI3537	5356129	466286	8.05	10.90	13.94	2.09	9.68	0.43	3.97	0.03	46.21	0.51	3.20	2.16
TI3920	5375488	466286	14.20	6.46	15.19	0.21	2.75	0.23	3.15	0.24	53.32	2.41	1.60	0.55
XBR033	5362646	449390	13.30	2.42	3.70	2.09	1.15	0.09	3.05	0.08	70.92	0.47	3.25	-
XBR034	5362574	449417	0.22	0.11	10.30	0.05	0.90	0.29	0.02	0.02	87.97	-0.01	0.66	-
XBR035	5362612	449435	0.12	0.00	4.72	0.03	0.03	0.07	0.01	0.04	95.00	-0.01	0.77	-
XBR036	5362574	449417	0.13	0.34	4.26	0.04	0.44	0.16	0.00	0.04	95.00	-0.01	0.60	-
XBR037	5362704	449559	0.52	0.14	7.91	0.04	0.43	0.21	0.00	0.02	89.99	0.02	1.55	-
XBR038	5362589	449693	9.98	5.55	9.86	1.42	3.67	0.17	0.73	0.05	59.44	0.84	6.39	-
XBR039	5362605	449685	10.81	0.39	9.54	2.10	0.23	0.05	2.01	0.06	68.78	0.39	4.63	-
XBR040	5362629	449512	1.14	0.38	1.57	0.02	0.08	0.01	0.59	0.05	96.38	0.01	0.21	-
XBR041	5362600	449512	16.79	2.31	1.87	1.39	0.30	0.03	5.83	0.09	68.03	0.23	2.81	-
XBR042	5362703	449481	0.29	0.07	1.25	0.01	0.03	0.01	0.11	0.05	98.27	-0.01	-0.01	-
XBR043	5363099	448980	9.38	0.54	1.19	3.15	0.37	0.03	0.16	0.10	83.50	0.33	1.77	-
XBR044	5363111	448972	14.83	0.09	0.92	8.81	0.17	0.00	1.43	0.09	72.91	0.43	0.78	-
XBR045	5363896	448798	10.19	0.23	2.02	2.79	0.35	0.01	0.25	0.07	82.57	0.13	2.12	-
XBR046	5363749	448775	1.20	4.09	3.22	0.27	1.71	0.10	0.09	0.03	83.96	0.03	5.95	-
XBR047	5363749	448775	3.30	1.32	3.18	0.48	1.39	0.04	0.10	0.09	87.57	0.15	2.38	-
XBR048	5363749	448775	12.71	2.43	4.93	1.87	1.14	0.08	2.93	0.11	69.45	0.40	4.23	-
XOR004	5363445	450433	0.89	0.32	1.25	0.03	0.08	0.01	0.46	0.06	96.80	0.01	0.10	-
XOR005	5363479	450493	8.34	0.33	36.90	0.06	4.08	0.50	0.01	0.00	36.13	0.31	13.20	-
XOR007	5362605	449696	8.52	0.34	3.91	2.48	0.55	0.02	0.48	0.12	82.32	0.11	2.06	-
XOR008	5363276	448952	12.50	0.29	2.72	3.84	0.20	0.04	2.34	0.12	77.09	0.15	1.42	-
XOR009	5363183	448915	7.63	0.12	17.21	1.54	1.54	0.07	0.09	0.12	62.44	0.25	7.53	-
XOR010	5363227	448810	13.91	1.42	3.69	2.25	0.52	0.11	3.96	0.20	72.13	0.48	2.12	-
XOR011	5363199	448935	13.45	7.74	10.86	3.53	4.01	0.26	1.87	0.81	43.00	1.32	11.13	-
XOR012	5362994	448959	4.30	10.44	23.03	0.05	11.28	0.31	0.18	0.14	41.94	2.60	1.83	-
XOR013	5363097	448970	16.14	0.95	4.65	3.90	0.61	0.12	2.73	0.23	68.74	0.61	3.04	-
XOR014	5363071	449039	13.70	1.11	2.83	4.32	0.68	0.08	0.16	0.20	75.17	0.48	2.60	-
XOR015	5363089	449240	13.95	6.23	11.68	0.52	5.37	0.18	2.80	0.18	49.32	1.05	7.89	-
XOR016	5363107	449235	11.87	1.38	2.68	1.39	0.50	0.08	3.95	0.19	76.72	0.39	1.89	-
XOR017	5363125	449298	14.08	7.61	13.77	0.60	2.58	0.16	3.82	0.36	49.30	2.08	3.84	-
XOR018	5363080	449348	12.43	8.20	16.78	0.66	4.85	0.25	2.39	0.26	49.40	1.81	1.36	-
XOR019	5363771	448790	15.77	1.74	10.08	3.34	1.62	0.16	1.64	0.20	59.69	1.07	4.78	-
XOR020	5363754	448834	12.79	1.28	4.26	3.07	0.50	0.06	0.35	0.15	75.73	0.29	2.89	-
XOR021	5363810	448844	11.28	3.39	2.80	0.97	2.22	0.04	1.82	0.09	76.87	0.13	1.75	-
XOR022	5363803	448839	8.26	10.66	12.47	0.10	12.89	0.15	0.26	0.07	48.70	0.09	4.11	-

SampleNo	Cr (ppm)	Y (ppm)	Sc (ppm)	Sr (ppm)	Zr (ppm)	Au (ppb)	Ba (ppm)	Cu (ppm)	Ni (ppm)	Pb (ppm)	Zn (ppm)	Fe/Fe+Mg	CO_2/CaO	Ishikawa Index	Chlorite Index	SCI	CSI	K/Al	CCPI
TI2640	-	62	5	69	329	2	288	3	2	1	88	0.81	0.93	37	42	47	53	0.24	54
TI2726	55	24	30	151	99	0	132	40	43	1	95	0.82	1.61	37	56	32	68	0.06	86
TI2728	21	32	38	159	122	0	23	28	19	1	117	0.84	1.05	37	67	30	70	0.00	86
TI3289	-	174	5	48	768	0	679	2	1	2	78	0.87	1.97	37	29	67	33	0.58	31
TI3537	3558	12	31	751	22	0	579	44	860	30	10	0.63	0.25	37	57	44	56	0.41	79
TI3920	14	41	33	403	172	1	110	29	29	1	105	0.86	0.11	37	63	27	73	0.02	83
XBR033	68	-	-	-	-	-	-	4	0	-	2	0.79	-	37	45	52	48	0.25	60
XBR034	68	-	-	-	-	-	-	7	0	-	4	0.93	-	37	91	35	65	0.36	92
XBR035	-	-	-	-	-	-	-	14	2	-	2	0.99	-	37	73	5	95	0.39	73
XBR036	-	-	-	-	-	-	-	1	0	-	0	0.92	-	37	48	16	84	0.48	49
XBR037	-	-	-	-	-	-	-	11	1	-	6	0.96	-	37	89	28	72	0.12	90
XBR038	137	-	-	-	-	-	-	12	0	-	2	0.76	-	37	62	42	58	0.22	85
XBR039	-	-	-	-	-	-	-	15	2	-	6	0.98	-	37	66	43	57	0.30	68
XBR040	-	-	-	-	-	-	-	484	63	-	1340	0.96	-	37	60	13	87	0.03	71
XBR041	-	-	-	-	-	-	-	6	1	-	14	0.88	-	37	17	50	50	0.13	22
XBR042	-	-	-	-	-	-	-	5	2	-	8	0.98	-	37	86	17	83	0.05	91
XBR043	-	-	-	-	-	-	-	1	1	-	6	0.79	-	37	27	75	25	0.53	30
XBR044	68	-	-	-	-	-	-	1	1	-	4	0.86	-	37	9	91	9	0.93	9
XBR045	68	-	-	-	-	-	-	40	4	-	14	0.87	-	37	40	69	31	0.43	42
XBR046	-	-	-	-	-	-	-	5	2	-	4	0.69	-	37	51	39	61	0.35	93
XBR047	137	-	-	-	-	-	-	6	1	-	2	0.73	-	37	69	45	55	0.23	88
XBR048	68	-	-	-	-	-	-	37	0	-	4	0.83	-	37	44	45	55	0.23	54
XOR004	68	-	-	-	-	-	-	310	107	-	662	0.95	-	37	60	17	83	0.05	71
XOR005	-	-	-	-	-	-	-	83	8	-	24	0.91	-	37	99	48	52	0.01	100
XOR007	68	-	-	-	-	-	-	17	2	-	2	0.89	-	37	55	59	41	0.46	58
XOR008	68	-	-	-	-	-	-	13	1	-	2	0.94	-	37	29	68	32	0.48	30
XOR009	-	-	-	-	-	-	-	28	6	-	12	0.93	-	37	91	51	49	0.32	91
XOR010	137	-	-	-	-	-	-	7	1	-	2	0.89	-	37	33	50	50	0.25	38
XOR011	68	-	-	-	-	-	-	53	0	-	4	0.76	-	37	51	46	54	0.41	72
XOR012	-	-	-	-	-	-	-	123	0	-	20	0.70	-	37	75	41	59	0.02	99
XOR013	137	-	-	-	-	-	-	13	2	-	10	0.90	-	37	39	59	41	0.38	42
XOR014	274	-	-	-	-	-	-	4	2	-	26	0.83	-	37	37	69	31	0.49	42
XOR015	342	-	-	-	-	-	-	66	1	-	2	0.72	-	37	62	39	61	0.06	83
XOR016	274	-	-	-	-	-	-	8	0	-	-	0.86	-	37	30	46	54	0.18	35
XOR017	137	-	-	-	-	-	-	73	2	-	6	0.86	-	37	55	28	72	0.07	77
XOR018	-	-	-	-	-	-	-	103	0	-	2	0.80	-	37	64	35	65	0.08	87
XOR019	205	-	-	-	-	-	-	47	0	-	2	0.88	-	37	61	49	51	0.33	68
XOR020	-	-	-	-	-	-	-	6	1	-	-	0.91	-	37	48	59	41	0.38	56
XOR021	-	-	-	-	-	-	-	12	1	-	18	0.59	-	37	43	47	53	0.13	63
XOR022	68	-	-	-	-	-	-	267	0	-	28	0.53	-	37	69	44	56	0.02	99

APPENDIX C

STABLE ISOTOPE DATA

Samples	UTM Northing (m)	UTM Easting (m)	$\delta^{13}C_{VPDB}$ (‰)	$\delta^{18}O$ SMOW (‰)
EVH13360	5356142	461712	-	15.76
EVH13367	5356463	458591	-	15.27
EVH13368	5363903	460116	-7.33	14.68
EVH13368	5363903	460116	-	14.76
EVH13369	5363929	460098	-	16.22
EVH13369	5363929	460098	-8.21	13.48
EVH13372	5355649	459541	-8.26	14.90
EVH13374	5355525	459541	-6.80	14.24
EVH13377	5360767	460687	-8.48	11.72
EVH13380	5360706	460722	-8.44	11.23
EVH13383	5355629	464502	-25.64	13.73
EVH13386	5355005	461896	-8.00	14.48
EVH13387	5355005	461896	-7.64	15.03
EVH13392	5356738	462807	-7.53	12.28
EVH13397	5361462	459623	-3.40	13.91
EVH13398	5361427	459643	-4.60	12.98
EVH16151	5365641	456127	-	9.88
EVH16152	5365885	459895	-	14.27
EVH16163	5366268	455843	-	10.74
EVH16167	5364711	455788	-	12.78
EVH16169	5364794	455788	-	12.94
EVH16177	5364687	461467	-5.93	13.45
EVH16198	5361369	461827	-4.94	11.16
EVH16202	5354024	455248	-	14.26
EVH16208	5366148	454842	-1.77	10.12
EVH16305	5363259	460064	-2.34	11.21
EVH16306	5363317	460025	-4.63	12.54
EVH16308	5359178	459071	-8.82	10.83
EVH16310	5362941	463392	-	12.92
EVH16313	5355261	459566	-8.56	14.35
EVH16315	5354700	458761	-7.22	14.44
EVH16320	5359186	458931	-8.44	14.88
EVH16321	5359186	458931	-	14.75
EVH16321	5359186	458931	-2.61	11.06
EVH16324	5358143	458673	-3.88	16.54
EVH16344	5353313	456191	-8.30	15.29
EVH16345	5358163	458744	-7.30	13.36
EVH16346	5358989	459142	-7.92	14.97
EVH16347	5358981	459142	-	15.15
EVH16355	5354872	462243	-6.99	13.20
EVH16364	5355103	461982	-6.64	15.13
EVH16365	5355101	461976	-6.10	15.60
EVH16366	5355095	461961	-7.33	14.07
EVH16368	5355080	461919	-6.89	15.38
EVH16369	5355090	461947	-7.13	14.46
EVH16372	5355010	461884	-8.44	13.59
EVH16373	5354998	461884	-7.97	18.29
EVH16375	5355007	461884	-8.15	15.84
EVH16382	5355201	461909	-6.73	12.64
EVH16383	5355201	461910	-6.79	11.54
EVH16385	5355173	461877	-6.86	15.52

Samples	UTM Northing (m)	UTM Easting (m)	$\delta^{13}C_{VPDB}$ (‰)	$\delta^{18}O$ SMOW (‰)
EVH16391	5355229	461906	-5.63	14.88
EVH16394	5355271	461843	-7.87	14.75
EVH16395	5355267	461838	-4.88	14.46
EVH16397	5355254	461823	-7.09	12.81
EVH16398	5355239	461805	-7.00	14.09
EVH16400	5355212	461772	-8.97	14.67
EVH16404	5354997	461896	-8.39	14.56
EVH16405	5355009	461910	-8.73	14.68
EVH16410	5355012	461876	-8.72	14.53
EVH16413	5355034	461902	-8.08	14.66
EVH16422	5355087	461909	-8.18	14.42
EVH16423	5355072	461910	-7.11	14.35
EVH16426	5355018	461936	-6.22	14.16
EVH19401	5363424	460198	-	13.70
EVH19405	5354969	462304	-7.33	14.07
EVH19408	5363323	460001	-	13.78
EVH19421	5362834	458847	-3.23	12.88
EVH19431	5360332	458746	-6.66	10.47
EVH19434	5360410	458710	-8.14	16.13
EVH19443	5354673	460951	-7.46	13.05

REFERENCES

Ayer, J. A., Thurston, P.C., Bateman, R., Gibson, H.L., Hamilton, M.A., Hathaway, B., Hocker, S., Hudak, G., Lafrance, B., Isopolatov, V., MacDonald, P.J., Peloquin, A.S., Piercey, S.J., Reed, L.E., Thompson, P.H., and Izumi, H., 2005a, Digital Compilation of Maps and Data from the Greenstone Architecture Project in the Timmins-Kirkland Lake Region, *in* Survey, D. A. I.-O. G., ed., Volume Miscellaneous Release - Data 155.

Ayer, J. A. T., P.C., Bateman, R., Dube, B., Gibson, H.L., Hamilton, M.A., Hamilton, M.A., Hathway, B., Hocker, S.M., Houle, M.G., Hudak, G.,Isopolatov. V.O., Lafrance, B., Lesher, C.M., MacDonald, P.J., Peloquin, A.S. Piercey, S.J., Reed. L.E., Thompson, P.H., 2005b, Overview of results from the Greenstone Architecture Project: Discover Abitibi Intiative, *in* Survey, O. G., ed., Volume Open File Report 6154, p. 177.

Bajc, A., Leney, S., Evers, S., van Haaften, S. and Ernsting, J. , 2001, A seamless Quaternary geology map of southern Ontario; in Summary of Field Work and Other Activities 2001: Ontario Geological Survey, Open File Report 6070, p. p.33-31to 33-35.

Barnes, H. L., 1997, Geochemistry of Hydrothermal Ore Deposits, 3rd Edition, John Wiley & Sons, p. 992.

Barrie, C. T., 2000, Geology of the Kamiskotia Area, *in* Survey, O. G., ed., Queen's Printer for Ontario, p. 79.

Blamart, D., 1991, Les concentrations tungstiferes et stanniferes: caracterisations isotopiques (H-O) des mineralisateurs, sur l'exemple du gisement Sn-W de Walmes (Maroc Central).Determination de quelques fractionnements isotopiques entre mineraux et eau. [Doctorate: L'Institut National Polytechnique de Lorraine, 160 p.

Blundy, J.D., Wood, B.J., 2001, Crystal-chemical controls on the partitioning of Sr and Ba between plagioclase feldspar, silicate melts, and hydrothermal solutions. Geochimica et Cosmochimica Acta, v.55, no.1, p.193-209

Brand, N. W., 2004, Geochemical Expressions of Nickel Sulphide Deposits, AIG Seminar, Advances and Innovations in the Exploration for Nickel Sulphide Deposits: Perth WA.

Burzo, Emil. Landolt-Börnstein: Numerical Data and Functional Relationships in Science and Technology Magnetic Properties of Non-Metalic Compounds Inorganic Compounds Based on Transition Elements - Phyllosilicates . 1. 27-I5. Berlin, New York: Springer, 2007. Print.

Cavey, G., 2006, Summary Geological Report on the Thorne Property - Bristol, Carscallen, Denton, and Thorneloe Townships: Porcupine Mining Division Ontario for Band-Ore Resources, p. 39

Corfu, F., Krogh, T.E., Y.Y. Kwok, L.S. Jensen, 1989, U-Pb ziron chronology in the southwestern Abitibi greenstone belt, Superior Province: Canadian Journal of Earth Sciences, v. 26, p. 1747-1763.

Davies, J. F., Grant, R.W., Whitehead, R.E.S., 1978a, Immobile trace elements and Archean volcanic stratigraphy in the Timmins mining area, Ontario: Canadian Journal of Earth Sciences, v. 16, no. 2, p. 305 - 311.

Davies, J. F., Luhta, L.E., 1978b, An Archean "Porphyry -Type" Disseminated Copper Deposit. Timmins, Ontario: Economic Geology, v. 73, p. 16.

Davies, J. F., Whitehead R.E.S., Cameron, R.A., , D., 1982, Regional and Local Patterns of CO_2-K-Rb-As Alteration: A Guide to Gold in the Timmins Area: Geology of Canada, p. 130-143.

Dinel, A. D. F., John Ayer, Alastair Still, Ken Tylee, Erik Barr, 2008, Lithogeochemical and Stratigraphic Controls on Gold Mineralization within the Metavolcanic Rocks of the Hoyle Pond Mine, Timmins, Ontario, Economic Geology, v. 103, p. 1341 - 1363.

Ferguson, S. A., 1957, Geology of Bristol Township, Ontario Department of Mines, Volume 66, p. 39.

Gray, M.D., Hutchinson. R. W., 2001, New Evidence for Multiple Periods of Gold Emplacement in the Porcupine Mining District, Timmins Area, Ontario, Canada: Economic Geology, v. 96, p.453-475.

Hawley, J. E., 1927, Geology of Ogden, Bristol, and Carscallen Townships, Cochrane District, *in* Survey, O. G., ed., Volume Annual Report, Ontario Ministry of Northern Development and Mines, Ontario Geological Survey, p. 102.

Hart, T.R. 1984, The geochemistry and petrogenesis of a metavolcanic and intrusive sequence in the Kamiskotia area; Timmins, Ontario; Unpublished M.Sc. thesis, University of Toronto, p. 179

Hocker, S. M., 2005, Volcanic stratigraphy, synvolcanic intrusions and controls on mineralization at the Archean Genex Mine, Kamiskotia area, Timmins, Ontario [Master of Science Dissertation/thesis]: Laurentian University, 256 p.

Hoffman, E. L., Clasrk, J.R., Yeager, J.R, 1998, Gold Analysis - Fire Assaying and alternative methods: Exploration and Mining Geology, v. 7, p. 155-160.

Jensen, R. H., 1976, Jensen Cation Plot: Using Geochemical Data, p. 63.

Jolly, W. T., 1978, Metamorphic history of the Archean Abitibi Belt, *in* Canada, G. S. o., ed., Metamoprhism in the Canadian Shield, Volume 78, p. 63-78.

K. Benn, J. A. A., B.R. Berger, C. Vaillancourt, E. Dinel, B. Luinstra, 2001, Structural Style and Kinematics of the Porcupine-Destor Deformation Zone, Abitibi Greenstone Belt, Ontario, *in* Survey, O. G., ed., Volume Open File Report 6070, p. 6-1 to 6-13.

Large, R. R., Gemmell J.Bruce, Paulick Holger, Huston, David, 2001, The alteration box plot; A simple approach to understanding the relationships between alteration mineralogy and lithgeochemistry associated wtih VHMS deposits: Economic Geology, v. 96, no. 5, p. 957-971.

MacLean, T. J. B. W. H., 1993, Lithogeochemical techniques using immobile elements: Journal of Geochemical Exploration, v. 48, p. 25.

Melnik-Proud, N., 1997, The geology and ore controls in and around the McIntyre Mine at Timmins, Ontario, Canada [Doctoral Thesis]: Queen's University.

P.C. Thurston, J. A. A., J. Goutier, M.A. Hamilton, 2008, Depositional Gaps in Abitibi Greenstone Bely Stratigraphy: A Key to Exploration for Syngenetic Mineralization: Economic Geology, v. 103, p. 1097-1134.

P.J. MacDonald, S. J. P., M.A. Hamilton, 2005, An Intergrated Study of Intrusive Rocks Spatially Associated with Gold and Base Metal Mineralization in the Greenstone Belt, Timmins Area and Clifford Township: Discover Abitibi Intiative *in* Survey, O. G., ed., Volume Open File Report 6160, p. 190.

Pyke, D. R., 1982, Geology of the Timmins Area, District of Cochrane; Ontario Geological Survey Report 219, *in* Survey, O. G., ed., p. 141.

R. Bateman, J. A. A., B. Dube, 2008, The Timmins-Porcupine Gold Camp, Ontario: Anatomy of an Archean Greenstone Belt and Ontogeny of Gold Mineralization: Society of Economic Geologists, v. 103, no. 6, p. 1285-1306.

R. Kerrich, R. W. H., 1982, Archean Lode Gold and Base Metal Deposits: Evidence for Metal Separation into Independent, *in* Canada, G. o., ed.: London, Ontario, University of Western Ontario, p. 144-160.

Rollinson, H.R. 1993: Using Geochemical Data: Evaluation, Presentation, Interpretation. Longman Scientific and Technical, England.

Madiesky, H.E., and Stanley, C.R., 1993, Lithogeochemical Exploration of Metasomatic Zones Associated with Volcanic-Hosted Massive Sulphide Deposits Using Pearce Element Ratios, International Geology Review, Vol. 35, pp.1121-1148

Taylor, H. P., 1974, Oxygen and hydrogen isotope studies to problems of hydrothermal alteration and ore deposition: Economic Geology, v. 69, p. 843-883.

Thompson, P. H., 2005, A new metamorphic framework for gold mineralization in the Timmins-Kirkland Lake are, western Abitibi greenstone belt: Discover Abitibi Intiative, *in* Survey, O. G., ed., Volume Open File Report 6162, p. 104.

Vaillancourt, C., 2000, Project Unit 00-011. New Geological Mapping and Compilation in the Timmins West Area-Bristol and Ogden Townships, in Open File Report 6032 Summary of Field Work and Other Activities, edited by J.A. Ayer, C.L Baker, R.I. Kelly, J.R. Parker, G.M. Stott and P.C. Thurston, *in* Survey, O. G., ed., p. 4-1 to 4-11.

van Hees, E. H., Shelton. K.L., Vennemann, T.W., O'neil, J.R., Kesler, S.E., 2000, Stable isotopes and fluid inclusion gases as exploration tools and ore guides in large-scale gold systems:Examples from the Yellowknife and Abitibi greenstone belts, Mining Millenium 2000 Convention Program with Abstracts, Prospectors and Developers Association of Canada, p. 54-55

Washington, G., 2008, Characterization and Significance of Lithogeochemical, Stable Isotope and Mineral Alteration Halos in the Hollinger-McIntyre Gold Deposit Timmins, Ontario, Canada [Master of Science: Wayne State University, 222 p.

Washington, G., Sirbescu, Jensen,K., van Hees, E.H., 2009, The nature and significance of lithogeochemical and stable isotope alteration halos in the Hollinger-Mcintyre gold deposit, Ontario, Canada, *in* Wayne State University, C. M. U., ed., International Applied Geochemistry Symposium: Fredricton, Canada, p. 273 - 277.

ABSTRACT

LITHOGEOCHEMICAL AND STABLE ISOTOPE CHARACTERISTICS OF BRISTOL AND NORTHERN THORNELOE TOWNSHIPS AND ITS CORRELATION WITH GOLD MINERALIZATION

by

ZACHARY G. STEVISON

May 2013

Advisor: Dr. Edmond H.P. van Hees

Major: Geology

Degree: Master of Science

The Porcupine Mining Camp located in the southwestend of the Abitibi Greenstone Belt has been mined extensively for its prolific precious and base metal enrichment. This study targeted Bristol and Northern Thorneloe, fifteen kilometers southwest of Timmins, ON, an area that is of economic interest for its gold mineralization. Rock samples were collected (drill- core and outcrop) throughout both townships and analyzed for their major and trace element composition, These were used to determine hydrothermal alteration signatures as well as specific elemental enrichment that relate to gold mineralization in Bristol-Thorneloe Township. Quartz-carbonate and quartz-carbonate-tourmaline vein samples were also collected near rock samples to determine $\delta^{18}O$ and $\delta^{13}C$ isotopic concentrations. These values were used to determine the fluid temperature and isotopic signatures for gold mineralization in the study area. After evaluation barium, strontium, phosphorus, and CO_2 enrichment was found in anomalous gold (>25 ppb) enrichment zones. These elements demonstrated evidence that

supports of mobilization in auriferous fluids in Bristol-Thorneloe Township. The isotopic analysis determined the gold bearing fluids in the study area to 303° to 403°C with $\delta^{18}O_{qtz}$ values of 13.5‰, similar to other mesothermal gold in and outside the Porcupine Camp.

AUTOBIOGRAPHICAL STATEMENT

I, Zachary Stevison, was born and raised in Algonac, Michigan a small town that enjoys the spoils that life out-of-doors in the “mitten” has to offer. Regarded as the “Venice of Michigan” during our adolescence my friends and I relied on our boats as primary transportation during the spring and summer months. With this freedom came with it the love of the outdoors by frequently fishing, hunting, and boating when away from school. However, over the course of my young life, a clear degradation of that once beautiful landscape was taking place. This went beyond mere disappointment and became my direction during my undergraduate studies where I earned a Bachelor of Science in Environmental Science at Oakland University (Rochester, MI). I had always planned on attending graduate school and my Oakland University professor introduced to Dr. van Hees at Wayne State University. Here a new world of geology was opened, and mining in particular appealed to my sense of adventure. After working a summer in Timmins, ON I knew the knowledge and experience this field had to offer would compliment my environment science background. That leads to me today where I am on the verge of closing this chapter at Wayne State University, and anxiously leave this autobiographical statement unfinished.